A Genetic Approach towards Modulating Pre-Harvest Pod Shatter in *Brassica napus* (Oilseed Rape)

By

Thomas Aidan Wood

The John Innes Centre
Norwich

A Thesis Submitted for
the Degree of Doctor of Philosophy
to the University of East Anglia,
School of Biological Sciences
December 2010

Dedicated to
My Mother and Father

Acknowledgements

I wish to offer my heart-felt thanks everyone who has assisted me during my PhD research at the John Innes Centre; to Lars for his benevolence, enthusiasm and support throughout, to Colin for his statistical expertise, to Eddie, Judith, Pauline, Rachel and Andrea for their practical guidance, to Ian and the Brassica Cluster for their support, the Østergaard lab for its engaging and enjoyable atmosphere, and Peter Werner at KWS for his pragmatic advise and commercial insight.

Abstract

Pre-harvest pod-shattering in *Brassica napus* (Oilseed Rape) is a serious agricultural and economic problem, with losses of 11-25% reported (Price *et al.,* 1996) resulting in lost revenues of an estimated £66 million per annum for the U.K. alone. Reductions in this loss will provide benefits for both society and the environment. Lines from a doubled haploid *B. napus* mapping population, segregating for Pod Shatter Resistance (PSR), termed POSH 1-3 exhibited a range of shatter resistance phenotypes. A Random Impact Test (RIT) was used to measure the difference between levels of PSR in population lines. An assessment of pod physiology among these lines revealed that PSR is associated with increases in the amount of vasculature and changes in vascular orientation as reported in the resistant DK142 parent line (Child *et al.* 2003). PSR was also found to result from differences in degradation of a key tissue required for valve separation in both *B. napus* and *Arabidopsis*. A genetic linkage map has been produced for the population and includes a number of candidate gene markers with established roles in fruit development in *Arabidopsis*. The linkage map was used as a basis to perform a QTL analysis where a number of loci associated with increases in PSR in *B. napus* have been identified. Genetic markers linked to these loci could provide a valuable tool for marker assisted selection (MAS) to improve pre-harvest pod shatter in *B. napus*. A novel assay has also been developed to investigate differences in PSR between *Arabidopsis* ecotypes. Shatter resistant ecotypes have been identified within the accessions tested. This could enable the differences between the model and crop species to be compared to assess if factors regulating such traits are conserved. This may also provide insight into new candidates to modulate pre-harvest pod shatter for agronomic improvement of *Brassica* species.

Contents

Chapter 1: Introduction

Chapter 3: Anatomical Assessment of Factors Contributing Towards PSR in the POSH 1-3 population

Chapter 4: POSH 1-3 Genetic Linkage Map Construction

Chapter 5: POSH 1-3 Single Marker Analysis

Chapter 6: Investigating Variation in Pod Shatter Resistance in Natural and Mutant Accessions of *Arabidopsis thaliana* using a Novel Assay

List of Figures

List of Tables

List of Appendices

Abbreviations

4-CPA- 4- Chlorophenoxyacetic Acid
ADPG1/2 – ARABIDOPSIS DEHISCENCE ZONE POLYGALATURONASE ½
AFLP – Amplified Frequency Length Polymorphism
ALC – ALCATRAZ
An-1- Antwerpen
ANOVA - Analysis of Variance
ARIT - *Arabidopsis thaliana* Random Impact Test
ASA – Allele Specific Amplification
A. thailiana - Arabidopsis thaliana
BACs- Bacterial Artificial Chromosome
Bay-0 - Bayreuth
BEN 2- BFA VISUALIZED ENDOCYTIC TRAFFICKING DEFECTIVE 2
BLAST- Basic Local Alignment Search Tool
B. napus - Brassica napus
B. nigra – Brassica nigra
B. oleracea - Brassica oleracea
bp- base pairs
Br-0 - Brünn
B. rapa - Brassica rapa
Brk. adj.LD50 – Broken Adjusted Lethal Dose 50
CAPS-Cleaved Amplified Polymorphic Sequences
CER - Controlled Environment Room
CIM – Composite Interval Mapping
Col-0 – Columbia
Cvi-0 - Cape verde island
DAA - Days after Anthesis
DArT – Diversity Array Technology
DH - Doubled Haploid
dH_20 – Distilled water
DNA – Deoxyribonucleic Acid
DUS – Distincness, Uniformity, Stability
DZ - Dehiscence Zone
enA – Endocarp layer A
enB - Endocarp layer B
Est-1 – Estland
EST – Expressed Sequence Tag
FAA - Formaldehyde Acetic Acid
FIL – FILAMENTOUS FLOWER
FUL – FRUITFULL
ga-2ox - GIBBERELIC ACID 2 OXIDASE
ga4-3ox - GIBBERELIC ACID 4-3 OXIDASE

GM-Genetic Modification
HEAR – High Erucic Acid Rapeseed
HNRT – Homeologous Non-Reciprocal Translocation
HRT - Homeologous Reciprocal Translocation
IND – INDEHISCENT
InDels – Insertion/Deletion
Int. adj.LD50 – Intact Adjusted Lethal Dose 50
IPTG - Isopropyl β-D-1-thiogalactopyranoside
JAG - JAGGED
Kin-0 - Kindalville
KW-Kruskal-Wallis
Ler-0 – Landsberg erecta
LD50 - Local Death 50 (Half life)
LL - Lignified layer
LN - Linkage Group
LN$_2$ - Liquid Nitrogen
LOD – Logarithmic of Odds
LRR - Leucine Rich Repeat
MAS - Marker Assisted Selection
MDE – Mutation Detection Enhancement
miRNA – MicroRNA
MIT – Manual Impact Test
Mrk-0 – Märkt
MQM – Multiple QTL Mapping
MVBV- Main Vascular Bundle of the Valve
N1-N19 - *B. napus* Linkage group
NASC - National Arabidopsis Stock Centre
Nok-3 - Noorwijk
OSR - Oilseed Rape (*Brassica napus*)
Oy-0 - Oytese
PAGE - Polyacrylamide Gel Electrophoresis
PCR-Polymerase Chain Reaction
PG - Polygalacturonase
PSR - Pod Shatter Resistance
PTGS-Post Transcriptional Gene Silencing
PWT - Pod Wall Thickness
QTG - Quantitative Trait Gene
QTL - Quantitative Trait Loci
RAPD - Random Amplified Polymorphic DNA
RECORD - Recombination Counting and Ordering
RNAi – Ribonucleic Acid interference
RPL- REPLUMLESS
RIT-Random Impact Test
RIL-Recombinant Inbred LIne

RT - Room Temperature
SHP1/2 – SHATTERPROOF 1/2
SPT - SPATULA
siRNA – Small interfering RNA
SL - Separation Layer
SMA - Single Marker Analysis
SMR - Single Marker Regression
SNPs- Single Nucleotide Polymorphism
SSCPs - Single Strand Conformation Polymorphism
SSRs- Simple Sequence Repeat
SRAPs – Sequence Related Amplified Polymorphism
TILLING – Targeted Induced Local Lesions In Genomes
TNDH – Tapidor/Ningyou7 Doubled Haploid
Van-0 - Vancouver
VM – Valve margin
Ws-2-Wasselewskija-2
WT – Wildtype
YAB3 – YABBY 3

Chapter 1: Pre-harvest Pod Shatter in *Brassica napus* (Oilseed Rape)

1.1 Introduction – Pre-harvest Pod Shatter in *Brassica napus* (Oilseed Rape); A Review

This introduction provides a background into *Brassica napus* as a crop, its related species and its uses and a description of pod development. I also discuss the previous approaches used to investigate pre-harvest pod shatter in oilseed rape (OSR), the technologies available to conduct genetic linkage mapping including the development of segregating *B. napus* populations, genetic markers and mapping procedures, and QTL analysis. Finally focus is placed on comparative genetics between members of the Brassicacea and the use of *Arabidopsis thaliana* as a basis for a candidate gene approach.

1.1.1 *Brassica napus* origins and uses

Brassica napus (B. napus) is a naturally occurring hybrid used worldwide for edible and industrial oilseed production. Oilseed rape is a member of the tribe Brassiceae, within the monophyletic Brassicacea family, itself comprised of nearly 3500 species and including many important annual and biennial vegetable, oilseed and fodder crops, and also the model plant species *Arabidopsis thaliana* (Warwick and Black, 1997; Weiss, 1983; Lagercrantz *et al.* 1996). The *Brassica* species are reported to a have diverged from *Arabidopsis thaliana* some 10-20 million years ago (Yang *et al.* 1999; Koch *et al.* 2000). Of the cultivated *Brassica* species six are identified to be of principle importance to agriculture. These comprise three diploid species; *B. nigra*, *B. oleracea* and *B. rapa* and three amphidiploids; *B. carinata*, *B. juncea* and *B. napus.* The allopolyploid species are a product of pair-wise, interspecific hybridisation between respective diploid progenitors (Figure 1.1). *Brassica* were some of the earliest domesticated plants, with reports of the use of vegetable varieties in the Neolithic period, whereas their use as oilseeds probably occurred more recently (Downey and Röbbelen, 1989). One of the earliest reports of the use as an oilseed was in 1570, where it was reported to be grown in the Rhineland, Germany, as lamp oil and as a cheaper alternative to olive oil (Heresbach, 1570). Rapeseed oil was used primarily for soap production and illumination in the middle ages (Appelqvist, 1972).
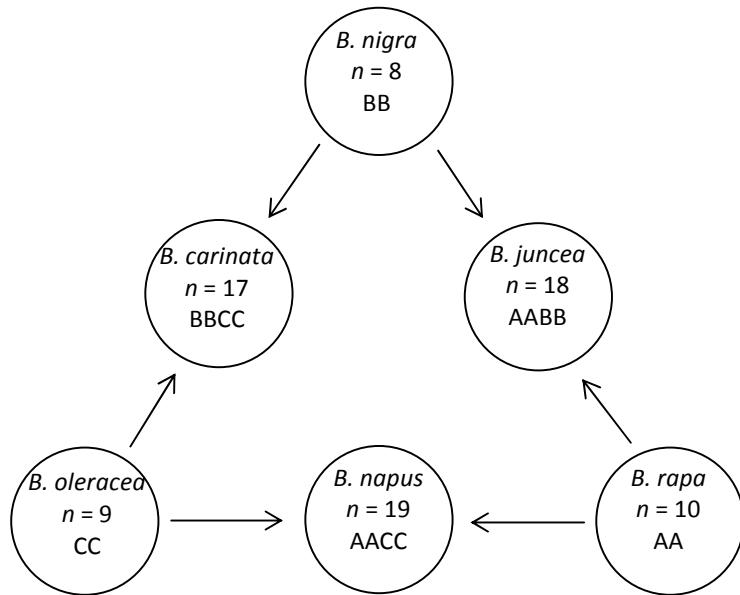
Figure 1.1: Triangle of U: Overview of genetic transfers and complements in between various species and hybrids of the genus *Brassica.* (U, 1935; Kimber and McGregor, 1995)

The amphidiploid species *B. napus* arose as a naturally occurring hybrid, from a cross between *Brassica rapa,* donating an 'A' genome (n=10) and *Brassica oleracea,* donating a 'C' genome (n=9), from Southern Europe with subsequent introduction in to Asia in the 18th Century (Snowdon *et al.* 2002; Downey and Röbbelen, 1989). *B. napus* is believed to have arisen less than 10,000 years ago (Rana *et al.,* 2004). In Europe, *B. napus* for edible oil has only been produced extensively in the western world since World War II, whereas, its use in Asia has been accepted for centuries (Kimber and McGregor, 1995). In the U.K. *B. napus* is grown predominantly as a break crop during cereal rotations. *B. napus* is cultivated as both spring and winter varieties, predominantly for the linolenic and oleic oils contained in the seed. These are used widely as a foodstuff, with the highest yields obtained in vernalization requiring winter cultivars (3.5 tonnes/ha) compared to spring varieties (2.5 t/ha) (www.defra.gov.uk,

www.hgca.com). Although this may appear low compared to wheat, with an average U.K. yield of 8 t/ha, it must be considered that the energy content in oilseeds is much greater (www.defra.co.uk; Diepenbrock, 2000).

In excess of 600,000 hectares of oilseed rape (OSR) was planted in the U.K. in 2010, yielding some 2.2 million tonnes of seed (www.defra.gov.uk). The approximate cost in 2010 was estimated at £300/tonne. (www.fwi.co.uk). The value and areas of oilseed rape being cultivated are increasing due to its potential use as a carbon-neutral bio-fuel, for lubricants and as a high price specialist food product, due to high levels of oleic oil. The cake remaining after oil extraction is also utilised as a high protein animal feed. Two distinct varieties are cultivated with 'double low' (low glycosinolates/low erucic acid) used for food varieties and high erucic acid rapeseed (HEAR) for non-food oils utilised in the plastics and lubricants industry. The low glycosinolate character was introduced from the Polish Bronowski variety after the Second World War and the low erucic acid was reported in spring Canadian *B. napus*, both improving the edibility of the oil considerably (Finlayson *et al.,* 1973; Stefansson *et al.,* 1961, 1964). Oilseed rape is now the third largest source of vegetable oil globally and in 2005 some 46 million tonnes of oilseed rape was produced worldwide (Gunstone, 2001; www.bayercropscience.co.uk).

Oil content in seed from commercial varieties is documented as ranging between 42 - 47% (Lööf, 1972). This is extracted using a mixture of mechanical and solvent based extraction techniques. Physical extraction techniques are first used to extract higher grade oils, followed by gaseous solvent extraction, using hexane to remove the residual oils (Anjou, 1972). Although cultivated since roman times *B. napus* is a relatively 'new' crop to contemporary agriculture and has only been cultivated extensively since the 1960s-70s. It is largely under-developed as a crop and exhibits a number of agronomically undesirable characters, removal of which can hinder breeding efforts to achieve the desired morphology, character and yield potential. One such character is indeterminacy, which permits continued flower set if a plant suffers from infertility or is damaged after flowering has been initiated, but also allows mature pods at the base of the raceme to dehisce whilst seeds in younger pods may not reach maturity

(Morgan *et al.,* 1998). This lack of developmental synchronicity also diverts resources into pods that may not fill properly before the end of the season. Yield in *B. napus* has remained relatively unaltered in the years it has been cultivated, whereas wheat yield has increased from around 4 t/ha in the 1960s to around 8 t/ha (Berry, 2006; Burgess and Morris, 2009). Much of the increases in wheat relate to the introduction of *Rht* genes, reducing height to divert biomass into grain filling, during the green revolution (Gale and Youssefsen, 1985).

1.1.2 Fruit Development in *Brassica napus*

Brassica napus pods are very similar in morphology to *Arabidopsis thaliana* siliques. On fertilisation, the gynoecium develops into a fruit consisting of a number of highly specific tissues associated with both the development and dispersal of germplasm (Figure 1.2a and b). The silique comprises of two valves attached to a lignified, dichotomous replum, divided laterally by a false septum. The beak of the fruit is formed from the remnants of the stigma and style. A row of seeds develop in each valve, either side of the replum. Valves exhibit an adaxial/abaxial symmetry and are composed of an outermost (abaxial) epidermal layer and two endocarp layers; A and B (enA and enB, Figure 1.2b), separated by 3-6 layers of mesophyll cells (Spence *et al.* 1996). The silique is joined to the raceme of the plant at the pedicel.

Figure 1.2a: Brassica silique var. Apex (actual size) B: Beak, P: Pedicel, V: Valve
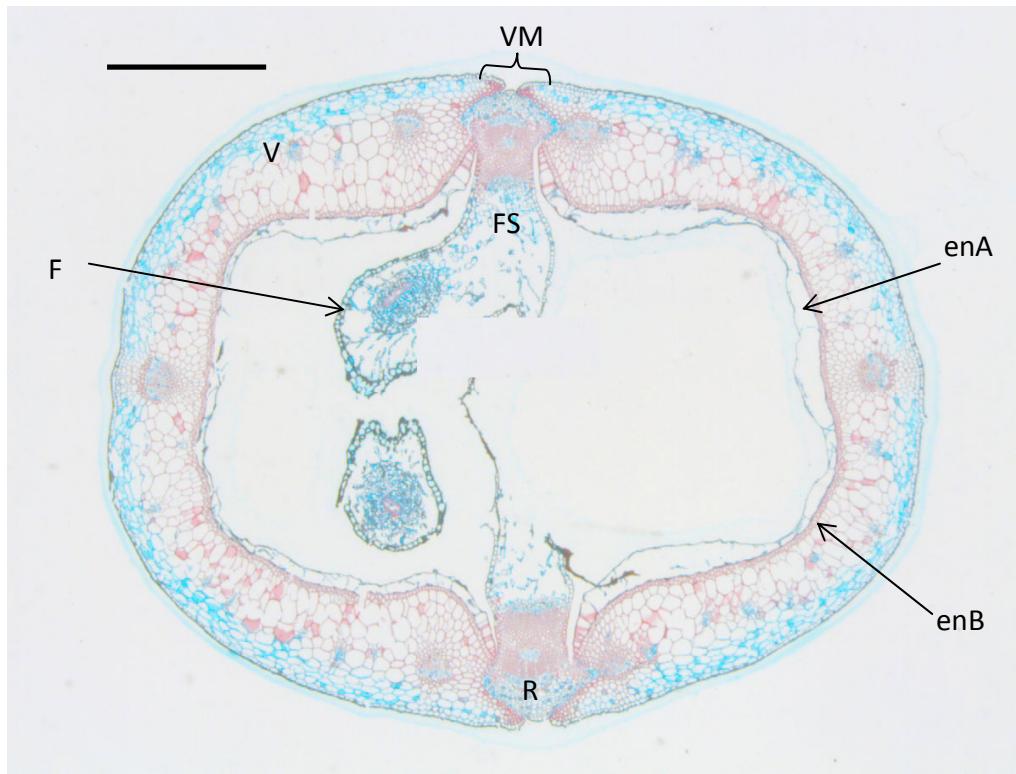
Figure 1.2b: Transverse section of a fully elongated *B. napus* silique enA: Endocarp A layer, enB: Endocarp B layer, F: Funiculus, R: Replum, FS: Septum, V: Valve, VM: Valve Margin Scale Bar: 1mm

The cell types constituting each of the tissues composing *Arabidopsis* and *Brassica* siliques differ greatly, each forming highly distinct boundaries along the valve margins, where the valve attaches to the replum (Meakins and Roberts, 1990a, Férrandiz *et al.* 1999, Sorefan *et al.,* 2009). Here, two distinct tissues, a rigid lignified layer (adjacent to valve) and a separation layer (adjacent to the replum) constitute the dehiscence zone (DZ). The silique has developed a number of distinct mechanisms to mediate pod-shatter. The DZ is directly involved in valve separation, with the lignified layer peeling away from the enzyme-secreting separation layer, as spring-like forces are generated as the silique desiccates (Spence *et al.,* 1996, Squires *et al.,* 2003).

This spring-like force is generated between the replum and the lignified tissue of the enB layer. On addition of a suitable mechanical stimulus, dehiscence at the valve margin can occur, with valves separating away from the main silique structure between the separation layer and lignified layers, shedding the seed. Valve separation predominantly initiates at the base of the silique along the dehiscence zone towards the beak, or from the beak when it is detached (Davies and Bruce, 1997).

The separation layer in *Brassica* pods secretes hydrolytic enzymes, causing breakdown of the middle lamella between adjacent cells, as is observed in *Arabidopsis* (Spence *et al.,* 1996, Meakins and Roberts, 1990b, Dinneny & Yanofsky, 2005, Ogawa *et al.,* 2009). Roles in the degradation of pectin at the middle lamella have been suggested for a range of polygalacturonases (PG), β-1, 4, glucanases and hemi-cellulases, many of which have been isolated from DZ tissue of *Arabidopsis, B. rapa* and *B. napus*. Many DZ hydrolyases show a high degree of homology, across different *Brassica* species (Sander *et al.,* 2001, Meakin and Roberts, 1990b; Ogawa *et al.* 2009; Jenkins *et al.* 1999; Petersen et al 1996). An increase in β-1, 4, glucanase has been correlated with a decrease in auxin during fruit senescence which suggests hormone signalling may contribute to regulate dehiscence (Chavaux *et al.,* 1997). Chavaux *et al.,* (1997) also demonstrated that application of an exogenous auxin analogue, 4-Chlorophenoxyacetic Acid (4-CPA), delayed the onset of separation layer degradation, inhibiting increases in cellulase activity. Application of 4-CPA was also demonstrated to perturb secretion of a rape dehiscence zone-specific polygalacturonase, RDPG1, into the cell wall of the separation layer (Petersen *et al.,* 1996; Dal Degan *et al.,* 2001). This suggests an important role for (reductions in) auxin at the valve margin in regulating separation layer degradation.

The duration of fruit growth/elongation in *B. napus* can be divided into distinct stages post-anthesis. After anthesis and fertilization, fruit elongation proceeds until approximately 35 days after anthesis (DAA) when the major phase of lignification has occurred, during which at 20DAA, replum differentiation occurs (Meakins and Roberts, 1990a). Rapid seed growth also begins around 20DAA, and seed are reported to attain 35% of their final weight when pods are fully elongated, after which oil production is initiated (Mendam and Salisbury, 1995). At 40-

45DAA activation of the hydrolytic enzymes required for separation layer degradation takes place (Meakins and Roberts, 1990b). At approximately 60DAA senescence begins as oil content continues to increase and at 75DAA pods are fully senesced, and oil content reaches a maximum (Mendam and Salisbury, 1995).

Smyth *et al.* (1990) have presented a more defined description of the developmental stages of *Arabiodopsis* siliques in the *Landsberg erecta* (Ler-0) ecotype. The first 12 stages are pre-anthesis and require approximately 13 days to occur, whilst stages 13-20 occur post-anthesis with a total duration of 13 days. Although many times smaller, *Arabidopsis* and *Brassica* fruit display a striking similarity with respect to physiology and also factors regulating their development and mechanism controlling seed dissemination. These similarities are demonstrated in depictions of transverse sections of *B. napus* and *Arabidopsis* siliques in Figures 1.3a and b. The major difference between the two types of silique is the noticeable reduction in the relative size of the replum in *B. napus* compared to *Arabidopsis*.
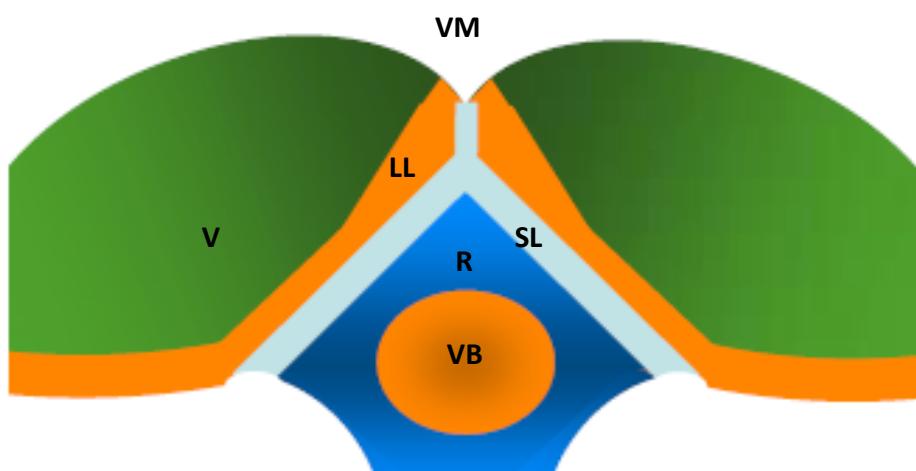
Figure 1.3a: Depiction of a transverse section of a *Brassica* dehiscence zone. LL: Lignified Layer, R: Replum, SL: Separation Layer, V: Valve, VB: Vascular Bundle and VM: Valve Margin (Adapted from Østergaard *et al.,* 2007).
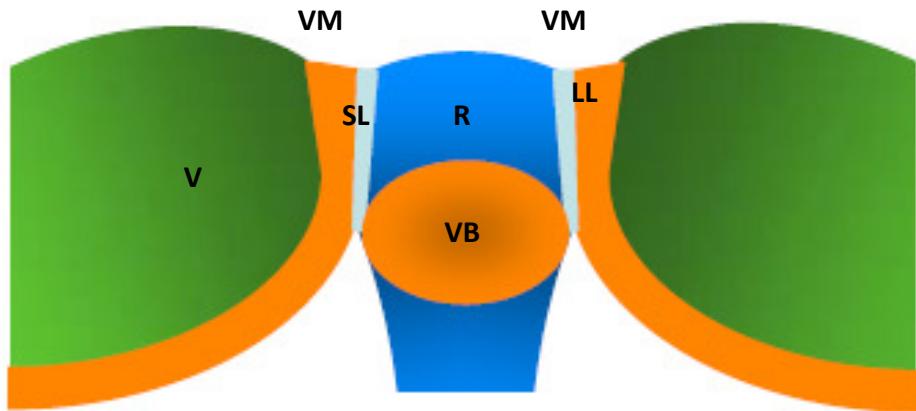
Figure 1.3b: Depiction of a transverse section of an *Arabidopsis* dehiscence zone. LL: Lignified Layer, R: Replum, SL: Separation Layer, V: Valve, VB: Vascular Bundle and VM: Valve Margin (Adapted from Østergaard *et al.,* 2007).

1.1.3 Pre-harvest Pod Shatter: Effects and contemporary control strategies

Sources highlight average seed losses through pre-harvest pod shatter of 8-12% (Kadkol *et al,* 1984). Losses are exacerbated during periods of adverse weather conditions such as wind, rain or hail, with losses increasing as high as 50% (Price *et al.,* 1996; Macleod, 1981). An average 10% loss in seed represents approximately £66 million pounds in lost revenue per annum in the U.K. (www.defra.co.uk). In conjunction with lost revenues, volunteer OSR plants caused by pre-harvest seed loss also contaminate fields, with reports estimating that 23% of winter cereal crops are contaminated with OSR in the U.K. (Whitehead and Wright, 1989). Although volunteers are easily controlled in subsequent cereal rotations with broadleaf herbicides, it is difficult to remove plants in adjacent OSR rotations and could result in contamination of foodstuffs with high erucic acid seed or through genetic contamination by cross pollination (Morgan *et al.,* 1998; Werner *et al.,* 2003c). *Brassica* seed is persistent in nature and can remain viable for a number of seasons, often confounding matters further. There are also considerations for the associated cost and environmental impact of removal all which detract

from the crops net value. A number of methods suitable to reduce premature seed shedding have been developed, but none are totally effective. These approaches are described below.

Genetic strategies to reduce pod shatter:

Conventional plant breeding and genetic mapping

In a natural environment, shatter resistance, would appear to be disadvantageous with respect to seed dispersal. However, this trait could hold the potential for modulating pod shatter in commercial crop varieties. Shatter resistance has been documented for a number of plant species including rice, the diploid parents of *B. napus, B. rapa* and *B. oleracea,* and other Brassicae, *B. carinata, B. nigra* and *B. juncea* (Li *et al.* 2006; Konishi *et al.* 2006; Kirk and Hurlstone, 1983; Prakash and Chopra, 1988, 1990). However, little variation for increases in pod shattering is reported in contemporary commercial *B. napus* cultivars (Bowman *et al.*, 1984; Morgan *et al,* 1998). A small number of *B. napus* lines are known to exhibit some degree of resistance to shattering, *i.e.* Apex, but this is still very poor (Werner *et al.,* 2003a).

The greatest improvement in studying the diverse characters contributing to pod shatter in *B. napus* has been made in the development of synthetic hybrids in *B. napus*, recreating the initial 'wild' hybridisation event between *B. rapa* and *B. oleracea* progenitors (Morgan *et al.,* 1998, 2000; Werner *et al.* 2003 a, b). Currently, there are no robust physical markers linked to pod shatter resistance (PSR) and therefore, the trait cannot be assessed in the field until pods have completely senesced. There is also a distinct lack of molecular markers linked to the PSR trait and a paucity of mapping resources to aid breeding efforts. In lines where shatter resistance has been identified, the character has been reported to be recessive, polygenic and highly complex, all hindering the application of conventional breeding methods (Morgan *et al.,* 2000; Child *et al.,* 2003; Werner *et al.,* 2003c).

Genetic modification

B. napus and its close relatives are amenable to transformation with *Agrobacterium tumefaciens*. Østergaard *et al.* (2006) demonstrated both a conserved role for *Brassica* fruit development genes using transgenic expression of an *Arabidopsis 35S::FRUITFULL (FUL)* construct in *B. juncea* and also its role in preventing dehiscence by perturbing conventional tissue patterning, completely fusing the valves to the replum. Although this could have the potential to reduce seed loss, a quantitative method of reducing the 'unbreakable' phenotype, would have to be developed to prevent the seed damage experienced on threshing *Brassica 35S::FUL* siliques. Unfortunately in the current climate a GM crop could not be licensed for cultivation in the U.K. and the cost of development is prohibitive compared to conventional varieties.

Post-Transcriptional Gene silencing (PTGS) or RNA interference (RNAi) is a powerful technique that has potential application to modulating pre-harvest pod shattering in oilseed rape. This technique allows the targeted down-regulation of selected genes or gene families through transformation with a silencing construct and has been applied successfully in a range of plant species including *Brassica* (Wood *et al.*, 2011, Yu *et al.* 2008). It has also been used to reduce pod shattering in *B. oleracea* through the silencing of *BolC.IND.a* gene, of which the orthologue in *Arabidopsis* is involved in valve margin specification (Wood, unpublished). Unfortunately due to legislation, the application of RNAi is prohibited in the same manner as other GM approaches.

Target Induced Local Lesions in Genomes (TILLING)

Although conventional GM and RNAi strategies may have limited application to commercial varieties, mutation breeding has seen widespread application to agriculture for many years. Therefore, identification of suitable phenotypes in TILLING resources may hold potential as a manner through which to identify important alleles contributing to reductions in pre-harvest pod shatter. An extensive *B. rapa* TILLING population is now publically available and a *B. napus* population is under development (Stephenson *et al.* 2010; www.revgenuk.jic.ac.uk;

Wells *et al.,* unpublished) and these may pose as important resources from which to introduce novel alleles into *B. napus* breeding material.

Agronomic approaches pod shatter:

Swathing

Wind-rowing or swathing involves cutting the crop around two weeks prior to the final harvest date and laying it in rows to dry. This method ensures the majority of the crop is at same level of maturity when harvested but losses due to mechanical vibration and damage are still evident (Kadkol *et al.,* 1984).

Application of desiccants

The use of chemical desiccants like diquat, glufosinate ammonia or glyphosate is another common technique to reduce seed loss. Glyphosate, licensed commercially as Round-up™ by Monsanto, is the most widespread contemporary treatment to tackle pre-harvest pod shatter and is favoured as it is trans-located systemically ensuring senescence throughout the entire plant. It is also is reported not to leach readily into groundwater as it rapidly becomes immobilised as it absorbs into the soil and shows relatively low eco-toxicity (Bayliss, 2000; Cook *et al.,* 2010).

Application of shatter reduction products

Products are now becoming available for spray application to OSR crops to reduce seed loss due to shattering. Pod-Stik™ (DeSangosse, U.K.) is a water-based polymer that prevents valve detachment and reduces seed loss compared to untreated plants (Wood, unpublished). However, due to agronomy of *B. napus*, the spray can only contact pods in the upper most layer of the canopy and is therefore not completely effective in stopping seed loss. There is also the associated extra cost of the spray to consider for the grower.

The production of shatter-resistant *B. napus* varieties using a synthetic source to reduce pre-harvest pod shatter is proposed as an alternative to agronomic and GM approaches which are

not completely satisfactory. This strategy could pose a potential solution to this serious agronomic issue and would be of great benefit to science and agriculture alike.

1.1.4 The Development of Shatter Resistant *B. napus* Varieties

In an effort to tackle the problem of pre-harvest pod shatter, a Doubled Haploid (DH) microspore-cultured mapping population termed POSH 1-3, segregating for Pod Shatter Resistance (PSR), was developed from select winter oilseed rape lines (Morgan *et al.,* 1998, 2000; Werner *et al.,* 2003b). The initial material from which this population was derived was a cross between a conventionally open pollinated elite cultivar, Apex (NK-Syngenta seeds Ltd, U.K.) and the shatter resistant DK142 line (Summers *et al.,* 2003). The DK142, a line selected from the DK3, DH population, was itself derived from a selfed DH line, which was generated from a cross between the DH winter oilseed rape N-0-109 (KWS, U.K.) and a synthetic interspecific hybrid of *Brassica rapa* var. chinensis and *Brassica oleracea* var. alboglabra (SYN1) developed at the John Innes Centre from which shatter resistance was introduced into the breeding program (Morgan *et al.,* 1998, 2000; Werner *et al.,* 2003a).

Issues of infertility were observed with DK142, resulting in poor pod and seed set. As these characters were commercially undesirable and made it hard to obtain selfed seed and assess pod strength, DK142 was crossed to the common cultivar Apex to improve its vigour. The Apex/DK142 cross yielded six F_1 hybrids, termed POSH 1 (1-1 to 1-6, respectively), which were selfed to produce F_2 lines. The POSH 1-3 DH mapping population was then derived from the F_2 POSH 1-3 lines, ensuring homozygous lines, segregating for the PSR trait, of which identical lines could be regenerated thorough selfed seed (Figure 1.4). The POSH 1-3 DH mapping population initially consisted of approximately 200 winter OSR lines segregating for PSR, which after initial experimentation and analysis, was reduced to approximately 120 lines, due to loss of lines to infertility (hence lacking selfed seed) and plant death.

Brassica rapa var. chinensis X *Brassica oleracea* var. alboglabra

↓

N-0-109 X SYN 1

↓

DK3

(DH Population)

↓

APEX X DK142

↓

POSH 1 F_1s

(six sets F_1 lines 1.1-1.6)

↓

F_2s

↓

POSH 1-3

(DH Mapping Population)

Figure 1.4: Origin of the POSH 1-3 mapping population (Adapted from Werner *et al.,* 2003a).

1.1.5 Pod and Dehiscent Zone Physiology in Shatter Resistant Lines

A wide range of physical characters have been assessed during cultivation of the POSH progenitor lines (Morgan *et al.* 1998, 2000; Child *et al.,* 2003; Summers *et al.,* 2003). Sources have highlighted that determinants of raceme morphology, such as pod angles, raceme length, thickness and width correlate poorly with pod shatter, suggesting the trait is likely to be selected for independently of other agronomically important characters (Morgan *et al.* 1998, 2000). This highlights the difficulty in identifying physical characters linked to the shatter resistance trait in *B. napus* that could be used as a marker to aid breeding efforts. However, a number of studies concerning the physiology of shatter resistant fruit from the DK142 lineage and shatter susceptible Apex cultivar have been conducted to identify causal factors attributed to increases in PSR (Child *et al.* 2003; Summers *et al.,* 2003). Pods from the DK142 line demonstrated differences in physiology compared to Apex, such as thicker pod walls, a 48% increase in the width of the dehiscence zone (DZ) and a 50% reduction in seed mass. However these differences were not strongly correlated with increases in PSR (Summers *et al.,* 2003; Child *et al.,* 2003).

Other anatomical and morphological features have been reported to directly contribute to increase in PSR; Summers *et al.* (2003) observed that increases in pod length and in the weight of the valves and of the beak/septum correlated with increases in PSR in DK142. Valves were 25% heavier and the beak/septum were 50% heavier in DK142 compared to Apex. Child *et al.* (2003) demonstrated how alterations in vascular tissue of the valve and DZ were evident in DK142 compared to Apex, with large increases in the size of the main vascular bundle of the valve (MVBV) and in secondary vasculature crossing the dehiscence zone. The MVBV is situated at the base of the valve, crossing the valve margin, at the point where the valve becomes detached from the replum and is proposed to be a key factor contributing to increased PSR in DK142 (Figure 1.5). Child *et al.* (2003) also demonstrated how the MVBV was orientated at a shallower angle in DK142 compared to Apex, and that longitudinally positioned secondary vascular bundles also encroached into the DZ of the resistant line, increasing the amount of vasculature that had to be broken to ensure valve detachment from the replum. This acted as a framework increasing the amount of energy

required to enable the silique to dehisce. Overall, DK142 pods were more robust than that of Apex, with a greater partitioning of dry mass towards the receptacle compared to the seed.
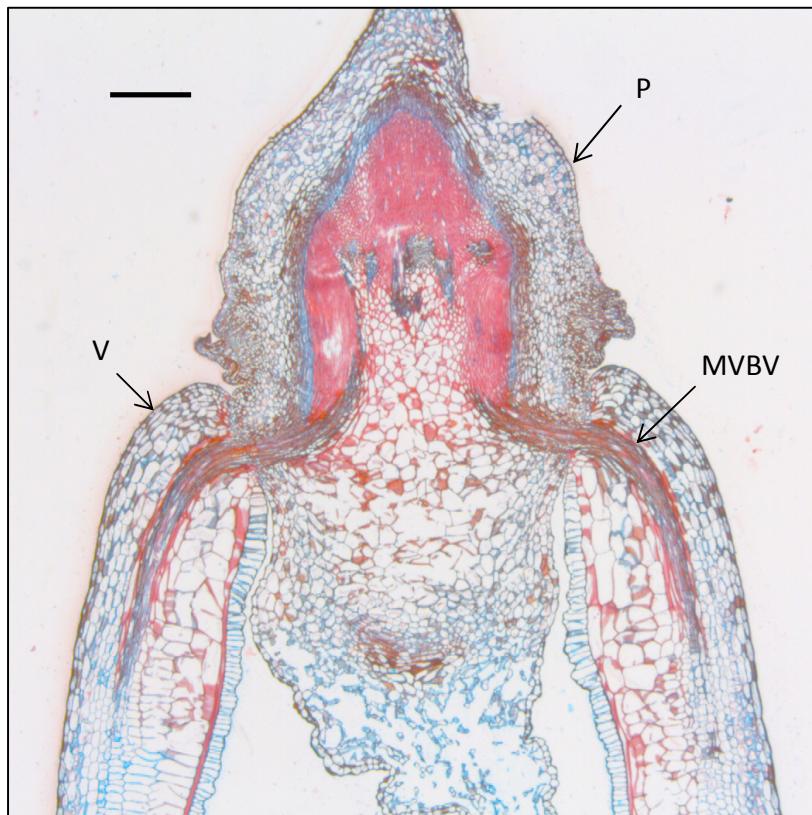
Figure 1.5: Longitudinal section of 35DAA Apex fruit base showing MVBVs. Scale bar: 500µm. MVBV: main vascular bundle of the valve, P: Pedicel and V: Valve

Differences at the DZ were also noted by Morgan *et al.* (1998), who demonstrated how pods from the shatter susceptible DK162 line shattered down multiple planes of fracture, whereas the resistant DK142 line fractured down a single plane due to the increased lignification of the valve margin tissues. The DZ in the susceptible line had a rough appearance and reduced MVBV, whereas shatter resistant DZ had a smooth appearance and increased MVBV (Figures 1.6 a and b).
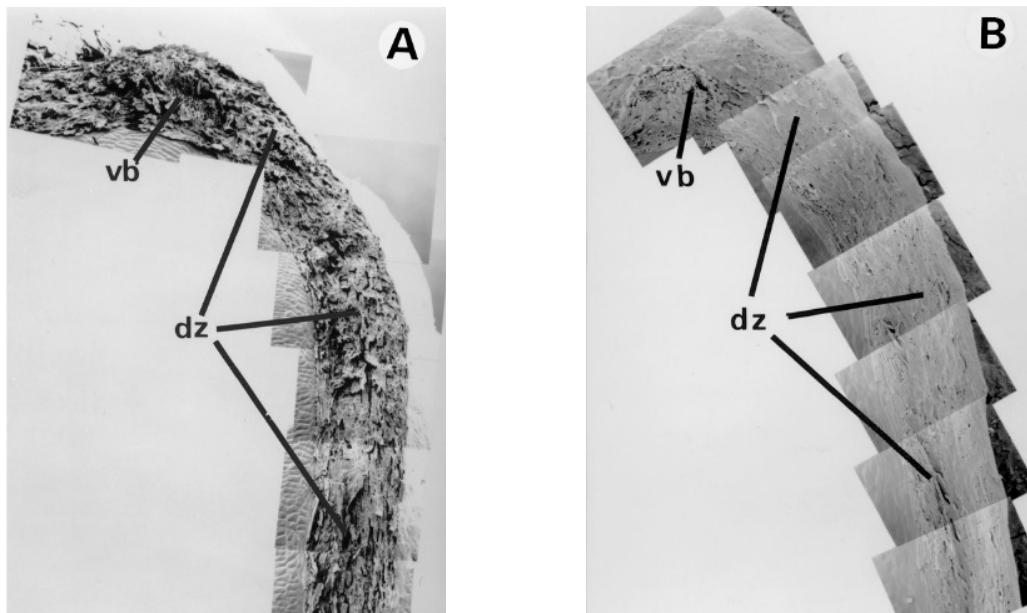
Figures 1.6 a and b : SEM images of the in fractured pods at the pedicel/valve juncture; A) from DK162 shatter-susceptible line and B) DK142 shatter resistant line. dz: Dehiscence Zone vb: Main Vascular Bundle of the Valve (Taken from Morgan *et al.,* 1998)

1.1.6 Roles for Hydrolytic Enzymes in Shatter Resistance

As indicated previously, roles in dehiscence have been suggested for a suite of hydrolytic enzymes in *B. napus* and in *Arabidopsis* (Meakins and Roberts, 1990b; Petersen *et al.,* 1996; Sander *et al.,* 2001; Ogawa *et al.,* 2009). It has been suggested that decreases in polygalacturonase activity maybe responsible for increased shatter resistance in DK142 and that this may also relate to problems experienced with fertility through failure of correct anther dehiscence, as the process involves very similar enzymes (Werner *et al.,* 2003a). However, no definite conclusion has yet been drawn and it could be of interest to assess if there is variation in enzyme activity between resistant, intermediate and susceptible POSH 1-3 lines, and their progenitors.

1.1.7 Physical Assessments of Pod Shatter Resistance

We have described how differences in the structure of siliques in *B. napus* lines contribute to increases in PSR in the POSH progenitors. A number of physical assessments have been developed to accurately determine levels of shatter resistance in *B. napus* pods and include:

Manual Impact Test (MIT) – The MIT is a basic assessment of pod strength made by hand in the field, to enable lines of significant interest to the researcher to be recorded for future analysis, also termed the cantilever bend test (Kadkol *et al.* 1984; Bruce & Hobson, 1995). It involves bending individual pods down whilst still attached to the raceme to see how much energy is required to initiate dehiscence at the base of the silique, principally at the MVBV. This is a somewhat arbitrary technique only allowing large differences in resistance to be indentified between lines and is subject to variation in relative water status and ripeness of the pods (personal observation).

Tensile separation test –This approach assesses the tensile force required to induce pod shatter along the dehiscent zone using a load test testing cell and was developed by Davis and Bruce (1997) (Figure 1.7). Morgan *et al.* (1998) utilised the assay to investigate PSR in the DK familial lines and observed it to be positively correlated with other shatter resistance test such as the Random Impact Test (Bruce *et al.,* 2002).
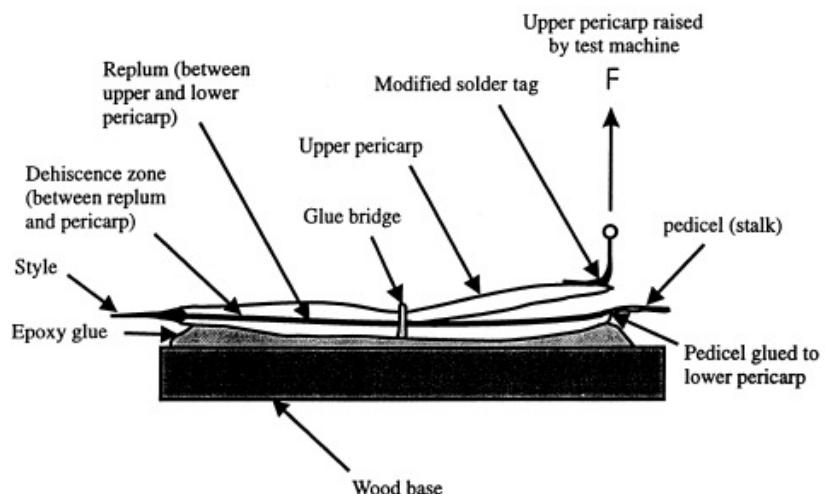
Figure 1.7: Diagram of tensile separation test (taken from Morgan *et al.* 1998)

Micro-fracture test (MFT)

A micro-fracture test (developed at Silsoe Research Institute) to establish the specific contribution of the main vascular bundle of the valve (MVBV) and non-vascular DZ tissue in medial regions of the fruit in the energy required to initiate separation of the valve from the replum (Child *et al.,* 2003). DK142 was reported to require 118% more force and 161% more energy to initiate fracture of the MVBV compared to Apex. These increases correlated with the thickness of MVBV in resistant DK142 line. For medial regions of the pod, although the DZ in DK142 was 48% wider, the peak force required to initiate fracture was increased by 50% indicating similar amounts of energy was required per unit area in both lines.

Random Impact Test (RIT) – The Random Impact Test was documented by Bruce *et al.* (2002). This test assesses pod-shatter resistance in a 'random' fashion. 20 pods are selected from samples equilibrated to 50% relative humidity and placed into a sealed, 20cm plastic container with six 12.5mm steel ball bearings in it (Figure 1.8). The vessel is then agitated for a set period of time, usually between 10-20 seconds, over a distance of 51mm at a rate of 4.98Hz. The container is opened between each agitation, and the number of intact, damaged and completely broken pods recorded. The times at which half of the pods remain intact are recorded and compared as a relative measure of resistance. This is termed the RIT_{50}.

The RIT provides the optimum approach through which to assess pod strength as large numbers of samples can be processed efficiently and reproducibly (Morgan *et al*., 1998, 2000). Using this approach Apex was reported to display a mean RIT_{50} of 15s whereas DK142 demonstrated a mean RIT_{50} of 29s, nearly two fold greater than the susceptible POSH 1-3 parent (Summers *et al.,* 2003). Assessments in F_1 offspring from crosses between Apex and DK142 demonstrated levels of shatter resistance similar to the susceptible Apex parent, whereas resistance in the F_2 was varied between levels demonstrated by the Apex and DK142, indicating that the PSR trait is recessive in nature.

Figure 1.8: RIT apparatus

1.1.8 Associated Issues of Conventional Breeding Strategies for Improving Pre-harvest Pod Shatter Using DK142 as a Source of Shatter Resistance

I have described how lines demonstrating PSR have been developed, and the techniques that can be used to assess variation in pod shatter in *B. napus*. I have also highlighted a number of physiological determinants contributing to increased PSR in these lines. The PSR character is reported to display a wide and continuous range of variation in pod shatter levels amongst DK142 lines, highlighting potential polygenic control (Child *et al.,* 2003).

The trait has also proven to be elusive and difficult to breed successfully into commercial material as it is recessive, selected for independently of other important agronomic characters, is environmentally sensitive, has a low correlation with scored traits, and is quantitatively controlled by a number of genes each contributing small effects (Morgan *et al.,* 2000; Werner *et al*. 2003a, c). These factors have made selection for the respective elements required to produce the shatter-resistant phenotype problematic using conventional breeding approaches such as pedigree analysis or single seed descent.

Currently the selection for shatter resistance can only be performed using physical markers at the end of the season when pods have fully senesced. This is limiting to the breeder and researcher alike. MAS utilising genetic markers linked to QTL or QTG (Quantitative Trait Loci,

19

Quantitative Trait Genes, respectively) of interest could expedite selection for shatter resistance as they could be screened for at a seedling stage greatly increasing the efficiency of a breeding programme. Identification of markers linked to PSR may also make it feasible to screen for similar loci in other related shatter resistant species, such as *B. carinata* or wild *Brassica* species. Although wide crosses are often associated with the introgression of undesirable alleles, MAS may act as a suitable approach to introgress beneficial traits into commercial breeding programmes.

It is therefore necessary to tackle the problem using a different strategy. It is proposed that a genetic approach utilising linkage mapping and a subsequent marker analysis would be the most successful method to identify the potential multiple factors contributing to increased shatter resistance in *B. napus.*

1.2 Genetic approaches to investigating pod shatter resistance in POSH 1-3

Genetic and molecular technologies, developed over the last thirty years, such as Polymerase Chain Reaction (PCR), DNA sequencing and high-density genetic linkage maps, have enabled an increased understanding of the structure and function of plant genomes (Mullis and Faloona, 1987; Sanger *et al.* 1977; Tanksley *et al.* 1992).The use of such techniques, encompassed with an ever-increasing array of powerful marker technologies, provides a platform through which to conduct investigations into identifying the key elements regulating fruit development and pre-harvest dehiscence in OSR.

DNA based markers have been used extensively for developing linkage maps and this information can be extrapolated to crop-improvement programmes for rapid transfer of beneficial QTL from wild or unadapted lines to elite cultivars (Tanksley and Nelson*,* 1996)*.* The use of such techniques could potentially aid efforts to modulate pod-shatter by identifying genes/QTL of interest using techniques such as marker assisted selection (MAS) (Collard *et al.,* 2005).

Linkage map production has three requirements: Two parental lines that are genetically diverse, from which a derived segregating population, such as an F_2, a doubled haploid (DH), or Recombinant Inbred Lines (RILs) can be developed; suitable genetic markers demonstrating polymorphism in the population; statistical software to calculate recombination frequencies between markers and convert them into map distances and marker order.

1.2.1 Mapping Populations

Genetic linkage map construction requires a suitable segregating population in which to identify polymorphism. A number of different types are available of which F_2, DH and RILs are most commonly utilised for mapping in *Arabidopsis* and *Brassica* species.

F_2 Populations

F_2 populations are the fastest, most basic type of segregating population that can be developed for genetic mapping. They require no tissue culture or inbreeding that can be required by other methods. However, due to the heterozygous nature of an F_2, the segregating genome affects replication of lines in trials and trial reproduction in subsequent years, unless clones are taken from the original lineage. F_2 populations have been utilised for genetic mapping and QTL analysis to identify loci linked to range of traits in *Brassica* including variation in flowering time in *B. oleracea* (Okazaki *et al.,* 2007), clubroot resistance in *B. rapa* (Suwabe *et al.,* 2003) and QTL relating to yield characters in *B. napus,* including plant height, silique length and silique density (Chen *et al.,* 2007).

Doubled Haploid (DH) Populations

The production of DH populations is a fast, efficient approach to generate homozygous lines and is employed by plant breeders and researchers alike. However, DH populations are only feasible in species amenable to tissue culture. In *Brassica* DH lines are often produced thorough microspore culture (Zaki and Dickinson, 1995). The process uses late unicellulate/early binucleate pollen grains, forcing them from gametophytic to embryonic development using media containing the anti-microtubule drug colchicine to induce

chromosome doubling by increasing levels of symmetrical division (Möllers *et al.,* 1994; Zaki and Dickinson, 1991). The use of DH lines ensures selfed seed is fixed/non-segregating, unlike an F_2, allowing identical lines to be grown in replicated trials, year on year. DH populations have been used in a wide array of investigations into *Brassica* QTL including traits such as fatty acid profile in *B. juncea,* and resistance to Phoma Stem Canker (*Leptosphaeria maculans*) and seed oil and erucic acid content in *B. napus* (Mahmood *et al.,* 2003; Delourme *et al.*, 2004; Qiu *et al.,* 2006).

Recombinant Inbred Lines (RILs)

Recombinant Inbred Populations or RILs are series of homozygous lines that can be multiplied and reproduced with minimal genetic change occurring, similar to DH lines. They are produced by inbreeding individual F_2 lines and require 6 to 8 rounds of selfing to ensure homogeneity (Collard *et al,* 2005). This could be a limiting factor in the development of RIL populations in *Brassica* due to long generation times and as is self-incompatibility reported in a number of *Brassica* species (Bateman *et al,* 1955)*.* RILs are however, suitable for development in autogamous species with a fast generation time tolerant, such as *Arabidopsis* (O'Neill *et al.*, 2008). RILs are also of benefit as they demonstrate a higher recombination frequency than DH lines (Jansen 2003). RIL populations have been utilised to identify QTL linked to traits in *B. napus* including seed mineral content and the agronomically-desirable character of yellow seed which is associated with a thinner testa and increased oil content (Ding *et al.,* 2010; Fu *et al.,* 2007).

1.2.2 Genetic Markers

Once a population segregating for the trait of interest has been developed, a suitable marker system to identify polymorphic loci must be employed. DNA marker technologies are required to be fast, robust, inexpensive and reproducible, enabling markers to be used across varieties improving the likelihood of production of consensus maps and comparative mapping studies. A number of different marker approaches have been developed for use in mapping genes in plants of which the main examples adopted in *Arabidopsis* and *Brassica* are described:

Randomly Amplified Polymorphic DNA (RAPDs)

Initially developed by Williams *et al.* (1990), this quick and simple marker technique can be used to generate multiple marker loci from single arbitrary primer pairs by identifying polymorphism at annealing sites and differences in product length between primers. This approach does not require any prior sequence information and is therefore is amenable to species which may not have previously been studied. RAPDs are dominant markers, amplifying in one parent and not the other when polymorphism is detected, so therefore cannot detect heterozygotes. They are reported to show poor reproducibility and transferability (Thormann *et al.,* 1994; Powell *et al.,* 1996). However they have applied successfully to investigate genetic diversity in a number of *Brassica* species and QTL linked to linolenic acid desaturation and linolenic/oleic acid content in *B. napus* (Lázaro *et al.,* 1998; Somers *et al.,* 1998; Hu *et al.,* 1999).

Restriction Fragment Length Polymorphisms (RFLPs)

RFLPs are a relatively old marker technology that has seen wide applications in both humans and plants. Botstein *et al.* (1980) utilised RFLPs to generate some of the first genetic linkage maps in humans. RFLPs are co-dominant markers making them useful for identifying heterozygotes. They are robust, reliable and transferable across species, enabling comparative mapping and QTL mapping (Tanksley *et al.,* 1989, Lander and Botstein, 1989). RFLPs are a powerful but highly laborious technique, requiring large amounts of DNA. This type of marker has been used to develop a number of genetic maps in *Brassica* and a

number of RFLP probes have been used to populate the original POSH 1-3 map (Teutonico and Osborn, 1994, Morgan *et al.,* unpublished). To date, one of the most densely populated *B. napus* maps was produced by Parkin *et al.,* (2005) and comprises of over 1000 RFLP probes. RFLP maps have been utilised to identify QTL in spring *B. napus* hybrids relating to seed yield, flowering time and bacterial leaf blight (Quijada *et al.,* 2006; Udall *et al.,* 2006).

Amplified Frequency Length Polymorphism (AFLPs)

AFLPs are a dominant marker which produces multiple loci with high levels of polymorphism (Vos *et al.,* 1995). This technique generates a large number of markers suitable for increasing marker density; however, they exhibit a complicated methodology and transfer to other populations is hampered by their complexity. AFLPs are similar to RFLPs as they detect genomic restriction fragments, although they use PCR, not southern hybridisation to identify differences in restriction products. Although AFLPs have been utilised to produce high density linkage maps in *B. juncea,* due to the dominant nature of the strategy, they are reported to be most suited towards diversity testing, and have been applied in *B. rapa* and also have been demonstrated to be amenable to automated fluorescent-labelling for *B. napus* cultivar fingerprinting, suitable for distinctness, uniformity and stability (DUS) tests (Warwick *et al.,* 2008; Sobotka *et al.,* 2004). As PCR and DNA sequencing technologies have expanded and become more cost effective, marker technologies have moved towards more reliable, efficient and transferable PCR based approaches.

SSRs: Simple Sequence Repeats

SSRs or microsatellites are short, tandemly-repeated nucleotide motifs of one to six bp, dispersed throughout the genome. Common representations of SSRs in *Brassica* are dinucleotide repeats such as $(AT)^n$, or trinucleotide repeats such as $(AGA)^n$ (Iniguez-Luy *et al.* 2008). SSRs are the product of slip-strand mispairing or from unequal crossing over during replication (Levison and Gutman, 1987). Unlike AFLPs, SSRs are co-dominant markers enabling heterozygotes to be identified (Powell *et al.,* 1996). Loci containing SSRs are often found to be very polymorphic due to the variation in the numbers of tandem repeats, making them excellent molecular markers. Microsatellite markers for mapping applications have been generated in a wide range of *Brassica* species including *B. rapa*, *B. oleracea* and *B.*

napus (Suwabe *et al.* 2002, 2003; Lowe *et al.* 2002, 2004; Piquemal *et al.* 2005). SSRs are now recognised as one of the most useful types of marker in marker assisted selection (MAS) (Gupta and Varshney, 2000).

Microsatellites are reported to be an important tool for applied *Brassica* research and have been developed for DUS testing when assessing *B. napus* varieties during national list trials, highlighting potential roles for assessing variation between varieties and even within a variety (Lowe et al. 2004; Tommassini *et al.* 2003). The major benefits of SSRs are that they are robust, reliable and transferable, enabling them to be used to anchor loci already mapped in other populations. Although SSRs require a large amount of time to develop suitable primers and initially required resolving using polyacrylamide gel electrophoresis (PAGE, figure 1.9), they are amenable to automated genotyping using capillary sequencers, dramatically increasing throughput as markers can be multiplexed using different fluorescent dyes (Collard *et al.* 2005; Schuelke, 2000).

Wide arrays of public SSR primer sets are available to screen *Brassica* species for polymorphism generated through AAFC Research (Saskatoon, Canada), BBSRC markers developed from *B. napus, B. nigra, B. oleracea, B. rapa,* (Lowe *et al.,* 2002, 2004), BRMS markers in *B. rapa* by Suwabe *et al.* (2002, 2003) and those developed by the Celera consortium (Piquemal *et al.,* 2005). Information on these resources can be obtained at www.cropstoredb.org. These resources could be utilised to screen for new polymorphic markers in the POSH 1-3 population and may expedite the discovery of potential candidate genes or agriculturally important QTL.
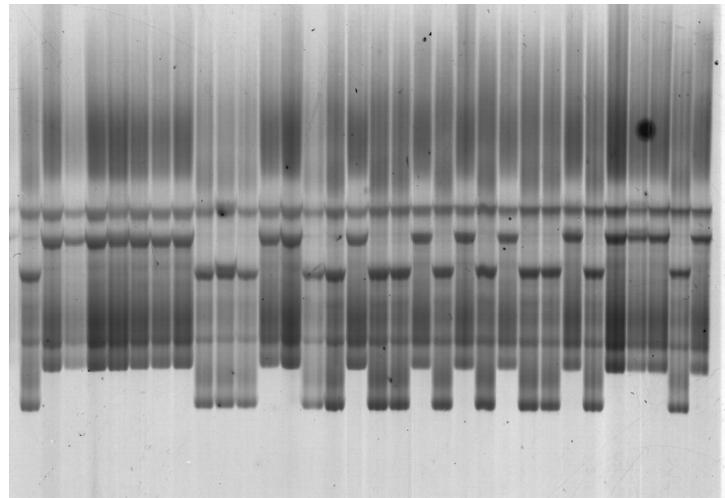
Figure 1.9: PAGE gel displaying segregating SSR bands in *B. napus*

Sequence Related Amplified Polymorphisms (SRAPs)

Another PCR based marker assay is SRAPs and these were designed specifically for us in *Brassica* (Li and Quiros, 2001). This strategy is a simple, reliable, reproducible and transferable method to identify both dominant and co-dominant markers suitable for genetic mapping, genomic and cDNA fingerprinting and map based cloning. The approach uses combinations of arbitrary primer pairs, with a forward primer targeting open reading frames (containing a CCGG motif) and a reverse primer targeting promoters and introns (containing an AATT motif) utilising the intrinsic differences in non-coding regions to generate polymorphic bands. This type of marker has been utilised to develop ultra-density linkage maps in *B. napus,* assess genetic diversity in different inbred *B. napus* varieties and also to assess colinearity between *Arabidopsis* and *B. oleracea* through direct transcriptome mapping (Sun *et al.,* 2007; Riaz *et al.,* 2001; Li *et al,* 2003).

SNPs: Single Nucleotide Polymorphisms

Single Nucleotide Polymorphisms, or SNPs, are single base differences in the DNA sequences of individuals of a species, present as bi-, tri- or tetra-allelic polymorphisms (Brookes, 1999). They can reside in both coding and non-coding regions of the genome (Lemieux, 2000). They contribute to the allelic variation between members of a species. SNPs are a very common

type of polymorphism, with reports of SNPs occurring, approximately every 300 – 1000bp in genomic DNA (Gupta *et al.* 2001). SNPs are associated with substitution mutations of bases either through a transition or a transversion. A transition occurs between purines A/G or pyrimidines C/T, whereas transversions are interchanges of purines and pyrimidines. Tranversions comprise; A or G to C/T and C or T to A/G (Jukes, 1987). In humans an average frequency of one SNP for every 1000bp is presented, whereas in plants, SNPs appear to be more abundant (Sachidanandam, 2001; Gupta *et al.,* 2001). For example, in US elite maize germplasm, rates of one SNP per 48bp in non-coding regions and one per 131bp in exons are reported (Bhattramakki *et al.,* 2002, 2001).

SNPs can be identified in a wide array of technologies including cleaved amplified polymorphic sequences (CAPS) (Konieczny *et al.,* 1993), oligonucleotide hybridisation using DNA chips and microarrays (Pease *et al.,* 1994; Southern *et al.,* 1996; Gupta *et al.,* 1999), denaturing high-performance liquid chromatography (dHPLC) (Giordano *et al.,* 1999), Taqman assays utilising fluorescent dyes to discriminate between alleles differing for SNPs (Livak *et al.,* 1995) and pyrosequencing (Ronaghi, 2001). Another approach is termed Diversity Arrays Technology (DArT) Jaccoud *et al.* 2001, Wenzl *et al.,* 2004). This is a microarray based technique detects polymorphism as the presence or absence of hybridisation of restriction fragments and has been successfully applied in *Arabidopsis* as a high-throughput method for genotyping SNPs (Wittenberg *et al.,* 2005).

A number of PCR based marker technologies have been developed to enable SNPs to be successfully genotyped such as allele specific amplification (ASA) which utilises allele specific primers to identify differences between lines (Ye, Humphries and Green, 1992, Bundock *et al.*, 2006) and single stand confirmation polymorphism (SSCP) (Hayashi*,* 1991; Bertin *et al.* 2005). SSCP markers are resolved on non-denaturing MDE (Mutation Detection Enhancement) gels using silver-staining to resolve the polymorphism. Structural conformation varies according to sequence and affects the rate at which the fragments are retarded in the gel. This type of marker does not require a size difference between PCR products but a difference in sequence and therefore conformation can be caused by SNPs,

insertion/deletion polymorphisms (InDels) or multiple base differences to enable the formation of secondary structures. InDels represent two classes of mutation: an insertion and a deletion. These types of mutation are sometimes associated with frameshifts, often resulting in alterations to transcribed mRNA sequences, leading to altered amino acid structure and function or even incomplete processing due to the generation of stop codons. SSCPs can also be automated using same approach as described for SSR markers increasing throughput dramatically (Scheulke, 2000). Both ASA and SSCP have been applied to genotyping and mapping in *Brassica* species; A series of ASA/InDel markers developed during the IMSORB (Integrated Markers System for Oilseed Rape Breeding) program (www.brassica.bbsrc.ac.uk/IMSORB) have been genotyped in the Tapidor/Ningyou7 DH (TNDH) *B. napus* population and are presented as a resource to screen for polymorphism in other varieties, whereas, SSCP has been used as a technique to successfully map genes in *B. oleracea* (Qiu *et al.,* 2006; Sato and Nishio, 2002; Inoue and Nishio, 2004).

SNPs present a robust, reliable and transferable source of DNA marker across species. The high frequency of SNPs can be discovered throughout the coding and non-coding regions of plant genomes makes them an excellent target for populating genetic linkage maps. Older, less efficient methods are making way for high-throughput, automated technologies enabling the fast, effective genotyping of whole populations. Next generation sequencing is becoming a powerful approach for SNP detection and genotyping for crop species, including *Brassica*. Trick *et al.,* (2009) have documented how Solexa transcriptome sequencing (Illumina) can be utilised for SNP discovery in *B. napus.* The technology has been used to generate 20 million expressed sequence tags (ESTs) in the varieties Tapidor and Ningyou7 and has identified approximately 30,000 SNPs between the two lines. Application of high-throughput approaches such as this increase the efficiency in producing dense genetic linkage maps suitable for accurate identification of loci associated with desirable traits such as increased PSR in *B. napus* and will likely impact greatly as the technology develops.

1.2.3 Genetic Linkage Maps

Once a population has been established, screened for polymorphism using suitable markers and subsequently genotyped, the position of the loci can be ascertained using computer software specifically designed for this procedure. The position of genetic markers in the genome is determined by the pair-wise recombination frequencies between loci, generated during chiasmata on cross-over in meiosis. A number of programmes are now available to calculate genetic maps including Mapmaker (Lander *et al.,* 1987), JoinMap (Stam, 1993, Van Ooijen and Voorrips, 2001), RECORD (Recombination Counting and Ordering) (Van Os *et al.,* 2005) and THREaD Mapper (Cheema, Ellis and Dicks, 2010). Mapping software first calculates recombination frequency then converts it into a map distance using a mapping function. This is due to recombination frequency and the frequency of crossing over not exhibiting a linear relationship (Kearsy and Pooni, 1996). A 1% recombination frequency between two loci equates to a distance of 1cM. The most widely used mapping functions are the Haldane function, assuming no interference between crossing-over and the Kosambi function, which assumes that recombination influences the occurrence of adjacent recombination events (Kearsey and Pooni, 1996; Hartl and Jones, 2001). Mapping techniques are well established in *Brassica* and a number of linkage maps have been produced for *B. napus* populations (Sharpe *et al.,* 1995; Lowe *et al.,* 2004; Parkin *et al.,* 1995, 2005, Qiu *et al.,* 2006).

The resolution of a linkage map is directly related to the number of individuals in a population as a greater number of lines provide more information about the recombination present in the population (Young *et al.,* 1994). Maps can often contain an array of different types of markers to maximise both coverage and density. Identifying loci already mapped in other populations can aid the process of linkage group identification in newly mapped populations. Such markers are termed anchors. One of the most comprehensive *B. napus* maps has been produced for the TNDH population and loci mapped in this could represent a good source of anchored markers to screen for in the POSH 1-3 population (Qiu *et al.,* 2006). The current POSH map contains 120 genotyped markers with a cumulative distance of approximately 800cM. When it is considered established maps demonstrate total distances

of 1700-1800cM (Parkin *et al.,* 2005; Qiu *et al.,* 2006), it is evident that less than half the POSH 1-3 genome has been successfully identified, and therefore the linkage map requires development Difficulties in obtaining an equal distribution of polymorphic markers throughout a map relates to the clustering of some loci in certain regions and absence in others (Paterson *et al.,* 1996).

Once a suitable genetic linkage map has been produced for a population and phenotyping conducted for a trait of interest performed, it should then be possible to perform analyses to identify regions of the genome contributing to variation in that trait using marker analysis approaches.

1.2.4 QTL Analysis

Traits displaying discrete, discontinuous, variation are often inherited in a Mendelian fashion. However, many agronomically important traits affecting crop yield demonstrate continuous quantitative variation (Kearsey and Pooni, 1996). Such traits are often complex, controlled by many genes of small effect and subject to influence from environmental factors and interactions between genes and the environment, termed G x E effects. Regions containing such genes are termed Quantitative Trait Loci (QTL) (Gelderman, 1975). QTL analysis can also be utilised to identify the position of major, Mendelian genes. QTL analysis attempts to detect an association between phenotype and the genotype molecular markers from a population (Collard *et al* 2005). Markers are used to partition the mapping population under analysis into genotypic groups. Groups relate to the presence or absence of a locus and are assessed for significant differences for the relevant trait (Tanksley, 1993, Young, 1996). As QTL can occur throughout the genome a large number of markers are required and a target of 10 to 50 markers per chromosome is desired to perform accurate QTL mapping (Kearsey and Pooni, 1996; Kearsey, 1998). A number of approaches to identify QTL are apparent, including single marker analysis, interval mapping and composite interval mapping (CIM), also termed multiple QTL mapping (MQM).

Single marker analysis is the most basic approach and does not require a complete genetic linkage map. This method uses basic statistical analyses such as t-tests, analysis of variance (ANOVA) or linear regression to associate particular genotypes with a phenotype. Linear regression is the most commonly used approach and acts to regress the mean of the marker genotype against the trait mean to identify significant relationships. This approach is beneficial as the R^2 (coefficient of determination) from the associated marker explains the phenotypic variation exhibited by the QTL. The disadvantage in this approach is that the further a QTL is from a marker the less likely it will be detected, as recombination can occur between QTL and marker, leading to the effect of the QTL being underestimated (Tanksley, 1993). A number of single marker analysis approaches are evident including Kruskal-Wallis and single marker regression. The Kruskal-Wallis is a ranked order, non-parametric, one-way ANOVA and is utilised in MapQTL 5 software (Van Ooijen, 2004). As a ranked order analysis it can handle non-normally distributed data. Single marker regression is a form of linear regression utilising numeric trait data for the analysis and is the basis for programmes developed by Morgan *et al.* (unpublished) which are now being used to investigate QTL in *B. napus*.

Interval Mapping utilises genetic linkage maps and analyses the interval between adjacent pairs of linked markers. This compensates for recombination between the paired markers and the QTL (Lander and Botstein, 1989). The approach assesses the trait data from each pair of adjacent markers and infers the likelihood of a QTL being positioned between them (Kearsey, 1998). A logarithmic of odds (LOD) value is generated for the markers on a chromosome and the QTL position is estimated in relation to the linkage map where the highest LOD score occurs (Collard *et al.,* 2005). The peak of the QTL must exceed a LOD threshold score of 3 to be considered statistically significant and is commonly determined using permutation tests (Churchill and Doerge, 1994). This acts to re-order the measured trait values whilst retaining the marker genotypic values and then QTL analysis is conducted between 500-1000 times to assess the level of false positive marker-trait associations (Doerge and Churchill, 1996; Hackett, 2002). Composite interval mapping (CIM), or multiple QTL mapping (MQM) mapping combines interval mapping and linear regression, including

additional markers to adjacent marker pairs, to improve accuracy and reduce issues associated with multiple QTL on a single linkage group (Jansen, 1993, Zeng, 1994).

QTL mapping has been performed in *Brassica* to identify a wide range of loci linked to agronomically important traits. Studies have been performed in *B. rapa* to identify markers linked to QTL related to clubroot resistance, one of the most serious pathogens affecting the species (Moriguchi *et al.,* 1999; Suwabe *et al.,* 2003). QTL for flowering time relating to *Bol.FLC2* gene have also been identified in *B. oleracea* which could aid insight into manipulating floral transition to control harvest period in important vegetable species (Okazaki *et al.,* 2007). Investigations have also identified QTL linked to a wide range of traits in *B. napus* including erucic and linolenic acid content, seed oil and fatty acid content, seed yield, flowering time and sclerotinia resistance (Thormann *et al.,* 1996; Burns *et al.,* 2003; Qui *et al.,* 2006; Udall *et al.,* 2006*;* Shi *et al.,* 2009; Long *et al.,* 2007; Yin *et al.,* 2010).

Many factors can influence the outcome of QTL analyses including the number of QTL associated with a trait, trait heritability, population size and environmental effects. The more QTL there are in a population, the smaller their individual effect and the harder they are to detect. Also, if trait heritability is below 50%, a QTL will represent a fraction of this percentage (Kearsey, 1998). Also, low QTL heritability can cause estimates of QTL position to have large confidence intervals making accurate identification of the definitive position of QTL problematic (Hyne et al. 1995). Population size can also affect accuracy in QTL studies, as a more accurate map can be produced with a greater number of recombinants, enabling QTL of smaller effect to be detected (Haley and Andersson, 1997). Environmental and G x E effects can infer large differences in the QTL identified between years (Snape *et al.,* 2007). Therefore repeat studies are required to verify if significant QTL are prevalent across years in different environments (Young *et al.,* 1999, Kearsey and Pooni, 1996). Experimental error such as inaccurate phenotype data and genotyping errors or missing data can also have large effects on map order and marker distances (Hackett, 2002).

QTL analysis poses as a powerful approach to identify important regions of the genome with potential for implementation as targets for Marker Assisted Selection (MAS) in crop improvement (Kearsey, 1998). The identification of key traits in *Brassica* relating to yield and quality have been highlighted using QTL analysis and it is proposed similar techniques could be applied to investigate sources of pod shatter resistance in the POSH 1-3 population in an aim to identify loci suitable for MAS to introgress the trait in commercial *B. napus* varieties.

1.3 Comparative Genetics in the Brassicacea : Resources for Comparative Mapping Approaches

1.3.1 Colinearity and Gene Duplication in Members of the *Brassicacea*

Comparative genetics is the study of genome structure and function across related species. It allows us to exploit the information gathered in one species and extrapolate it into other, often more complex, less understood organisms. An example of this is the use of our knowledge in the model Brassicacea*, Arabidopsis thaliana* and how this can be used to study crop *Brassica.* Studies suggest that *Arabidopsis* and *Brassica* originated through a common ancestor, diverging approximately 10-20 million years ago (Lysak *et al.,* 2005; Yang *et al.,* 1999; Koch *et al.,* 2000). Conserved segments of the *Arabidopsis* genome have been demonstrated to be represented in *Brassica* species and chromosome 4 and 5 from *Arabidopsis* have been shown to be colinear with regions of *B. oleracea* genome (Lagercrantz *et al.,* 1996, 1998; O'Neill and Bancroft, 2000; Parkin *et al.,* 2002). Schranz *et al.* (2007) have highlighted how 24 genomic blocks are represented in both the *Arabidopsis* and *Brassica* genomes and have been maintained from an ancestral karyotype prior to divergence. It is this colinearity and conservation of regions of the genome between the species which enables a comparative genetics approach to be adopted. Colinearity is not limited to the *Brassicacea,* and the use of comparative genetics has been reported for in members of the Fabaceae, Poaceae and Solanaceae (Gale and Devos, 1998 a, b).

As well as being highly conserved, the *Brassica* genome is extensively duplicated, with three copies of each *Arabidopsis* region in the diploid *Brassica* and six copies in the amphidiploids

due to the presence of two constituent genomes (Lagercrantz and Lydiate, 1996; Parkin *et al.,* 2003). This indicates a triplication event has occurred after the diploid *Brassica* diverged from *Arabidopsis* (Lysak *et al.,* 2005)*.* Although allopolyploid, *B. napus* behaves as a diploid and its respective A and C genomes are demonstrated to be highly syntenous (Udall *et al.,* 2005). The respective A genome, comprised of chromosomes N1-N10 is representative of the 10 *B. rapa* chromosomes, whereas the C genome comprised of chromosomes N11-N19 represents the nine *B. oleracea* chromosomes (Parkin *et al.,* 1995; Udall *et al.,* 2005). This genetic synteny allows us to exploit our knowledge from the diploid *Brassica* species and extrapolate it to the amphidiploid. Although high levels of colinearity are evident between *Brassica* species, diploid *Brassica* genomes are reported to demonstrate structural rearrangements, whereas *B. napus* retains the structure of its individual *B. rapa* and *B. oleracea* progenitor genomes (Schmidt, Acarkan and Boivin, 2001). However, homeologous recombination between *Brassica* chromosomes has been reported and homeologous reciprocal (HRTs) and non – reciprocal translocation events (HNRTs) are evident in *B. napus* demonstrating rearrangements affecting synteny are still prevalent (Sharpe *et al.,* 1995; Parkin *et al.* 2003; Udall *et al.,* 2005).

Due to their colinearity, we can utilise both *Arabidopsis* and *Brassica* species as comparative genetic resources to investigate *B. napus. Arabidopsis* is a powerful tool to study gene function and we have access to a complete genome sequence and also a huge array of genetic and molecular information concerning the regulation a multitude of biological processes/fruit development (Kaul *et al.*, 2000). A wide range of genetic resources have also been established in diploid *Brassica* species including sequence databases (brassicadb.org, brassica.bbsrc.ac.uk), genetic markers and linkage maps, and the delivery of the complete *B. rapa* sequence through the international sequencing consortium is anticipated shortly. Next-generation sequencing technology is currently being utilised to produce a high density linkage map for the TNDH which will provide an important resource for studying *B. napus* (Trick *et al.,* unpublished).

We therefore have at our disposal a number of resources through which to investigate the genetic basis of pre-harvest pod shatter in oilseed rape. As indicated previously, fruit development in *Arabidopsis* and *Brassica* appears to be very similar. We can therefore exploit the knowledge gained in these species to ascertain if candidate genes with established roles in *Arabidopsis* are regulating fruit development in *B. napus*, and if it is possible to manipulate them to increase pod shatter resistance.

1.3.2 Candidate Genes in *Arabidopsis*: The Regulation of Fruit Development in *Arabidopsis thaliana*

Candidate gene strategies exploit the knowledge of previously sequenced genes of known function contributing to major loci (Pflieger *et al.,* 2001). The striking similarity between *Arabidopsis* and *Brassica* fruits suggests that the underlying mechanism of their development is conserved and potentially controlled by orthologues genes. This hypothesis is now supported by experimental data, with studies demonstrating that ectopic expression of the *FUL* gene from *Arabidopsis* controlled by a CaMV35S promoter in *Brassica juncea* results in plants with a similar phenotype to an *Arabidopsis 35S::FUL*, over-expression line with fruit that lack both the lignified valve margin layer and the separation layer, through inactivation of *SHATTERPROOF 1/2* genes (Østergaard *et al.*, 2006, Ferrándiz *et al.*, 2000).

This suggests that the genetic pathway regulating valve margin development in both species is conserved. A similar occurrence is documented for the *MADSB* gene*,* a *FUL* homolog from mustard (*Sinapis alba*). When expressed ectopically with a *35S* promoter, similar effects in silique development, producing rigid, lignified, fruit preventing precocious seed dispersal (Chandler *et al.* 2005). Similar regulatory roles for such transcription factors and the fact they can be manipulated makes them a potential target to modulating pod shatter resistance. The development of the specialized tissues of the *Arabidopsis* dehiscence zone are believed to be regulated by a suite of transcription factors, such as those highlighted in flower and silique formation in *Arabidopsis*. These key regulators are thought to be similar in

Brassica and therefore genes from the model could act as candidates to search for homologues in a crop species.

Investigations into fruit development in *Arabidopsis* have generated a wealth of both physiological and molecular data, highlighting roles in silique development and tissue patterning for a host of transcription factors (Ferrandiz *et al*., 2000; Lilijegren *et al*., 2000, 2004; Rajani and Sundaresan, 2001; Roeder *et al*., 2003). A number of genes, encoding a range of transcription factors involved in *Arabidopsis* fruit development, have been deduced using EMS (ethyl methane sulphonate), over-expression and knockout mutation to induce defects in normal development. Characterisation of these genes has enabled the successful identification of a number of essential regulatory elements of Arabidopsis fruit development (Østergaard and Yanofsky, 2004). Studies of this nature have generated a plethora of information on how key regulators interact to pattern and differentiate the distinct cell types that comprise mature siliques which are now aiding understanding of similar processes in *Brassica* species.   Genes documented in regulating fruit development in Arabidopsis include:

REPLUMLESS (RPL) - *RPL* encodes a BELL1-subfamily, homeodomain protein regulating replum development. This gene is reported to negatively regulate *SHP1/2,* by repressing ectopic expression in the replum and is also required for development, preventing replum cells adopting a valve margin cell-fate. Together, negative regulation by *RPL* and *FUL* defines narrow stripes of *SHP 1/2* expression, restricting valve margin development to the valve/replum boundary (Roeder *et al. 2003)*.

FRUITFULL (FUL) - FUL encodes a MADS box transcription factor reported to prevent ectopic lignification of valve cells. This is achieved by promoting valve margin differentiation by negative regulation of *SHATTERPROOF 1/ 2* expression in the valves (Férrandiz et al., 2000).

SHATTERPROOF 1/2 (SHP1/2)– The functionally redundant *SHP1/2* genes encode MADS box transcription factors which are both required for fruit dehiscence (Lilijegren et al. 2000). Both are associated with lignification at the valve margin and give rise to the replum and valve margin cells. In wild type *Arabidopsis* and either the *shp1* and *shp2* single mutants, the valve margin and the dehiscent zone are clearly visible, whereas in the *shp1/shp2* double mutant, no valve margin is present and hence, pods are indehiscent (Figure 1.13a and b). The gene pair is thought to positively regulate *INDEHISCENT* and *ALCATRAZ* genes also associated with key roles in fruit development, specifically in tissues involved in silique dehiscence.
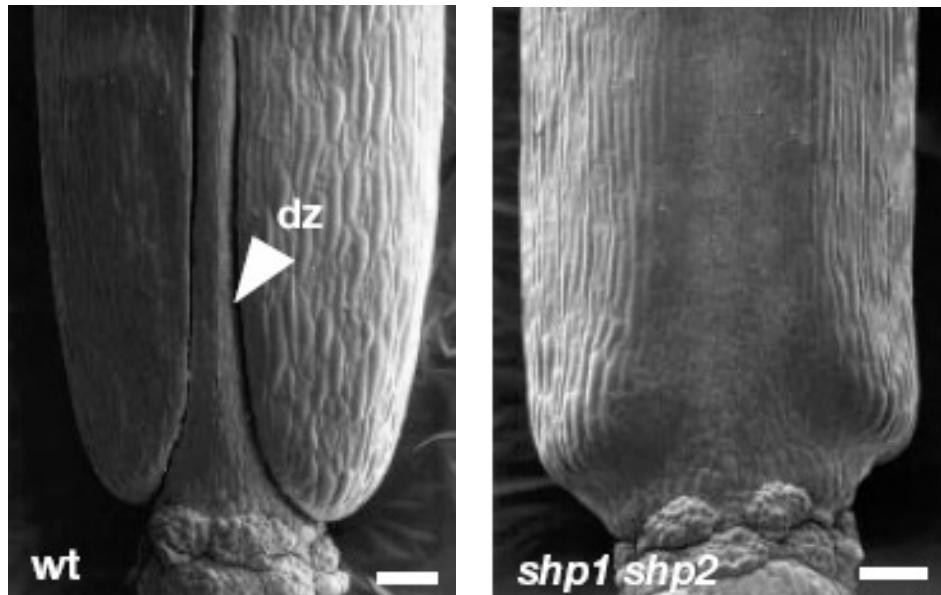
Figure 1.10 a & b: Scanning Electron Micrograph (SEM) images of siliques
Wildtype (WT) and *shp1/2 Arabidopsis* silques. dz: Dehiscence zone
(Taken from Lilijegren *et al.* 2000)

INDEHISCENT (IND) – *IND* encodes a basic helix – loop – helix (bHLH) transcription factor reported to act downstream of *SHP 1/2*, functioning to control valve margin formation. *IND* is responsible for regulating development of both the separation layer and lignified layer and also lignification of enB layer. Mutant lines deficient for IND exhibit fruit that will not shatter

(Liljegren *et al.* 2000, 2004). *IND* has been demonstrated to be a key regulatory element in valve margin development, coordinating auxin efflux, to generate minima required for the correct patterning of the DZ (Sorefan *et al.,* 2009). *IND* has also been demonstrated to interact with GA3 oxidase 1 to promote gibberellic acid production at the valve margin required for development of the lignified and separation layer (Arnaud *et al.,* 2010). I have previously described how down-regulation of the orthologous *BolC.IND.a,* using an RNAi strategy resulted in indehiscent siliques in *B. oleracea* (Wood, unpublished). This highlights how perturbing *IND* function can result in a similar phenotype in both *Arabidopsis* and *Brassica.*

ALCATRAZ (ALC) - *ALC* is a bHLH transcription factor that promotes development of the separation layer, but not the lignified layer. *ALC* also has roles linked to lignification of the endocarp layer B. An *ALC*:GUS reporter-gene construct highlighted expression in a broad range of silique tissues, with expression becoming restricted to the valve margins later on in development. Expression is also reported in the seed. The gene was identified during a genetic screen, in a gene trap transposon line bearing indehiscent fruit (Rajani and Sundaresan, 2001).

ARABIDOPSIS DEHISCENCE ZONE POLYGALACTURONASE 1/2 (*ADPG1/2*) – *ADPG1/2* encode dehiscent zone-specific polygalacturonases associated with separation layer degradation and are essential for valve detachment during dehiscence (Ogawa *et al.,* 2009). Although they do not act as development factors they play an important role in seed dissemination. *ADPG1* was isolated and identified according to its homology with the *Brassica* RDPG1 protein (Sander *et al.,* 2001; Petersen *et al.,* 1996).

A prospective model, describing the regulatory role for each respective gene highlighted in the development and patterning of the DZ is presented in figure 1.11. Upstream regulators of fruit development, termed *JAGGED (JAG)*, *FILAMENTOUS (FIL)* and *YABBY3 (YAB3)* are included in this model and have been highlighted in activating *FUL*, *SHP* and *IND* expression in undeveloped valve and valve margin in unfertilized gynoecia (Dinneny & Yanofsky, (2005).
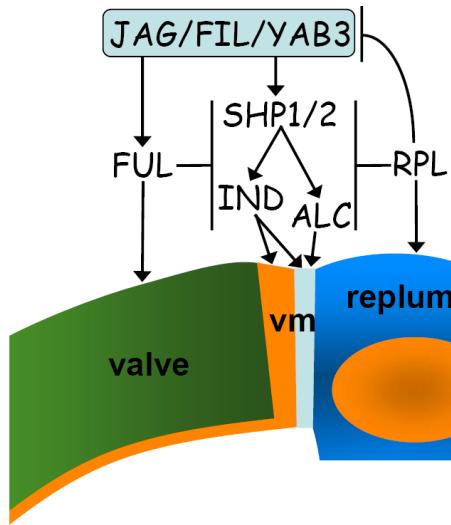
Figure 1.11: Diagram depicting a model of the genes involved in fruit development in *Arabidopsis* (Adapted from Østergaard *et al.,* 2007)

As certain elements in pathways regulating fruit development in *Arabidopsis* and *Brassica* have been demonstrated to be conserved, genes such as *ADPG1/2, ALC, FUL, IND* and *SHP1/2* could hold the potential to act as candidate genes to study fruit development and pod dehiscence in *B. napus*. Gene orthologues could therefore be targeted to develop linked markers to aid identification and characterisation of genetic elements involved in regulating silique development and dehiscence in *Brassica* in a breeding programme. Factors regulating vascularisation in *Arabidopsis* siliques still remain to be elucidated and could provide important candidates for investigating vascular architecture in *B. napus.*

Much is known about the regulation of fruit development in *Arabidopsis* and genes involved in such signalling networks may have also conserved roles in *B. napus* silique development. However, little research has been conducted into shatter resistance in *Arabidopsis* and it could be of interest to investigate variation for the trait in natural accessions and if this could provide new insight into pod shatter in oilseed rape.

1.3.3 Natural Variation in Seed-Shattering in *Arabidopsis*

Arabidopsis ecotypes are observed to demonstrate a diverse range of phenotypes for a wide range of traits (Koorneef *et al.* 2004). It is assumed that some of these differences have arisen due to the range of environmental effects at different geographical locations, favouring selection for different traits that may be beneficial to the plant (Pigliucci, 1998). This selection will have enabled adaptation to a particular habitat or environment and resulted in a wide range of diversity. Natural variation is an important basic resource for plant biology and is, currently, somewhat under-exploited. Approaches have focussed on investigating the genetic basis of multi-genic traits such as flowering time and vernalization response/requirement, using data generated from natural variation in populations (Alonso-Blanco & Koornneef, 2000; Koornneef *et al.* 2004). Natural variation in *Arabidopsis* has been demonstrated in a number of traits including glucosinolate accumulation, phytate and phosphate content, sulphate content and also adaptive traits such as flowering time, drought tolerance and vernalization response (Kleibenstein *et al.,* 2001; Bentsink *et al.,* 2003; Loudet *et al,* 2007; Clarke *et al.,* 1995; McKay *et al.,* 2008; Shindo *et al.* 2005)

Although little information exists relating to natural levels of variation in shatter resistance in *Arabidopsis* as a species, We have observed different levels of shattering apparent between Columbia (Col-0) and Landsberg erecta (Ler-0) ecotypes, with siliques dehiscing prior to complete senescence in Ler-0 (Personal Observation). It would be very interesting to investigate the cause of potential differences and also any links between PSR and geographical origin. If QTL could be isolated in ecotypes with improved PSR it would be of great benefit to compare these loci to those isolated in *B. napus*, to assess if similar physiological factors and QTL are regulating shatter resistance in both species. Identification of loci contributing to PSR in *Arabidopsis* may also provide extra candidate genes to search for new targets in *B. napus* to tackle pre-harvest pod shatter.

1.4 Conclusion

Pre-harvest Pod Shatter is a serious economic and environmental issue leading to lost revenues and contamination of subsequent crop rotations. *Brassica napus* is a relatively new

crop to contemporary agriculture and retains many unadapted and weed-like traits (Morgan *et al.,* 1998, 2003). A number of investigations have been conducted into measuring variation in pod shatter resistance in oilseed rape and also in the physiology of pods exhibiting shatter resistance (Davies & Bruce, 1997; Morgan *et al.* 1998, 2000; Child *et al.,* 2003; Summers *et al.,* 2003). Studies have identified that alteration in pod length and weight, and differences in vascular architecture contribute significantly to increases in pod shatter resistance (PSR). However due to a complex, recessive and polygenic nature, successful introgression of the trait into breeding lines has remained elusive (Werner *et al.,* 2003 a, b).

We have discussed how a number of techniques have been applied in *Brassica* species to develop mapping populations, how to apply a range of genetic marker technologies to identify polymorphism, the production of genetic linkage and how QTL associated with a wide range of important traits have been identified. It is proposed that a genetic approach using the techniques described to identify QTL contributing to the PSR trait may provide greater insight into the process of pod shatter and present a potential method through which to manipulate this undesirable agronomic issue. The basis of this approach would include thorough phenotyping of the POSH 1-3 population for PSR, the production of a genetic linkage map through the screening and genotyping for polymorphic markers and a subsequent QTL analysis to identify contributory loci. Knowledge of key regulatory loci from *Arabidopsis* with established roles in fruit development could be used as a basis for a candidate gene approach to develop genetic markers with which to investigate if similar genes are contributing to fruit growth and pod shattering in *B. napus*.

A physiological analysis could then be conducted to ascertain if similar factors contributing to differences in shatter resistance between the Apex and DK142 parent lines are also evident in the population lines. Variation in shatter resistance in accessions of *Arabidopsis* could also be investigated to identify if differences are apparent between ecotypes and to address any physiological determinants contributing to potential differences in an attempt to better understand the process of pod shatter and to elucidate new potential candidate

genes that may be applicable to studying the process in *B. napus.* Identification of suitable markers linked to QTL contributing to increased pod shatter in oilseed rape could then have potential for application to breeding programmes using methods such as marker assisted selection (MAS).

1.5 Aim of Investigation

The main focus of this investigation is to develop the POSH 1-3 genetic linkage map to elucidate QTL contributing to pre-harvest pod shattering in *B. napus* and approaches through which to modulate this. This will be addressed using a dual approach to identify the physiological determinants of shatter resistance and the molecular basis of trait regulation. A candidate gene strategy will be utilised, selecting factors known to regulate fruit development in the model plant species *Arabidopsis thaliana,* to develop markers in *Brassica napus* to ascertain if similar genes are contributing to increases in shattering. Identification of markers linked to QTL associated with increases in shatter resistance could provide targets through which to manipulate the trait and introduce alleles suitable for crop improvement into commercial *B. napus* lines via marker assisted selection (MAS). In an effort to bridge the ground between model and crop species, a novel assay has also been developed to investigate differences in pod shatter resistance in *Arabidopsis*. *Arabidopsis* ecotypes exhibit a wide range of phenotypic variation and this may relate to their natural geographical distributions. This could provide new insight into the process of dehiscence and a greater number of candidate genes for improving pod shatter in *B. napus.*

Chapter 2: Physical Assessment of Pod Shatter Resistance in the POSH 1-3 population

2.1 Introduction

Brassica napus retains a number of undesirable, weedy characters compared to other arable crops. Susceptibility to pod shattering, exacerbated by indeterminacy, is a widespread agronomic issue in cultivated varieties of Oilseed Rape (OSR). This relates to the short period OSR has been bred for commercial cultivation, selective breeding and the relatively narrow range of germplasm from which modern varieties have been adapted due to the requirement of low levels of glucosinolates and erucic acid in edible oils resulting in close similarities among cultivars (Morgan *et al.,* 1998, Smooker *et al.,* 2010). Efforts have been made to improve pre-harvest losses through swathing and contemporary approaches such as herbicide-mediated desiccation of the crop, ensuring a greater synchronicity in pod ripening and hence shattering (Kadkol *et al.,* 1984, Morgan *et al.,* 1998). However, this treatment is not completely effective and there are still the associated costs of spraying and potential negative environmental impacts.

Recent attempts to introduce shatter-resistance into varieties have proved largely unsuccessful due to an apparent lack of variation for the trait in contemporary commercial germplasm (Morgan *et al.,* 1998). Although Pod Shatter Resistance (PSR) has been noted in some *B. napus* lines, the polygenic and apparent recessive nature of the trait, identification of specific genetic candidates and their subsequent introgression into elite material have so far proved largely unsuccessful (Morgan *et al.* 2000, 2003, Werner *et al.,* 2003a). In an effort to address this issue, a mapping population observed to segregate for Pod Shatter Resistance, termed POSH 1-3, has been produced in conjunction with scientists from the John Innes Centre (Norwich, U.K.) and Plant Breeders from KWS (formerly CPB-Twyfords, Hertfordshire, U.K.) to help aid the identification of physiological and genetic factors contributing towards such important agronomic traits.

In this chapter we will describe the cultivation and assessment of pod shattering in lines from the doubled haploid mapping population (DH) POSH 1-3 population cultivated in a series of field trials. A shaking assay, termed the Random Impact Test (RIT) (Bruce *et al.* 2002; Summer *et al.* 2003), was used to assess variation in the duration it takes for equivalent pod samples from the POSH lines to degrade under agitation. Progress curves were then fitted to pod-degradation data to enable the accurate estimation of the time point at which half the pods from a sample remain intact or broken. Subsequent statistical analyses of field data are described and the findings discussed.

2.2 Materials and Methods

2.2.1 Plant cultivation

Lines from the POSH 1-3 DH mapping population were cultivated in two separate years at the John Innes Centre, Norwich, UK to produce material for assessing PSR. A 'complete' field trial consisting of 120 lines, grown in a triplicated randomised block design including guard rows was conducted in 2006 (Figure 2.1). 120 lines were selected for the 2006 trial, which consisted of 105 population lines and 15 lines of parental origin (including reciprocal crosses, selfs and progenitor and ancestral lines). Subsequently a subset of 13 select POSH 1-3 with a range of shatter resistance were selected and grown in a randomised block design, in 2009 (Figure 2.2).

Seedlings were germinated in soil in a glasshouse and grown to the six leaf stage prior to a six week vernalization period at 5°C. After vernalization, plants were moved to cold frames to acclimate for a period of five to seven days, prior to transplanting into the field. Field plots consisted of triplicated randomized blocks, arranged in staggered doubled rows, 1.5 m apart and 0.5m between plants within rows. Guard rows (var. Apex) were included at either side and the top and bottom of the plot to reduce potential edge effects. Any plants that died shortly after transplanting or before elongation of the primary raceme were replaced with guard plants.

GRD	GRD	GRD	GRD	GRD	GRD	GRD	GRD	GRD	GRD	GRD	GRD	GRD	GRD	GRD	GRD	GRD
GRD	155	280	149	142 x 142	160	155	24/31	205	152	129 self	238	145	274	Apex	177	GRD
GRD	198	GRD	175	238	206	226	185	234	272	191	208	195	205	192	182	GRD
GRD	129-1	147	185	272	24/27	238	201	193	142-2	190	DK3016	166	207	170	259	GRD
GRD	224	233	259	291	223	173	GRD	DK3016	223	245	180	198	143	191	228	GRD
GRD	187	24/31	191	24/29	151	198	228	188	147	GRD	185	235	278	217	148	GRD
GRD	195	174	171	24/32	226	144	281	218	259	129-1	210	24/33	249	163	187	GRD
GRD	243	202	215	274	182	DK142-1	263	272	213	145	224	234	216	272	GRD	GRD
GRD	218	216	197	182	201	247	166	182	24/27	249	193	291	202	245	276	GRD
GRD	153	158	227	170	217	148	113	149	24/32	24/29	129 self	DK142-1	150	24/26	GRD	GRD
GRD	275	263	245	173	177	192	150	233	197	206	194	24/30	152	GRD	GRD	GRD
GRD	196	GRD	GRD	210	166	216	180	168	202	24/30	222	206	263	215	GRD	GRD
GRD	24/30	DK3016	150	193	211	195	183	187	207	151	155D	173	247	218	GRD	GRD
GRD	163	GRD	234	190	246	291	280	175	170	160	226	24/27	149	163	GRD	GRD
GRD	207	148	145	208	129 self	211	243	275	163	227	144	188	171	244	GRD	GRD
GRD	143	194	144	244	Apex	208	160	217	196	147	223	201	174	262	GRD	GRD
GRD	207	192	183	213	169	171	235	246	GRD	190	GRD	GRD	175	153	GRD	GRD
GRD	24/26	188	249	168	153	224	174	210	143	253	197	168	213	275	GRD	GRD
GRD	DK142-2	180	235	152	227	215	24/33	151	142 x 142	GRD	158	211	GRD	GRD	GRD	GRD
GRD	281	169	228	142-1	244	24/26	177	194	158	196	290	246	280	24/28	GRD	GRD
GRD	GRD	GRD	GRD	GRD	GRD	GRD	GRD	GRD	GRD	GRD	GRD	GRD	GRD	GRD	GRD	GRD

Figure 2.1: POSH 1-3 Randomised Field Design 2006. Sub-Block 1: White, Sub-Block 2: Lt. Grey, Sub-Block 3: Dk Grey, GRD: Guard

GRD	GRD	GRD	GRD	GRD
GRD	Apex	MC177	MC168	GRD
GRD	DK142	MC259	MC246	GRD
GRD	Tapidor	Apex	MC226	GRD
GRD	MC148	MC228	MC243	GRD
GRD	MC168	Tapidor	MC259	GRD
GRD	MC169	MC216	DK142	GRD
GRD	MC177	MC148	MC228	GRD
GRD	MC216	MC169	MC148	GRD
GRD	MC226	MC243	Apex	GRD
GRD	MC228	MC168	MC216	GRD
GRD	MC243	MC226	MC169	GRD
GRD	MC246	DK142	MC177	GRD
GRD	MC259	MC246	Tapidor	GRD
GRD	GRD	GRD	GRD	GRD

Figure 2.2: POSH 1-3 Randomised Field Design 2009. Block 1: White, Block 2: Lt. Grey, Block 3: Dk Grey, GRD: Guard

2.2.2 Pod Selection and Equilibration

Whole plants were harvested and hung in a cool, dry environment for a minimum of four weeks prior to pod selection to ensure uniform desiccation. Pods were selected non-randomly throughout the primary and secondary racemes, alternating the position from which pods were taken moving up and around the raceme to reduce positional bias (Figure 2.3). Pod selection was preferentially targeted towards fully elongated, fertile pods. Fruit were detached from the raceme using secateurs leaving the entire pedicel intact. Three 20 pod sub-samples were taken from each line per block, bagged individually and equilibrated for a minimum of 3 days at 25°C at 50% relative humidity (RH) in a controlled environment chamber prior to testing. Air was pumped into the controlled environment chamber through silica pellets to remove excess moisture and maintained at 25°C using a heating element.
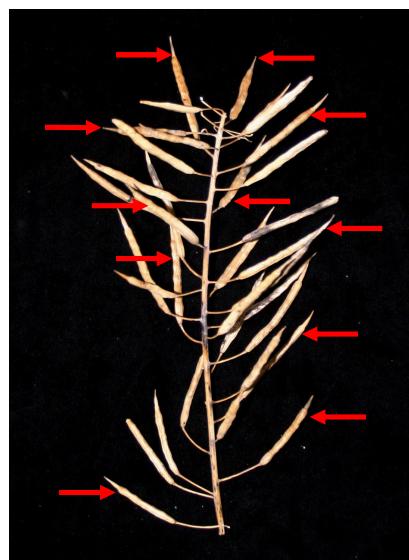
Figure 2.3: Image of oilseed rape raceme, with arrows illustrating typical selection of pods selected for assessment

2.2.3 Investigating differences in PSR using a Random Impact Test (RIT)

A Random Impact Test (Bruce *et al.* 2002) was utilised to assess relative resistance to pod shattering in POSH 1-3 lines. 20 equilibrated, undamaged pods were placed with six 10mm diameter steel balls, weighing 50.08g, in a 20cm cylindrical sealed plastic container. This assay was modified slightly from the method utilised by Bruce *et al.* (2002) by reducing the diameter (and hence weight) of the balls in the shaker from 12.5 mm to 10 mm, to decrease the amount of force transferred to *Brassica* pods and hence reduce the rate at which they break. The container was then mechanically shaken at a frequency of 4.98Hz over a stroke length of 51mm for two 5 s periods, five 10 s periods and up to thirty 20 s periods or until all pods had completely shattered.

After each period, pod condition was monitored. The number of intact pods, damaged pods without detached valves, damaged with one detached valve and dehisced pods were recorded. Pods with no damage were regarded to be intact whereas siliques with one or both valves detached were considered to be broken. The RIT induces a progressive degradation in pod material of which the time course of pod breakage can be accurately estimated. For the 2006 field trial three 20 pod samples from block one and single 20 pod sample from blocks two and three were subjected to the RIT. For the 2009 subset field trial three 20 pod samples from each of three blocks were analysed using the RIT.

2.2.4 Physical Trait Measurement

Morphological data for pod samples was obtained by assessments of the following traits:

Pod Mass (g): Each 20 pod sample was weighed after equilibration and before pod shatter testing using a pan balance in the 2006 and 2009 trials

Seed Mass (g): The seed from each 20 pod sample was cleaned using a separator and weighed after shatter testing using a pan balance in 2006 samples. The percentage seed content of 20 pod samples was also calculated, by dividing Seed Mass (g) by Pod Mass (g) and multiplying by 100.

Seed Damage: Seed damage was estimated post-Random Impact Testing on a 0 – 9 scale (0 – No Damage, 9 – Complete Destruction) in the 2006 material

Intact pods: The frequency of intact pods was logged after each RIT shaking interval to derive the Intact RIT_{50}; the time (secs) at which 10 pods from a 20 pod sample remain intact after shatter testing was estimated using a curve fitting-model on pod degradation data generated during the Random Impact Test (RIT).

Broken RIT_{50}: The frequency of broken pods was logged after each RIT shaking interval to derive the Broken $RIT_{50;}$ the time (secs) in seconds at which 10 pods from a 20 pod sample were observed to have one or both valves detached was estimated using a curve fitting model on pod degradation data generated during the Random Impact Test (RIT)**.**

2.2.5 Progress Curve fitting and RIT_{50} estimation

To enable comparison of the relative level of PSR in each respective POSH 1-3 line tested, the time point at which 10 pods (half) was estimated. This was achieved by fitting a curve to the values for intact and broken pods over their progressing shaking period to generate an 'RIT_{50}' value (seconds) according to the value at the X/Y intercept when 10 pods remained intact or were broken. This value is also referred to as sample 'half-life'. A curve-fitting model (Morgan, unpublished), which utilised a four parameter Chapman curve, was automated using Genstat V.12 software (Payne *et al.* 2009) and enabled efficient, accurate estimation of the respective RIT_{50} value for each sample tested. Regression parameters for the sigmoidal curve were: Y: Maximum asymptote (20/0, Intact/Broken respectively), A: Minimum asymptote (0/20, Intact/Broken, respectively), B: Gradient of regression and C: Inflection point required for the curve fitting equation. The quality of curve fitting was determined according to the percentage variance accounted for by the model (coefficient of determination, R^2 value). Where the model 'failed' to accurately fit progress curves and hence RIT_{50} estimation (R^2 <0.95), regressions were fitted by hand using Sigmplot V.11 software (Sysat software Inc.). RIT_{50} scores for intact and broken pods from each individual 20 pod

sample were recorded. Intact RIT$_{50}$ scores only included undamaged pod frequency, whereas broken RIT$_{50}$ was derived from the number of pods with one and/or both valves detached. An example of the Intact pod progress curves generated in POSH 1-3 parents is displayed in Figure 2.4.
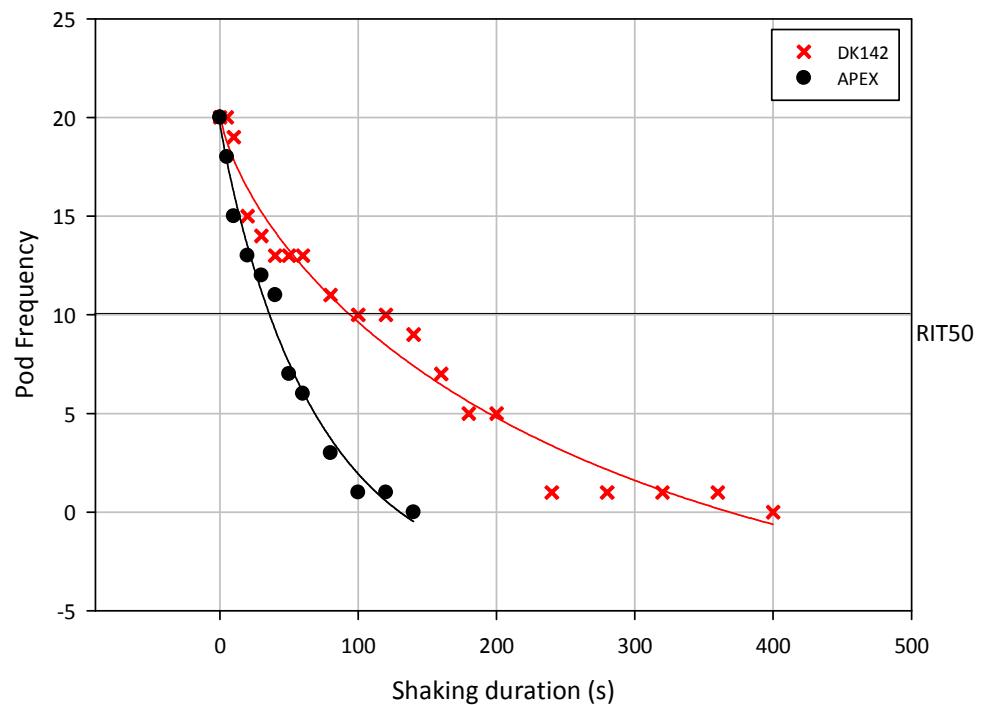
Figure 2.4: Progress curves generated for intact pod degradation in Apex and DK142 lines displaying decreasing pod frequency over increasing shaking duration

2.2.6 Estimations of Pod Shatter Resistance in POSH 1-3 using a Random Impact Test

A range of measurements of the progressive breakdown of the 20 pod samples generated using the RIT was utilised to obtain the most accurate observations of potential differences in levels of shatter resistance amongst the lines assessed. These included:

Adjusted Intact and Broken Lethal Dose 50 (Intact/Broken Adj. RIT$_{50}$)

Previously, Summers *et al.* (2003) reported significant differences in PSR in POSH progenitors and F$_2$ lines which were correlated with increases in pod weight, specifically valve and septum/beak weight and also increases in pod length, regardless of seed weight/number. Pod Mass may have deleterious/confounding effects when trying to identify associated markers contributing to increases in PSR. For this reason we analysed Intact/Broken RIT$_{50}$ using Pod Mass (g) as a covariate in the Generalized Linear Model (GLM). The covariate was highly significant and was observed to decrease RIT$_{50}$ values in heavier pod samples and increase RIT$_{50}$ values in lighter pod samples (2.3.4.1-2.3.4.4).(Appendix 2.1-2.4 (pages 242-246)). The adjusted values have been used as they dissociate any effects (extreme) differences between different population lines may have influenced RIT$_{50}$.

2.2.7 Statistical Analysis: Tests for Normality of Data Distribution, Analysis of Variance, Correlations and Trait Heritability

Statistical analyses were conducted using Genstat V.12 software (Payne *et al.* 2009). Data was tested for normality using the Shapiro-Wilk (W-test). Analyses were performed using Generalized Linear Model (GLM) for Pod Mass, Seed Mass, Seed Damage, Intact/Broken RIT$_{50}$, Intact/Broken adjusted RIT$_{50}$ and the 'B' curve fitting parameter for all available POSH 1-3 lines in both trials as the data was unbalanced due to sampling structure. GLM/ANOVA for Intact and Broken RIT$_{50}$ with Pod Mass (g) as a covariate was utilised to modulate data to generate adjusted RIT$_{50}$ values for Intact and Broken pods. Broad-sense heritability was calculated to determine relative genetic and environmental contribution to trait phenotypes. Trait means for each character from samples from all blocks present were calculated. As an unbalanced dataset formed the basis for the

analyses, with respect to the number of replicate samples assessed from each line, the harmonic mean for the population was first calculated using the formula:

$$1/H = 1/n \, \Sigma \, (1/Y_i)$$

(H: Harmonic mean, n: no. of lines, Y_i: no. of replicates)

The expected means squared (EMS) was then calculated for each trait, using the following formula:

$$EMS = (\sigma^2 g - \sigma^2)/n$$

(σg: Line means squares, σ: Residual means squares, n: Harmonic mean)

Then the EMS was then used to derive heritability (H^2) using:

$$H^2 = EMS/Total\ EMS, \text{ or } H^2 = G/G + E$$

(EMS: Expected mean squares, Total EMS: EMS + Residual, G: Genotype, E: Environment).

Relationships among the traits were assessed using the correlation co-efficient, r and coefficient of determination, R^2, were calculated to determine if any relationship between traits could be established in POSH 1-3. GLM was used to assess for differences between lines, sub-blocks and independent trials performed in different years to test the validity of the experimental design due to the confounding of blocks two and three only containing a single technical replicate (Appendix 2.9, 2.11, 2.13, 2.15 (pages 251, 254, 256 and 258, respectively)).

2.3 Results

2.3.1 Assessing Pod Shatter Resistance in the POSH 1-3 population using a Random Impact Test

A RIT was used to measure Pod Shatter Resistance (PSR) in POSH 1-3. Prior to shaking, Pod Mass (g) was determined for each 20 pod sample. A total of 371 pod samples, from 93 lines were measured in 2006 and 60 samples from 13 lines in 2009 (including Tapidor as control material), with the progressive breakdown and subsequent reduction in frequency of intact/increase in broken pods recorded. In the 2009 an excessively wet period during harvest meant that pods of MC216 line matured very late and were harvested as green pods. Therefore, samples from this line were excluded from the RIT analysis and subsequent assessment.

In lines from the 2006 trial levels of seed damage post-shaking were recorded for each sample assessed (0-9 scale), as was seed mass (g), percentage seed content (%) and values for the 'B' curve fitting parameter, whereas for the 2009 trial as well as pod mass and the 'B' regression parameters were recorded (Appendix 2.1-2.4).

2.3.2 Tests for Normality and Distribution of Data

The distribution of trait data for the population was tested for normality using the Shapiro-Wilk W-test. Histograms for RIT_{50} traits for POSH 1-3 lines (from 2006 trial) are shown in Figure 2.5. Histograms for the other characters are given in Appendix 2.5.

In pods from the lines assessed in the 2006 trial Pod Mass (g), Seed mass (g) Percentage Seed (%) were normally distributed (Appendix 2.5, 2.6). However, Intact/Broken mean RIT_{50} in the POSH 1-3 population were observed to exhibit a highly non-normal distribution ($P<0.001$) (Appendix 2.7) as was Seed Damage. Reanalysis of RIT_{50} values, using the adjusted values after using Pod Mass (g) as a covariate reduced RIT_{50} values in larger heavier pods and increased it in smaller, lighter pods. However, on reanalysis, the distribution of adjusted RIT_{50} was also observed to be non-normal ($P<0.001$). This was due to the complex, polygenic nature of the PSR trait resulting in a small number of outliers with increased shatter resistance.
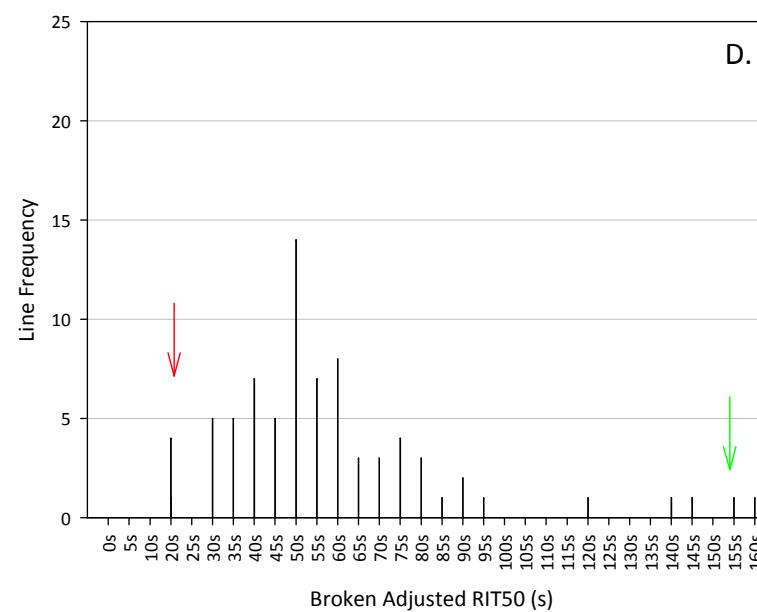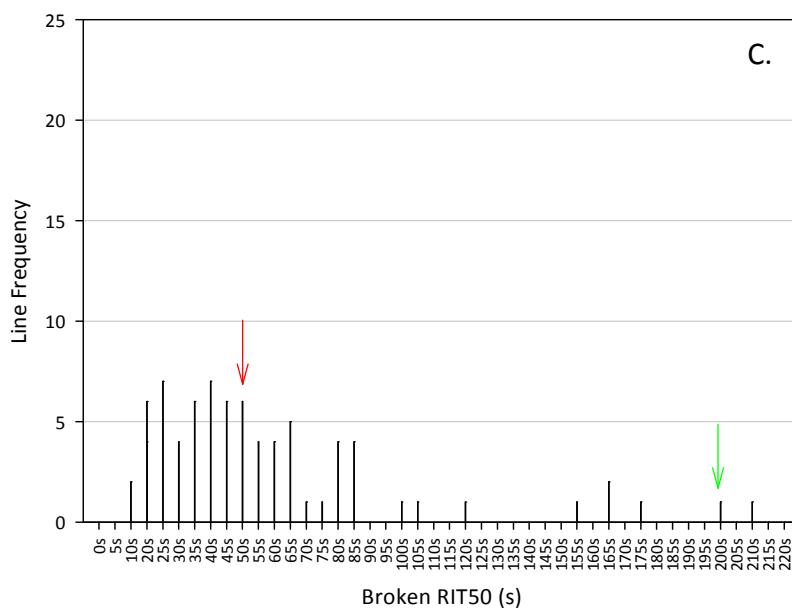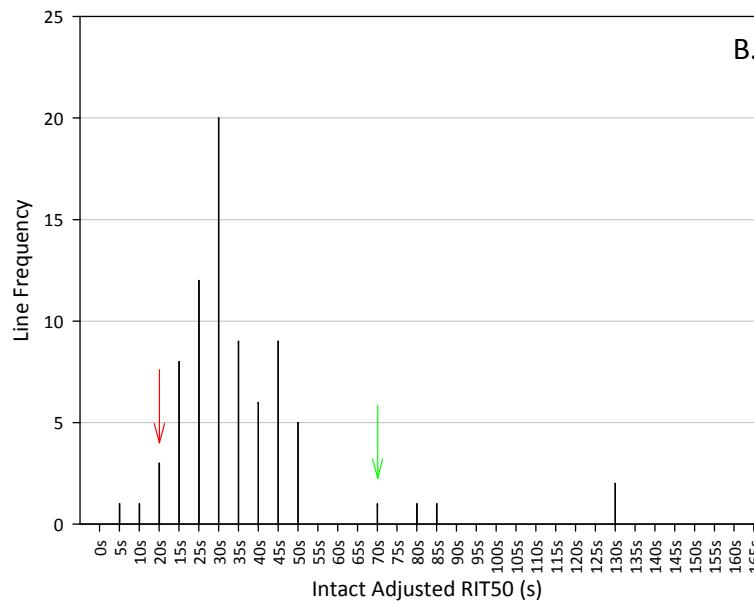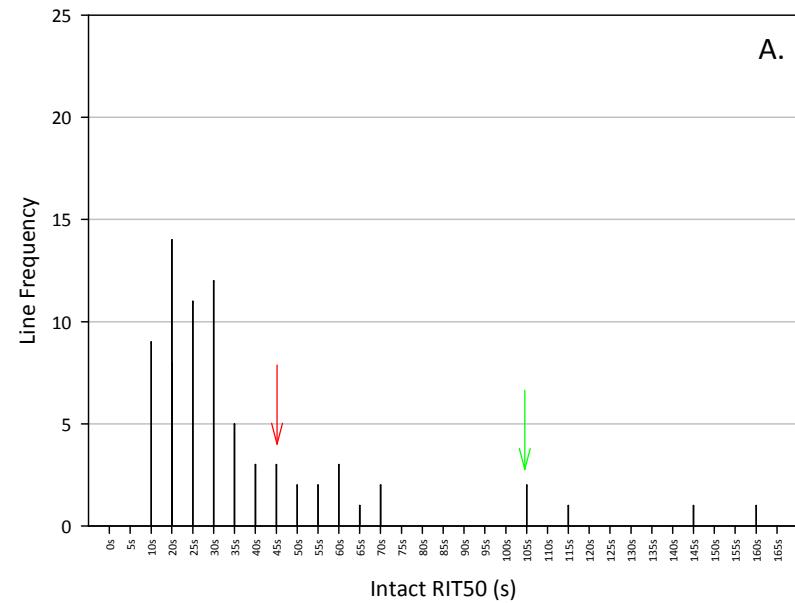
Figure 2.5: Histograms displaying mean LD50 distribution for POSH 1-3 lines in 2006 trial: A) IntactLD50, B) Intact Adj. LD50, C) Broken LD50 and D) Broken Adj. LD50 (Apex: red arrow/ DK142: green arrow)

For Intact pod data adjustment for the covariate reduced the range of the distribution from 157 s to 125 s (from a min 6 s/max 162 s to min 4 s/max 129 s). For Broken pod data the range was reduced from 200 s to 144 s (min 8 s/ max 209 s to min 12 s /max 156 s). Transformation of (RIT_{50}) data, using log and logit functions, did not improve the distribution/achieve normality (data not shown).

2.3.3 Differences in Scored Traits in the POSH 1-3 Population

A summary of the GLMs for the 2006 trial (Appendix, 2.8-2.11) are displayed in Table 2.7 (page 73) including trait probabilities for Pod Mass, Seed Mass, Seed Damage Intact/Broken RIT_{50}, Intact/Broken adjusted RIT_{50}, and also estimates of broad sense heritability (H^2). A summary of trait probabilities for Pod Mass, Intact and Broken RIT_{50}, Intact and Broken adjusted RIT_{50}, and estimates of broad sense heritability (H^2) from the 2009, is displayed in Table 2.8 (page 74). Correlation and coefficient of determination (R^2) were calculated for Pod Mass, Seed Mass, Seed Damage, Intact/Broken RIT_{50}, Intact/Broken adjusted RIT_{50}, and 'B' regression parameters in 2006 trial (Figure 2.6 and Figure 2.8 (pages 75 and 77, respectively), whereas Pod Mass, Intact/Broken RIT_{50}, Intact/Broken adjusted RIT_{50} and 'B' parameter were calculated in 2009 (Figure 2.7 and Figure 2.9 (pages 76 and 78, respectively). As data from Intact and Broken pods was utilised to derive half life, associations with other physical traits are also represented for each measure of resistance in the results. These are generally observed to be similar but in some cases, different associations have been identified.

2.3.3.1 Physical Trait measurement
Pod Mass (g) in the 2006 and 2009 trials
2006
Significant differences in Pod Mass (g) ($P<0.001$) were observed between POSH 1-3 lines in 2006 (Appendix 2.8, 2.10 (pages 249 and 252, respectively)). Pod Mass ranged between a minimum of 1.251g in MC208 to a maximum of 5.959g in MC148. No significant differences in Pod Mass (g) were apparent between Apex and DK142 ($P=0.1471$, Appendix 2.17 (page 263), with means of 5.672g and 5.195g respectively. Significant positive correlations were identified between Intact

Pod Mass (g) and Seed Mass (g) (r=0.885, *P*<0.0001), Intact RIT$_{50}$ (r=0.729, *P*<0.0001) and Intact adjusted RIT$_{50}$ (r=0.32, *P*<0.01) (Figure 2.6, page 75). Significant positive correlations were also identified between broken Pod Mass (g) and Seed Mass (g) (r=0.888, *P*<0.0001), Broken RIT$_{50}$ (r=0.737, *P*<0.0001), Broken adjusted RIT$_{50}$ (r=0.344, *P*<0.01). As Seed Mass is a component of Pod Mass we expected these traits to be auto-correlated (r=1). However this was not always the case and relates to variation in pod wall thickness, seed size and fertility in pods. On further assessment of the relationship between the individual components of Pod Mass, Pod Material Mass and Seed Mass the correlation was observed to be still significant (r=0.451) Greater Pod Mass was associated with increased Seed Mass, Intact/Broken RIT$_{50}$ and adjusted RIT$_{50}$ values. Significant correlations indicated heavier pods exhibited greater Seed Mass and also demonstrated greater RIT$_{50}$ and hence levels of PSR. However, with RIT$_{50}$ adjustment, utilising Pod Mass as a covariate, the level of significance in these relationships was observed to be reduced in both Intact and Broken adjusted RIT$_{50}$ values.

It therefore may be possible to select for increased PSR independently of Pod Mass. Significant negative correlations were observed between Intact and Broken Pod Mass and the 'B' regression parameter (r=-0.349, *P*<0.01 and r=-0.468, *P*<0.0001, respectively). Therefore, an increase in Pod Mass was associated with a decrease in the slope of the progress curve, indicating heavier pods were damaged at a slower rate, potentially as they could absorb more energy, resulting in slower degradation.

2009

In the 2009 trial material, significant differences were also identified amongst lines for Pod Mass (*P*<0.001, Appendix 2.12 (page 255). Significant differences were observed between Apex and DK142 (*P*<0.05, Appendix 2.17), with a mass of 4.984g recorded for Apex and 5.765g for DK142. In the subset of lines, Pod Mass ranged from 3.768g in MC259 to 5.957g in MC148. MC148, as in the 2006 trial, demonstrated the greatest Pod Mass of the lines assessed. Pod Mass was seen to demonstrate a highly significant correlation with Intact and Broken RIT$_{50}$ values in the 2009 trial (r=0.508, r=0.718, *P*<0.001, respectively) (Figure 2.7). Adjustments using Pod Mass as a covariate

resulted in a non-significant correlation with Intact adjusted RIT_{50}, whereas Broken adjusted RIT_{50} was identified to be reduced compared to unadjusted RIT_{50}, but still significantly correlated with Pod Mass in the 2009 trial post adjustment (r=0.41, $P<0.001$). Significant negative correlations were observed with Pod Mass and the 'B' regression parameter for both Intact and Broken Pod data (r=-0.362, $P<0.01$ and r=-0.439, $P<0.001$), indicating increases in Pod Mass decreased the gradient of the progress curve.

2006|2009

Significant differences in mean Pod Mass were observed amongst the nine lines ($P<0.005$, Appendix 2.16 (page 259)), common to 2006 and 2009, but there was no environmental effect between years ($P=0.394$). No significant interaction was observed between Years and Lines ($P=0.5$). Pod Mass increased by 3% from 4.59 g to 4.74g in 2006 and 2009 respectively (page 259). The greatest changes in Pod Mass were observed in MC243 and MC246 increasing 12% and 27% respectively and in MC226 which decreased by 12%

2.3.3.2 Seed Mass (g) and Percentage Seed Content in the 2006 trial

There were significant differences in Seed Mass amongst lines ($P<0.001$, Appendix 2.8, 2.10 (pages 249 and 252, respectively)). Mean Seed Mass ranged from a minimum of 0.141g in line MC151 to a maximum 2.621g in line MC211. Lines with a greater Seed Mass (g) were generally observed to demonstrate a greater Pod Mass (g). No significant differences in Seed Mass between Apex and DK142 parental lines were evident ($P=0.154$, appendix 2.18 (page 264)) each exhibiting respective values of 3.317g and 2.628g. Significant positive correlations were observed between Intact and Broken Seed Mass (g) and Pod Mass (g) as described in 2.3.3.1, respective Intact and Broken RIT_{50} (r=0.5, $P<0.001$, r=0.475, $P<0.001$, respectively, Figure 2.6). However adjusted RIT_{50} values were found not to be significantly correlated with Seed Mass. This indicated that Seed Mass was influencing RIT_{50} indirectly as a component of Pod Mass. Significant negative correlations were observed between Seed Mass and Seed Damage (r= -0.363, -0.356, $P<0.01$). Hence increases in Seed Mass results in reduced Seed Damage.

Highly significant differences were observed for Percentage Seed Content (Seed / Pod Mass) ($P<0.001$, Appendix 2.8, 2.10). Percentage Seed Content in lines with the lowest and highest Seed Mass was observed to range from a minimum of 8.9% in MC151 to a maximum of 52.4% in MC211, between which highly significant differences were identified ($P<0.000001$, Appendix 2.19 (page 264)). This reflects variation in the level of seed set and fertility in POSH 1-3 lines. Significant differences were observed between Percentage Seed Content between Apex and DK142 lines ($P<0.001$, Appendix 2.19), with respective seed percentages of 60.5% and 46.4%. The partitioning ratio of seeds compared to the receptacle was observed to be 1.52:1 in Apex and 0.86:1 DK142.

2.3.3.3 Seed Damage in the 2006 trial

Significant differences were observed between lines and Seed Damage induced during the RIT for Intact and Broken pods ($P<0.001$, Appendix 2.8, 2.10). The population displayed a range of levels of Seed Damage with seven lines (MC150, MC160, MC195, MC206, MC210, MC228 and MC274) exhibiting the lowest levels of Seed Damage, scoring a value of 0, whereas line MC249 displayed the greatest level of damage with a value of 8.75. High levels of damage were also observed in MC169, MC205, MC280, with respective levels of 7.7, 7.8, and 8. Significant differences were observed between parental lines ($P<0.05$, Appendix 2.20 (page 264), with Apex demonstrating a mean damage score of 1.75 whereas DK142 scored 3. Samples from resistant lines were on average, shaken for greater durations that susceptible lines, subjecting them to more energy, thus exposing the seeds to higher levels of potential degradation. This explains the non-normal distribution observed in Seed Damage for the population, also observed for the half life traits.

Samples from the most resistant lines such as DK142, MC169 and MC205 did exhibit high levels of damage. However, the most resistant line MC148 however was observed to display only a moderate level of Seed Damage (4.6), whereas, MC177, which demonstrated an Intact RIT_{50} values in excess of 100 s was observed to display a seed damage score of only 2.6. An increase in Seed Damage was significantly correlated with unadjusted/adjusted Intact RIT_{50} ($r=0.271$, $P<0.05$, 0.378, $P<0.001$ respectively) and unadjusted/adjusted Broken RIT_{50} ($r=0.342$, $P<0.01$, $r=0.481$, $P<0.0001$, respectively) (Figure 2.6). Increases in RIT_{50} are therefore associated with increases in Seed

Damage. Significant negative correlations were identified between Seed Damage and the 'B' curve fitting parameter (slope) for both Intact and Broken pods (r=-0.312, *P*<0.01 and r=0.394, *P*<0.001, respectively). Increased Seed Damage is associated with decreases in the gradients of the slope. This was due to decreases in gradient in resistant lines with protracted RIT_{50} with a longer shaking period.

2.3.4 Pod Shatter Resistance Trait Measurement: Intact and Broken RIT_{50} in 2006 and 2009 Trials

2.3.4.1 Intact RIT_{50}

2006 Trial

Significant differences in Intact RIT_{50} were observed between POSH lines (*P*<0.001, Appendix 2.8). No significant differences were observed between Apex and DK142 parents (*P*=0.213, Appendix 2.21 (page 265), each displaying respective mean Intact RIT_{50} values of 40 s and 101 s. This was due to high levels of inter-sample variation between replicates. The lowest intact RIT_{50} was recorded at 5.5 s for MC152, whereas the greatest was 162 s in MC148 and hence the most shatter resistant line. A total of sixteen lines were observed to display intact RIT_{50} values greater than the shatter susceptible Apex parent. The remaining 62 lines were seen to perform less well compared to Apex and were identified as negative transgressive segregants.

Three lines, MC205, MC169 and MC148 were observed to display positive transgressive segregation for mean intact RIT_{50}, with half-lives in excess of the shatter resistant DK142 parent (110 s, 147 s and 162 s, respectively). Significant differences could not be established between the positive transgressive segregants and DK142 (*P*=0.86, *P*=0.544 and *P*=0.345, respectively). However, significant differences between Apex, MC205 and MC148 (*P*<0.05) were observed. Significant positive correlations were identified between Intact RIT_{50} and Intact adjusted RIT_{50} (r=0.882, *P*<0.0001), Pod Mass (g) (2.3.3.1), Seed Mass (g) (2.3.3.2), and Seed Damage (2.3.3.3) (Figure 2.6). Therefore increases in Intact RIT_{50} result in increases in Intact adjusted RIT_{50}.

Although assumed to be auto-correlated differences in between adjusted and unadjusted half-life is due to the removal of the Pod Mass covariate. This demonstrates how Pod Mass affects half-life.

Significant negative correlations (r=-0.349, *P*<0.01) were observed with the 'B' regression parameter, indicating greater Intact RIT_{50} is associated with decreases in the gradient of the slope of the progress curve. More resistant pods can therefore absorb more energy than susceptible pods and degrade more slowly.

2009

Significant differences in Intact RIT_{50} were also observed amongst 11 lines from the 2009 trial (*P*<0.001, Appendix 2.12). MC148 was observed to exhibit the greatest Intact RIT_{50} value (54 s), as was observed in 2006 trial, whereas MC259 was observed to display the shortest Intact RIT_{50} (14 s). Significant differences could not be identified between Apex or DK142 lines and Intact RIT_{50} values were observed to be near identical (18 s and 18 s, respectively) (*P*=0.97, Appendix 2.22 (page 266). This is due to potential out-crossing in DK142. Significant differences were identified between MC148 and both Apex and DK142 (*P*<0.01, *P*<0.05, respectively). Significant positive correlations were observed between Intact RIT_{50} and Intact adjusted RIT_{50} (r=0.883, *P*<0.0001) (Figure 2.7) as in 2006. Significant negative correlations were observed between Intact RIT_{50} and the 'B' parameter (r=-0.819, *P*<0.0001, respectively) as in 2006. Increases in Intact RIT_{50} were associated with a decrease in the gradient of the progress curve.

2006|2009

In the nine lines common to both trials, significant differences in RIT_{50} were observed between years (*P*<0.005, Appendix 2.16), but not between lines, due to the range of inter-sample variation and subset of lines selected for the analysis. This indicated environmental affects were influencing Intact RIT_{50} in different trial years. Total Intact RIT_{50} for the common lines was observed to be reduced in the 2009 trial to 25 s compared to 73 s in 2006. A reduction in relative Intact RIT_{50} was observed for all but one line tested; Only MC246 demonstrated an increase in Intact RIT_{50} from 9 s to 14s (+53%). However, even with a reduction in the overall level of shatter resistance, MC148 was observed to demonstrate the greatest Intact adjusted RIT_{50} in both trial years. MC169 also demonstrated a high relative RIT_{50} across the two years. This indicates that although environmentally sensitive at a population level the most resistant lines in the population remain

prevalent. In the two parental lines, significant differences were observed between Apex samples from 2006 and 2009 ($P<0.01$, Appendix 2.25 (page 268), but not in DK142 samples due to high levels of variation within samples, even though respective means were quite dissimilar (101 s in 2006/18 s in 2009, respectively). Although DK142 was observed to be resistant to shattering under the RIT assessment in 2006, it appeared to exhibit an extremely reduced level of PSR in 2009 (82.5%). This could relate to out-crossing, environmental sensitivity ot the PSR trait or through erroneous planting. However, significant differences were also observed in the most resistant line, MC148 ($P<0.01$), with Intact RIT_{50} reduced from 162.5s in 2006 to 54.3s in 2009 (a decrease of 67%). This indicates a high degree of environmental variability in Intact RIT_{50} and hence PSR between trial years.

2.3.4.2 Broken RIT_{50}

2006 Trial

Significant differences in mean broken RIT_{50} were observed between lines ($P<0.001$, Appendix 2.10 (page 252). 44 negative transgressive segregants were observed, displaying mean broken RIT_{50} values less than Apex parent, whereas, 34 lines exhibited mean broken RIT_{50} values greater than Apex. The greatest Broken half life was displayed by MC148 (208 s) and the shortest exhibited by MC152 (8 s). Only MC148 was observed as a positive transgressive, with a mean broken RIT_{50} greater than the DK142 parent. The 77 remaining lines demonstrated reduced values compared to the resistant DK142 parent. No significant differences were established between Apex and DK142 ($P=0.056$) or between MC148 and DK142 ($P=0.899$), due to high inter-sample variation (Appendix 2.23 (page 267). However, significant differences were observed between Apex and MC148 ($P<0.05$). Significant positive correlations were identified between broken RIT_{50} and broken adjusted RIT_{50} ($r=0.888$, $P<0.0001$), and Pod Mass (g), Seed Mass (g) and Seed Damage (2.3.3.1, 2.3.3.2, 2.3.3.3, respectively) (Figure 2.6). The lack of auto-correlation between adjusted and unadjusted Broken half-life resulted from removal of the Pod Mass covariate, again demonstrating the affect the weight of the pods has on half-life.   Significant negative correlations were observed with the 'B' regression parameter ($r=-0.584$, $P<0.0001$). Increases in Broken RIT_{50} were associated with a decrease in the gradient of the progress curve. This again demonstrates

that the more resistant a line, the slower pod break-down occurs, indicating it could absorb more energy than more susceptible lines.

2009

Broken RIT_{50} was observed to be significantly different between the 11 POSH 1-3 lines from the 2009 trial (P<0.001, Appendix 2.14 (page 257)). Significant differences were also observed in Broken RIT_{50} between Apex and DK142 parents (P<0.001, Appendix 2.24 (page 267)), with Apex demonstrating a Broken half life of 27 s and DK142 46 s. This was the conserve to that observed for the Intact RIT_{50} in the 2009 trial as was expected. This indicated that although the number of intact pods degraded equally as fast in Apex and DK142, siliques in DK142 did not reach a broken stage as quickly. This indicates that factors such as secondary vasculature could be contributing to the phenotype in DK142, holding the valves on even after breakdown has been initiated. MC148 was observed to display the greatest Broken RIT_{50} value (86 s), whereas MC226 exhibited the shortest (19 s). Significant differences were observed between MC148 and Apex (P<0.01). Significant positive correlations were identified between Broken RIT_{50} and Pod Mass (2.3.3.1), and also Broken adjusted RIT_{50} (r=0.93, P<0.0001) (Figure 2.7). This highlights that increases in Broken RIT_{50} are associated with an increase in Broken adjusted RIT_{50}. Unadjusted/adjusted RIT_{50} were auto-correlated and deviation from r=1 is likely an effect of adjustment for the Pod Mass covariate. Significant negative correlations (r=-0.784, P<0.01) were also observed with 'B' regression parameter, as in the 2006 trial, with increases in Broken RIT_{50} associated with decreases in the gradient of the slope of the progress curve. This indicates resistant lines are behaving in a similar fashion to those identified in the 2006 trial.

2006|2009

Significant differences in Broken RIT_{50} were observed between trial years in the nine lines assessed ($P<0.01$, Appendix 2.16). No significant differences were observed between lines and no significant interactions were established between line and year ($P=0.135$, $P=0.5$, respectively). This related to the level of variation between samples and the selection of the subset of lines. Total Broken RIT_{50} was observed to be different between trial years, with a mean RIT_{50} value of 101 s in 2006 and 47 s in 2009. A reduction in Broken RIT_{50} was observed in all lines in the 2009 trial, barring MC246, compared to 2006, as observed for Intact RIT_{50}. MC246 was observed to display an increase in Broken RIT_{50} of 29 s in 2006 to 60 s in 2009 (+ 48 %). Significant differences in Broken RIT_{50} were identified between years in Apex ($P<0.05$) and DK142 ($P<0.01$) (Appendix 2.26 (page 269). MC148 demonstrated the greatest Broken RIT_{50} in both trial years and hence was the line most resistant to pod shatter. Significant differences were observed in MC148 between the trial years ($P<0.05$) with Broken half life reduced from 208 s in 2006 to 86 s in 2009 (- 48%). Therefore environmental effects between years could have influenced Broken RIT_{50} and hence PSR.

2.3.4.3 Intact adjusted RIT_{50}

2006

Significant differences in Intact adjusted RIT_{50} (Int. adj. RIT_{50}) were observed between lines and the Pod Mass covariate ($P<0.001$, Appendix 2.8). This indicated that accounting for the covariate significantly influenced the Intact RIT_{50} character. Significant differences were also observed between blocks ($P<0.05$) and the Pod Mass covariate ($P<0.001$) (Appendix 2.9 (page 251). This is an effect of adjusting for the covariate and indicates that RIT_{50} is more variable when the Pod Mass component has been accounted for. This is supported by the observation that trait heritability is reduced from approximately 60% to 35% on selection of Pod Mass as a covariate (Table 2.7). However, the significance level is not extremely high. Five lines were identified to display mean Int. adj. RIT_{50} less than Apex and 73 DH lines were observed to exhibit mean Int. adj. RIT_{50} greater than Apex. 74 lines exhibited reduced mean RIT_{50} compared to the resistant DK142 parent. Four lines were demonstrated to be positive transgressive segregants with a mean Int. adj. RIT_{50} greater than DK142. These included MC148, MC169 and MC205 which were identified

exhibit greater Intact RIT_{50} and now also MC177. This indicated that although Pod Mass was influencing the PSR trait, some factors contributing in the most resistant lines appeared to be selected for independently. In the two lines demonstrating the most extreme differences in Intact RIT_{50}, Int. adj. RIT_{50} was increased five-fold in the shatter susceptible MC152 from 5 s to 29 s, and decreased 26% in the resistant MC148 from 162 s to 129 s (Figure 2.7). MC246 was the identified to exhibit the shortest half life of 4 s with a decrease of 59% compared to the unadjusted Intact RIT_{50} (9 s). Int. adj. RIT_{50} was observed to be reduced in both Apex and DK142 compared to Intact RIT_{50} as both lines demonstrated relatively heavy pods (reductions of 62.29% and 32%, respectively). These results indicate that Pod Mass has a significant influence on half life, especially in more shatter susceptible lines.

Significant positive correlations were observed with Pod Mass, Seed Damage and Intact RIT_{50} (2.3.3.1, 2.3.3.3 and 2.3.4.1) (Table 2.1). Significant negative correlations with the 'B' regression parameter ($P<0.05$) were identified. Therefore increases in Int. adj. RIT_{50} and hence PSR were associated with a decrease in the regression slope. The level of association between the slope parameter and Int. adj. RIT_{50} was reduced compared to Intact RIT_{50} due to the removal of the influence from Pod Mass.

Line	Apex	DK142	MC148	MC152	MC246
Pod Mass (g)	5.195	5.672	5.959	1.844	3.826
Intact RIT_{50} (s)	40.2	101.5	162.5	5.5	9.1
Intact adj. RIT_{50} (s)	15	69.4	128.7	28.7	3.7
Percentage change +/-	-62.29	-32	-26	+521	-59

Table 2.1: 2006 Intact RIT_{50}/Intact Adjusted RIT_{50} comparisons

2009

Significant Differences in Int. adj. RIT_{50} were observed between lines ($P<0.001$, Appendix 2.12 (page 255) and the covariate ($P<0.05$). MC148 was identified to exhibit the greatest Int. adj. half life (44 s) and MC246 the shortest (10 s) (Table 2.2). Respective decreases in half life, post-adjustment, were noted at 18.8% for MC148 and 31.4% for MC246. Apex and DK142 were

observed to display respective half lives of 16 s and 9 s (respective decreases of 12.3% and 48.4%). Significant positive correlations were identified between Int. adj. RIT_{50} and Pod Mass (2.3.3.1) and Intact RIT_{50} (2.3.4.1) (Figure 2.7). Significant negative correlations were observed between half life and the 'B' regression parameter (r=-0.752, $P<0.0001$), as observed in the 2006 trial. Increases in Int. adj. RIT_{50} were associated with a decrease in the gradient of the progress curve.

Line	Apex	DK142	MC148	MC246
Pod Mass (g)	4.984	5.765	5.959	5.25
Intact RIT_{50} (s)	17.9	17.8	54.3	14
Intact adj. RIT_{50} (s)	15.7	9.2	44.1	9.6
Percentage +/-	-12.3%	-48.4%	-18.8	-31.4%

Table 2.2: 2009 Intact RIT_{50}/Intact Adjusted RIT_{50} comparisons

2006|2009

No significant differences between Int. adj. RIT_{50} and lines were observed for the lines common to both trials (P=0.138, Appendix 2.16 (page 259)). This related to the level of variation between samples and the selection of the subset of lines. Significant differences were observed between years amongst the same respective lines ($P<0.05$). This indicated that Int. adj. RIT_{50} and hence PSR was subject to environmental effects between the two trials. No significant interactions between line and year were identified (P=0.5). The resistant MC148 line was identified to demonstrate a decrease in adjusted half life of 65.8% in 2009 compared to 2006, whereas the most susceptible line from 2006, MC246, exhibited an increase of 259% (Table 2.3). In general terms, Int. adj. RIT_{50} was reduced in 2009 compared to 2006, with total Int. adj. RIT_{50} reduced from 55.46 s in 2006 to 25 s in 2009. Although slightly increased in MC246, Int. Adj. half life and hence PSR was reduced in 2009 compared to 2006. Intact/Int. adj. RIT_{50} was extremely variable in MC246 between the two years and indicates this line is highly sensitive to environmental effects. The DK142 line also demonstrated a large reduction in adjusted half life (86.8%) in 2009 compared to 2006 and could be attributed to environmental effects, through out-crossing and subsequent cultivation of segregating material, not a selfed DH line or through erroneous planting.

However Apex was observed to behave similarly in both years with an Int. adj. RIT_{50} of 15 s in 2006 and 16 s in 2009. This indicates that once the effects of Pod Mass have been accounted for in Apex, although relative susceptible to shattering, the level of PSR remains stable.

Line	Apex	DK142	148	246
Pod Mass (g) (2006)	5.195	5.672	5.959	3.826
Intact adj. RIT_{50} (s) (2006)	15	69.4	128.7	3.7
Pod Mass (g) (2009)	4.984	5.765	5.957	3.77
Intact adj. RIT_{50} (s) (2009)	15.7	9.2	44.1	9.6
Percentage difference +/-	+4.5	-86.8	-65.8	+259

Table 2.3: 2006/2009 Intact RIT_{50}/Intact Adjusted RIT_{50} comparisons

2.3.4.4 Broken adjusted RIT_{50}

2006

Significant differences were identified between Broken adjusted RIT_{50} (Brk. Adj. RIT_{50}) and lines (*P*<0.001,), and the covariate (*P*<0.001) (Appendix 2.10 (page 252). All the population lines were observed to exhibit an increased Brk. adj. RIT_{50} compared to Apex (10 s). This was due to the high Pod Mass and low initial Broken RIT_{50}. Brk. adj. RIT_{50} was observed to be reduced in both Apex and DK142 compared to Broken RIT_{50} (88% and 34%, respectively) (Table 2.4). This demonstrated that Pod Mass was contributing to Broken RIT_{50} and hence PSR, especially in Apex. MC163 was identified to have the shortest Brk. adj. RIT_{50} value for (11.8 s) for the population. Only MC148 was observed to display Brk. adj. RIT_{50} greater than the resistant DK142 parent (156 s and 153 s, respectively). In the resistant MC148 Brk. adj. RIT_{50} a decrease in half life of 25.4% compared to Broken RIT_{50} was observed and in the susceptible MC163 line adjustment decreased the RIT_{50} value by 61.4%. These findings reiterated the how Pod Mass influenced Broken RIT_{50} and hence PSR. However, these also indicated that some factors contributing to PSR in MC148 may potentially be selected for independently of Pod Mass.

Line	Apex	DK142	MC148	MC163
Pod Mass (g)	5.195	5.672	5.959	4.346
Broken RIT_{50} (s)	47.1	199.8	208.6	30.6
Broken adj. RIT_{50} (s)	10.4	153.1	155.8	11.8
Percentage +/-	-88 %	-34%	-25.4%	-61.4%

Table 2.4: 2006 Broken RIT_{50}/Broken Adjusted RIT_{50} comparisons

Significant positive correlations were observed between Pod Mass, Seed Damage and Broken RIT_{50} (2.3.3.1, 2.3.3.2 and 2.3.4.2, respectively). Significant negative correlations were evident between Brk. adj. RIT_{50} and the 'B' regression parameter (r=-0.493, P<0.0001) (Figure 2.6). Therefore an increase in Brk. adj. RIT_{50} was associated with a reduction in the gradient of the slope.

2009

Significant Differences in Brk. adj. RIT_{50} were observed between lines (P<0.005, Appendix 2.14 (page 257)) but not for the Pod Mass covariate (P=0.076). This highlighted that adjustment for Pod Mass had no significant effect on Broken RIT_{50} and is thought to be due to the non-random selection of lines in the sub-trial. The resistant line MC148 demonstrated the greatest Broken adj. RIT_{50} (72 s), as observed in the complete 2006 trial, whilst MC226 displayed the shortest duration (28 s) (Table 2.5). Brk. adj. RIT_{50} was reduced by 16 % in MC148 compared to Broken RIT_{50}, whilst in MC226 it was increased by 52%. Broken adjusted RIT_{50} was also reduced compared to unadjusted half life in Apex and DK142 (10 % and 24 %, respectively). Significant positive correlations were observed between Brk. adj. RIT_{50} and Pod Mass and Broken RIT_{50} as described in 2.3.3.1 and 2.3.4.2., respectively (Figure 2.7). Highly significant negative correlations were observed with the 'B' regression parameter (r=-0.794, P<0.0001). Increases in Brk. adj. RIT_{50} and hence PSR were associated with a decrease in the gradient of the progress curve.

Line	Apex	DK142	148	226
Pod Mass (g)	4.984	5.77	5.957	3.77
Broken RIT_{50} (s)	26.7	46.3	85.6	18.7
Broken adj. RIT_{50} (s)	23.9	35	72.2	28.4
Percentage +/-	-10.5	-24.4	-15.7	+52

Table 2.5: 2009 Broken RIT_{50}/Broken Adjusted RIT_{50} comparisons

2006|2009

In lines common to both years, no significant differences were evident between Brk. adj. RIT_{50}, lines (P=0.19), years (P=0.068) or interactions between line and year were evident (P=0.5, Appendix 2.16). This relates to the non-random selection of lines and variation between replicate samples. A mean reduction in Brk. adj. RIT_{50} from 76 s in 2006 to 46 s in 2009 was observed in the lines assessed. Increases in Brk. adj. RIT_{50} were observed in MC228, MC246 and MC259, whereas, the remaining lines demonstrated decreases in half life (Table 2.6). In the resistant MC148, the Brk. adj. RIT_{50} was reduced from 157 s in 2006 to 72 s in 2009 (-54%), whereas in the most susceptible line MC246, half life increased from 19 s in 2006 to 54 s in 2009 (+178%) on adjustment. Apex was observed to display an increased Brk. adj. RIT_{50} in 2009 compared to 2006 (+129%), whereas DK142 was greatly reduced (-77%). As for Intact/Intact adj.RIT_{50} the reduction could have been due to environmental variation, out-crossing or incorrect planting of the DK142 line. Although Int. adj. RIT_{50} appeared to be similar across both trials in Apex, differences in Brk. Adj. RIT_{50} indicates pods in 2009 were more resistant to degradation after breakdown had been initiated.

Line	Apex	DK142	148	228	246	259
Pod Mass (g) (2006)	5.195	5.67	5.957	4.501	3.826	3.77
Broken adj. RIT_{50} (s) (2006)	10.4	153.1	156.78	33.8	19.35	31.84
Pod Mass (g) (2009)	4.984	5.77	5.957	4.217	3.826	3.77
Broken adj. RIT_{50} (s) (2009)	23.9	35	72.2	47.7	53.9	35.6
Percentage +/-	+129	-77	-54	+41	+178	+10.6

Table 2.6: 2006/2009 Broken RIT_{50}/Broken Adjusted RIT_{50} comparisons

2.3.4.5 Progress Curve Fitting Parameter B

2006

Significant differences were observed between 'B' regression parameter and lines for Intact and Broken Pod data ($P<0.001$, Appendix 2.8, 2.10). Significant negative correlations were observed between the 'B' parameter and Pod Mass and Seed Damage, for Intact and Broken pods (2.3.3.1 and 2.3.3.3, respectively). Negative correlations were also identified between the 'B' parameter and Intact RIT_{50}, Broken RIT_{50}, Int. adj. RIT_{50} and Brk. adj. RIT_{50} as discussed previously (2.3.4.1, 2.3.4.2, 2.3.4.3 and 2.3.4.4, respectively). This highlights that as half life increases the gradient of the regression slope decreases, with resistant pods degrading at a slower rate than in susceptible lines. This indicates that resistant pods can absorb more energy endured during the Random Impact Test (RIT) than susceptible pods.

2009

Significant differences were observed between the 'B' parameter and lines for Broken pods ($P<0.001$, Appendix 2.14). The lack of significance between the 'B' parameter and lines in Intact pods is likely due to the non-random selection of lines and variability between replicates. Significant negative correlations were identified between the 'B' parameter and Pod Mass for Intact and Broken pods (2.3.3.1) and between Intact and Broken adjusted RIT_{50} (2.3.4.3 and 2.3.4.4, respectively).

2.3.5.1 Coefficient of Determination (R^2)

The coefficient of determination is a measure of the proportion of variability accounted for by the statistical model, utilising the correlation coefficient (r) as a basis to estimate this variation and the level of contribution from each characterised trait. This has been calculated for traits scored in the 2006 and 2009 trials (Figures 2.8 and 2.9 (pages 77 and 78, respectively)).

2006

It was evident that although a number of traits demonstrate significant correlations between each other, only those exhibiting highly significant associations ($P<0.0001$), were identified to

contribute to an excess of 20% or more of the variation accounted for. Correlations exhibiting lower levels of significance ($P<0.05$ to $P<0.001$) were observed to account for only small proportions of the variation identified between paired traits (<20%).

Of the traits identified demonstrating highly significant correlations, Pod mass (g) and Seed Mass were observed to contribute to approximately 78% of the variation between lines in both Intact and Broken pod data (Figure 2.8). This highlights that Seed Mass and Pod Mass are strongly associated. Evidently, these characters are auto-correlated with Seed Mass a constituent component of Pod Mass. The lack of a 100% association relates to variation in pod wall thickness, seed size and seed filling between lines. Association between Pod Mass and RIT_{50} was also identified and proposed to contribute to approximately 53% of the variation between the traits. This highlights the contribution towards PSR by Pod Mass. For broken pod data differences in Pod Mass and the 'B' regression parameter were observed to be responsible for 21.9% of the variation between traits, whereas, for intact pods only 12% of the variation could be accounted for between Pod Mass and the 'B' parameter. It appears that Pod Mass has a greater effect on the gradient of the regression and hence the rate at which degradation occurs in broken pods than in intact pods.

Seed Mass and RIT_{50} were also observed to be associated, with 22.56% of the variation accounted for in Intact Pods and 25 % in Broken Pods. This is suggests that Seed Mass is contributing to PSR either thorough absorbing energy from the RIT or by acting as component of Pod Mass. This is supported by the dissociation of the relationship observed in the adjusted RIT_{50} traits where the percentage of the variation is reduced to <1% when Pod Mass is accounted for. Differences in Seed Damage and adjusted RIT_{50} in Broken pods were attributed to 23% of the variation accounted for. This is suggested to be an effect of the adjustment of the RIT_{50} value for the covariate, removing the contribution of Pod Mass on PSR, resulting in a greater percentage of the variation accounted for. This was also observed for adjusted RIT_{50} in Intact pods but only 14% of the variation was accounted for.

In Broken pods, 34% of the variation was accounted for between Broken RIT_{50} and the 'B' parameter traits. This suggests that differences in Broken RIT_{50} are associated with differences in the gradient of the progress curve. This is supported by the finding that a highly significant negative correlation exists between Broken RIT_{50} and the 'B' parameter gradient. However, only 13% of the variation between Intact RIT_{50} and the 'B' parameter was observed between the traits, indicating the Intact RIT_{50} accounts for less of the variation in the slope.

Approximately 78% of the variation between Intact and Broken RIT_{50} and adjusted RIT_{50} s were accounted for by the model. This indicates a significant contribution between the two traits for Intact and Broken pods. This was anticipated as adjusted RIT_{50} is derived from RIT_{50}. As the traits were expected to be auto-correlated the lack of a higher percentage of accounted variation relates to the removal of the effects on half life contributed by Pod Mass.

Broken adj. RIT_{50} and the 'B' parameter accounted for 24% of the variation in half life. This is reduced by approximately 10% compared to the variation accounted for between Broken RIT_{50} and the 'B' parameter. This reduction in the variation accounted for between Broken adjusted RIT_{50} and 'B' parameter is a product of adjusting for the Pod Mass covariate. This reiterates the influence Pod Mass has on Pod shatter, at least in the Broken pod data set. Relationships between Pod Mass and Intact and Broken RIT_{50} have been established, with approximately 53% variation accounted for by the model. On adjustment for the covariate the amount of variation that can be accounted for is reduced to between 10-12% for adjusted RIT_{50} indicating that adjustment for Pod Mass may enable the identification of factors contributing to PSR which are independent of factors regulating pod architecture.

2009

With respect to the sub-trial from 2009, correlations between Pod Mass and RIT_{50} accounted for approximately 26% of the variation in Intact pods and 51% in Broken pods (Figure 2.9). However after adjustment for the covariate the amount of variation was reduced as observed for the 2006 trial further supporting the process of modulation to aid the identification of factors affecting PSR

independently of Pod Mass. As in the 2006 trial, a relationship between RIT_{50} and adjusted RIT_{50} was evident with Intact RIT_{50} observed to account for 78% of the variation in Intact adjusted RIT_{50}, whereas 86% of the variation could be accounted for between Broken RIT_{50} and Broken adjusted RIT_{50}. This was expected as the adjusted RIT_{50} is derived directly from the RIT_{50} value. Intact and Broken RIT_{50} were also observed to account for 67% and 61% of the variation for the 'B' regression parameter respectively. Therefore, half life appears to account for relatively large amounts of the variation in the slope of the regression for both pod categories, across trial years. Intact and Broken adjusted RIT_{50} were observed to account for approximately 56% and 63% of the variation in the 'B' parameter, respectively. This again highlights the relationship between increases in half life and effects on the regression gradient, as observed in the unadjusted RIT_{50} values.

2.3.5.2 Trait Heritability (H^2)

Broad-sense trait heritability for characters scored in POSH 1-3 lines are displayed in Table 2.7 for the 2006 trial and Table 2.8 for the 2009 trial (pages 71 and 72, respectively). The physical traits scored in the POSH 1-3 population were identified to be highly heritable in the 2006 trial. Pod Mass (g) and Seed Mass (g) exhibited high levels of heritability, both in excess of 75%. This was anticipated as crossing of the DK142 to the Apex parent was performed to improve agronomic potential and overall fertility of the POSH 1-3 population. Seed Damage was also identified to show high levels of heritability amongst POSH lines, with a value of 70% estimated for the trait. Intact and Broken RIT_{50} were also identified to demonstrate relatively high heritability of approximately 57% and 56%, respectively. This suggests that the traits are relatively robust and could perform well as targets for crop improvement. However, when the heritability of adjusted Intact and Broken RIT_{50} characters were calculated, it was evident that modulation for the Pod Mass covariate resulted in lower values of 35% and 30%, respectively.

We also identified significant variation between blocks in adjusted RIT_{50}. This indicates that when Pod Mass has been accounted for the trait is subject to more environmental variation than initially anticipated and highlights why the trait has been hard to introgress into commercial lines through conventional breeding strategies. This highlights the influence of Pod Mass on assessing PSR, and

that differences in Pod Mass may have confounded identification of differences in POSH 1-3 in previous outings. Trait heritability in the 2009 is not accurately represented due to the non-random of selection of lines in the sub-trial. This resulted in extremely high estimations of heritability for Pod Mass, RIT_{50} and adjusted RIT_{50}, all of which were identified to exhibit values in excess of 90%.

Trait	Source of Variation	d.f.	m.s.	v.r.	P	H^2 (%)
Pod Mass (g)	Line	77	3.5928	11.04	<0.001	75.904
	Residual	235	0.3253			
Seed mass (g)	Line	77	1.1996	10.89	<0.001	75.611
	Residual	234	0.1102			
Damage	Line	77	13.869	8.5	<0.001	70.162
	Residual	234	1.632			
Intact RIT_{50}	Line	77	3412.8	5.33	<0.001	57.609
	Residual	235	639.9			
Broken RIT_{50}	Line	77	6017	5.02	<0.001	55.846
	Residual	234	1199			
Intact Adj. RIT_{50}	Line	77	1569.8	2.73	<0.001	35.11
	Covariate	1	15605.4	27.09	<0.001	
	Residual	234	576			
Broken Adj. RIT_{50}	Line	77	2724	2.53	<0.001	30.198
	Covariate	1	29954	27.84	<0.001	
	Residual	233	1076			

Table 2.7: Trait Heritability for physical traits from 2006 trial displaying Traits, Sources of Variation, Trait degrees of freedom (d.f.), Mean sum of squares (m.s.), Variance Ratios (v.r.), Probability values *(P)* demonstrating significance levels and calculated broad-sense heritability (H^2) percentages

Trait	Source of variation	d.f.	m.s.	v.r.	P	H^2 (%)
Pod Mass(g)	Line	11	3.3425	10.6	<0.001	97.513
	Residual	67	0.3153			
Intact RIT_{50}	Line	11	1062.1	6.46	<0.001	98.570
	Residual	67	164.4			
Broken RIT_{50}	Line	11	2632.2	5.31	<0.001	96.869
	Residual	67	495.8			
Intact Adj. RIT_{50}	Line	11	729.4	4.93	<0.001	96.574
	Covariate	1	1242.6	8.39	0.005	
	Residual	66	148.1			
Broken Adj. RIT_{50}	Line	11	1611.2	3.53	<0.001	94.358
	Covariate	1	3077.2	6.74	0.012	
	Residual	67	456.6			

Table 2.8: Trait Heritability for physical traits from 2009 trial displaying Traits, Sources of Variation, Trait degrees of freedom (d.f.), Mean sum of squares (m.s.), Variance ratios (v.r.) and Probability values (P) demonstrating significance levels.

2006 Intact pods

	Pod Mass (g)	Seed mass (g)	Damage	Intact LD50	Y	A	B	C	Intact Adj. LD50
Pod Mass (g)	1								
Seed mass (g)	0.885	1							
Damage	-0.003	-0.363	1						
Intact LD50	0.729	0.5	0.271	1					
Y	-0.169	-0.256	0.113	-0.09	1				
A	0.014	-0.081	0.085	0.047	0.268	1			
B	-0.349	-0.122	-0.312	-0.362	-0.385	0.035	1		
C	0.205	0.289	-0.168	0.081	-0.812	-0.159	0.49	1	
Intact Adj. LD50	0.32	0.082	0.378	0.882	-0.008	0.055	-0.26	-0.03	1

	+ive	-ive
	<0.0001	<0.0001
	<0.001	<0.001
	<0.01	<0.01
	<0.05	<0.05

2006 Broken pods

	Pod Mass (g)	Seed mass (g)	Damage	Broken LD50	Y	A	B	C	Broken Adj. LD50
Pod Mass (g)	1								
Seed mass (g)	0.888	1							
Damage	-0.007	-0.356	1						
Broken LD50	0.737	0.475	0.342	1					
Y	-0.106	0.019	-0.214	-0.169	1				
A	0.033	-0.04	0.081	0.035	-0.78	1			
B	-0.468	-0.194	-0.394	-0.584	0.44	-0.373	1		
C	0.228	0.232	-0.086	0.316	0.293	-0.498	-0.024	1	
Broken Adj. LD50	0.344	0.055	0.481	0.888	-0.163	0.026	-0.493	0.284	1

Figure 2.6: 2006 POSH 1-3 trial Intact and Broken Pod Correlation (r) matrices

75

2009 Intact pods

	Pod Mass (g)	Intact LD50	Y	A	B	C	Intact Adj. LD50
Pod Mass (g)	1						
Intact LD50	0.508	1					
Y	0.096	0.027	1				
A	0.296	0.042	0.468	1			
B	-0.362	-0.819	0.255	0.126	1		
C	-0.401	-0.41	0.134	-0.203	0.736	1	
Intact adj. LD50	0.044	0.883	-0.021	-0.113	-0.752	-0.257	1

	+ive	-ive
	<0.0001	<0.0001
	<0.001	<0.001
	<0.01	<0.01
	<0.05	<0.05

2009 Broken pods

	Pod Mass (g)	Broken LD50	Y	A	B	C	Broken Adj. LD50
Pod Mass (g)	1						
Broken LD50	0.718	1					
Y	-0.2	-0.236	1				
A	-0.301	-0.217	0.512	1			
B	-0.439	-0.784	0.104	-0.233	1		
C	0.377	0.085	0.143	-0.593	0.175	1	
Broken Adj. LD50	0.41	0.93	-0.203	-0.125	-0.794	-0.088	1

Figure 2.7: 2009 POSH 1-3 Intact and Broken pods Correlation (r) matrices

2006 Intact pods

	Pod Mass (g)	Seed mass (g)	Damage	Intact LD50	Y	A	B	C	Intact Adj. LD50
Pod Mass (g)	100								
Seed mass (g)	78.3225	100							
Damage	0.0009	13.1769	100						
Intact LD50	53.1441	25	7.3441	100					
Y	2.8561	6.5536	1.2769	0.81	100				
A	0.0196	0.6561	0.7225	0.2209	7.1824	100			
B	12.1801	1.4884	9.7344	13.1044	14.8225	0.1225	100		
C	4.2025	8.3521	2.8224	0.6561	65.9344	2.5281	24.01	100	
Intact Adj. LD50	10.24	0.6724	14.2884	77.7924	0.0064	0.3025	6.76	0.09	100

2006 Broken pods

	Pod Mass (g)	Seed mass (g)	Damage	Broken LD50	Y	A	B	C	Broken Adj. LD50
Pod Mass (g)	100								
Seed mass (g)	78.8544	100							
Damage	0.0049	12.6736	100						
Broken LD50	54.3169	22.5625	11.6964	100					
Y	1.1236	0.0361	4.5796	2.8561	100				
A	0.1089	0.16	0.6561	0.1225	60.84	100			
B	21.9024	3.7636	15.5236	34.1056	19.36	13.9129	100		
C	5.1984	5.3824	0.7396	9.9856	8.5849	24.8004	0.0576	100	
Broken Adj. LD50	11.8336	0.3025	23.1361	78.8544	2.6569	0.0676	24.3049	8.0656	100

Figure 2.8: 2006 POSH 1-3 trial Intact and Broken Pod Coefficient of Determination (R^2) matrices

2009 Intact pods

	Pod Mass (g)	Intact LD50	Y	A	B	C	Intact Adj. LD50
Pod Mass (g)	100						
Intact LD50	25.8064	100					
Y	0.9216	0.0729	100				
A	8.7616	0.1764	21.9024	100			
B	13.1044	67.0761	6.5025	1.5876	100		
C	16.0801	16.81	1.7956	4.1209	54.1696	100	
Intact Adj. LD50	0.1936	77.9689	0.0441	1.2769	56.5504	6.6049	100

2009 Broken pods

	Pod Mass (g)	Broken LD50	Y	A	B	C	Broken Adj. LD50
Pod Mass (g)	100						
Broken LD50	51.5524	100					
Y	4	5.5696	100				
A	9.0601	4.7089	26.2144	100			
B	19.2721	61.4656	1.0816	5.4289	100		
C	14.2129	0.7225	2.0449	35.1649	3.0625	100	
Broken Adj. LD50	16.81	86.49	4.1209	1.5625	63.0436	0.7744	100

Figure 2.9: 2009 POSH 1-3 trial Intact and Broken Pod Coefficient of Determination (R^2) matrices

2.4 Discussion

Investigation Summary

Pod Shatter Resistance (PSR) was investigated in the POSH 1-3 population using a Random Impact Test to generate relative estimations of resistance in each line. This was achieved by fitting regressions using an automated model to pod degradation data to estimate the half life in Intact and Broken pods. Pod Mass (g), Seed Mass (g) and Seed Damage (0-9) were also assessed amongst lines to ascertain if these characters demonstrated any influence on PSR. We have observed that the PSR appears to be a complex trait and is influenced by environmental effects and physiological variation between lines. A full trial, comprising some 370 samples, was conducted in 2006 to gather as much information as possible from the population regarding shatter resistance and a number of physical characters perceived to potentially influence this. A reduced sub-trial comprising of a number of select lines demonstrating a range of shatter susceptibility and resistances were then cultivated to obtain replicated trial data. Although this could potentially reduce the accuracy and validity of future marker analysis, this approach was deemed suitable to assess levels of pod shatter across trial years in a coherent and manageable fashion. A previous year's trial data, generated from the same material, using a similar approach generated in 2000, was also available for subsequent marker analysis. Therefore, 10 population lines and the Apex and DK142 progenitors were selected as a basis for comparison with the initial 2006 trial.

Distribution of data in lines in 2006 trial

Initial assessments of scored traits in the 2006 dataset demonstrated that Pod Mass (g), Seed Mass (g) and Percentage Seed content (%) exhibited normal distributions. However, RIT_{50} for Intact and Broken pod data was observed to be highly non-normal, as was Seed Damage. The non-normal distribution of the half life trait was anticipated due to the complex, polygenic basis of the character. As Pod Mass demonstrated a normal distribution, and RIT_{50} did not, it could be suggested that the traits are selected independently of each other. However Summers *et al.* (2003) proposed that increases in Valve and Septum Mass (g) and in pod length are correlated with increases in PSR in POSH material. We also observed highly significant correlations between RIT_{50} and Pod Mass (g) in Intact and Broken pods. A more in depth dissection of characters

contributing to PSR in POSH lines conducted by Child *et al.* (2003) identified a number of physiological factors influencing shatter resistance more significantly than pod architecture, such as the thickness and orientation of vascular bundles within the fruit. Therefore, in this investigation utilising only RIT_{50} values as a basis for trait and QTL analysis may have biased selection in the identification of factors contributing to Pod Mass or size, not shatter resistance alone.

Due to its synthetic derivation, the range of variation in Pod Mass in POSH lines were observed to vary greatly compared to that of commercial parental cultivar Apex and potentially confounded the issue further. For this reason we decided to adjust half life in Intact and Broken pods by selecting a covariate in the generalized linear model, to attempt to dissociate the potential effects of extreme differences in Pod Mass between lines may have imposed. Adjustment for the covariate did not greatly improve normality, but did appear to improve the relative distribution in susceptible and intermediate lines and also reduce the range of the RIT_{50} distribution in all lines. Further transformation of the data using log and logit functions did not ameliorate the distribution of RIT_{50} or adjusted RIT_{50} traits. Although the distribution of Intact and Broken half life values and Seed Damage were non-normal, GLM (unbalanced analysis of variance (ANOVA)) was utilised to interrogate the data sets. This approach has been used previously to assess RIT_{50} in *B. napus* (Morgan *et al.* 2000), and McDonald (2006) proposed that as a regression based analysis ANOVA, is not too sensitive to moderate deviations away from normality, with normality not a requirement for calculation of sums of squares or degrees of freedom, estimation of constraints, main effects or interactions.

Differences in Pod Mass in POSH 1-3 lines have been observed

Pod Mass was identified to be significantly different between lines as was anticipated for a synthetically-derived segregating population. Previous crossing with the elite N-0-109 line and the SYN1 line and with the Apex and DK142 aimed to retain the shatter resistance trait whilst improving agronomic potential, pod set and mass and also decreasing infertility in the F_2 lines and derived DH lines of the POSH 1-3 population (Werner *et al.,* 2003a). However recurrent crossing

would be required to reduce this variation in pod characteristics and would risk loss of variation for other important traits. No significant differences were noted between lines and years indicating minimal environmental effects in the population. Pod Mass was observed to demonstrate a high level of heritability and therefore should not be subject to large environmental effects within or across different years. Significant differences in Pod Mass between Apex and DK142 were only observed in the 2009 trial although Summers *et al.* (2003) had previously reported that DK142 displayed a 23% reduction in pod weight compared to Apex. This could relate to out-crossing in the DK142 affecting Pod Mass in 2006 and 2009.

Pod Mass was positively correlated with Seed Mass accounting for 78% of the variation in Intact and Broken pods, suggesting heavier siliques also displayed greater seed weights. As these characters are auto-correlated this was anticipated. Correlations between Pod Material Mass (Silique tissue not including the seed) and Seed Mass demonstrated a lower significance, indicating differences in pod wall thickness, seed size; seed number or fertility leading to variation in seed filling may have affected the relationship between Pod Mass and Seed Mass.

Pod Mass was also negatively correlated with the 'B' regression parameter in Intact and Broken pods from 2006 and in Broken Pods from 2009, indicating that increases in mass are associated with decreases in the gradient of the progress curve. This suggests that Pod Mass contributes increase in half-life, and hence may also contribute to increases in shatter resistance.

Evidently, Pod Mass was also positively correlated with Intact and Broken RIT_{50} in the 2006 trial accounting for 53% of the variation, indicating larger, heavier pods were associated with an increased shaking duration and hence increases in resistance to shattering. Pod mass was also correlated with Intact and Broken RIT_{50} in the 2009 trial, with approximately 26% of the variation for Intact pods and 51% of the variation in Broken pods accounted for. This is in agreement with Summer *et al.* (2003), who identified that increases in valve and septum/beak mass correlated with PSR in POSH 1-3 progenitors and F_2 lines. It seems logical that a larger receptacle could endure more force per unit area during the assessment with the RIT. Adjustment of the RIT_{50}

values, selecting Pod Mass as a covariate, reduced the significance of the association in both Intact and Broken pods in both trial years, suggesting PSR may be selected for at least partially independently of Pod Mass. Child *et al.* (2003) also proposed physiological factors which contributed more significantly than increases in Pod Wall Thickness (PWT) and Summers *et al.* (2003) demonstrated that taller, more vigorous, plants exhibited increased levels of shatter resistance, as did individuals which had racemes removed, reducing pod number. It may simply be that plants with heavier pods have had better establishment, enabling the individual to grow larger, permitting the diversion of resources into pod growth or be more resilient to variation in environmental pressures such as weather and therefore have a greater ability to produce shatter resistant pods. More rigorous assessment of growth characters, such as height, pod number per plant, pod length, components of pod mass or pod wall structure may help gain insight into how differences in Pod Mass affect PSR in *B. napus*.

Differences in Seed Mass have been observed in POSH 1-3 lines

We identified significant differences in Seed Mass between POSH lines. Heritability of the Seed Mass trait was relatively high and therefore should not be subject to large environmental effects within or across different years. As Seed Mass is a component of Pod Mass, it is proposed that the wide range of variation observed in individual lines relates to the synthetic derivation of the populations progenitors. The basis for this difference could relate to a number of factors including; poor fertility through self incompatibility, lack of pollen production or misregulation of anther dehiscence, through poor agronomic background resulting in weak, weedy or stressed plants or potentially due to chromosomal rearrangements resulting from reciprocal or non-reciprocal translocation events during meiosis (Werner *et al.,* 2003b). We observed significant differences between Apex and DK142 for Seed Mass, although this was considerably reduced compared to the levels of a 55% reduction in DK142 suggested by Summers *et al.* (2003). This suggests a degree of out-crossing may have occurred in the DK142 material confounding results. Highly significant positive correlations were identified between Seed Mass and Intact and Broken RIT_{50}, as for the Pod Mass character, although this only accounted for approximately 22% of the variation in Intact pods and 25% in Broken pods. This indicated that increases in Seed Mass are associated with

increases in half life and hence resistance to shattering. However no significant correlation was evident between Seed Mass and adjusted half life, indicating that the relationship with RIT_{50} is due to the influences of Pod Mass and not Seed Mass directly.

Negative correlations with Seed Damage highlight that as Seed Mass increases the relative amount of Damage is decreased. This could be explained by greater relative amounts of seed absorbing the energy from shaking, resulting in less energy input per seed, by relatively larger seed in lines with greater Seed Mass, or through heavier seed exhibiting a character rendering it less susceptible to damage *i.e.* a thicker testa or greater seed fibre content. It would of interesting to investigate the relationship between Seed Mass, Seed Size and relative resistance to damage.

Variation in Percentage Seed Content was also investigated in POSH 1-3 lines. This was derived from the difference in Seed Mass compared to Pod Mass. Significant differences between Apex and DK142 were observed, with a greater Percentage Seed Content evident in the susceptible parent. This highlights that the partitioning of seed compared to the receptacle was greater in Apex as indicated by Summers *et al.* (2003). Variation in Percentage Seed Content in the population relates to reduced fertility in the DK142 parent line and also an increase in Pod Wall Thickness (PWT) compared to Apex (Werner *et al.* 2003a; Child *et al.,* 2003). The relationship in PWT and PSR will be investigated and discussed in the subsequent chapter.

Differences in Seed Damage have been identified in POSH 1-3 lines

Investigations were conducted in to the levels of Seed Damage in pod samples after RIT assessment. We observed significant correlations between Seed Damage and RIT_{50} and adjusted RIT_{50} values. Therefore pods from resistant lines exhibit greater levels of Seed Damage compared to less resistant lines. Seed Damage was also observed to be non-normally distributed and its range is comparable to RIT_{50} distribution so may potentially be linked with half life. As only approximately a quarter of the variation is accounted for by the model by the Broken adjusted RIT_{50} trait and less that 15% for Intact RIT_{50} character this suggests other factors are also contributing to higher levels of Seed Damage. It must also be considered that although most

resistant lines display moderate to high levels of damage they are shaken between an average of 40 and 140 seconds longer compared to the nearest line exhibiting moderate levels of damage. Therefore, it is likely pods from resistant lines have received increased energy inputs compared to more shatter susceptible samples and are subsequently subjected to higher levels of damage. This could suggest that Seed Damage is acting as a proxy for RIT_{50}. The negative association between Seed Damage and 'B' regression parameter is suggested to be due to effects from RIT_{50} and adjusted RIT_{50} values and not necessarily a true representation of the relationship between damage and its effect on the gradient parameter.

An approach to overcome the issue of accurate trait assessment may be to investigate Seed Damage in a subset of lines demonstrating similar half lives or only in those lines represented within a normal distribution (and not in strongly resistant lines with extended shaking durations). It is suggested that an assessment enabling measurement of the progressive level of damage, *e.g.* the rate of seed degradation on shaking, maybe an approach to potentially gain greater insight into differences seed breakdown between lines. The RIT was observed to be an extremely vigorous assay generating somewhat arbitrary data with respect to Seed Damage. Therefore, it would be desirable to develop a more discreet, quantifiable technique to assess differences in *Brassica*. Investigation into variation in levels of Seed Damage are of interest to industry with respect to identifying seed coat characters that could be exploited to improve agronomic potential, such as testa thickness or seed fibre content to improve oil yield or protein meal quality (Wittkop *et al.,* 2009). It would also be of interest to study variation in Seed Damage in wild *Brassica* or Brassicacea species, to investigate if differences in seed strength provide a selective/adaptive advantage in 'extreme' environments. It could be perceived differences in seed strength or testa thickness may promote selective advantage, with respect to seed dormancy or persistence. For example do natural accessions of *Arabidopsis thaliana* demonstrate variation in seed strength? Investigating natural variation in *Arabidopsis* ecotypes for the trait could potentially an approach to attempt this and may provide targets to study this in related *Brassica* species.

Differences have been observed in unadjusted and adjusted Intact/ Broken RIT$_{50}$ in POSH 1-3 lines

To enable the most accurate assessment of variation in PSR in the POSH 1-3 population we utilised two different measures; that of the frequency of Intact pods and Broken pods over the shaking duration of the RIT. This provided the most informative method of pod breakdown available, allowing assessment of potential differences in the shattering profile. RIT$_{50}$ distribution and hence PSR in the full trial was observed to be wide and non-normal, as reported by Child *et al.,* (2003). The majority of POSH 1-3 lines were observed to display Intact and Broken RIT$_{50}$ equal to or less that the susceptible Apex parent. Only three lines were demonstrated to exhibit Intact half-lives greater than the resistant DK142 parent and only one line displayed a Broken RIT$_{50}$ in excess of DK142. Only a small frequency of offspring demonstrate the shatter resistant phenotype supporting the suggestion that the PSR trait is under polygenic control and regulated by multiple potentially recessive factors and hence only manifested in a small number of POSH lines (Morgan *et al.* 1998; Child *et al.,* 2003; Summer *et al.,* 2003; Werner *et al.,* 2003a). The observation of positive transgressive segregants, demonstrating increased Intact and Broken RIT$_{50}$ values compared to the resistant DK142 may also reflect a degree of out-crossing in the parent line. Transgressive segregation could also be attributed to positive heterotic effects on crossing, although, with a lack of data of shatter resistance data in F$_2$ lines to make comparisons to RIT values in DK142 in Summers *et al.,* (2003), this is difficult to substantiate as we do not have a true-breeding DK142 line to assess.

Significant correlations were detected between RIT$_{50}$ scores and Pod Mass (g), Seed mass and Seed Damage and also adjusted RIT$_{50}$. Correlations between Intact and Broken RIT$_{50}$ and respective adjusted RIT$_{50}$ values for the 2006 and 2009 trials were highly significant, with variation in excess of 75% accounted for by the model. This finding was anticipated as adjusted RIT$_{50}$ was derived from the initial half- life in each case and suggests that although some influences from Pod Mass appear to contribute to the characters, it may be possible to select for factors regulating RIT$_{50}$/adjusted RIT$_{50}$ independently to those selecting for increases in mass.

We also identified significant negative correlations between RIT_{50} and the 'B' regression parameter. This is was anticipated as, with increasing duration of the shaking period inferred through increased resistance to shattering in both Intact and Broken pods, one would predict a greater RIT_{50} value and hence reduced gradient of the regression.

With respect to Intact and Broken pod half-life, we observed significant differences between lines in 2006 trial. Although a representative subset of susceptible, intermediate and resistant lines was selected for the 2009 sub-trial, significant differences could not be established for half-life. This was due variation in replicate samples and also the reduced level of PSR experienced in the trial year. However, in the nine lines common to both trials, although differences between lines were observed not to be significant between each other, they were for individuals across years. This indicated that the PSR trait was subject to environmental effects. Trait heritability in 2006 was observed to be in excess of 50%, suggesting that the RIT_{50} characters, and hence PSR, were not subject to large influences from environmental effects and therefore factors contributing the trait pose potential targets for crop improvement. However, when trait heritability was calculated from the adjusted RIT_{50} values, the initial estimates were reduced to approximately 35% for Intact adjusted RIT_{50} and 30% for Broken adjusted RIT_{50}. PSR therefore may be subject to greater levels of environmental variation than first anticipated in this investigation and supports the difficulties found in attempting to breed successfully with the POSH 1-3 material (Werner *et al.,* 2003a).

Between POSH 1-3 lines, year effects, resulting from large-scale environmental differences such as in rainfall, wind conditions or temperature across a season, impact on the trait as a whole within the population, not solely in individual lines. Variation in the level of shattering has also been observed in a commercial *B. napus* variety Castille (Dekalb, U.K.) grown in separate trial years (Wood, unpublished). Reports have also highlighted how factors such as plant height and the number of pods per plant could affect PSR in POSH lines (Morgan *et al.* 1998; Summers *et al.* 2003). The reduction in PSR in the majority of lines grown in 2009 relates to growth conditions within a trial year, and resulting in differences in the status of the plants compared to that in 2006. Child *et al.* (2003) identified roles for physiological factors in increased PSR in POSH lines;

specifically differences in the vasculature of the silique. Potentially, if growth conditions were sub-optimal in a one year compared to another, it is feasible that a relatively 'weaker' plant may produce less resistant pods than a plant grown under better conditions. To establish if this is the case, an extended investigation, encompassing measurement of a range of environmental factors across trials years that may influence such occurrences would have to be performed. Assessment of the same line grown under different conditions, i.e. drought/non drought, high/low temperature, different light conditions or high/low wind conditions may also provide insight into the effects of variation observed between trial years.

It should be noted that growth conditions were different between the two trials with a long, dry spring and summer in 2006 compared to a dry spring and wet summer in 2009 (www.metoffice.gov.uk/climate/uk).   However, although subject to environmental effects and therefore variable between years, the most resistant lines in the POSH 1-3 population were identified consistently in both trials. Therefore although the PSR trait is environmentally sensitive it appears that it could still be successfully selected for as a target to improve pre-harvest pod shatter in *B. napus.*

In this investigation, with a desire to try to assess PSR independently of the effects of Pod Mass, we decided to adjust RIT_{50} using a covariate. This was conducted to improve the accuracy of subsequent marker analyses, where loci contributing to Pod Mass may have inadvertently been selected due to the correlations identified with the initial Intact and Broken RIT_{50} measurement. Adjustment for the covariate resulted in a reduction in the initial ranges of the distribution of Intact and Broken, decreasing the half life in samples with heavy pods and increasing the duration in lighter samples. In the assessment we identified significant differences between lines in Intact and Broken adjusted RIT_{50} values and the covariate in both trial years.

Due to the adjustment process estimating the modulated RIT_{50} as a mean value and not for individual samples, comparison for statistical significance was not feasible within or across trial years. However comparisons could still be made; With respect to the relationship between

parental lines DK142 was observed to display increased adjusted RIT_{50} durations compared to Apex during the 2006 trial and Broken adjusted RIT_{50} during 2009. However, Intact adjusted RIT_{50} in the 2009 was observed to be reduced in DK142 compared to Apex. Adjusted half life in DK142 was strongly reduced, raising the suggestion as previously, that out-crossing, may be responsible for this outcome. Although, Broken adjusted RIT_{50} in DK142 was increased compared to Apex, this level was still reduced compared to other shatter resistant lines supporting the argument for loss of homozygosity in DK142. Potentially, sequencing of the two parent lines and a selection of the population may give more insight in to the DK142 line.

Intact and Broken half-lives inform us of differences in the shatter profiles of the lines being tested. Intact RIT_{50} gives us insight into pod integrity *i.e.* the difference in the energy required to begin to initiate pod opening and Broken pods informs us about valve shedding and the energy required to ensure pods completely dehisce. Assessment of different measures of shatter resistance also gives a greater degree of resolution when conducting marker analysis to aid identification of QTL contributing to increases in PSR. It would be interesting to assess the difference between the Intact and Broken half life in lines as this may shed further light on characters contributing to shatter resistance. Reduced association with the covariate in adjusted RIT_{50}, compared to RIT_{50}, suggests that factors contributing to adjusted RIT_{50} values and hence PSR, may be selected for independently of Pod Mass. Due to the inherent variability in POSH lines with respect to Pod Mass, it may be of benefit to assess the trait in background where such variation is minimised, but not at the expense of genetic diversity. The new Temple x MC169 mapping population, itself derived from a shatter resistant POSH 1-3 line may present a valuable resource for such an investigation.

We have successfully identified differences in Pod Shatter Resistance between lines of the POSH 1-3 populations. The data generated from this investigation will form the basis from which to conduct a QTL analysis to aid the identification of potential candidates contributing to PSR in *B. napus*, with scope for developing tools for use in marker assisted selection (MAS)*.* We have observed that RIT_{50}, a measure of PSR in POSH lines, is relatively heritable and robust trait.

Although subject to the effects of environmental variation across years, factors regulating shatter resistance may pose as viable targets for selection and introgression into commercial OSR cultivars to improve the effects of pre-harvest pod shatter. We will now describe investigations into physical factors contributing to increases in PSR in the POSH 1-3 population.

Chapter 3: Anatomical Assessment of Factors Contributing Towards PSR in POSH 1-3

3.1 Introduction

In nature, pod shattering is common in a wide range of plant species, allowing seed to be disseminated, only when fully mature. From the perspective of domestication, uncontrolled seed-shattering is an undesirable feature retained from wild progenitor species and is a direct target for crop improvement to reduce the loss of seed for the grower. Anthropogenic selection against this trait has already been identified in cultivated crops species such as rice (Konishi *et al.,* 2006; Lin *et al*., 2007) and although some reports have identified resistance to seed shattering in *Brassica* species, the majority of modern commercial *B. napus* cultivars are relatively susceptible to pre-harvest seed loss due to pre-harvest pod dehiscence (Prakash and Chopra*,* 1990; Wang *et al.*, 2007; Morgan *et al.,* 1998, 2003).

Decreases in pre-harvest pod shatter have been reported in synthetic *B.napus* lines, developed from inter-specific hybridization between *B. rapa* var. chinensis and *B. oleracea* var. alboglabra (Morgan *et al.,* 1998, 2000). A doubled haploid (DH) mapping population derived from this material, termed POSH 1-3, has also been identified to demonstrate increased PSR (Summers *et al.,* 2003). Differences in the levels of PSR in POSH 1-3 progenitor DK142 and F_2 lines are mediated through a number of anatomical differences in pod structure; including the size and orientation of the major vascular bundle of the valve (MVBV) and also increases in pod length and weight (Child *et al.* 2003; Morgan *et al.,* 1998; Summers *et al.* 2003). The MVBV is reported to be a key contributory factor in the PSR phenotype in DK142 and F_2 lines. Roles for cellulases are also important in *B. napus* pod dehiscence, mediating degradation of a thin file of cells, termed the separation layer (SL), ensuring valves can detach freely from the replum during pod shattering (Meakins & Roberts 1990 a, b; Petersen *et al.* 1996).

In this chapter, investigations to identify potential physiological differences in vascular architecture and pod structure in shatter susceptible and resistant lines POSH lines are described and were performed to ascertain if similar factors identified in the resistant DK142

progenitor can be attributed to increased levels of PSR. Sectioning and staining will be utilised to elucidate both size and orientation of vascular potentially contributing to increases in shatter resistance. Investigations to identify differences in the degradation of the separation layer (SL) and a range of assays utilised to address potential differences in the activity of hydrolytic enzymes in SL breakdown are discussed.

3.2 Materials and Methods

3.2.1 Plant material

POSH 1-3 seedlings were germinated in soil in a glasshouse and grown to the six-leaf stage prior to a six-week vernalisation period at 5°C in a CER with reduced lighting. Post vernalization, plants were transplanted into 1 litre pots and arranged in a quadruple randomised design, in the greenhouse (Figure 3.1). Plants were grown in natural light, under long day conditions. Plants were shaken vigorously at daily intervals to encourage pollination. Individual flowers were tagged at anthesis. Fruits for sectioning/staining were harvested, at intervals of 10, 35, 40 and 60 days after anthesis (DAA) and fixed in 3.7% FAA solution (formaldehyde acetic acid) (3.7% formaldehyde, 5% acetic acid, 50% ethanol (EtOH) In ddH_2O). 70DAA senesced fruit were also collected and kept in a dry, cool environment prior to assessment. Investigations were principally targeted towards susceptible and resistant lines (Apex, DK142, MC148 and MC169). Tapidor, an 'old' relatively shatter-susceptible elite variety was included in the trial as a control, and behave similarly to Apex.

Apex	DK142	Tap	148	169	177	226
148	Tap	177	Apex	226	169	DK142
169	226	DK142	177	148	Apex	Tap
Tap	177	Apex	169	DK142	226	148

Figure 3.1: Randomised planting design for greenhouse grown POSH 1-3 lines

3.2.2 10 DAA and 40 DAA Pod Tissue Fixation, Clearing and Staining

Whole 10 DAA and basal regions of 40 DAA pods, from select POSH 1-3 lines, were placed in 10 ml 3.7% FAA (Formaldehyde Acetic Acid) solution in 20 ml scintillation vials. Vials were loosely covered and vacuum infiltrated for 15 mins until all fruit sank on release of the vacuum. Pod material was then rinsed in 10 ml 0.1 M KH_2PO_4 for 2 hrs and subsequently cleared in 10 ml, 8M NaOH, whilst shaking for 12 hrs. Fruit was rinsed in 10 ml 0.1M KH_2PO_4 for 2 hrs, followed by 30 mins staining in 0.1% Aniline Blue dye solution (KH_2PO_4 0.1 M buffer, 0.1 g/100 ml Aniline Blue dye) for specific staining of callose in the vasculature. Pods were rinsed for a further 2 hrs in 0.1 M KH_2PO_4 buffer post-staining to remove residual stain. Cleared, stained fruits were visualized under a Leica MZ16 (Leica, U.K.) dissecting microscope. Five different pods from each line were assessed.

3.2.3 35, 40 and 60 DAA Tissue Fixation, Sectioning and Staining

Harvested pods were cut into apical, medial and basal sections using a razor blade and immediately placed in 20 ml scintillation vials containing 10 ml 3.7% FAA solution (see below). Vials were loosely covered and vacuum infiltrated for approximately 15 mins, until all fruit sank on release of the vacuum.

Samples were left to fix overnight on a shaker then subsequently rinsed with 50% ethanol (EtOH) and subsequently taken through the following series of 50%, 60%, 70%, 80% and 90% for 30 mins at each stage, whilst shaking at room temperature (RT), followed by overnight incubation at 4°C in 95%with three subsequent washes in 100% EtOH

This was followed by Histoclear washes (National diagnostics, Hull, U.K.) consisting of a series of 75% EtOH/25% Histoclear (75E/25H) , 50%E/50%H, 25%E/75%H and 100% Histoclear again conducted at RT, with 30 minutes incubation whilst shaking, followed by an overnight incubation in Paraplast (Paramat-Gurr, VWP International)/Histoclear (50/50). Samples were then incubated over-night at 60°C in an oven. Six subsequent changes of Paraplast with incubation at 60°C for four hours between each change were made. Tissue

was then embedded in Paraplast within a plastic tissue cassette for sectioning and stored in the fridge at 4°C.

Sectioning

Tissue sectioning was conducted on a Leica microtome. Sections of 12 μm were prepared from select POSH 1-3 lines (Apex, DK142, MC148 and MC169) from 35, 40 and 60 DAA pods. Longitudinal sections were generated in 35 DAA and transverse sections in 40 and 60 DAA fruits. Paraplast ribbons produced when sectioning were floated on a water bath at 40°C. Ribbons were linked adjacently and attached to a polysine-coated glass slides using a fine paint brush to guide the wax strips. Prepared slides were dried on a slide warmer overnight at 45°C. Slides could be stored indefinitely at 4°C.

Staining

Prior to staining, slides were de-waxed through immersion in two, 10 mins washes, of 100% Histoclear, and two subsequent, two mins washes, of 100% EtOH. Slides were air dried for 30 mins. Siliques were stained using a 0.1% Alcian Blue/0.05% Safranin-O dye solution (solubilised in 0.1M Na-acetate buffer pH5.0) for 30 mins until colour had developed and then rinsed in ddH$_2$O. Slides were air dried for 1 hr, set in Histomount (National diagnostics, Hull U.K.), and covered with a glass shield. Slides were dried overnight at RT in the dark. Slides were observed under a Leica MZ16 dissecting microscope.

3.2.4 Physiological Trait Measurements in 35, 40 and 70 DAA POSH 1-3 Siliques

A series of physical measurements were performed on POSH 1-3 sections from 35 and 40 DAA pods and 70 DAA detached senesced valves. Imaging of samples was performed using the Leica MZ16 microscope followed by assessment with Sigma scan Pro 5 software. Statistical analyses were performed on Genstat V.12 (Payne *et al.* 2009), using two-sample paired/unpaired *t*-tests to identify potential significant differences between individual lines and one-way analysis of variance (ANOVA) for assessment between all lines.

3.2.4.1 Vascular Orientation and Height in Longitudinal Sections from 35 DAA Pods

The thickness and orientation of the MVBV in select POSH lines were assessed in 35 DAA longitudinal sections stained with 0.1% Alcian Blue/0.05% Safranin-O dye solution. Sections were mounted vertically with the pedicel pointing upwards. Vascular bundles were assessed as they cross the valve margin at the base of the fruit, across the dehiscent zone, into the valve. The angle of the MVBV was estimated by positioning a horizontal line to the base of the MVBV at the point it crosses the valve margin and a second angled line, through the centre and in the same orientation as the bundle, from the valve until it reached the pedicel (Figure 3.2). Five different MVBVs were measured for each line assessed.

To assess potential differences in MVBV height (millimetres, mm), a straight line was fitted horizontally across the bundle at the interface between the Lignified layer (L.L.) and Separation Layer (SL) (Figure 3.3). This was performed in five different MVBVs per line.
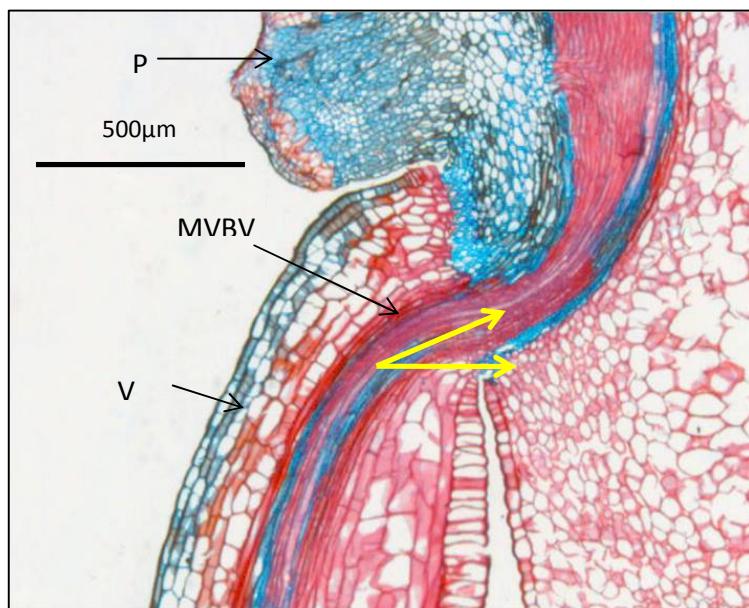
Figure 3.2: 35 DAA longitudinal section of *B. napus* POSH 1-3 MC169 silique. Yellow arrows fitted for measuring MVBV orientation, scale: 500µm, MVBV: Main vascular bundle of valve, P: Pedicel and V: Valve
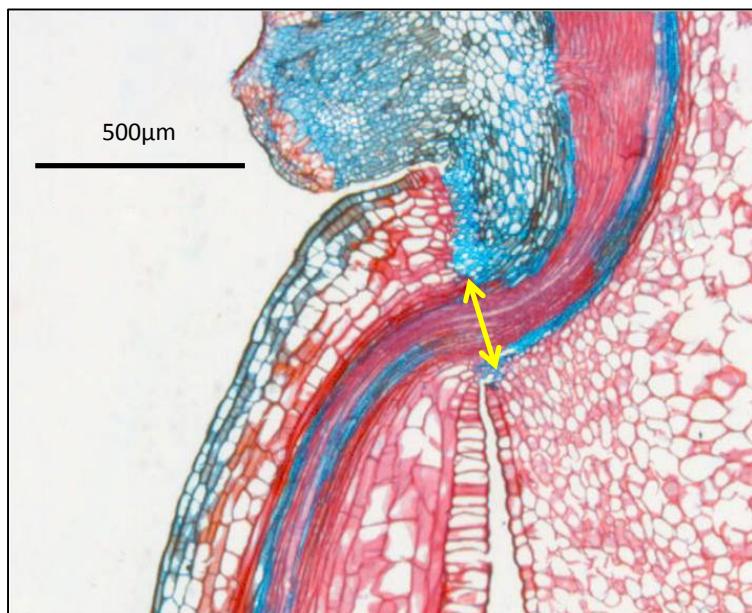
Figure 3.3: 35 DAA longitudinal section of *B. napus* POSH 1-3 MC169 silique. Yellow arrow fitted for measuring MVBV thickness (mm), scale: 500µm

3.2.4.2 Assessing Pod Wall Thickness (PWT) in POSH 1-3 Lines

The thickness of pod walls (mm), in medial transverse sections from 40 and 60 DAA pods from select POSH lines was assessed after staining with 0.1% Alcian Blue/0.05% Safranin-O dye solution (Staining non-lignified and lignified tissues, respectively). Measurements were made by fitting a straight line from the outer epidermis to endocarp layer B using Sigmascan pro 5 software (Sysat software, Inc). Three random measurements were taken from each of three independent sections per line (Figure 3.4). Mean values for PWT for each section were derived from the three biological replicates.
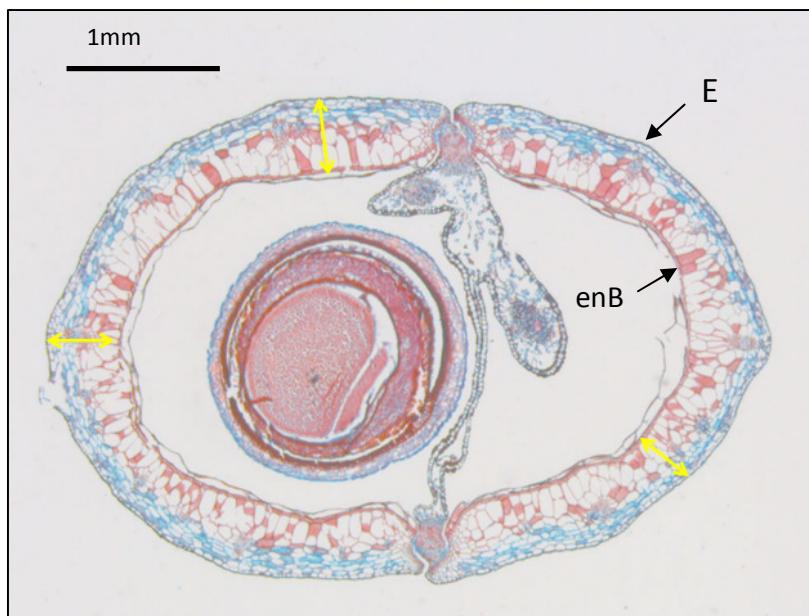
Figure 3.4: 40 DAA transverse section of a *B. napus* silique (Apex). Yellow arrows highlight regions measured for pod wall thickness. E: Epidermis, enB: Endocarp layer B, scale: 1mm

3.2.4.3 Vascular Bundle Thickness in 70 DAA Detached, Senesced Valves

The width of the MVBV was measured in detached valves from 70 DAA senesced pods in select POSH lines using Sigmascan pro 5 software (Figure 3.5). 10 valves were assessed from each line.
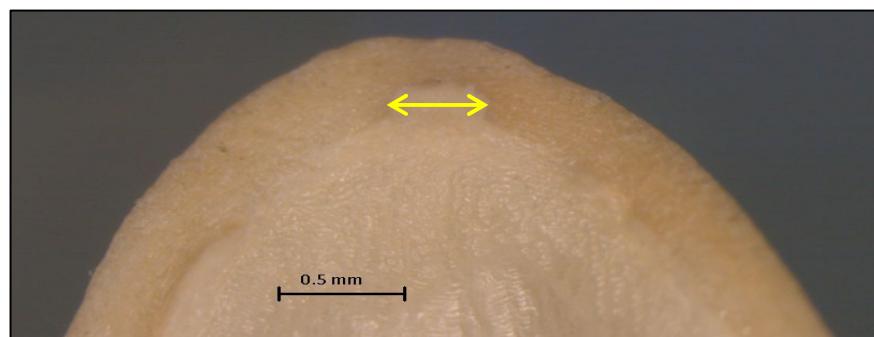
Figure 3.5: Image of basal region of senesced 70 DAA detached valve for MVBV width assessment. The yellow arrow highlights the vascular bundle width, scale: 0.5mm

3.2.4.4 Visual Assessment of Separation Layer Degradation in Select POSH 1-3 Lines

A visual comparison of separation layer (SL) integrity pre and post-cellulase activation was performed in medial and basal sections of 40 and 60 DAA pods in select POSH lines (Figures 3.10 and 3.11). Differences in Alcian Blue staining and changes in appearance of the cells at the SL indicated potential breakdown caused by enzyme activity in susceptible and resistant lines.

3.2.5 Assessment of Cellulase Activities in POSH 1-3 Lines

3.2.5.1 Fruit Collection for Cellulase Activity Assays

Select POSH 1-3 lines were cultivated as described in 3.2.1. For viscometric and colorimetric cellulase assays, pods at 40, 45, 50, 55 and 60 DAA were collected from Apex, DK142, MC148, MC169, MC177, MC226 and Tapidor lines. The dehiscence zone (DZ) and replum were dissected away from the valve tissue with a razor blade and frozen immediately on liquid nitrogen (LN_2). Samples were then transferred to a -80°C for storage. For global cellulase assays fresh 45 DAA pods were harvested immediately prior to assessment.

3.2.5.2 Enzyme Extraction

Prior to viscometric and colorimetric testing, 500 mg of frozen DZ/replum and valve samples were ground separately on liquid nitrogen to a fine powder, then 1000 µl Na-acetate pre-extraction buffer added (50mM pH 6.0 Na-acetate buffer with PMSF 1 mM). Samples were transferred to a 2 ml eppendorf tube, sealed and centrifuged at 13,000 rpm, at 4°C for 30 mins. The supernatant containing the soluble protein fraction was then discarded. Samples were kept on ice and re-suspended in 1000µl 1M Sodium chloride (NaCl) extraction buffer (1M NaCl in pH 6.0 Mcilvaine buffer (12.63 ml 0.2 M Na_2HPO_4/ 7.37 ml 0.1 M Citric acid per 20 ml)). Tubes were transferred to a cold room (4°C) and spun on an eppendorf mixer at 60 rpm for 2 hours. Samples were then re-spun 13,000 rpm, at 4°C for 30 mins and the supernatant (containing solubilised polygalacturonase fraction) aliquotted into fresh eppendorf tubes. All tubes were then stored on ice. (Adapted from Pressy, 1986; Truelsen and Wyndaele 1991)

A Bradford assay was utilised to determine the relative protein concentration in each extracted sample. A standard curve was generated using BSA at a concentration of 0, 100, 250, 500, 750 and 1000 µg/ml and relative absorbance determined at 595 nm (Bradford, 1976).

3.2.5.3 Substrate Solution Preparation

1% solutions of carboxy-methyl cellulose (CMC), pectin and polygalacturonic acid (Sigma-Aldrich, U.K.) were prepared, respectively, by dissolving substrates in Mcilvaine buffer (10.30 ml 0.2 M Na_2HPO_4/9.70 ml 0.1 M Citric acid per 20 ml) at pH 5.0 at 60°C. The solution was maintained at 60°C whilst stirring with a motorised flea. The solution was left for 30 mins until substrates had completely solubilised. The solutions were stored at 4°C until use.

3.2.5.4 Viscometric Assay for Cellulase Activity Assessment

A 2 ml glass pipette was mounted in a clamp stand in a controlled environment room (CER) at 22°C. Standard solutions containing 2 ml of 1% polygalacturonic acid, 1% carboxymethylcellulose substrate and 1% pectin substrates were prepared as in 3.2.5.3. The pipette was filled with the substrate and equilibrated for 30 mins. The initial outflow rate (secs) of three consecutive runs was recorded. After the standard outflow rate had been ascertained, 200 μl of respective enzyme extracts from Apex, DK142, MC148 and MC169 pods were added to individual 2 ml aliquots of substrate, immediately prior to viscometric analysis. Three consecutive initial outflow periods were recorded, followed by three outflows after 5 min and 10 min incubation intervals, for each respective sample tested. (Adapted from Truelsen and Wyndaele, 1991).

3.2.5.5 Neocuproine Assay to Detect Reducing Sugars Associated with Polygalacturonase Activity

A neocuproine (2, 9-dimethyl-1, 10-phenanthroline) based colorimetric assay, to detect the reducing sugars generated by polygalacturonase, was utilised to assess enzyme activity in select POSH 1-3 lines (Apex, DK142, MC148 and MC169) (Dygert *et al.*, 1965; Besada *et al.*, 1989). A 1% polygalacturonic acid substrate was prepared as described in section 3.2.5.3.

A series of reaction tubes was prepared in triplicate; consisting of reagent blanks containing 1 ml of Mcilvaine buffer (pH 5.0) and 5 ml of PGA substrate, sample assays containing 1 ml of enzyme extract and 5 ml of 1 % PGA and sample blanks containing 5 ml of buffer and 1 ml of enzyme. Tubes were incubated in a water bath at 37°C for 60 mins. A D-galacturonic acid

standard at 1 mg/ml in Mcilvaine buffer (pH 5.0) was prepared and aliquotted in triplicate to produce a series of standard tubes at concentrations of 10 µg, 25 µg, 50 µg, 75 µg, 100 µg and 125 µg with respective dilution in Mcilvaine buffer (pH 5.0) for generating a standard curve. After incubation, the reaction tubes were immediately placed on ice to halt the reaction. 100 µl from each tube was then aliquotted in fresh tubes. To each reaction tube and standard tube aliquot were added 2 ml of reagent 'A' and 2 ml of reagent 'B'. For reagent 'A': 40g Na_2CO3, 16 g glycine and 450 mg $CuSO_4$ 5H2O was dissolved in 600 ml ddH_2O and brought up to 1 litre with ddH_2O. For reagent 'B': 1.2 g Neocuproine-HCl was dissolved in 1 litre ddH_2O. Tubes were mixed and placed into boiling water for 12 minutes. Tubes were immediately cooled in tap water and 2 ml ddH_2O added to each tube. Tubes were mixed and their absorbance read at 450 nm against a water blank. A standard curve was generated from the standard series (Figure 3.6) (Dygert *et al.,* 1965; Worthington Biochemical Corporation protocol, www.worthington-biochem.com/PASE/assay.ht ml)
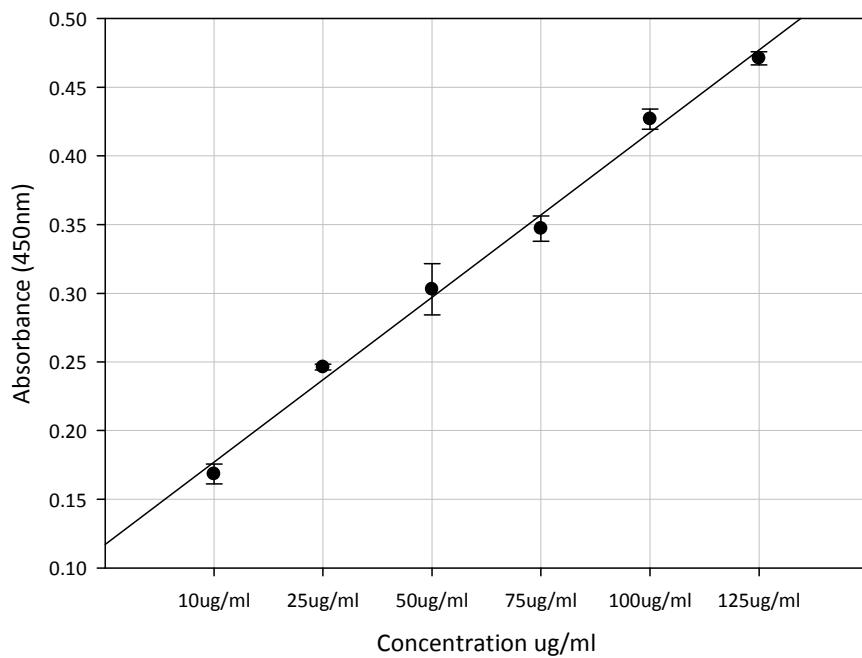
Figure 3.6: D-galacturonic acid standard curve 10-125µg/ ml in pH 5.0 Mcilvaine buffer

3.2.5.6 Global Polygalacturonase Assay

A 1.5 % agar/0.5 % polygalacturonic acid substrate was prepared by first heating agar in Mcilvaine buffer (pH 5.0) until it dissolved and addition of the polygalacturonic acid when cooled to 60°C. 600 µl of the solution was then pipetted onto glass slides and allowed to solidify in a sealed container. Whole 45 DAA pods were collected from Apex, DK142, MC148, MC169, MC177, MC226 and Tapidor. Pods were cut into apical, medial and basal sections, and dissected along the valve margin using a razor blade, leaving the DZ exposed. Each section of the fruit was then positioned with the DZ in contact with the substrate and incubated at 37°C in a sealed container for 24 hours. Slides were then stained with 0.05 % Ruthenium red (dissolved in pH 6.0 Mcilvaine buffer) for 10 mins.

3.3 Results

3.3.1 Differences in Vascular Patterning in 10 DAA Pods in Resistant and Susceptible POSH 1-3 Lines

Vascular architecture was assessed in whole, cleared *B. napus* pods with subsequent staining with Aniline Blue dye solution. This was performed in 10 DAA and 40 DAA fruit respectively. Clearing enabled the successful visualisation of vasculature in 10 DAA fruit. However, in 40 DAA pods, staining resulted in complete saturation of the sample rendering visualisation of vasculature impossible. Reduction in the dye concentration, staining duration and extended rinse periods did not improve this. In 10 DAA fruit, increases in staining of secondary vascular bundles were observed in DK142 and MC169 lines compared to Apex and the shatter-susceptible variety Tapidor (Figure: 3.7). Apparent differences in vascular orientation and size were also observed, but, due to difficulties in accurate positioning of whole fruit for imaging, this approach was considered unsuitable for accurately measuring angles or distances.
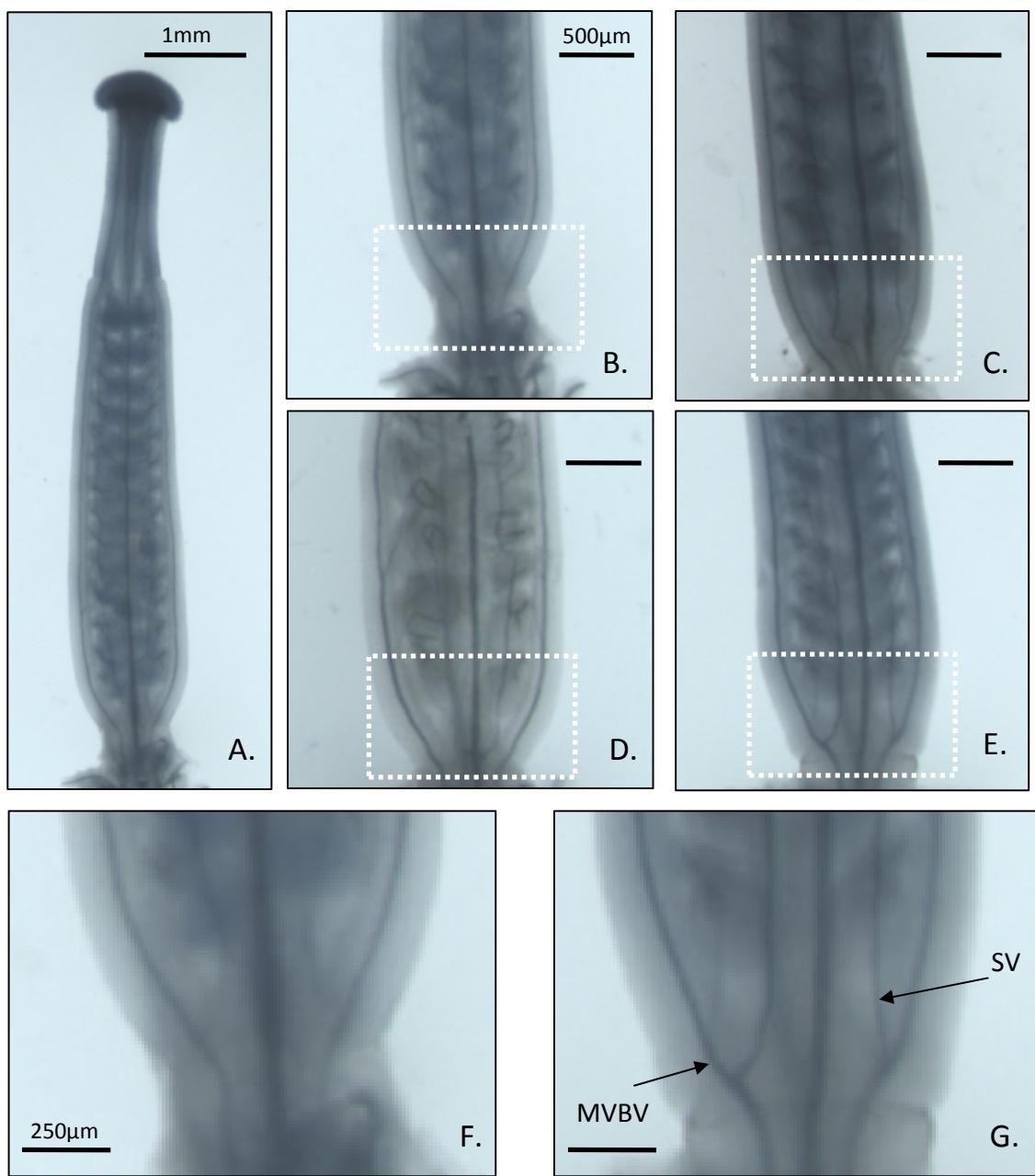
Figure 3.7: 10 DAA cleared fruit, stained with 0.1% Aniline Blue dye highlighting MVBV and secondary vasculature in A) Apex whole fruit, scale: 1 mm. B) Apex, C) DK142, D) Tapidor and E) MC169 MVBV in basal regions, scale: 500 μm.Close-ups of MVBV and secondary vasculature in F) Apex and G) MC169, scale: 250 μm. MVBV: Main vascular bundle of the valve SV: Secondary Vascular Bundle

3.3.2 Variation in the Orientation of the Major Vascular Bundle of the Valve (MVBV) in 35 DAA Fruit

Longitudinal sections from the basal region of 35 DAA fully-elongated pods from susceptible and resistant POSH 1-3 lines were prepared to enable assessment of their vasculature architecture. The angle of orientation and height of the Major Vascular Bundle of the Valve (MVBV), spanning from the pedicel, across the base of the valve margin, into the valve were assessed in five different samples per line (Figure 3.8).

Significant differences in the orientation of the MVBV were observed between lines assessed ($P<0.01$) (Appendix 3.1 (page 270)). The MVBV in DK142, MC148 and MC169 lines appeared to be more robust and positioned at a different angle than those in the susceptible Apex line. Significant differences in the angle of the MVBV, were identified between Apex and DK142 lines ($P<0.005$), and MC148 and MC169 ($P<0.001$, $P<0.005$, respectively (Appendix 3.2 (page 270)). It appears the angle of the MVBV as it crosses the dehiscence zone and enters the valve is increased in resistant lines. The mean angle of the MVBV in DK142 was twice as great as the mean angle in Apex (Table 3.1). Mean MVBV angle in MC148 and MC169 was seen to be similar to DK142. Therefore, in Apex sections the MVBV is positioned in a more horizontal orientation compared to the more longitudinal orientation in DK142, MC148 and MC169.

Line	Mean MVBV Angle (°)	Range (°)
Apex	11.99	9.032-16.76
DK142	24.68	22.06-27.92
MC148	25.4	23.53-27.3
MC169	23.52	20.94-25.70

Table 3.1: Mean and range of MVBV angles (°) in Apex, DK142, MC148 and MC169 pods

3.3.3 Variation in the Thickness of the Major Vascular Bundle of the Valve (MVBV) in Susceptible and Resistant 35 DAA Pods

The thickness of the MVBV as it exited the pedicel and joined the valve was also measured in 35 DAA pod sections (Figure 3.8). MVBV height was observed to be significantly different amongst Apex, DK142, MC148 and MC169 ($P<0.01$, Appendix 3.3 (page 271)). Highly significant differences were observed between Apex and between DK142, MC148 and MC169 respectively ($P<0.0005$, $P<0.01$ and $P<0.005$ respectively, Appendix 3.4 (page 271)). The MVBV was greater in size in the resistant lines compared to the susceptible Apex parent. Significant differences were not identified between DK142 and shatter-resistant MC148 and MC169 lines. The mean height of the MVBV in DK142 was 69% greater compared to Apex. Mean MVBV height in MC148 and MC169 was similar to DK142, with respective increases of 73% and 77% compared to Apex (Table 3.2).

Line	Mean MVBV Height (μm)
Apex	123.8
DK142	209.5
MC148	214.4
MC169	219.8

Table 3.2: Mean height of MVBV (μm) in Apex, DK142, MC148 and MC169
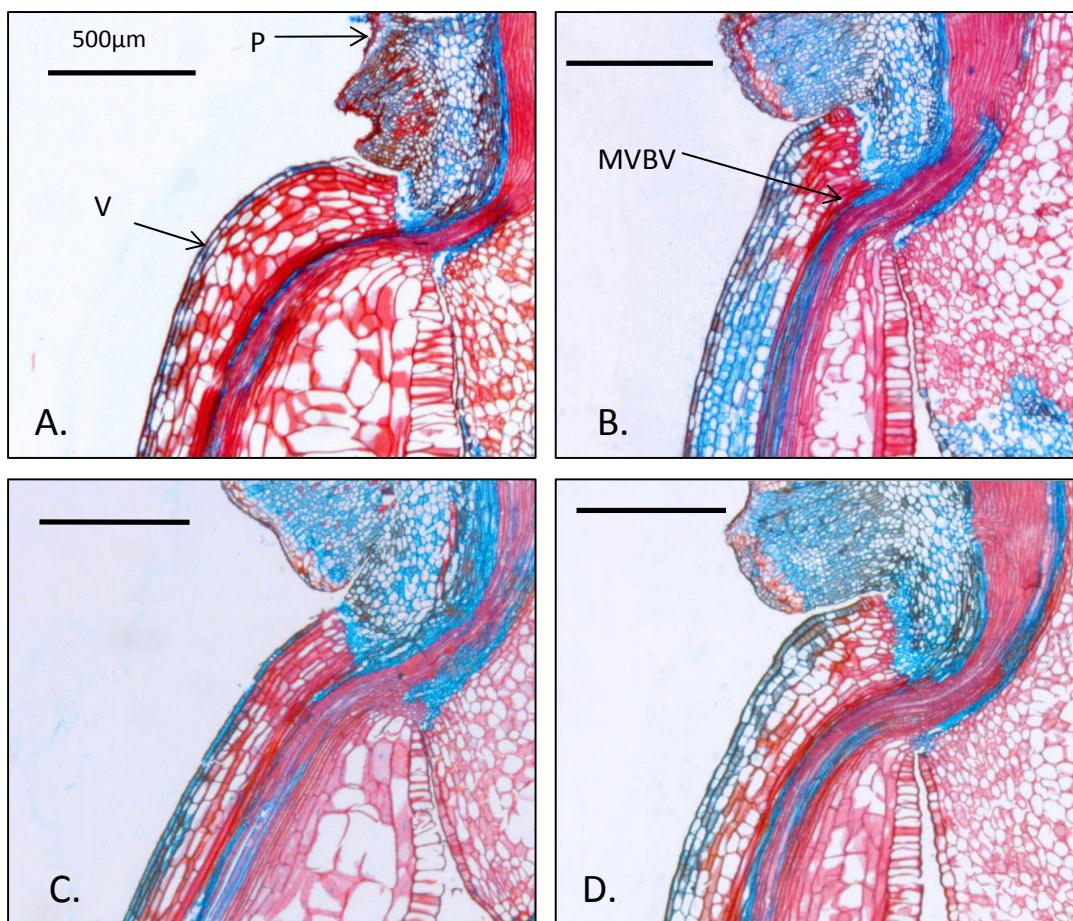
Figure 3.8: Examples of longitudinal 35 DAA sections in A) Apex, B) DK142, C) MC148 and D) MC169 pods used to measure vascular orientation and height, scale: 500 μm. MVBV: Main vascular bundle of the valve, P: Pedicel and V: Valve

3.3.4 Variation in the Width of the MVBV in Susceptible and Resistant 70 DAA Pods

Significant differences in the mean width of the MVBV protruding from detached valves in 70 DAA senesced pods from Apex, DK142, MC148 and MC169 pods were observed (Appendix 3.5 (page 272)). Highly significant differences in the mean width of MVBV were identified between the shatter susceptible Apex and resistant MC148 and MC169 lines (P<0.001 and P<0.005, respectively, Appendix 3.6 (page 272)), and between the resistant DK142 parent and MC148 and MC169 (P<0.00001 and P<0.0001, respectively). However, differences between the resistant DK142 parent and Apex were observed not to be significant, with both lines demonstrating almost identical widths at the MVBV (P=0.99). MC148 and MC169 exhibited respective increases of 37% and 55% compared to the parental lines (Table 3.3).

Line	Mean MVBV Width (µm)
Apex	342.3
DK142	342.1
MC148	470.2
MC169	529.7

Table 3.3: Mean widths of MVBV (µm) in Apex, DK142, MC148 and MC169

3.3.5 Variation in Pod Wall Thickness in Susceptible and Resistant POSH 1-3 Lines in 40 DAA Pods

Pod wall thickness (mm) (PWT) was measured in the medial region of 40 DAA transverse sections in pods from select POSH 1-3 lines. Significant differences were observed between lines ($P<0.001$, Appendix 3.7 (page 273)). Highly significant differences were observed for PWT between parental Apex and DK142 lines ($P<0.0001$, Appendix 3.8 (page 273)). DK142 was also observed to exhibit a significantly greater PWT than MC148 and MC169 ($P<0.0005$ and $P<0.05$, respectively). Both MC148 and MC169 demonstrated significantly greater mean wall thickness compared to the Apex parent ($P<0.01$ and $P<0.005$, respectively). However, differences in PWT between MC148 and MC169 were found not to be statistically significant ($P=0.35$). DK142 demonstrated a mean PWT 90% greater than Apex, whilst MC148 and MC169 were 39% and 49% greater than Apex respectively (Table 3.4). PWT in DK142 was 37% greater than in MC148 and 28% greater than MC169.

Line	Mean PWT (µm)
Apex	426.3
DK142	814.1
MC148	594.4
MC169	636.9

Table 3.4: Mean widths of MVBV (µm) in Apex, DK142, MC148 and MC169
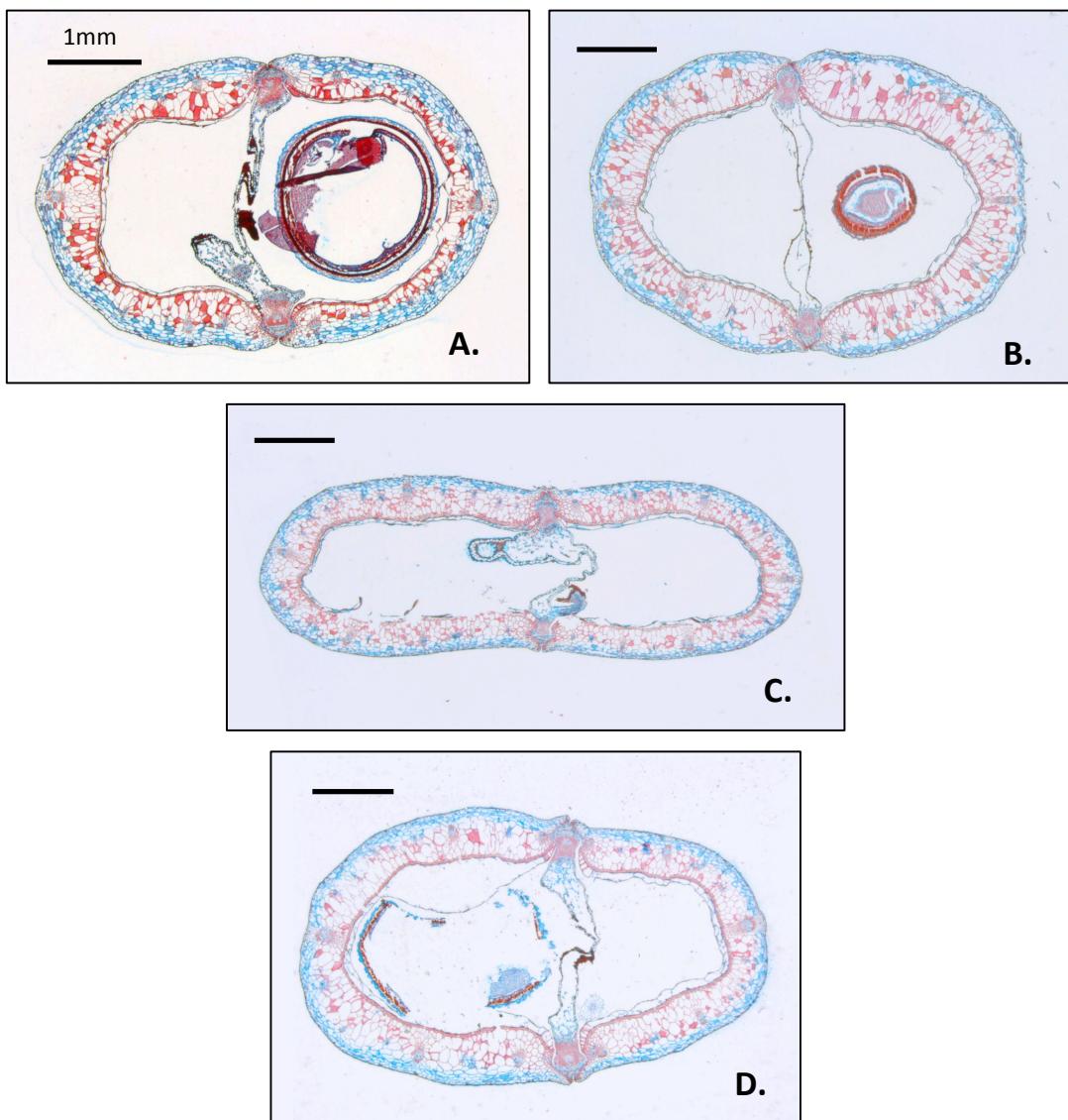
Figure 3.9: Examples of 40-50 DAA Transverse sections used for pod wall thickness (PWT) measurements in A) Apex, B) DK142, C) MC 148 and D) MC 169, scale: 1mm

3.3.6 Observation of Differences in the Degradation of Separation Layer in Resistant and Susceptible Lines in 40 and 60 DAA Pods

40 DAA pods

In transverse sections from medial and basal (pedicel) regions of 40 DAA pods, no breakdown of the middle lamella at the separation layer (SL) was evident in parental (Figure 3.10 images A and B) or resistant lines. The separation layer (stained blue) was situated adjacent to the lignified layer (stained red) and the replum at the centre of the image.

60 DAA pods

In 60 DAA pods, degradation of separation layer was evident in both the medial and basal regions of fruit in Apex and DK142 (Figure 3.10 C and D, Figure 3.11 A and B). The separation layer was ragged in appearance or was completely absent post-sectioning in samples from Apex and DK142 pods. It was discovered that mechanical handling in 60 DAA tissues was sufficient to degrade the integrity of the SL much more easily than in 40 DAA fruit sections. In sections from 60 DAA pods in the shatter-resistant MC148 and MC169 POSH DH lines, the relative level of separation layer degradation induced through mechanical handling appeared to be reduced compared to susceptible parents/lines (Figure 3.10 E and F, Figure 3.11 C and D). Degradation in medial sections in resistant lines was also observed to be reduced compared to parental lines, although not as obvious as in basal sections, where little or no degradation of the SL was identified. At higher resolution, a progressive reduction in the level of degradation of the S.L. can clearly be observed; with almost total dissolution in Apex, partial degradation in DK142 and little or no identifiable breakdown in the resistant MC148 and MC169 lines. Observation of the valve margin in MC169 also highlighted resistant lines to exhibit vascular bundles transecting the dehiscence zone compared to the susceptible parent Apex. The shape of the replum contacting the SL in MC169 also appeared to be more angular compared to the curved morphology observed in Apex, DK142 and MC148.
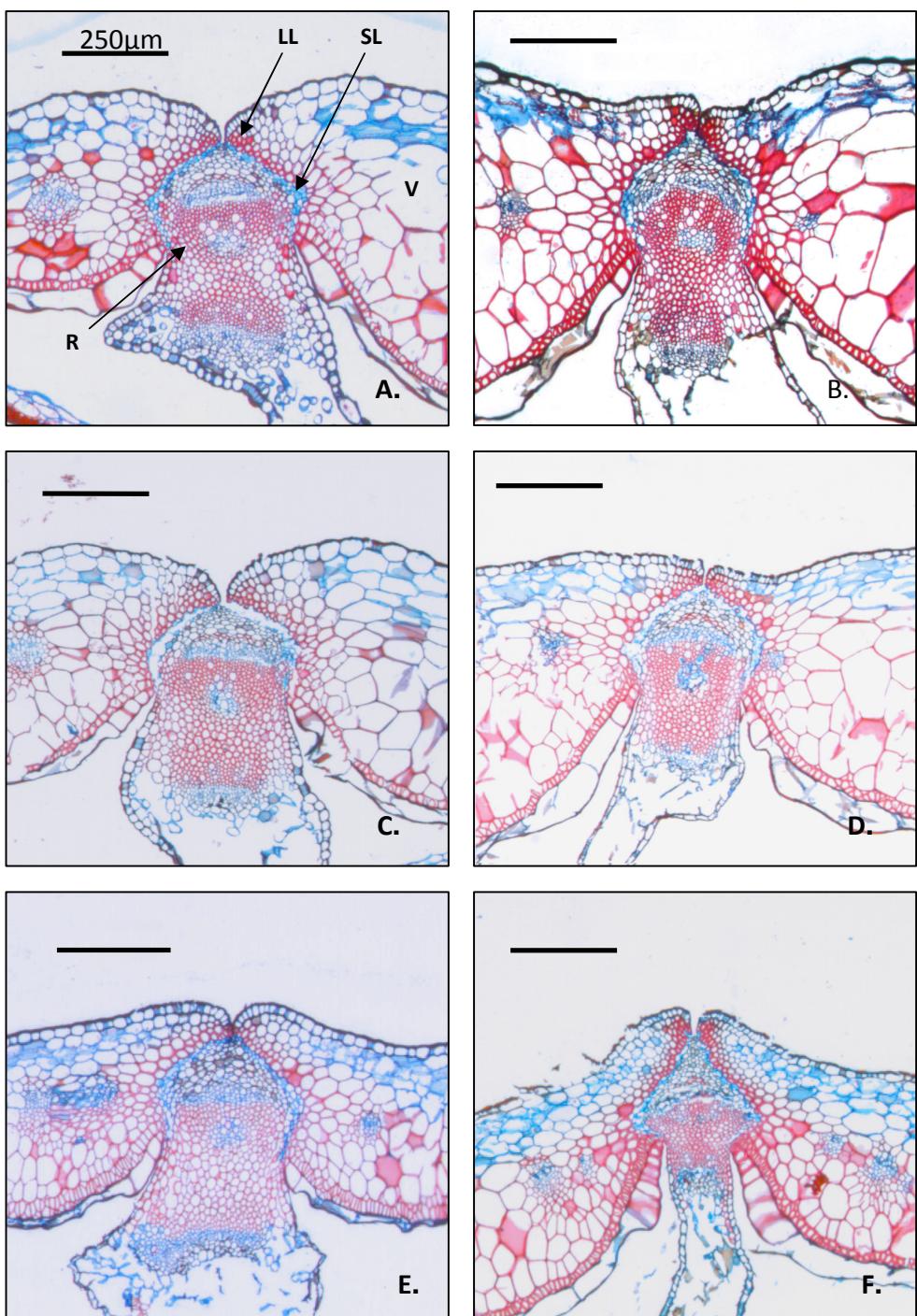
Figure 3.10: 40 DAA medial transverse sections of valve margin in A) Apex, B) DK142. 60 DAA, medial transverse sections of the valve margin in C) Apex, D) DK142, E) MC148 and F) MC169. LL: Lignified Layer, SL: Separation Layer, R: Replum, V: Valve. Scale bar: 250 μm
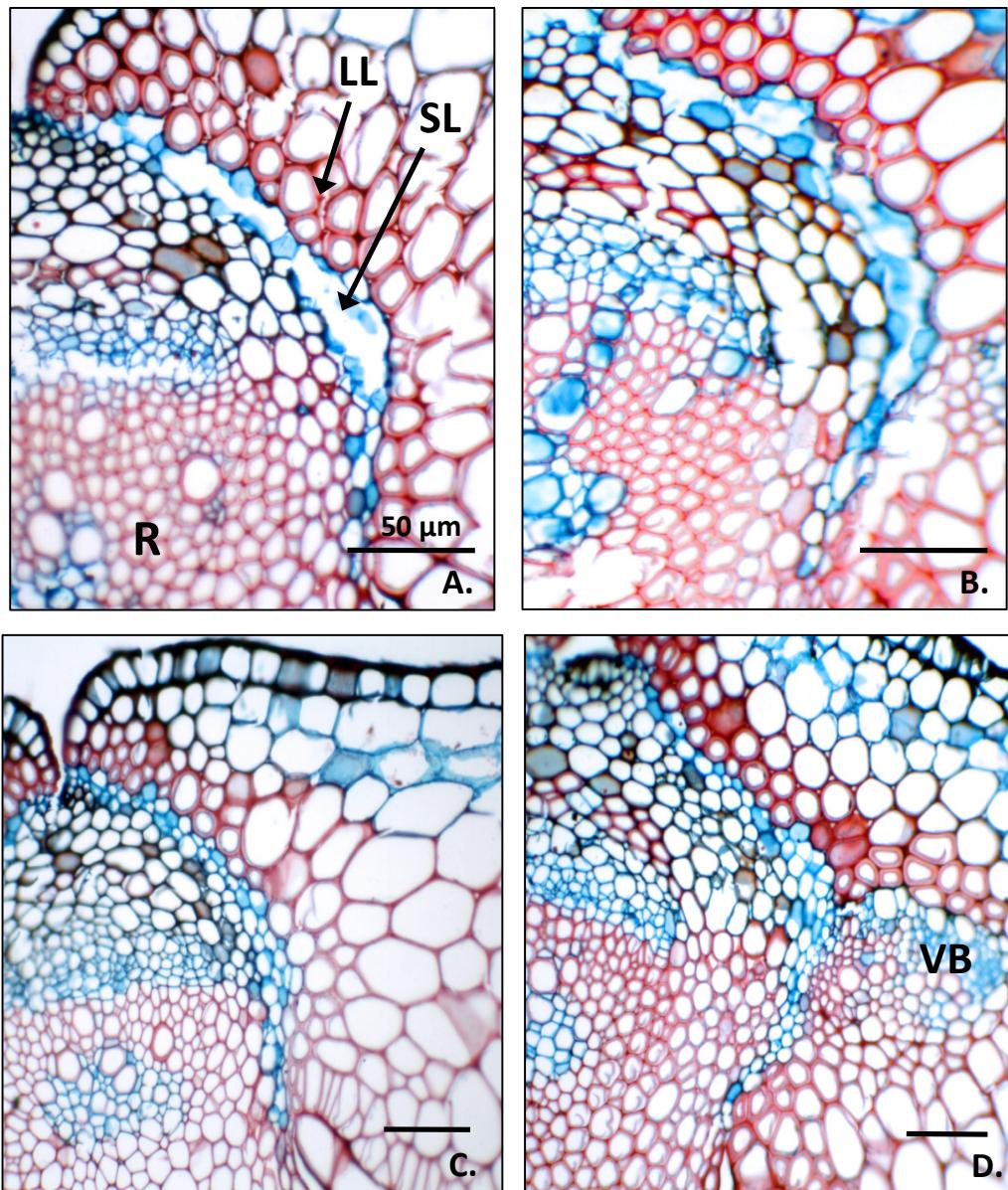
Figure 3.11: Close-up of basal transverse sections of 60 DAA valve margins in A) Apex, B) DK142, C) MC148 and D) MC169. LL: Lignified Layer, SL: Separation Layer, R: Replum, V: Valve, VB: Vascular Bundle at DZ in MC169, scale: 50 μm

3.3.7 Variation in Cellulase Activities in Susceptible and Resistant POSH 1-3 Lines

Potential differences in the activity of DZ-specific cellulases were investigated in susceptible, intermediate and resistant POSH 1-3 lines. Three approaches were utilised to assess the activity of the extracted enzymes: 1) viscometric analysis 2) a copper based, neo-cuproine colorimetric assay to detect differences in reducing sugars produced as a product of hydrolytic enzyme activity and 3) dissection of the DZ with exposure to an agar/polygalacturonic acid substrate and subsequent staining with pectin-specific Ruthenium Red stain (0.05%) to detect global differences in enzyme activity. Enzyme extractions were performed on ground valve and dehiscent zone samples, before attempting to quantify their activity against specific substrates for viscometric and colorimetric assays. Apical, medial and basal regions were dissected to expose the DZ/Separation Layer for the global polygalacturonase assay.

3.3.7.1 Viscometric Assessment of Differences in Cellulase Activity

Viscometric assessments of cellulase enzymes in crude protein extracts from susceptible and resistant POSH lines, to assess β 1, 4-glucanase, pectinase and polygalacturonase activity, using specific substrates were conducted. Initial outflow times could be measured accurately, but subsequent decreases in substrate viscosity after incubation with extracts could not be generated accurately or reproducibly for any of substrates tested, although the approach had been validated previously using an identical technique to extract and assess cellulases from tomato (*Lycopersicon esculentum* var. Tigerella) and in a commercial pectinase enzyme preparation on a pectin substrate (Sigma Aldrich U.K.) (Figure 3.12 and 3.13, respectively). Therefore results from the investigation were deemed to be inconclusive.
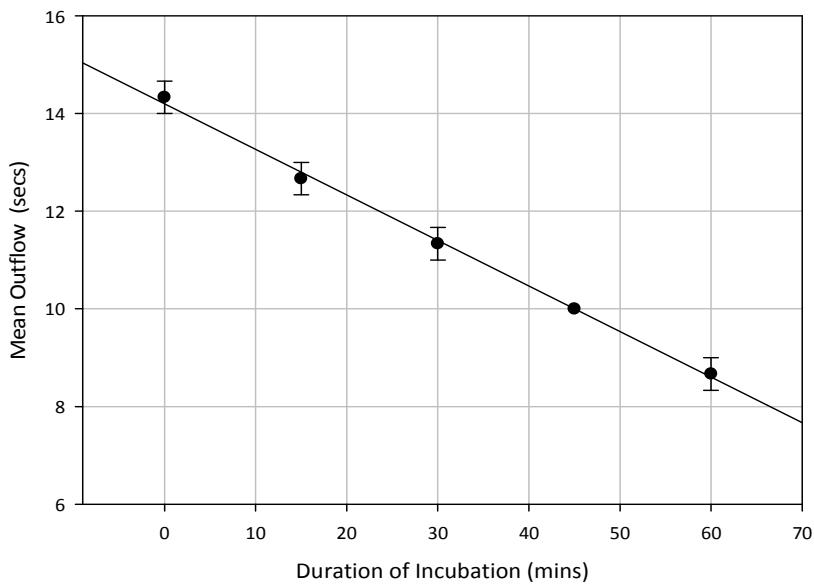
Figure 3.12: Decreasing viscosity in 1% pectin solution with Tomato pectinase extract @ 37°C (25°C)
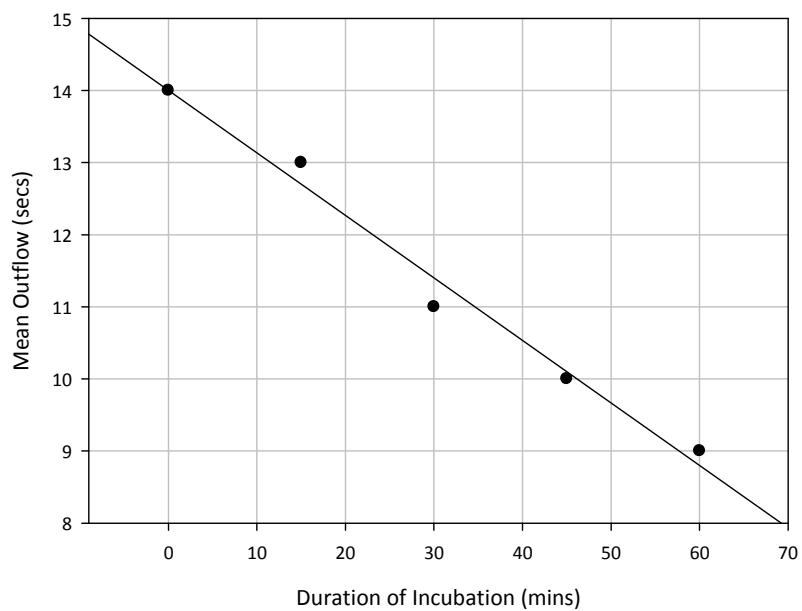
Figure 3.13: Decreasing viscosity in 1% pectin solution with 2 units commercial pectinase @ 37°C (25°C)

114

3.3.7.2 Neocuproine Assay for Determination of Reducing Sugar generated by Polygalacturonase Activity

A neocuproine (2,9-dimethyl-1,10-phenanthroline) based colorimetric assay, to detect the reducing sugars generated by polygalacturonase on the hydrolysis of pectin-rich middle lamella of the separation layer, was utilised to assess potential differences in enzyme activity in select POSH 1-3 lines (Apex, DK142, MC148 and MC169). Neocuproine is highly selective for copper, and the Copper (II)-neocuproine reagent forms a yellow-orange, Copper (I) (neocuproine)$_2$+ chelate complex when reduced by the presence of sugars, the production of which can be measured using a spectrophotometer at an absorbance of 450-460nm (Dygert *et al.*, 1965; Besada *et al.*, 1989). Polygalacturonase activity results in production of galacturonic acid residues on the degradation of polygalacturonans present in pectin (Bélafi-Bakó *et al.,* 2007). Increases in the quantity of sugars resulted in a greater level of production of copper-neocuproine complex.

Differences in the relative concentration of reducing sugars generated as a product of polygalacturonase activity between extracts from susceptible or resistant lines, between each harvest period (DAA) and between dehiscence zone (DZ) and valve samples from the same line, could not be accurately estimated or were non-reproducible. Absorbance data generated during reactions were also observed to be variable between replicate samples and similar results were obtained between DZ and valve extracts, even after adjustment for the quantity of protein identified using the Bradford assay. An example of this is depicted in samples from 50DAA Apex and DK142 samples (Figure 3.14). Standard curves, using a D-galacturonic acid, were however reproducible using this technique (Figure 3.6). Results from the assay are therefore reported to be inconclusive due to the variability of the results obtained.
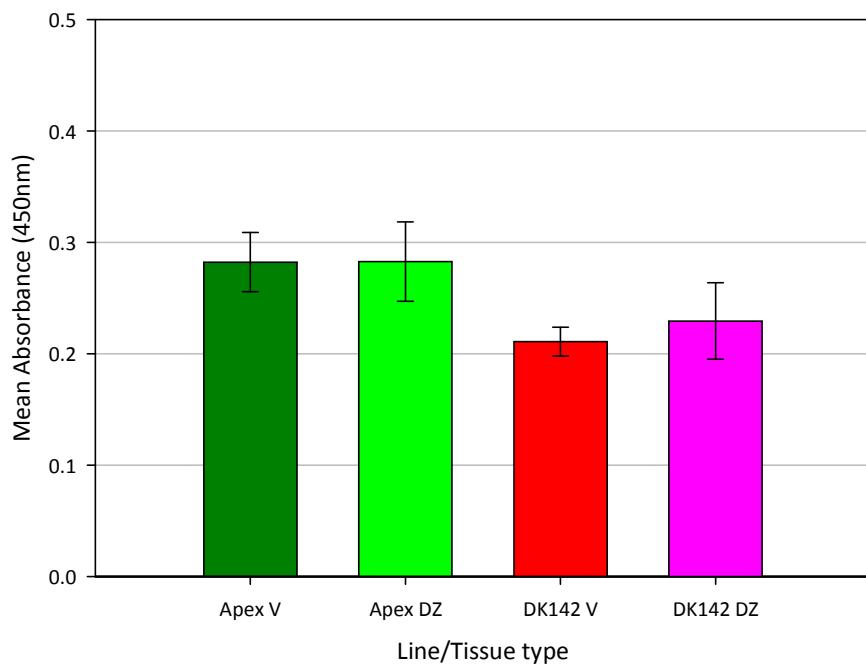
Figure 3.14: Histogram depicting Neocuproine assay absorbance data in 50DAA Apex and DK142 Valve and Dehiscence Zone extract samples

(including standard error bars).

3.3.7.3 Global PG assay

No differences could be detected in the staining of the agar/polygalacturonic acid substrate exposed to either apical, medial or basal regions of susceptible or resistant pod samples. All slides were stained with an equal intensity on exposure to the ruthenium red dye solution (Data not shown).

3.4 Discussion

Variation in the orientation of the Main Vascular Bundle of the Valve in POSH 1-3 resistant DH lines

This investigation has identified statistically significant differences in the orientation of pod vasculature vascular architecture in resistant POSH 1-3 lines compared to the susceptible Apex parent. This was first identified in 10 DAA whole fruit and subsequently quantified in 35 DAA longitudinal sections. Differences in the angle of the main vascular bundle of the valve (MVBV) in 10 DAA pods were apparent between Apex and DK142 parental lines and also in the resistant MC148 and MC169 lines. However, accurate measurements of the vasculature could not be achieved in whole fruit due to differences in relative depth of bundles situated within tissues and the ability to reproducibly position the fruit for imaging. Secondary vasculature also appeared to be increased in 10 DAA pods from resistant lines, although accurate assessment also proved problematic due the same issues associated with primary vasculature. Measuring vascular angles in immature fruit may provide an 'earlier' score-able trait than assessment of vascular angle in elongated fruit or PSR in senesced fruit, but a full assessment in young and mature fruit would have to be conducted to corroborate if angles remained constant throughout development.

40 DAA pods were also assessed in an effort to address potential changes in vascular orientation after fruit elongation and vascular growth had ceased, but these were completely stained by the aniline blue dye, making vascular orientation measurements impossible. This is suggested to be due to callose deposition throughout tissues in the elongated 40 DAA fruit, whereas in 10 DAA samples only callose present in vascular bundles was stained.

Significant differences in MVBV orientation were observed in 35 DAA pods between the susceptible Apex parent and resistant DK142, MC148 and MC169 lines. The angle of the MVBV as it crossed the valve margin in Apex appears at approximately 90° (horizontally) compared to the orientation of the bundle running through the valve and pedicel, whereas in DK142 it is reported to be orientated more longitudinally (Child *et al.* 2003). We observed

increases in the angle of elevation of the MVBV in resistant DK142 and POSH DH lines MC148 and MC169 compared to Apex, resulting in a decrease in the angle of the MVBV in relation to its orientation compared to the valve/pedicel. Therefore it is concluded that the orientation of the MVBV also is orientated more longitudinally in the resistant POSH1-3 DH lines as reported for the resistant DK142 parent. We have observed that the angle of elevation on average is doubled in resistant lines, increasing by a mean of 108% in DK142 compared to Apex, 112% in MC148 and 96% in MC169. Therefore, in resistant lines, the MVBV is situated at approximately 45° compared to 90° in the shatter susceptible Apex line. The increase in angle of elevation/decrease in angle of orientation of the MVBV is suggested to potentially contribute to greater levels of PSR in the resistant POSH 1-3 DH lines by increasing the relative surface area subject to fracturing during valve detachment.

The force induced during fracturing is suggested to be distributed diagonally in resistant lines, compared to a more horizontal distribution in shatter susceptible pods, requiring more tissue to be broken prior to dehiscence. This agrees with the suggestion by Child *et al.* (2003) that the more longitudinal vasculature of DK142 and F_2 lines is stronger per unit area than Apex. It is suggested that the same anatomical determinants contributing to increases in PSR in DK142 and F_2 lines are evident in resistant lines from the POSH 1-3 DH population.

Differences in the size of the Main Vascular Bundle of the Valve in POSH 1-3 resistant DH lines

We have also identified significant differences in the thickness of the MVBV at the point the bundle crosses the dehiscence zone in the DK142 parent and resistant DH population lines. An increase in the size of the MVBV of 60% has been reported previously in DK142 compared to Apex and an increase in PSR is directly attributed to this, in both DK142 and F_2 lines (Child *et al.* 2003). An average increase in the height of the MVBV of 69% in DK142 compared to Apex, and 73% in MC148 and 77% in MC169 was observed. An increase in the height of the MVBV in resistant lines MC148 and MC169 is suggested to contribute to increases in PSR, as observed in DK142. It is suggested that an increase in thickness of MVBV

(and secondary bundles) could increase the amount of fracture energy required to shed valves, strengthen pods at point where dehiscence is initiated.

Differences in the width of the Main Vascular Bundle of the Valve in POSH 1-3 resistant DH lines

Significant differences were observed in the width of the Main Vascular Bundle of the Valve (MVBV) in detached 70 DAA valves when comparing the POSH 1-3 parents and resistant DH lines. The MVBV observed in the resistant MC148 and MC169 lines were visibly wider than that in Apex and DK142, with respective increases in mean width demonstrated of 37% in MC148 and 54% in MC169. This suggests a similar contributory role for increases in the width of the MVBV as a key component in the shatter resistant phenotype of DK142, as described by Child *et al.,* (2003). However the lack of significant variation identified between Apex and DK142 in MVBV width, which is contrary to that reported by Child *et al.* (2003), may be attributed to potential out-crossing in the resistant DK142, POSH progenitor line.

The increased size and longitudinal orientation of the MVBV (and observation of increases in size of secondary vascular bundles) in resistant lines is likely to contribute to increases in PSR, with vascular bundles acting like a scaffold, increasing the amount of energy required to detach valves, inferring a greater level of pod integrity and therefore pods that are more shatter resistant under the RIT assessment described in Chapter Two. Secondary bundles transecting the replum have also been suggested to contribute to increased pod integrity in DK142 (Child *et al.* 2003). Similar bundles have were observed in MC169. Interestingly, secondary vascular bundles in medial and apical regions in DK142 were not often apparent and seemingly reduced in comparison to the MC169 line during this investigation. This is suggested to potentially relate to out-crossing in DK142 parent line resulting in differences reported in the original phenotype.

A more in-depth investigation into the range of variation in the size and angle of the MVBV in the POSH 1-3 population may enable QTL analysis to potentially identify factors

contributing to differences in the MVBV. Such factors are likely to be associated with increases in PSR and are therefore promising targets for crop improvement.

Differences in Pod Wall Thickness of the Valve in POSH 1-3 resistant DH lines

Significant differences in the pod wall thickness (PWT) have been identified in the lines assessed. The greatest differences in PWT were observed between Apex and DK142, however, MC148 and MC169 were also observed to demonstrate significantly thicker pod walls than the shatter susceptible parent. It has been reported previously that significant increases in thickening in the endocarp of DK142 compared to Apex did not correlate strongly with RIT measurements and that changes in pod wall architecture did not contribute to differences in shatter resistance (Child *et al.,* 2003), whereas, overall pod dimensions, particularly pod length and weight of septum and valves did correlate significantly (Summer *et al.,* 2003). Although PWT does not seemingly contribute strongly to increases in PSR in POSH 1-3 parents or F_2 lines, it would be of interest to investigate the relationship between increases in pod mass, pod length, relative PWT, levels of lignification and increases in shatter resistance in POSH 1-3 DH lines. Especially when it is considered that although DK142 pods were 15% shorter and held 55% less seed than Apex their relative mass was 25 % greater (Summers *et al.,* 2003).

Differences in the level of Separation Layer degradation in POSH 1-3 resistant lines compared to the susceptible Apex parent

Here, We have identified differences in the relative level of degradation of the separation layer (SL), a key tissue required for the pod dehiscence process. Sections from 40 DAA pods were observed to demonstrate no obvious differences in the breakdown of the middle lamella of the S.L. in either resistant or susceptible lines, at medial or basal regions of the fruit. This was expected as cellulase activity in *B. napus* pods is not reported to peak until 45-50 DAA in *B. napus* (Meakins and Roberts, 1990b; Chavaux *et al.,* 1997). However, in 60 DAA pod sections, degradation of the S.L. was apparent at medial regions in Apex, DK142 and in MC148 and MC169. However, in basal regions, closer to the pedicel, the level of breakdown appeared to be slightly reduced in DK142, with further reductions in MC148 and MC169. The

SL in the resistant POSH 1-3 DH lines appear to be almost completely intact close to the pedicel, the region where pod shattering is reported to be initiated (Davies and Bruce, 1997).

It is suggested that this could be contributing to increases in LD50 value and hence PSR resulting in a greater amount of energy being required to induce dehiscence. A decrease in degradation could be due to differences in hydrolytic enzyme activity or in the temporal activation of cellulase activity at the DZ in resistant lines compared to susceptible lines. Potentially differences could be attributed to damage induced during sectioning, although MC148 and MC169 appeared to be less subject to the effects of manual handling, also indicating a more robust SL in comparison to Apex and DK142. The observed increase in SL degradation in DK142 compared to MC148 and MC169 may be due to out-crossing in DK142.

Attempts to identify differences in cellulase activity in Dehiscence Zone specific enzymes
Previously, roles have been established for hydrolytic enzymes in the breakdown of the middle lamella of cells constituting the separation layer, with cell separation preceded by an increase in β 1, 4-glucanase at the DZ(Meakins and Roberts, 1990b). Cellulase activity has been also been proposed for polygalacturonases, including RDPG1 (Rape Dehiscence Zone Polygalacturonase 1) although, no temporal or spatial correlation could be determined with respect to cell separation and polygalacturonase in *B. napus* (Petersen *et al.*, 1996; Sander *et al.* 2001; Meakins and Roberts, 1990b). However, it was suggested this should not preclude the enzyme from involvement in the cell separation process (Meakins and Roberts, 1990b; Berger and Reid, 1979).

Experiments were designed to identify potential differences in cellulase activity at the dehiscence zone utilising three separate approaches on salt-soluble protein extracts from susceptible and resistant POSH 1-3 lines. A viscometric assay was first utilised to address potential differences in β 1, 4-glucanase, pectinase and polygalacturonase activities by utilising respective CMC, pectin and polygalacturonic acid substrates. However, no measurable differences in cellulase activity, between lines, in any of the substrates tested

could be obtained utilising this approach. This may have been due to an inefficient extraction procedure, although similar approaches have been described previously to successfully obtain salt-soluble cellulase fractions (Pressey, 1986, Meakins and Roberts, 1990 b, Truelsen and Wyndaele, 1991). In this approach an ammonium-sulphate ($(NH_4)_2SO_4$) precipitation step to concentrate the protein was not conducted as this was perceived to potentially reduce enzyme activity and thus may have had negative effects on proceedings (Pressey, 1986).

In defence of this, an salt-soluble protein extraction was previously performed in tomato (*lycopersicon esculentum* var. Tigerella) without $(NH_4)_2SO_4$ precipitation and subsequently measured changes in pectinase activity utilising the same viscometric assay used to assess for differences in *B. napus.* The viscometric assay had also been validated previously using commercial pectinase enzyme. Therefore, it is suggested that the quantity of tissue used for cellulase extraction, or the amount of enzyme extract used in the analysis may have been sub-optimal to yield measurable results as opposed to the lack of differences in hydrolytic enzyme activity between POSH lines. However this cannot be substantiated without further investigation. Limitations to the amount of pod material due to infertility in POSH lines and the number of plants that could be cultivated were also considered a limiting factor to the investigation.

A neocuproine based colorimetric assay to detect reducing sugars generated as a product of polygalacturonase activity was also found to be inconclusive in identifying potential differences amongst susceptible and resistant POSH lines. Results were observed to be variable between replicate samples from the same tissue and similar between dehiscence zone and valve extracts. The assay was utilised successfully to generate reproducible standard curves, using a D-galacturonic acid substrate and was therefore observed to be effective in identification in even low concentrations of reducing sugars. Therefore, it is suggested that the lack of differences identified between susceptible and resistant lines could be attributed to variation in efficacy of extraction procedure, too smaller quantity of tissue from which the extract was procured, variation in cellulase concentrations between

pods from the same line or simply no measurable increases in PG activity between the lines tested. The amount of pods available to the experiments due to infertility was also a limiting factor to the investigation. Meakins and Roberts (1990 b) previously reported that similar colorimetric assays, specifically the Nelson-Somogyi method, did not identify tissue-specific significant increases in polygalacturonase activity at the dehiscence zone during development, however without more rigorous testing this cannot be validated within the POSH lines tested.

A slide based assay using an agar/polygalacturonic acid substrate to assess for variation in polygalaturonase levels between susceptible and resistant lines was also employed. No differences in the level of substrate degradation could be identified in dissected pods from susceptible or resistant lines. This could potentially be due to ineffective dissection technique, rendering the SL unexposed to the substrate, due to only small quantities of cellulase present in pods or a low relative activity resulting in little or no degradation over the assay duration. Longer exposure durations did not result in any noticeable substrate degradation.

These results do not preclude differences in cellulase activities in the variation in degradation of the SL in susceptible and resistant POSH lines. It could be that differences observed in SL degradation, at basal region of the pod in MC148 and MC169 compared to Apex, may be related to temporal variation in the activation of cellulase activities. However more in depth analyses must be performed to verify this and it is proposed more accurate approaches, with a greater amount of pod material, would need to be employed to elucidate if differences do exist in cellulase activities between POSH 1-3 DH lines.

The work presented here demonstrates that increases in the size and differences in the orientation of the MVBV, which have previously been reported to contribute to increases in PSR in the POSH progenitors, are also responsible for greater levels of PSR in specific resistant lines from the POSH 1-3 population. Potential differences in the degradation of the separation layer between resistant and susceptible lines have also been identified. Traits

such as these could pose as potential targets for introgression as targets to reduce pre-harvest pod shattering in commercial varieties of *B. napus*. Principle steps in the identification of genetic factors for this purpose would require the construction of a robust genetic linkage map containing a diverse population of markers. The production of such a resource for the POSH 1-3 population will be described in the next chapter.

Chapter 4: POSH 1-3 Genetic Linkage Map Construction

4.1 Introduction

Genetic linkage maps estimate marker position within the genome of a population, using a mapping function to convert recombination frequency into map distance (cM). Direct requirements to conduct mapping studies include a stabilised population derived from diverse parents to ensure sufficient polymorphism at a large number of loci and a robust method for amplification and detection of differences in genetic markers to permit accurate and efficient genotyping from lines within the population.

A number of *B. napus* genetic maps have been constructed using this general approach, presenting important resources for understanding *Brassica* genome structure and through which to potentially isolate important genes (Lowe *et al.,* 2004; Parkin *et al.,* 2005; Qiu *et al.,* 2006; Radoev *et al.,* 2008). A Genetic linkage map forms the basis for performing QTL analysis to identify important regions of the genome associated with phenotypic traits. Synthetic hybridization, through interspecific crosses between *B. napus* progenitors *B. rapa* and *B. oleracea,* has been used in an attempt to introgress a more diverse array of alleles into mapping populations (Morgan *et al.* 1998; Werner *et al.,* 2003a).

This chapter describes marker screening and linkage map development in the synthetically derived, POSH 1-3 Doubled Haploid population, using suites of publicly accessible SSR and InDel markers. A series of candidate-gene specific SSCP markers whose orthologs have established roles in *Arabidopsis* fruit development were also screened in the population. Genotyping of markers and genetic linkage map construction are also detailed. Construction of an improved version of the POSH 1-3 map will present an important resource, through which to identify loci contributing to an increase in PSR in *Brassica napus*.

4.2 Materials and Methods

4.2.1 Cetryltrimethylammonium bromide (CTAB) Genomic DNA Extraction

Genomic DNA was extracted using the CTAB extraction protocol (Doyle & Doyle, 1987; Steward & Via 1993) for 120 POSH lines cultivated during the 2006 season. Approximately 3-5 g of young, frozen leaf tissue was ground to a fine powder with liquid nitrogen in a pestle and mortar. Ground leaf samples were transferred to 50ml Corning tubes, into which 25 ml of CTAB was buffer heated to 65°C prior, was aliquotted. Tubes were incubated at 65°C for 1 hr with agitation every 15 mins. 10 ml of Chloroform was added, the tubes shaken, and then inverted on a rotor at RT for 20 mins. Tubes were centrifuged at 3,000 rpm for 5 mins to separate phases. The aqueous phase (containing the DNA) was transferred to a fresh 50 ml tube, to which 2 volumes of propan-2-ol was added to precipitate the DNA.

Tubes were inverted and placed on ice for 10 mins followed by centrifugation at 3,000 rpm for 5 mins. Residual liquid was removed and then the tubes re-centrifuged to condense the DNA pellets. Any remaining liquid was pipetted off and the pellets allowed to air dry for 1 hr. Pellets were dissolved in 1.8 ml TE buffer (0.05M). 50 µg of RNase was added (10 µg/µl) and the tubes incubated at 37°C for 30 mins. 2 ml of Phenol/Chloroform was added to the tubes, followed by shaking and further addition of 2 ml Chloroform. Tubes were centrifuged at 3,000 rpm for 5 mins. The aqueous phase was recovered and 2 ml of ddH$_2$0 added to the phenolic phase, shaken and re-centrifuged. The aqueous phase was recovered.

Two volumes of EtOH were added to the retained aqueous phase and the tubes placed on ice for 5 mins to precipitate the DNA. Tubes were centrifuged at 3,000 rpm for 10 mins and the liquid decanted off. Pellets were rinsed with 10 ml 70 % EtOH to remove any residual phenol. Tubes were re-centrifuged and the remaining liquid pipetted off. Pellets were air dried and re-dissolved in 250 µl TE buffer. DNA concentration was quantified using an Implen Nanophotometer and working dilutions of 20 ng/µl prepared.

4.2.2 *Taq* Polymerase Production

Escherichia coli clones containing a p*Taq* plasmid were streaked out on two LB-amp plates and incubated at 37°C overnight. Single colonies were transferred into 10ml LB-amp broth and incubated at 37°C overnight. 2 x 2 litre of pre-warmed, 37°C LB-amp broth were inoculated with 500µl of the overnight culture and incubated for 7 hrs at 37°C, until the OD_{600} ~0.8. IPTG (Isopropyl β-D-1-thiogalactopyranoside) was added to a concentration of 125 mg/l to induce protein translation/*taq* polymerase production and the cultures incubated for 12 hrs at 37°C.

E. coli cells were pelleted by centrifugation at 3,000 rpm for 10 mins in 200 ml aliquots. Pellets were re-suspended in 50 ml/litre of the original culture in pre-lysis buffer (Buffer A + lysozyme) and incubated at RT for 15 mins. 50 ml/litre of the original culture Lysis buffer was added and incubated at 75°C for 1 hr. Tubes were centrifuged at 15,000 rpm for 10 mins at 4°C.

The supernatant was transferred to a sterile pyrex flask to which ammonium sulphate (30 g/litre of original culture) was added to precipitate the *taq* protein. Tubes were centrifuged at 15,000 rpm for 10 mins at RT. The surface and pelleted precipitate was collected and re-suspended in 20 ml/litre of the original culture in Buffer A.

Dialysis tubing was prepared by first boiling for 10 mins in 2 % sodium hydrogen carbonate, rinsing twice with ddH_2O and re-boiling for 10 mins in 1 mM EDTA. Tubing was cooled and stored at 4°C. The *taq* solution was then transferred to dialysis tubing and dialysed for two 12 hr periods in 1 litre of storage buffer at 4°C (50 mM Tris-HCl pH 7.9, 50 mM KCl, 0.1 mM EDTA, 1 mM DTT, 0.5 mM PMSF, 50 % glycerol). The solution was then diluted 1:1 with storage buffer and stored at -70°C. Taq polymerase was titrated against commercial taq preparation in standard PCR to ascertain relative concentration before use in screening and genotyping markers.

4.2.3 Molecular Marker Screening and Development

4.2.3.1 Microsatellites (SSR)

For SSR screening and genotyping conventional PCR was utilised, with subsequent resolution of products using Polyacrylamide Gel Electrophoresis (PAGE) to visualise genotypic differences. PCR was conducted with the following reaction using 20 µl reaction consisting of 9.65 µl ddH$_2$0, 2 µl 10 x PCR buffer (15 mM MgCl$_2$), 1.3µl dNTPs (2 mM), 1 µl each of forward primer and reverse primers (2 mM), 0.05 µl *taq* polymerase (~20 U/ µl) and 5 µl DNA (20 ng/µl). PCR was conducted on an M J Research PTC-200 thermo-cycler using the following programmes. For BBSRC SSRs an initial denaturation at 94°C for 10 minutes was followed by 35 cycles of a denaturation at 94°C for 30 s (0.5°C /s ramp), annealing at 53°C for 1 min 0.5°C/s ramp and extension at 72°C for 1 min 0.5°C/s ramp with a subsequent final extension at 72°C for 10 mins. For BRMS and Saskatoon SSRs an initial denaturation at 94°C for 10 mins was followed by denaturation at 94°C for 30 s (0.5°C /s ramp), annealing at 50°C for 1 min (0.5°C/s ramp), extension at 72°C for 1 min 0.5°C/s ramp with a subsequent final extension at 72°C for 10 mins.

4.2.3.2 Visualisation of PCR Products for Genotyping using PAGE

PCR products were visualised using PAGE followed by silver staining. PCR samples were denatured by addition of an equal volume of formamide loading buffer (10 ml formamide, 200 µl 0.5 M EDTA pH 8.0, 1 mg/ml xylene cyanol and 1 mg/ml bromophenol blue) and heating at 95°C for 5 mins. Samples were immediately put on ice. 2.5 µl of each sample was then loaded into the wells of a denaturing 19:1, 5%, 380 x 310 x 0.35mm polyacrylamide gel, in conjunction with two lanes of 100 bp marker (Invitrogen, U.K.). Gels were run at 70 watts for 1hr 30 mins, until the bromophenol blue marker had migrated into the buffer. Gels were fixed in 10% acetic acid solution for 30 mins on a shaker, the fixer retrieved, and then rinsed in ddH$_2$0 for 10 mins.

Gels were soaked in silver stain for 30 mins (12 ml 1.010 N silver nitrate solution, 3 ml formaldehyde (37.5%) in 2 litre ddH$_2$0) on a shaker. Immediately prior to development,

300 µl sodium thiosulphate (0.1 N) and 3 ml formaldehyde were added to 2 litres of chilled sodium carbonate solution (30 g/litre ddH$_2$0). Gels were removed from the silver stain and immersed three times in 2 litres of ddH$_2$0, drained and then immersed in the sodium carbonate solution whilst shaking. On satisfactory development of the stain, the fixer solution was poured in the developer to halt the reaction. After effervescence had ceased gels were rinsed in ddH$_2$0 for 20 minutes and allowed to air dry overnight.

4.2.3.3 Fluorescent Labelled M13 tail PCR/Capillary Sequencer Genotyping

For automated SSR screening and genotyping amplification was performed with one of four fluorescent labelled M13 adaptors (Applied Biosystems) per primer pair enabling multiplexing of PCR products (4 x) after amplification had been conducted using the following reaction and PCR cycles. Universal primers tailed with a M13 adaptors (5'-TGT AAA ACG ACG GCC AGT-3') were labelled with one of four fluorescent dyes (FAM, VIC, PET or NED) and utilised in the following reaction mix; for 110 reactions 5.16 µl fluorolabelled adaptor (100µM),. 5.16 µl reverse Primer (untailed, 10µm), 0.35 µl, Qiagen Hotstar PCR mastermix, 343.75 µl Sterile ddH$_2$O. PCR was conducted utilising a hotstart and denaturation at 95°C for 15 mins followed by 40 cycles denaturing at 95°C for 1 min, ramping to annealing at 50°C (0.5°C/sec) for 1 min, with subsequent ramping to 72°C (0.5°C/sec), Extension at 72°C for 1 min, a final extension 72°C for 10 mins, finally holding at 8°C.

After PCR, samples were multiplexed by first centrifuging and then diluting them 1/40 by adding 1 µl of each labelled PCR product and 36 µl of ddH$_2$O. 1 µl of each dilution was added to 8.9 µl of Hi-Di formamide (Applera, U.K.) and 0.1 µl of LIZ 500 size standard (Applied Biosystems, U.K.). Electrophoresis was conducted on a Life Technologies 3730XL sequencer and analysed using Genemapper software (Applied Biosystems). Markers were genotyped and subsequently verified manually to ensure data quality. Figure 4.1 displays the peaks generated in a polymorphic marker in Apex and DK142 lines.
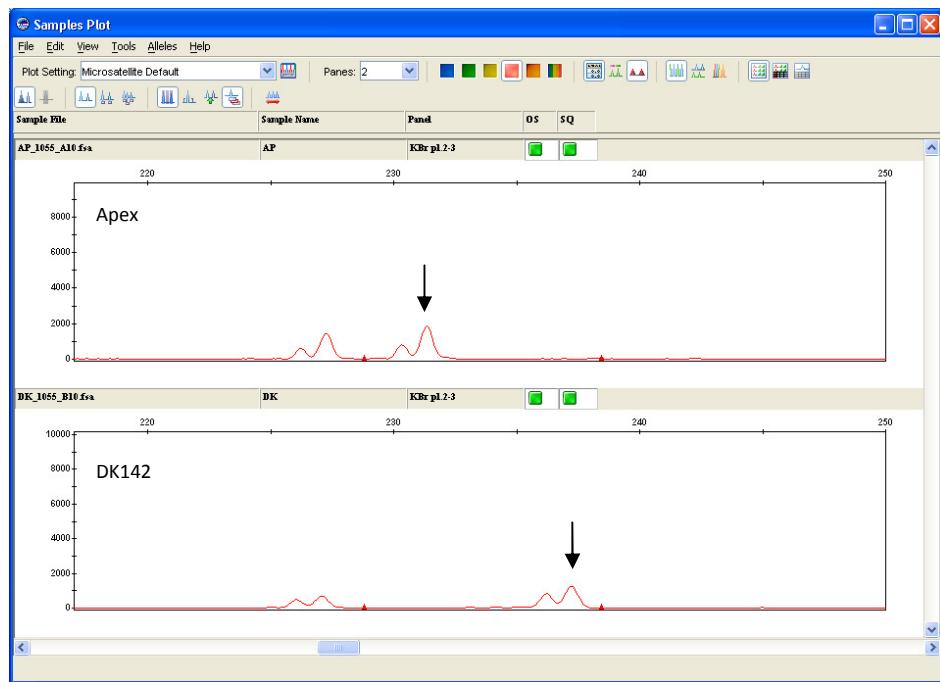
Figure 4.1: Example of SSR polymorphism detection in Apex and DK142 using M13 tailed fluorescent labelled primers, using ABI3730 sequencer and Genemapper software (Applied Biosystems Limited). Difference in position of peak indicated by arrows demonstrates size difference between lines (approx. 232bp in Apex/238bp in DK142).

4.2.3.4 IMSORB Insertion/Deletion (InDels) Marker Screening

PCR for IMSORB allele specific amplification/InDel markers was conducted on an MJ Research PTC-200 thermo-cycler using a 'touchdown' programme, reducing the annealing temperature by $1°C$ per cycle during the first 15 cycles. This acts to increase primer specificity, through reducing mis-priming and also negates the requirement to identify optimum primer annealing temperature for each primer pair. Non-specific binding is more likely to take place at lower temperatures. Therefore, initiating a at higher annealing temperature and subsequently reducing it minimises the quantity of non-specific product at early stages of the PCR, resulting in a higher quantity of the specific product. The touchdown approach means differences in Tm between correct and incorrect annealing will give an

advantage of 2 fold per cycle or 4-fold per ° C to the correct product (Don et al., 1991), therefore enriching for the correct product over any mis-primed products.

Primary rounds of PCR were conducted using the following reaction and 'touch-down' PCR cycle with a primary round of PCR using 20 µl reactions consisting of 7.65 µl ddH$_2$0, 2 µl 10 x PCR buffer (15 mM MgCl$_2$), 1.3 µl dNTPs (2 mM), 2 µl each of forward and reverse primers (2 mM), 0.05 µl *taq* polymerase (~20 U/µl) and 5 µl DNA (20 ng/µl). The touchdown PCR cycle consisted of an initial denaturation at 94°C for 5 mins followed by 15 Cycles with a denaturation at 94°C for 30 s, annealing at 63°C for 30 s (-1°C /cycle) with extension at 72°C for 30 s. These initial cycles were followed by 30 cycles with denaturation at 94°C for 30 s, annealing at 53°C for 30 s, extension at 72°C for 30 s and final extension at 72°C for 10 mins.

For the second stage of PCR a 1 µl of 1/1000 dilution of the primary PCR product was utilised as template to prevent annealing of primers to homologues regions in the genome. Amplification was conducted using two specific primers for small InDels, enabling identification of a size difference between the two parents, whereas one universal and two allele-specific primers were required for SNPs markers. As only two primers were required for the small InDels the volume of ddH$_2$0 was adjusted accordingly. The second round of PCR was conducted using the following conditions using an identical touchdown cycle to the primary round of amplification with 20 µl reactions consisting of 9.65 µl ddH$_2$0, 2 µl 10 x PCR buffer (15 mM MgCl$_2$), 1.3 µl dNTPs (2 mM), 2 µl Primary primer (F or R) (2 mM) 2 µl of allele 1 primer (F orR) (2 mM), 2 µl of allele 2 primer (F/R) (2 mM), 0.05 µl *taq* polymerase (~20 U/µl) and 1 µl DNA (1/1000 dilution of primary PCR product).

Products were visualised using PAGE and genotyped on the population.

4.2.3.5 Candidate Gene Markers - Amplification of Candidate Gene specific PCR products and SSCP analysis

Primer pairs were designed to identify polymorphism in candidate genes identified in *Arabidopsis* using Single Strand Confirmation Polymorphism (SSCP) analysis. Ten sets of primers, termed TW-001-TW-010, were designed using sequence data obtained from *B. rapa, B. oleracea* and *B. napus,* to amplify select regions of *ALCTRAZ, FRUITFUL, INDEHISCENT, RAPE DEHISCENT ZONE POLY GALACTURONASE 1, REPLUMLESS* and *SHATTERPROOF 1 and 2* genes. Primers were designed to span from exons across introns, to identify intronic polymorphism, due to the high levels of sequence similarity within exons between gene homeologues. In the case of the IND gene, which only has one large exon, promoter regions with sequence differences between homeologues ('A' and 'C' genome) were targeted. Oligonucleotides were designed to the following criteria: 18-20 bp in length, a G/C content of 50% and a 3' end with a CC/CG/GG clamp to ensure tight annealing.

A set of 11 primers, termed AP (Amandine Perez), designed around the *BraA.IND.a* gene were also screened in the POSH progenitors. Sequences of primer sets developed during the investigation are displayed in Appendix 4 (page 274). Amplification was conducted using 20 µl reactions consisting of 7.65 µl ddH$_2$0, 2 µl 10 x PCR buffer (15 mM MgCl$_2$), 1.3 µl dNTPs (2 mM), 2 µl of each forward and reverse primers (2 mM), 0.05 µl *taq* polymerase (20 U/µl) and 5 µl DNA (20 ng/µl). PCr was conducted with an initial denaturation at 94°C for 5 mins followed by 35 cycles with denaturation at 94°C for 30 secs, annealing at 50°C for 1 min, extension at 72°C for 1 min and a final extension at 72°C for 10 mins

Amplification products were resolved using SSCP-PAGE. PCR products were denatured for 5 mins at 94°C, with an equal volume of formamide, immediately placed on ice and resolved on a 380 x 310 x 0.35 mm SSCP gel, using mutation detection enhancement (MDE) gel solution (2x, Lonza, Rockland, Me). The gel mix was made to a final volume of 65.5 ml, containing 16.5 ml MDE (2X), 2 ml 20x TTE buffer (National Diagnostics, Hull, U.K.), 35 ml sterile ddH$_2$0, 12 ml 50% glycerol and polymerised on addition of 36 µl

tetramethyllenediamine (TEMED) and 400 µl of 10% ammonium persulphate. PCR products were electrophoresed for 16 hours, at 2 W, in a CER at 5°C. Gels were visualised using silver staining as described for PAGE, but with elongated fixation, rinsing and staining durations of 1 hr, 30 mins and 1 hr respectively.

4.3 Results

4.3.1 Marker Screening and Genotyping

4.3.1.1 Marker Screening

224 SSR primer sets from four different libraries were screened for polymorphism in the POSH 1-3 progenitors, Apex and DK142. These consisted of 73 BBSRC markers (Lowe *et al.* 2004), 66 BRMS markers (Suwabe *et al.* 2002), 7 KBr markers predicted directly from sequenced *Brassica* BACs (www.brassica.bbsrc.ac.uk) linked to candidate genes and 78 markers from AAFC Saskatoon Research Centre (www.brassica.agr.gc.ca/index_e.shtml). Polymorphic primer pairs were then genotyped against the entire POSH 1-3 population.

A further 329 primer pairs consisting of 103 BBSRC markers, 58 BRMS, 34 Celera (Piquemal *et al.* 2005; Radoev *et al.*, 2008), 34 FITO (Iniguez-Luy et al 2009), 100 KBr (www.brassica.bbsrc.ac.uk) were screened in POSH 1-3 parents and polymorphic markers subsequently genotyped in the population using an automated M13 tailed fluorescent labelled approach (see Schuelke, 2000). This included a number of primers observed to amplify poorly using conventional PCR and PAGE screening (68 BBSRC and 58 BRMS primer pairs, respectively). The fluorescent labelled approach utilises the incorporation of an M13 adaptor sequence into the PCR product. This is achieved by generating a primer containing the target sequence and an M13 tail at its 5' end (21 bp). The quantity of this primer/adaptor sequence is reduced compared to the complementary primer (Forward/Reverse) so it is used up in the initial of cycles of PCR. Subsequently the fluorescently labelled M13 universal primer, with a sequence complementary to the adaptor sequence now present at the 5' end in the PCR product, will be used to prime amplification in each new round of PCR. Hotstart taq polymerase is utilised to avoid mispriming during the

beginning of the reaction. Incorporation of a fluorochrome into PCR products enables differences in fragment size to be resolved on a capillary sequencer.

A series of IMSORB (integrated markers system for oilseed rape breeding) primers (Brassica.bbsrc.ac.uk/IMSORB) were also screened in POSH 1-3. These are a set of 35 allele-specific and 9 InDel markers developed for the Tapidor x Ningyou 7 DH *B. napus* population (Qiu *et al.,* 2006). Primers were developed from sequences linked to specific homologues of *Arabidopsis* genes were designed from BAC end sequences to first generate a template fragment of approximately 500bp in both parents. PCR products were then sequenced and aligned to identify small InDels or SNP polymorphisms between the two parent lines which were identified in a subsequent round of PCR. Amplification and potential polymorphism in large InDels in the primary round of PCR was verified using a 1.5% agarose gel. For small InDels, a subsequent round of PCR using two primers selective for the InDel between parents was utilised, resulting in an equivalent size difference.

For primers amplifying SNPs the second round PCR was conducted using one universal and two allele specific primers. Allele specific primers were designed at ~20 bp in length with a deliberate mismatch in the penultimate 3' base to improve primer specificity. This relates the requirement of complementarity at the 3' to ensure efficient polymerase extension (Ayyadevara *et al.* 2000). Therefore extension can only occur in the allele that is complementary to the primer and not in the allele containing the penultimate mis-match. To each Tapidor primer, 15 bp of non-annealing sequence was incorporated, to create a size difference between alleles. Both small InDels and SNPs were designed to be resolved on a 3% metaphor gel, but to increase resolution further PCR products were visualised using PAGE.

In total, 423 primer pairs, from nine individual sets, were screened in the progenitors of the POSH 1-3 population. 99 primer sets were identified as being polymorphic in the population (approximately 24 %). Primers genotyped in the population consisted of 88 SSRs

(32 conventional, 56 M13), four IMSORB InDel/SNP primers and seven SSCPs designed to specific candidate genes. 47 primers produced in excess of one polymorphic locus, with the majority of these represented in the M13 tailed class of SSRs. 32 out of 56 M13 tailed primers produced multiple loci compared to 15 out of 43 conventional primers resolved using PAGE. Of the conventional primers producing multiple loci, five SSCP primers were identified as generating multiple loci and two single loci only. Polymorphic primers generated a total of 177 new loci for genetic linkage mapping, corresponding to ~1.8 loci generated per genotyped primer pair. This increased the number of genotyped loci in the POSH 1-3 population from 162 to 340. Automated genotyping was observed to be more efficient than manual marker genotyping through the ability to multiplex PCR products although the rates of polymorphisms detected between techniques were similar (Conventional 16.5% (43/260) compared to 17% (56/329) for M13 tailed). Multiple loci that could be successfully genotyped were more likely to be identified using the M13 approach.

4.3.1.2 Polymorphism in SSRs and IMSORB Markers

Rates of polymorphism in the POSH 1-3 population varied between primer sets

BBSRC primers demonstrated a polymorphism rate of approximately 10%, with 21 new loci generated from 10 primer pairs, from 107-set screen (5 manual, 6 M13 tailed with 8 and 10 loci, respectively). Of the 21 markers amplified by the BBRSC primers, 12 were generated from primers developed from *B. nigra,* four from *B. napus,* and four from *B. oleracea* and one in *B. rapa.* The rate of polymorphism in POSH 1-3, at least for the BBSRC markers, appears to be reduced compared to other populations they have been screened in (62% for primers tested in Lowe et al., 2004).

BRMS markers demonstrated a polymorphism rate of 32% with 21 of 66 primers observed to be polymorphic in POSH lines (8 manual, 13 automated). This generated a total of 31 new loci for genotyping. Amplification of BRMS primers was relatively unsuccessful under conventional PCR and PAGE analysis (8 polymorphic primers from 66 screened identified). For this reason 63 of 66 BRMS primers were re-screened using the M13 tailed approach and

13 more polymorphic primer sets were identified and genotyped accordingly, including five markers that were difficult to genotype using conventional PCR/PAGE.

Of the 34 Celera markers screened in the POSH parents, 20 were observed to be polymorphic, yielding 56 loci for genotyping and exhibiting the highest polymorphism rate amongst marker sets screened (58%). FITO primers were demonstrated to be less effective, with only 6 polymorphic primers (17%), generating 12 new loci.

Nine polymorphic primers from the 107 KBr assayed (2 manual, 7 automated) were identified, producing 15 loci for genotyping. This set of markers displayed the lowest polymorphism rate of marker sets tested (8%) due to non-reproducibility during genotyping. The two manually genotyped KBr SSR markers were identified to be adjacent to (on the same BAC) copies of candidate *FRUITFUL* and *RDPG1* genes.

For AAFC Saskatoon primers screened in POSH 1-3, a polymorphism rate of approximately 22% was established, with 17 of 78 primers identified to be polymorphic. Markers were subsequently genotyped generating 24 new loci for mapping.

IMSORB primers produced four genotyped loci from 35 primer sets screened (11%). Three markers were observed to be small InDels whilst the other represented a SNP in the 500 bp target amplicon.

4.3.1.3 Polymorphism in SSCP candidate gene markers

Intragenic SSCP markers for candidate genes were successfully developed and screened for copies of *ALCATRAZ* (*BnaA.ALC.*x and *BnaC.ALC.*x), *REPLUMLESS* (*BnaX.RPL.x*), *SHATTERPROOF 1* and *2* (*BnaX.SHP1.a* and *Bna*X.*SHP2.a*, respectively) and *INDEHISCENT* (*BnaA.IND.a* and *BnaC.IND.a*). Individual primer pairs amplified multiple copies of target candidate genes for *ALC* and *IND* markers, although homeologue-specific amplification was initially desired. Markers for the *BraA.IND.a* (*BnaA.IND.a*) gene were also generated by two

of the AP SSCP primers. Each individual AP primer pair generated two loci which were identified to behave as co-segregants.

4.3.2 Genetic Linkage Mapping

4.3.2.1 Genetic Linkage Map Construction

Genetic linkage mapping was conducted using Joinmap Version 3.0 software, using the Kosambi mapping function to translate recombination frequency into map distance (centimorgans (cM)) (Van Ooijen & Voorrips, 2001). The Joinmap program functions to position markers sequentially/systematically (one followed by another) starting with the most tightly linked pair of markers with a measure of goodness of fit (X^2 chi-squared) is calculated for each marker.

Initially a LOD tree is generated for all the loci present. The grouping is based on a test for independence, translated into a LOD score. The tree represents loci in groups of associated markers at nodes with increasing LOD stringency. As the LOD increases, only loci with significant pair-wise associations, with at least one other marker in the group, will be retained in the mapping node.

Individual groups of markers at a given node can then be selected for mapping. An initial round of mapping is performed with no forcing of problematic loci allowed. A second and a third round of mapping are then conducted, re-testing all associated markers in a group to position them against the other loci or by forcing the marker into the map at the best estimated point, disregarding requirements of maximum allowed reduction in goodness of fit and no negative distances (Van Ooijen & Voorrips, 2001). Any markers observed to display high mean chi squared values (markers mean contribution to the goodness-of-fit) were more likely to be mapped erroneously and were assessed or removed before the maps were re-calculated.

Polymorphic loci genotyped in 140 POSH 1-3 lines were used as the basis for the linkage map. Maps were calculated using pair-wise data from genotyped marker loci. However only markers which have a recombination frequency smaller than recombination (REC) threshold (0.4 default) and a logarithm of the odds of the differences value larger than the LOD threshold (1.0 default) were included by the program. A maximum LOD groupings threshold of 20 was imposed during the initial stages of mapping to ensure sufficient separation due to the apparent association between markers from duplicated or homeologous regions within the POSH 1-3 *B. napus* genome. Most mapping was conducted between LODs of 10-15, to ensure separation of homeologous linkage groups.

After initial identification marker groupings stage two or three maps were mapped individually. Reducing the LOD resulted in linking/transposition of marker groupings with similar homologies. Individual/multiple markers could be assessed for their relative goodness-of- fit compared to the remaining markers in the linkage group enabling the most accurate construction possible. Markers were excluded on the basis of low goodness of fit (high mean chi square value), due to abnormalities in allele scoring resulting from segregation distortion (an imbalance in relative A to B ratio, which would be expected to be similar in loci situated from the same region), or due to a high frequency of un-scored alleles (U). Markers were rescored and remapped where any errors were identified. Finally locus genotype frequencies (A/B ratios) were re-assessed for segregation distortion in marker groupings. Large increases in segregation distortion highlighted potential areas where map order may require refinement.

4.3.2.2 Results from Genetic Linkage Mapping

Ninety-nine of four-hundred and twenty three primer pairs screened for polymorphism were genotyped in the POSH 1-3 population, with 47 pairs generating multiple loci. This generated 178 new loci, more than doubling the markers previously available, providing a total of 340 genotyped loci for genetic linkage mapping.

Initial rounds of mapping were conducted at LODs of 10-15 (Max. LOD groupings threshold 20), to resolve issues with linkage group separation caused by homeologous or duplicated regions in the POSH genome. Mapping at lower LOD threshold resulted in decreasing numbers of large, compound, marker groupings (with excessively large distances (>100cM)). 39 linkage groups have been identified, of which 17 can be designated as representative of regions of associated A/C genome homeologues (Figure 4.2). Representative linkage groups are presented for N1-N14, N17 and N18. The current POSH 1-3 linkage map consists of 218 markers with 120 loci remaining as doublets or single markers still to be integrated. Markers comprising the map include 2 AP SSCPs, 67 BBSRC SSRs, 16 BRMS SSRs, 36 Celera SSRs, 5 FITO SSRs, 9 KBr SSRs, 11 RFLPs, 2 IMSORB InDel/SNP markers, 58 Saskatoon SSRs and 12 TW SSCPs. A cumulative map distance of 1123cM is suggested for mapped loci.

The original POSH 1-3 map consisted of 120 markers spanning over 19 linkage groups with a cumulative map distance of 841 cM. The addition of new markers and conducting mapping at a higher stringency/LOD has highlighted the limitations associated with the original map such as lack of coverage and density of population and the mixing of linkage groups.

Due to the current status of the POSH 1-3 and issues with accurately designating specific linkage groups to groups of markers, a global view of segregation distortion in constituent markers was preferred. From a total of 30098 genotyped alleles in 140 lines, it was discovered that alleles were slightly skewed towards the DK142 parent with 48.2% exhibiting a B, whereas, A-alleles from Apex represented 42.1% of scored loci. Approximately 9.6% of alleles remained un-scored (U).

A number of markers mapped in POSH 1-3 have also been mapped in other more developed *B. napus* mapping populations and can therefore be described as anchors. 70 markers were observed to be anchored the Tapidor/Ningyou-7 (TN) map (Qiu *et al.,* 2006), 25 in the BBSRC consensus map (Lowe *et al.* 2004), 29 in the Piquemal *et al.* (2005) consensus map and 45 in the AAFC Saskatoon map.

BnaA.IND.a and *BnaC.IND.a* were subsequently mapped in the Tapidor/Ningyou 7 (Qiu *et al.* 2006), doubled haploid, *Brassica napus* population using SSCP (Single Strand Conformation Polymorphism) analysis to verify their relative position in the *B. napus* genome (Girin *et al.* 2010). This was to anchor the markers in the TN population, aiding to verify the suggested position of the markers on the POSH 1-3 genetic map. Each predicted A and C genome specific marker appeared to map to the same respective linkage groups in both populations (LN3 (N3) and LN13 (N13)).
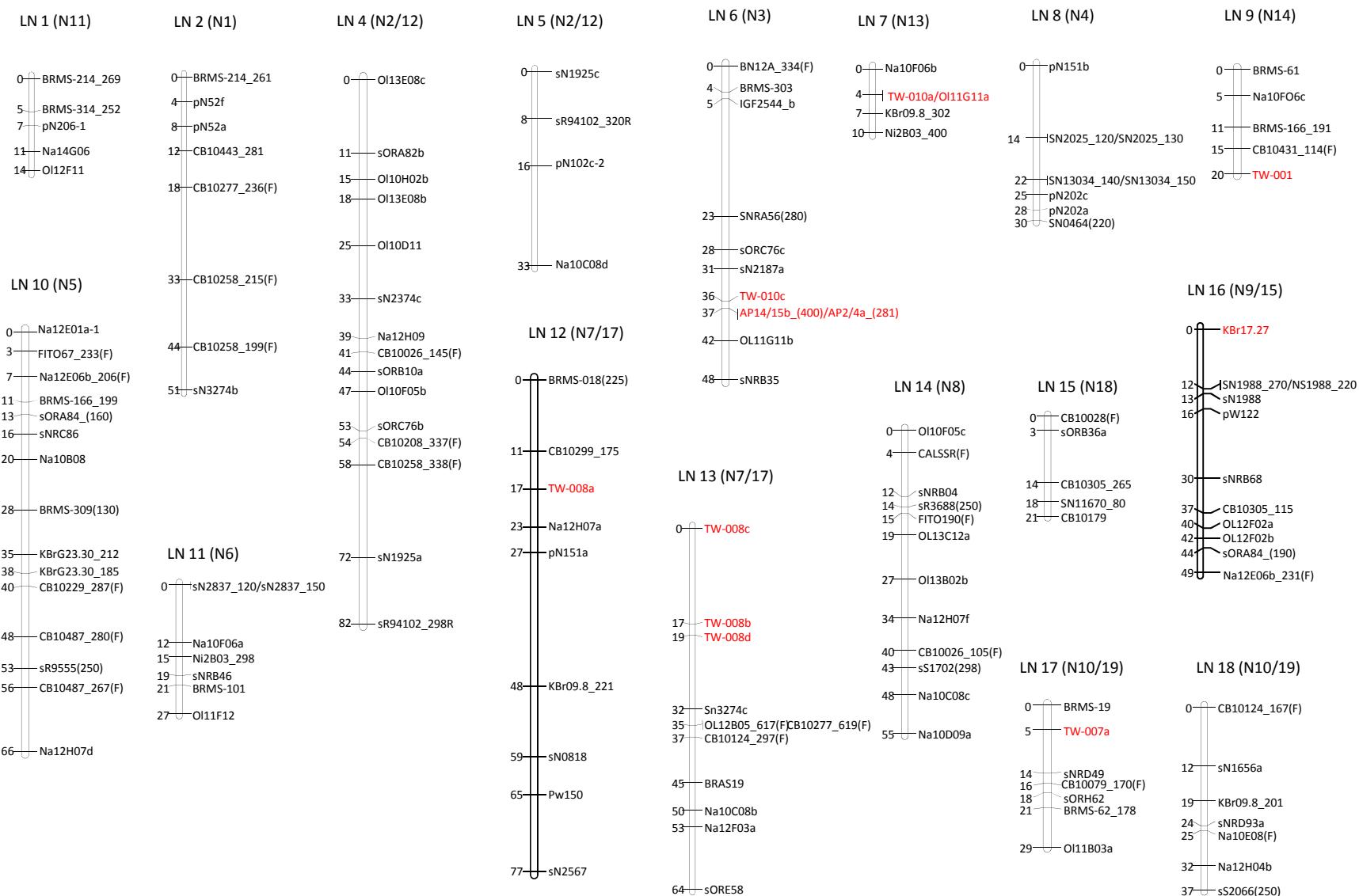
Figure 4.2: Preliminary POSH 1-3 Genetic Linkage Map composed of 218 loci. Candidate gene loci are marked in red

LN 19 (N3/N13)
0 — BN12A_303(F)
11 — Ni2-B03_148
18 — BRMS-6_159
26 — sS2368b
37 — Na10G10b
40 — CB10079_201(F)
52 — CB10106_139

LN 20
0 — Ol10A11a
10 — Na14D09
15 — CB10373(F)
23 — Na14B03
24 — sNRD76
26 — SN11670_115
37 — TW-006

LN 21
0 — Ni4-A07_250
7 — Na12A08c
10 — Ol10H02c
20 — Ol13A10
21 — Na12F12
22 — sORB36b

LN 22
0 — sNRB68
5 — Na12F03b
10 — OL12F02a
12 — OL12F02b
15 — CB10305_115
20 — Na12E06b_231(F)

LN 23
0 — BRMS-108_148
2 — sN360/Na12D04
25 — Na12H04a
36 — KBrA14.8_221
37 — KBrA14.8_238
41 — Ol10G05

LN 24
0 — BRMS-93_256
16 — Na12H07e
21 — Na10C01a
34 — CB10109

LN 25
0 — FITO135
11 — pN52d-1
21 — Ni2B03_198
33 — Ni2-B03_180

LN 26
0 — KBr09.8_221
12 — sN0818
19 — Pw150
32 — sN0212b

LN 27
0 — sS1949(180)
9 — sNRB93
15 — KBr11.30_231
27 — CB10258_595(F)

LN 28
0 — FITO122_113
6 — sS1854a
13 — sORH43
21 — Na10C01c

LN 29
0 — Na12H06
9 — Ol13E08a
13 — Ol10H02a
25 — sORA82a

LN 30
0 — TW-007b
17 — Ol11B03b
30 — BRMS-62_173

LN 31
0 — CB10587_185(F)
15 — Na12G03
27 — SN11641(395)

LN 32
0 — IGF5154_c
10 — CB10079_205(F)
22 — Na10G10a

LN 33
0 — CB10299_175
10 — TW-008a
18 — Na12H07a

LN 34
0 — TW-010b
9 — sN2187c
14 — Na12H07g

LN 35
0 — Ol10D10a
9 — sS1854b
13 — sN0212a

LN 36
0 — Ol10F05a
19 — sN2321

LN 37
0 — CB10208_344(F)
14 — CB10258_325(F)

LN 38
0 — Na12A08a
10 — SR11644_250/SR11644_350

LN 39
0 — BN12A_266(F)
3 — FITO66_208

4.4 Discussion

The investigation was targeted towards improving the coverage and population of the POSH map as well as identifying key candidate genes involved in pod shatter resistance. Marker screening and genotyping has generated 178 new loci for genetic linkage map construction, bringing a total of 338 markers for the POSH 1-3 population. This includes a series of intragenic markers designed from candidate fruit development genes with established function in *Arabidopsis*. The utilisation of automated sequencing and genotyping greatly increased the rate at which polymorphic loci could be identified in the POSH population, whilst decreasing the relative cost of marker identification, thus enabling a greater frequency of markers to be added to the linkage map.

Differences in the level of polymorphism in SSR Markers in POSH1-3 were observed

Relatively low levels of polymorphism were identified in all but one of the six SSR primer sets during marker screening in the POSH 1-3 population. SSR markers are reported to show high levels of transferability across *Brassica* species between members of *Brassicacea* (Lowe *et al.,* 2002, 2004). However this did not appear to be the case for the POSH 1-3 population with respect to BBSRC, BRMS, FITO, KBr derived and Saskatoon SSRs. Celera markers displayed a rate of polymorphism of 58%, a figure similar to that reported for BBSRC markers in four other *Brassica* species (Lowe *et al.,* 2004). Although the PSR trait was introgressed from a synthetic hybrid, with introduction of other diverse alleles into the population (Morgan *et al.* 1998), it would appear the level of polymorphism in the POSH 1-3 is potentially reduced compared to other populations, at least for the SSRs screened.

Out-crossing in the DK142 may have confounded issues further, reducing the amount of detectable polymorphism between the shatter resistant parent and Apex during marker screening. A lack of identifiable polymorphism amongst lines compared to polymorphism between progenitors during genotyping was also observed for some markers supporting this hypothesis. A lack of polymorphism could relate to the similarity of the N-0-109, used in the initial cross to derive the DK142 line, with Apex which was subsequently used to derive the

POSH 1-3 lines in the cross with the DK142. Although crossing with these elite cultivars was conducted at each respective stage to improve agronomic quality, this may have potentially reduced diversity in the population, confounding polymorphism rate.

IMSORB SNP/InDel markers were observed to exhibit a polymorphism rate of only 11%, similar to that observed for BBSRC and KBr derived markers. Markers were demonstrated to amplify successfully in POSH lines but a lack of polymorphism was evident for these loci. This could be related to the design of the IMSORB markers as they were developed to identify specific polymorphism in the TNDH population (Qiu *et al.* 2006) and these sites may not be present in POSH 1-3.

Candidate Gene Specific Markers were Developed and Mapped in POSH 1-3

Candidate gene specific SSCP markers were used to successfully map orthologues of five key fruit regulatory genes. This will enable us to identify specific genes during subsequent marker analysis to ascertain if orthologues of key genes involved in *Arabidopsis* fruit development contribute to differences in pod shatter in *B. napus.* Although the initial aim was to identify individual copies of specific *B. napus* candidate genes in POSH lines, and this was attained, copy specific PCR could not be achieved due to similarity of primer sites between homeologues. Primer pairs were observed to often amplify both A and C genome homeologues or even multiple copies of a specific candidates, although the differences in genotyping could be resolved due to differences in DNA conformation on MDE gels.

This method highlights the benefits of a candidate gene approach and basis of genomic synteny in *Brassica,* which have enabled us to exploit sequence information from key regulatory genes first identified in the model, but also identifies the problem of achieving copy-specific PCR due to sequence similarity. Homeologue specific markers designed in the *IND* gene have aided linkage group designation in N3 and N13, through reverse genotyping and mapping of these markers in the more comprehensively mapped TN population (Qiu *et al.,* 2006, Girin *et al.,* 2010). This highlights that these markers may be transferrable across *B.*

napus populations and could be used as a resource to map candidate genes in other populations*.

Regions of segregation distortion were identified within the POSH 1-3 genome due to preferential selection for regions of Apex or DK142 genome. On a global scale, markers were slightly skewed in favour of the DK142 parent opposed to the Apex parent, although without a more complete map, with a greater degree of linkage between fragments, its is difficult to draw firm conclusions.

The Coverage and Marker Density of the POSH 1-3 Linkage Map has been improved

For the skeleton POSH 1-3 linkage map, we set a target of ten markers per linkage group. This figure was only achieved in six linkage groups and is suggested to be due to a lack of identifiable polymorphic markers from some regions of the genome, coupled with a lack of linkage between the markers that have been mapped. An average marker density of 5.6 markers per linkage group is presented for the current POSH 1-3 map. However, it must be considered that the current map is represented as 39 linkage groups, not 19 individual groups representative of each *B. napus* chromosome, due to an apparent lack of linkage between some segments. It was not possible to designate specific linkage groups to all marker groupings identified due to this lack of linkage between fragments and a lack of common, anchored markers, between POSH and other more densely mapped populations.

However, a number of anchored markers positioned in the genetic maps of other populations have been successfully genotyped in the POSH 1-3 population, allowing the distinction of a number of regions pertaining to homeologous (A and C) pairs of linkage groups. Identification of specific linkage groups has been hindered by a general lack of coverage/linkage and also by the multi-allelic nature of SSRs, resulting in multiple loci mapping at different regions within the genome, usually in homeologues or duplicated regions (as predicted by Parkin map (Parkin *et al.,* 2005)). It is suggested that a greater

number of locus-specific anchored markers, with a known location in multiple populations, would aid identification of individual linkage groups in POSH.

Efforts to improve POSH 1-3 linkage map have resulted in a greater level of coverage, with an increase in cumulative map length of 841 cM to 1123 cM and an increase in marker population from 120 mapped loci to 226. More comprehensively mapped populations, namely the Parkin and TNDH maps present cumulative distance of 1837 cM (~9Mb) and 1724 cM respectively. Only prospective group LN13 (64 cM) representing N7 (or N17) exhibited a length similar to that suggested according to Parkin *et al.,* (2005) (N7: 66.3 cM). Evidently, this suggests there are still regions of the POSH 1-3 linkage map that remain to be elucidated. Further genotyping efforts to increase map coverage could increase association between disparate fragments and help integrate the remaining 113 unmapped loci. Inclusion of centromeric markers could also aid linkage group designation.

Although not a 'complete' skeleton map, the much improved POSH 1-3 map, with both greater marker coverage and density, is comprised of a suitable number of markers on which to perform QTL analysis. The map, along with trait data collected during POSH field trials, will form the basis of the single marker analysis from which to identify factors contributing to PSR. This process is described in the next chapter.

Chapter 5: POSH 1-3 Single Marker Analysis

5.1 Introduction

Many important characters relating to crop development and yield demonstrate continuous, quantitative variation, where desirable phenotypes arise from the contribution of multiple genes, each having small effects (Kearsey and Pooni, 1996, Shi *et al.* 2009). Due to the polygenic nature of many traits, and minor contributory effects which are often difficult to detect, approaches have been developed to identify regions of the genome conferring such phenotypes (Collard *et al.* 2005). Regions contributing to this type of variation are referred to as quantitative trait loci (QTL) (Gelderman, 1975). Identification of QTL requires two main elements; two or more individuals, that differ genetically for the trait in question and genetic markers that distinguish between the parental lines amongst a derived population segregating for the trait (Miles & Wayne, 2008).

Identification of QTL contributing to quantitative variation is dependent on linkage between specific markers and a QTL, demonstrating non-independent segregation, resulting in markers being associated with different trait phenotypes (Kearsey, 1998). Also required is a robust manner in which to measure the trait being assessed and suitable statistical software to identify associations with the trait and genotyped molecular markers. A number of statistical approaches have been developed to identify QTL. The simplest technique is Single Marker Analysis which uses analysis of variance (ANOVA) or t-tests to establish if marker means are significant for the trait, or through Linear Regression, by regressing the trait value onto the marker genotype (Kearsey, 1998, Kearsey and Hyne, 1994). Other approaches include Interval Mapping, which uses genetic linkage maps and intervals between adjacent pairs of linked markers (Lander and Botstein, 1989), and Composite Interval Mapping, which combines both Linear Regression and Interval Mapping (Jansen *et al.* 1993, Zeng *et al.* 1994).

QTL analysis has been applied in *Arabidopsis* and a range of *Brassica* species, including *B. napus,* to identify regions of the genome linked to important traits including seed oil content and fatty acid profile (Ecke *et al.* 1995, Burns *et al.,* 2003, Qiu *et al.,* 2006), seed erucic and

147

linolenic acid content (Thormann *et al.,* 1996), flowering time, Long *et al.* 2007) and seed yield (Udall *et al.,* 2006, Shi *et al.* 2009).

The genotyping and mapping of a range of genetic markers to generate a partial genetic linkage map was described in Chapter Four and a phenotypic evaluation of Pod Shatter Resistance in the POSH 1-3 population was described in Chapter Three. This data will form the basis for a QTL analysis. This chapter discusses a Single Marker Analysis performed using two separate approaches to identify loci significantly contributing to Pod Mass (g), Seed Mass (g), Seed Damage, RIT_{50} and adjusted RIT_{50}. It describes techniques to aid the elucidation of targets for crop improvement with potential for use in Marker Assisted Selection (MAS), with scope for introgression into commercial *B. napus* varieties, to reduce pre-harvest pod shattering.

5.2 Materials and Methods

5.2.1 Single Marker Analysis

Trait and genotyping data from both the complete 2006 field trial and the 2009 subset trial (Chapter Two) were analysed using two methods to ascertain if different markers could be identified to be significantly associated with the measured characters. As the POSH 1-3 genetic linkage map still required refinement, MapQTL software was used to conduct a Single Marker Analysis (SMA), to investigate the statistical significance of loci linked to important traits, as opposed to Interval Mapping or Composite Interval Mapping approaches. A Single Marker Regression (SMR) model (Morgan, unpublished) was also tested due to the non-normal distribution of PSR in the population.

The SMA was first performed using MapQTL utilising a non-parametric Kruskal-Wallis (KW) analysis giving a ranked order value for each loci, from which statistical significance is calculated individually, with no reference to map order. Segregating QTL are indicated by large differences in the average rank of the marker genotype classes and a test statistic based on the genotype rank classes is calculated (Van Ooijen, 1993, 2004). As a rank order test KW analysis is not affected by non-normal distribution of data.

The SMR was then utilised to analyse loci associated with traits in POSH 1-3. The SMR is a parametric analysis, using direct numerical values for each individual marker for a selected trait. This approach was used to assess if the distribution of RIT_{50} data affected QTL detection. Using trait values can result in more leverage in data points from outliers in the population and therefore can be affected by data distribution. Marker regression detects QTL by assessing the relationship between the mean value of a random variable and the corresponding value of one or more independent variables. In this case, regression analysis identified the additive difference between marker genotypes at a given locus, against a function of the recombination frequency between that locus and the putative QTL (Kearsey and Hyne, 1994). The coefficient of determination (R^2) from markers explains the phenotypic variation from linked QTL in the SMR approach (Collard *et al.,* 2005). As with the KW analysis

markers are treated individually, regardless of map order. Additivity is also calculated using the SMR, demonstrating how much a locus contributes to the absolute trait value and indicates which parent is increasing and which is decreasing. Positive additivity values in SMR highlighted the main contribution to a trait was from the DK142 allele, whereas, negative additivity indicated contribution from the Apex allele.

Markers demonstrating a $P<0.05$ were accepted to be significantly associated with traits. Genotyping data for the 338 loci was prepared for the 73 lines and trait data was obtained during the 2006 field trials and also for the 9 lines from the 2009 sub-trial to enable single marker analysis. For the 2006 trial marker associations were investigated for Pod Mass (g), Seed Mass (g), Seed Damage (induced during Random Impact Testing (RIT) (0-9 scale 0-none, 9- severe), and Intact and Broken RIT_{50}/adjusted RIT_{50} traits, whereas only Pod Mass (g) and Intact and Broken RIT_{50}/adjusted RIT_{50} were investigated in the 2009 dataset. Both Intact and Broken measures of RIT_{50} and adjusted RIT_{50} were included in the analyses to ascertain if differences could be identified to provide a greater insight into the factors potentially regulating the complex, polygenic trait of pod shatter resistance.

Markers were named after the suites they were derived from and alleles of the same locus were distinguished either alphabetically *i.e.* TW-008 a, b, c, or d, or by inclusion of the size of the PCR product amplified after the name of the primer pair *i.e.* BRMS-62_173, BRMS-62_178, thus giving reference to the size of the allele generated.

Linkage groups were designated with a numeric value LN 1-LN 39 during the linkage map procedure (Chapter Four) and also with specific *Brassica napus* chromosome names (N1-N19) where accurate determination of constituent markers was possible. Undesignated homeologous chromosome (from A and C genomes) are identified by both terms *i.e.* N7/N17 (LN 12) and N7/N17 (LN 13).

A separate analysis, utilising the SMR approach was also conducted on the 9 lines common to the 2006 and 2009 trials to investigate if similar markers were contributing to traits in the same lines across different years. The SMR approach was also conducted on data collected from a previous trial conducted in 2000 in the POSH 1-3 population (Morgan *et al.*, unpublished). 44 Lines common to the 2000 and 2006 trials were assessed for similarities in marker associated to Intact and Broken RIT_{50} and Pod Mass using the improved genotyping data produced during our investigation (discussed in Chapter Four).

Markers identified as having a significant association with Intact and Broken adjusted RIT_{50} (*P*<0.05) were selected for subsequent multiple regression analysis to establish the percentage variance loci may account for, if multiple loci contribute to traits with differing degrees and also to identify potential interactions between loci.

5.2.2 Multiple marker regression

Genstat V.12 software (Payne, 2009) was utilised to perform a multiple regression to identify specific combinations of loci in the 2006 trial for Intact and Broken adjusted RIT_{50}. Markers were selected on their relative significance in the preliminary Single Marker Regression (SMR) analysis. This model also enabled interactions between loci to be identified. The multiple regression could not be used to assess the 2009 sub-trial due to the lack of information associated with a small sample size.

5.2.3 Marker Homologies

Primer homologies of significant markers were interrogated using BLAST software (www.blast.ncbi.nlm.nih.gov/Blast.cgi) to identify similarities between other *Brassica* and *Arabidopsis* sequences to attempt to designate gene candidacy.

5.3 Results

Marker data from KW analysis for 2006 and 2009 datasets are displayed in appendices 5.1-5.12, whereas data from the SMR for 2006, 2009 and nine select lines from 2006 are displayed in appendices 5.13- 5.29. The most statistically significant loci for each linkage group for Pod Mass, Seed Damage and Intact/Broken RIT_{50} and Intact/Broken adjusted RIT_{50} traits are displayed in Figure 5.1 (p 153). Data from the 44 lines common to 2000 and 2006 datasets are displayed in appendices 5.30 – 5.35. Multiple regression data for Intact and Broken adjusted RIT_{50} is included in appendices 5.36 and 5.37, respectively, and multiple regression data highlighting interactions for Intact and Broken adjusted RIT_{50} is included in appendices 5.38 and 5.39, respectively.

5.3.1 Pod Mass (g)

2006 Trial

QTL analysis was performed using KW and SMR. Similar markers were identified using both approaches for the Pod Mass trait for the 2006 dataset, but with slight variation in the ranking of the significance of these loci (Appendix 5.1, 5.13 (pages 275 and 284, respectively). In total 49 markers were significantly associated with the Pod Mass trait ($P<0.05$) using KW, whereas 44 loci were observed to be associated with the SMR ($P<0.05$). 39 loci were coincident between the analyses. Loci demonstrating the highest levels of significance mapped to N2/N12 (LN 5), N3 and a number of markers resided in undesignated linkage groups or unmapped regions of the genome, in both approaches (Table 5.1). Major QTL were identified on N2/N12 ($P<0.001$) and N3 ($P<0.001$). Major QTL were also observed for the unmapped Na12E01b ($P<0.005$) and KBrM6.12 ($P<0.01$) markers.
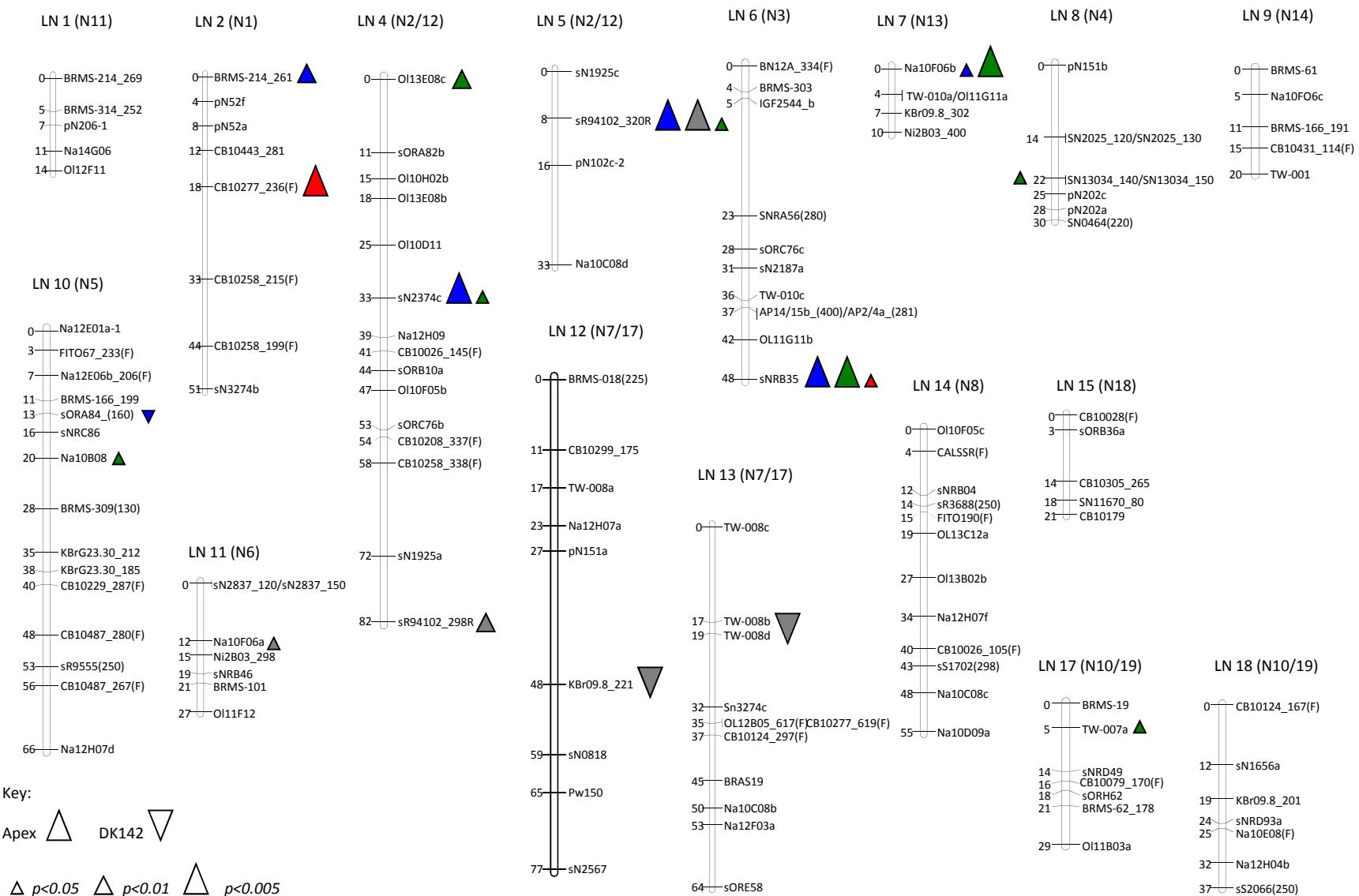
Figure 5.1: POSH 1-3 genetic linkage map displaying the most significant markers for each linkage group for Pod Mass (blue), Seed Damage (grey), Intact/Broken RIT$_{50}$ (green) and Adjusted Intact/Broken RIT50 (red) identified using Single Marker Analysis.

LN 19 (N3/N13)
- 0 — BN12A_303(F)
- 11 — Ni2-B03_148
- 18 — BRMS-6_159
- 26 — sS2368b
- 37 — Na10G10b
- 40 — CB10079_201(F)
- 52 — CB10106_139

LN 20
- 0 — Ol10A11a
- 10 — Na14D09
- 15 — CB10373(F)
- 23 — Na14B03
- 24 — sNRD76
- 26 — SN11670_115
- 37 — TW-006

LN 21
- 0 — Ni4-A07_250
- 7 — Na12A08c
- 10 — Ol10H02c
- 20 — Ol13A10
- 21 — Na12F12
- 22 — sORB36b

LN 22
- 0 — sNRB68
- 5 — Na12F03b
- 10 — OL12F02a
- 12 — OL12F02b
- 15 — CB10305_115
- 20 — Na12E06b_231(F)

LN 23
- 0 — BRMS-108_148
- 2 — sN360 Na12D04
- 25 — Na12H04a
- 36 — KBrA14.8_221
- 37 — KBrA14.8_238
- 41 — Ol10G05

LN 24
- 0 — BRMS-93_256
- 16 — Na12H07e
- 21 — Na10C01a
- 34 — CB10109

LN 25
- 0 — FITO135
- 11 — pN52d-1
- 21 — Ni2B03_198
- 33 — Ni2-B03_180

LN 26
- 0 — KBr09.8_221
- 12 — sN0818
- 19 — Pw150
- 32 — sN0212b

LN 27
- 0 — sS1949(180)
- 9 — sNRB93
- 15 — KBr11.30_231
- 27 — CB10258_595(F)

LN 28
- 0 — FITO122_113
- 6 — sS1854a
- 13 — sORH43
- 21 — Na10C01c

LN 29
- 0 — Na12H06
- 9 — Ol13E08a
- 13 — Ol10H02a
- 25 — sORA82a

LN 30
- 0 — TW-007b
- 17 — Ol11B03b
- 30 — BRMS-62_173

LN 31
- 0 — CB10587_185(F)
- 15 — Na12G03
- 27 — SN11641(395)

LN 32
- 0 — IGF5154_c
- 10 — CB10079_205(F)
- 22 — Na10G10a

LN 33
- 0 — CB10299_175
- 10 — TW-008a
- 18 — Na12H07a

LN 34
- 0 — TW-010b
- 9 — sN2187c
- 14 — Na12H07g

LN 35
- 0 — Ol10D10a
- 9 — sS1854b
- 13 — sN0212a

LN 36
- 0 — Ol10F05a
- 19 — sN2321

LN 37
- 0 — CB10208_344(F)
- 14 — CB10258_325(F)

LN 38
- 0 — Na12A08a
- 10 — SR11644_250/SR11644_350

LN 39
- 0 — BN12A_266(F)
- 3 — FITO66_208

Minor QTL associated with differences in Pod Mass were identified on N5, N6 and N13 (*P*<0.05). A minor QTL (*P*<0.05) was also identified on the corresponding N2/N12 homeologue (LN) in both. The sNRB35 marker from N3 was observed to exhibit the greatest association with the Pod Mass trait and mapped to a region corresponding to *Arabidopsis* chromosome 3 (*P*<0.001). However, homology could not be established with the locus between identified *Arabidopsis* or *Brassica* sequences. The unmapped KBrM6.12_241 marker was identified to demonstrate homology with a Leucine Rich Repeat (LRR) extensin protein and is likely to be linked to roles in the plant cell wall (Shirsat *et al.,* 1996). Markers demonstrating significant association with Pod Mass also resided on N5 and N6 (*P*<0.05).

In the SMR analysis the two most significant QTL were linked to respective sNRB35 and KBrM6.12_241 loci. Additivity from the sNRB35 marker accounted for 0.6g of the differences in Pod Mass whereas; the unmapped KBrM6.12_241 marker demonstrated an additivity of 0.58g, for Pod Mass. The majority of lines demonstrating the heaviest Pod Mass were observed to carry an Apex allele for major effect QTL associated with sNRB35, Na12F06b and the unmapped KBrM6.12_241 (Data not shown).

LN	N	Position	Locus	Signif. (KW)	Reg Fprob (SMR)	Additivity (g)
LN 5	N2/N12	7.920	sR94102_320R	*P*<0.00005	0.00051	-0.4
LN 6	N3	48.443	sNRB35	*P*<0.00005	0.00001	-0.6
LN 10	N5	13.033	sORA84_160	*P*<0.05	0.01913	0.27
LN 7	N13	0.000	Na10F06b	*P*<0.05	0.01057	-0.29
LN 11	N6	36.116	KBrA14.8_221	*P*<0.05		
U	U		KBrM6.12_231	*P*<0.005	0.00107	-0.58
U	U		Na12E01b	*P*<0.0001	0.00011	-0.47

Table 5.1: 2006 Pod Mass Single Markers

2009

SMA in the 2009 dataset identified different significant loci associated with Pod Mass than those identified in 2006. 8 Loci were identified to be significantly associated with the Pod Mass trait using KW, whereas, 14 markers were observed to be significant using SMR ($P<0.05$) (Appendix 5.2, 5.14 (pages 276 and 284, respectively). With the KW associations were observed to be of minor effect ($P<0.05$), with QTL noted on N7/N17 (LN 13) and N10/N19 (LN 17) or for unmapped loci. With the SMR, major QTL ($P<0.01$) were observed on N10/N19 and minor QTL ($P<0.05$) on N7/17 (LN 13) and N8 or were associated with unmapped loci (Table 5.2). Similar loci were identified to be significant in both approaches..

The level of accuracy in the determination of significant QTL and overall significance of markers were reduced in the 2009 subset-trial. Identical significance values were evident in multiple markers from the same linkage group. The major QTL peak on N10/N19 contributed 0.57g in the variation in Pod Mass and the increasing allele came from the DK142 parent. Although only demonstrating minor significance ($P<0.05$), a number of unmapped loci were associated with increases in Pod Mass, such as sS2368a, which demonstrated an additivity of 0.76g for the Pod Mass trait.

LN	N	Position	Locus	Signif. (KW)	Reg Fprob (SMR)	Additivity (g)
LN 13	N7/17	50.429	Na10C08b	$P<0.05$	0.023946	-0.63
LN 17	N10	13.688	sNRD49	$P<0.05$	0.005206	0.57
LN 17	N10	15.704	CB10079_170(F)	$P<0.05$	0.005206	0.57
LN 17	N10	18.422	sORH62	$P<0.05$	0.005206	0.57
LN 17	N10	21.437	BRMS-62_178	$P<0.05$	0.005206	0.57
U	U		Na10C01a	$P<0.05$	0.047495	0.46
U	U		CB10045	$P<0.05$		
U	U		sS2368a		0.035352	0.76

Table 5.2: 2009 Pod Mass Single Markers Analyses

2006/2009

Markers with significant association to Pod Mass were observed to be different when comparing lines common to both 2006 and 2009 trials using the SMR (Appendix 5.15, 5.14 (pages 285 and 284, respectively). 15 loci were observed to be significant in the 2006 subset compared to the 14 loci indentified in the 2009 trial. Only minor QTL ($P<0.05$) were evident in mapped regions in the 2006 subset and resided on N2/N12 (LN 4), N3 and N18 Of the 15 significantly associated loci from the reduced 2006 set, four were coincident with those observed in 2009; sS2368a, CB10443_290, FITO122_365 and FITO122_461.

 This indicates that although environmental effects across years are evident, some QTL contributing to the Pod Mass phenotype, are concurrent across trial years. However, accurate determination of QTL peaks in loci in lines from the 2006 subset was not possible due to the reduction in resolution caused by the small number of lines.

5.3.2 Seed Mass (g)

Genetic markers associated with Seed Mass (g) were investigated using KW and SMR in the 2006 trial dataset. 47 loci were identified to be significantly associated with PSR utilising the KW analysis, whereas 56 were observed with the SMR (Appendix 5.3, 5.16, (pages 276 and 286, respectively)). 39 coincident markers were identified using both methods, with significant loci observed to reside on N3, both N2/12 homeologues, N5, N9/N15, N7/17, N12 and N13. A Major QTL ($P<0.01$) was identified on N2/12 (LN5) at the same position as Pod Mass, whereas a major QTL on N3 ($P<0.0005$) was associated with the same sNRB35 marker using SMR and the adjacent Ol11B11b locus in KW ($P<0.001$) (Table 5.3). A Major QTL was also situated above the unmapped Na12E01b as identified for Pod Mass ($P<0.001$). Minor QTL ($P<0.05$) were observed on N5, N9/N15 and two on the corresponding N2/N12 homeologue (LN4) and for the unmapped KBrM6.12 markers. A minor QTL on N13 ($P<0.05$) was represented by Na10F06b, also identified for its association with Pod Mass. A minor QTL ($P<0.05$) was identified on N7/N17 (LN 13), coincident with a marker within the candidate *BnaX.ALC.a* gene. The orthologous *ALCATRAZ* gene from *Arabidopsis* is observed to regulate

separation layer development, but is also reported to be expressed in the seed (Rajani and Sundaresen, 2001). *BnaX.ALC.a* may therefore act in the seed in the *B. napus* also. Major QTL identified during the SMR analysis for sNRB35 displayed an additivity of 0.3g, whereas the sR94102_320R marker at the peak of the QTL on N2/N12 (LN 5) displayed an additivity of 0.22g. The majority of the lines demonstrating the heaviest Seed Mass were observed to carry Apex alleles for the most significantly associated loci, as observed for the Pod Mass trait.

LN	N	Position	Locus	Signif. (KW)	Reg Fprob (SMR)	Additivity (g)
LN 4	N2/N12	0	Ol13E08c	*P*<0.05	0.02052	-0.16
LN 4	N2/N12	33.022	sN2374c	*P*<0.05	0.01073	-0.2
LN 5	N2/N12	7.92	sR94102_320R	*P*<0.005	0.00092	-0.22
LN 6	N3	41.872	OL11G11b	*P*<0.00005	0.00051	-0.3
LN 6	N3	48.443	sNRB35	*P*<0.00005	0.00019	-0.3
LN 13	N7/N17	0	TW-008c	*P*<0.05	0.01068	-0.18
LN 7	N13	0	Na10F06b	*P*<0.05		
U	U		Na12E01b	*P*<0.0001	0.00064	-0.25

Table 5.3: 2006 Seed Mass Single Marker Analyses

5.3.3 Seed Damage

Loci associated with Seed Damage were assessed in the 2006 dataset. 19 markers were identified using the KW analysis and 24 markers using the SMR, (Appendix 5.4, 5.17 (pages 277 and 287 respectively). Similar significant associations were identified using both analyses of which 15 were coincident. This indicates that although the distribution of Seed Damage is non-normal, both analyses identify similar significant loci. Major QTL were identified on N2/N12 (*P*<0.01) associated with sR94102_298, and on both N7/N17 homeologues with one QTL linked to the TW-008b (*P*<0.0005) locus on LN13 and the other on the corresponding N7/17 (LN12) homeologue, represented by sN0818 in the KW analysis and KBr9.8_221 for the SMR (P<0.005) (Table 5.4).

This demonstrated how peaks shifted between the two methods. Significant QTL were also associated with CB10258_595(F), sN0212b, CB10443_290 ($P<0.01$) and sN2442a using SMR ($P<0.005$), but these could not be accurately ascribed to specific linkages groups, nor homology established between known *Arabidopsis* or *Brassica* genes with information from the sequence databases. The TW-008b marker on N7/N17 (LN 13) was observed to exhibit an additivity of 0.8 in Seed Damage level (0-9 scale), whereas the significantly associated sN2442a and CB10443_290 markers contributed to differences of 1.61 and 1.21 on the damage scale, respectively. The increasing allele was indicated to come from the resistant parent and lines demonstrating the greatest levels of Seed Damage were generally observed to carry DK142 alleles for the major QTL associated with the TW-008b, sN0818 and sN212b loci whereas for the sN2442a and CB10443_290 loci, lines with the most damage displayed Apex alleles, although the additivity suggested the DK142 contributed the increasing allele. Therefore, it appears that loci contributing to Seed Damage are conferred from both parents.

LN	N	Position	Locus	Signif. (KW)	Reg Fprob (SMR)	Additivity
LN 4	N2/N12	82.123	sR94102_298R	*P*<0.01	0.001773	-0.7
LN 13	N7/N17	16.993	TW-008b	*P*<0.00005	0.000304	0.8
LN 12	N7/N17	48.386	KBr09.8_221		0.002732	0.67
LN 12	N7/N17	59.148	sN0818	*P*<0.005		
U			CB10258_595(F)	*P*<0.005	0.002234	0.72
U			sN0212b	*P*<0.005	0.000535	0.75
U			CB10443_290	*P*<0.005	0.002271	1.21
U			sN2442a		0.002532	1.61

Table 5.4: 2006 Seed Damage Single Marker Analyses

5.3.4 Intact RIT_{50}

2006

Similar numbers of loci were identified to show significant association with Intact RIT_{50} using both marker analyses. We observed 58 significantly associated markers using the KW method and 59 using the SMR approach (Appendix 5.5, 5.18 (pages 279 and 288, respectively). The high number of QTL indicates the complexity associated with the trait. 30 common markers were identified with both approaches, but QTL peaks were observed to shift between the two methods. Many QTL were observed to be coincident with those identified for Pod Mass (g) and multiple major and minor QTL were observed to contribute to RIT_{50}. Major QTL were identified on N3 and N13 using KW and SMR ($P<0.0005$) and also on N3/N13 ($P<0.01$). The SMR indicated that two putative QTL may be present on N3, one associated with AP2/4a (an intra-genic *BnaA.IND.a* marker) and the other with sNRB35 ($P<0.0001$) (Table 5.5) However, only one peak over sNRB35 was identified in the KW approach. A major QTL was also evident at the top of N13 ($P=0.01$) associated with the Na10F06b locus. The sNRB35 and Na10F06b loci were observed as the most significant QTL on N3 and N13, respectively, as observed for the Pod Mass (g) trait.

Major QTL were identified on N2/N12 (LN4) using KW ($P<0.005$). Minor QTL contributing to Intact RIT_{50} were also identified further down N2/N12 using the KW method ($P<0.05$). KBrM6.12_231/241 and Na12E01b were identified amongst these highly significant markers ($P<0.005$), as they were for Pod Mass and Seed Mass. In the SMR, KBrM6.12_231 was observed to be highly significantly associated with Intact RIT_{50} ($P<0.00005$). This locus also demonstrated a high additivity contributing to approximately 22 s to the Intact RIT_{50} trait.

LN	N	Position	Locus	Signif. (KW)	Reg Fprob (SMR)	Additivity (s)
LN 4	N2/N12	0.000	Ol13E08c	$P<0.005$	0.01735	-8.26
LN 4	N2/N12	39.455	Na12H09	$P<0.05$	0.03473	-7.65
LN 6	N3	37.302	AP2/4a_(281)	$P<0.05$	0.00009	-16.64
LN 6	N3	48.443	sNRB35	$P<0.00005$	0.00003	-16.98
LN 7	N13	0.000	Na10F06b	$P<0.005$	0.00457	-9.35
LN 14	N8	33.581	Na12H07f	$P<0.01$		
LN17	N10/N19	4.657	TW-007a	$P<0.05$		
U	U		KBrM6.12_231	$P<0.0001$	0.00002	-21.83
U	U		KBrM6.12_241	$P<0.005$	0.00002	-22.46
U	U		Na12E01b	$P<0.005$	0.00004	-14.75
U	U		Na10C08a	$P<0.05$	0.01609	8.27

Table 5.5: 2006 Intact RIT$_{50}$ Single Marker Analyses

Minor QTL were observed on N7/N17 and two more on N9/N15 ($P<0.05$) using the KW approach, the latter included associations with the TW-007a marker (*BnaX.RPL.x*). Although only of minor significance it appears the *BnaX.RPL.x* may be contributing to increases in PSR. With the SMR approach, minor QTL were identified on N4 and N6, that were not observed using the KW analysis, but no association was observed with the TW-007a marker. The unmapped Na10C08a locus was also observed to be significantly associated with Intact RIT$_{50}$ in both approaches ($P<0.05$). This marker is of interest as lines demonstrating the greatest Intact RIT$_{50}$ carry a DK142 allele at this locus. Homology has also been established with an *Arabidopsis* haloacid-dehalogenase, At3g10970, identified to exhibit hydrolase activity. Therefore this may potentially be linked to genes responsible for contributing PSR in the DK142 parent, such as those function to degrade to Separation Layer, prior to dehiscence.

Although some differences were identified between the analyses with respect to minor QTL the distribution of data did not appear to affect the SMR adversely compared to the KW analysis.

Lines demonstrating the greatest Intact RIT_{50} values were generally observed to carry Apex alleles for the most significantly associated markers Ol13E08c, sNRB35, Na10F06b and KBrM6.12 loci. This indicated a contribution towards PSR from the Apex parent. Additivity in loci demonstrating the greatest level of association with Intact RIT_{50} were observed at 8.26 s for Ol13E08c, 16.98 s for sNRB35, 9.35 s for Na10F06b and 22.46 s for KBrM6.12_241. These loci are therefore observed to have relatively large effects on the duration of Intact RIT_{50} and hence PSR.

2009

For the 2009 trial data 25 loci were observed to be significantly associated with the Intact RIT_{50} trait using the KW analysis, whereas, 29 were identified using the SMR approach (Appendix 5.6, 5.19, respectively). 17 loci were coincident between analyses. All associations using the KW method were seen to be of minor significance ($P<0.05$). Coincident minor effect QTL were present on with QTL identified on N3/N13, N6, N7/N17, N9/N15, N10/N9 and N18 (Table 5.6). Two putative major QTL were observed on N3/N13 ($P<0.01$) and minor QTL on N6, N7, N9/N15 and N18 using the SMR. However accurate determination of the markers most significantly associated with major and minor QTL in the approaches could not be established due to similar regression probabilities in adjacent and non-adjacent markers. This again indicates the reduced resolution of QTL analysis using only a small number of lines.

LN	N	Position	Locus	Signif. (KW)	Reg Fprob (SMR)	Additivity (S)
LN 19	N3/N13	0.000	BN12A_303(F)	$P<0.05$	0.00588	-10.81
LN 19	N3/N13	25.637	sS2368b	$P<0.05$	0.00588	-10.81
LN 11	N6		sN2837_120		0.02694	-10.99
LN 11	N6		Ni2B03_298		0.03889	-10.36
LN 12	N7/N17	59.148	sN0818	$P<0.05$	0.02676	9.48
LN 12	N7/N17	77.292	sN2567	$P<0.05$	0.03787	10.06
LN 16	N9/N15	35.933	sN1988	$P<0.05$	0.01699	9.95
LN 16	N9/N15	36.783	SN1988_220	$P<0.05$	0.03223	10.09
LN 30	N?	0.000	TW-007b	$P<0.05$	0.02101	-11.79
LN 30	N?	17.013	Ol11B03b	$P<0.05$	0.02433	-10.11
LN 30	N?	30.081	BRMS-62_173	$P<0.05$	0.01699	-9.95
	U		Na10C08a	$P<0.05$	0.00866	11.54

Table 5.6: 2009 Intact RIT$_{50}$ Single Marker Analyses

2006/2009

20 loci were identified to exhibit significant association with Intact RIT$_{50}$ in the nine lines from 2006 compared to 25 loci identified in the 2009 subset (Appendix 5.20, 5.19, (page 289). 10 QTL were coincident between years. When comparing the results from the SMR the major effect QTL from N3/N13 was observed to be only of minor effect in 2006 compared to 2009. QTL on N6 and N9/N15 were identified in the subsets from both trial years, with the sN1988 locus coincident with the peak. These were observed to be of minor effect ($P<0.05$), apart from one on N6 in 2006, which demonstrated highly significant association with the Ni2B03_298 locus ($P<0.005$). Positions of the QTL varied between years, with alternate markers observed to demonstrate the greatest significance in each year. This indicated environmental effects were influencing the position of significant QTL in different years. The N6 linkage group was not identified to represent any significant QTL in 73 lines using either analysis approach. Although only observed to be of minor significance the Na10C08a locus was observed in the 2006 subset, as identified in the full 2006 trial and 2009 subset.

This again highlights conservation of QTL potentially contributing to PSR across years in the POSH 1-3 population.

5.3.5 Broken RIT$_{50}$

2006

Multiple loci contributing to the Broken RIT$_{50}$ trait were investigated using both analyses. 65 loci were identified using KW and 52 using the SMR Table 5.6 (Appendix 5.7, 5.21 (pages 279 and 290, respectively)). 35 markers were observed to be coincident between analyses and some variation in minor QTL was observed. Many of the loci identified to be significantly associated with the Broken RIT$_{50}$ trait were coincident with those identified for Intact RIT$_{50}$, Pod Mass and Seed Mass. In mapped regions of the genome a total of five putative major QTL ($P<0.01$) were identified using the KW and four major QTL ($P<0.01$) utilising the SMR. A number of other highly significant loci were observed to reside in undesignated and unmapped areas ($P<0.01$) (Table 5.7). A major QTL ($P<0.01$) was observed to be associated with the Ol13E08c locus on the N2/N12 (LN4) homeologue using the SMR and another putative QTL may reside on this linkage group. The Ol13E08c marker was observed to be associated with a similar QTL under KW analysis although this was of minor effect ($P<0.05$), as was a second minor QTL ($P<0.05$) separated by a distance of 39cM.

A major effect QTL ($P<0.005$) was observed to be associated with the Na10G10b locus on N3/N13 (LN 19) under SMR analysis. Two major QTL were also observed on N13, with the greatest association with Na10F06b ($P<0.01$), as observed for Pod Mass, Seed Mass and Intact RIT$_{50}$ characters and the second associated with the Ni2B03_400 locus ($P<0.01$). The Ni2B03 locus is identified to exhibit homology with an *Arabidopsis* electron transfer flavoprotein, termed ETF beta, a putative subunit of the mitochondrial electron transfer chain (At5g43430). A major QTL was also observed on N2/N12 (LN5, $P<0.005$) under KW analysis, although under SMR analysis this was observed to be of minor effect ($P<0.05$). Another Major QTL was identified on N10/N19 with the KW analysis, but was only of minor significance using the SMR ($P<0.05$). Two major QTL were identified on N7/N17 (LN 13)

($P<0.01$), whereas these were observed to be of minor effect using the KW ($P<0.05$). A number of unmapped markers were also observed to be significantly associated with Broken RIT$_{50}$. These included KBrM6.12 loci, Na12E01b and Ol10F04a ($P<0.005$). With respect to additivity in the most significantly associated loci, the *BnaA.IND.a* marker, AP2/4a demonstrated an additivity of 20 s whereas, sNRB35 contributed to 24 s to the accounted variation, Na10F06b to 14 s and KBrM16.12 to 30 s. As with Intact RIT$_{50}$, the majority of lines demonstrating the greatest Broken RIT$_{50}$ carried an Apex allele for highly significant markers. This indicates a contribution from the Apex parent in Broken RIT$_{50}$ and hence PSR in POSH 1-3 DH lines.

LN	N	Position	Locus	Signif. (KW)	Reg Fprob (SMR)	Additivity (s)
LN 6	N3		AP14/15b_(400)		0.001331	-16.83
LN 6	N3	48.443	sNRB35	$P<0.005$	6.431E-06	-23.99
LN 19	N3/N13		Na10G10b		0.0043737	-16.25
LN 7	N13	0	Na10F06b	$P<0.0001$	0.0012846	-14.01
LN 7	N13	9.884	Ni2B03_400	$P<0.01$	0.0051862	-13.48
U	U		KBrM6.12_231	$P<0.00005$	8.842E-06	-30.09
U	U		KBrM6.12_241	$P<0.0001$	9.693E-06	-31.09
U	U		Na12E01b	$P<0.01$	8.703E-05	-18.73
U	U		Ol10F04a	$P<0.00005$	0.0033617	-12.94
U	U		Na10C08a		0.0254207	10.26

Table 5.7: 2006 Broken RIT$_{50}$ Single Marker Analysis

2009

Marker analyses in the 2009 dataset identified fewer associated markers than in 2006 with 13 significant coincident loci were identified using the KW approach and 16 using the SMR (Appendix 5.8, 5.22, (pages 281 and 290, respectively)). The unmapped AP14/15a marker was observed to be the only candidate gene marker associated with Broken RIT$_{50}$ in the 2009

dataset (Table 5.8). As seen for markers in the other subset marker analysis, accurate determination of significance was confounded by a lack of data due to the small number of lines assessed. The Na10C08a locus was observed to be associated with Broken RIT_{50} in the 2009 subset as it was for Intact RIT_{50}.

LN	N	Position	Locus	Signif. (KW)	Reg Fprob (SMR)	Additivity (s)
LN 19	N3/N13	0.000	BN12A_303(F)	$P<0.05$	0.0283588	-14.26
LN 19	N3/N13	25.637	sS2368b	$P<0.05$	0.0283588	-14.26
LN 14	N8	27.065	Ol13B02b	$P<0.05$	0.0093407	-15.86
LN 17	N10/N19	13.688	sNRD49	$P<0.05$	0.004441	16.65
LN 17	N10/N19	15.704	CB10079_170(F)	$P<0.05$	0.004441	16.65
LN 17	N10/N19	18.422	sORH62	$P<0.05$	0.004441	16.65
LN 17	N10/N19	21.437	BRMS-62_178	$P<0.05$	0.004441	16.65
LN 1	N11	4.197	pN52f	$P<0.05$	0.042648	-19.08
	U		Na10C08a	$P<0.05$	0.0438046	14.88
	U		AP14/15a(400)	$P<0.05$	0.0283588	-14.26
	U		CB10079_205(F)	$P<0.05$	0.0276755	17.1
	U		BRMS-6_177	$P<0.05$	0.0093407	-15.86

Table 5.8: 2009 Broken RIT_{50} Single Marker Analysis

2006/2009

A total of 16 loci from each year were observed to demonstrate significant association when comparing SMR results from the nine lines common to both 2006 and 2009 (Appendix 5.24, 5.23 (page 291, respectively)). However, five markers were coincident between years with two on N3/N13 and three unmapped loci. A major effect QTL was observed on N6 in the 2006 set, whereas, highly significant markers indicating major QTL were observed on N8 and N10/N19 ($P<0.01$ and $P<0.005$) for the 2009 lines. Na10c08a was identified in both years ($P<0.05$).

This indicates that although the RIT_{50} and hence PSR, demonstrate a heritability of approximately 35% and are subject to environmental effects, coincident QTL are evident across trail years and may act as source through which to modulate PSR as a target of crop improvement.

5.3.6 Intact adjusted RIT_{50}

2006

The KW method identified 60 loci significantly associated with Intact adjusted RIT_{50} and 62 markers utilising the SMR. 31 loci were coincident between analyses. Multiple major and minor effect QTL were observed using both marker analyses, many of which were coincident with those identified for Intact RIT_{50}, Pod Mass and Seed Mass (Appendix 5.9, 5.24 (pages 282 and 291, respectively). However a number of minor effect QTL appear to be selected for independently of those identified for Pod and Seed Mass. Utilising the KW, major effect QTL associated with single markers were identified on N1, N2/N12 (LN 4) ($P<0.005$) and two highly significant QTL on N3/N13 (LN19) ($P<0.0001$). The QTL associated with the sN1925a locus on N2/N12 (LN4) was in a different position than for significant markers identified for the Intact RIT_{50} trait (table 5.9). This indicates that adjustment for the covariate has identified markers significantly associated with the PSR trait which are independent of Pod Mass. A number of unmapped loci and markers from unspecified linkage groups also demonstrated high levels of significance ($P<0.01$). Minor QTL ($P<0.05$) were observed on N3, both N7/N17 homeologues, N9/N15 (LN 16) and N10/N19, represented by the TW-007a marker (*BnaX.RPL.x*). This suggests that *BnaX.RPL.x* may contribute to increases in PSR independently of Pod Mass.

Major QTL were observed on N3, one peak represented by the AP2/4a marker (*BnaA.IND.a*) and the other by sNRB35 ($P<0.005$, $P<0.01$, respectively). Another major QTL was observed on N3/N13 ($P<0.0005$) with the peak linked to the Ni2B03_148 locus. A number of unmapped and unspecified loci also demonstrated strong associations with Intact adjusted RIT_{50} including KBrM6.12_231 ($P<0.0005$), as did the undesignated, co-segregating

sR11644_250/_350 markers ($P<0.01$). Minor QTL ($P<0.05$) were observed to reside on N4, N6, N7/N17 (LN12), N9/N15 coincident with the sN1988 locus, N13 and a number of unmapped or undesignated loci. As observed with other traits, many of the lines displaying the greatest Intact adjusted RIT$_{50}$ values carried an Apex allele for the most significantly associated markers. Interestingly, the series of sN1988 markers, although only associated with minor effect QTL ($P<0.05$), were identified to be significant across both years, in all combinations of lines, in both analyses.

Additivity was reduced in Intact adjusted RIT$_{50}$, due to accounting for the Pod Mass covariate. This indicated that Pod Mass was contributing to increases in Intact RIT$_{50}$ and hence PSR. In highly significant loci, coincident with the Intact RIT$_{50}$, additivity for AP2/4a was observed at 10 s, 8 s for sNRB35 and 14 s for KBrM6.12 for 14 s.

LN	N	Position	Locus	Signif. (KW)	Reg Fprob	Additivity (s)
LN 2	N1	18.368	CB10277_236(F)	$P<0.005$		
LN 4	N2/N12	71.920	sN1925a	$P<0.005$		
LN 6	N3		AP2/4a_(281)		0.002255	-9.72
LN 6	N3	48.443	sNRB35	$P<0.05$	0.0051814	-8.46
LN 19	N3/N13	11.315	Ni2-B03_148	$P<0.00005$	0.0003361	-9.64
LN 19	N3/N13	25.637	sS2368b	$P<0.00005$	0.0008032	-8.25
LN 16	N9/N15	35.933	sN1988	$P<0.05$	0.0229865	5.67
LN 17	N10/N19		Ol11B03b		0.0479264	-4.92
	U		KBrM6.12_231	$P<0.01$	0.000154	-13.78
	U		Na10C08a	$P<0.01$	0.0064067	6.76
	U		sN0212b	$P<0.005$	0.0066027	6.74
	U		Na12F03b	$P<0.005$	0.0290273	5.59

Table 5.9: 2006 Intact adjusted RIT$_{50}$ Single Marker Analysis

2009

Analysis of the 2009 subset identified a reduced number of associated loci to Intact adjusted RIT$_{50}$ compared to the 2006 dataset. Some 12 markers were identified during the KW analysis and 22 using SMR (Appendix 5.10, 5.25 (pages 282 and 292, respectively)). The loci identified using KW were all coincident for those observed in the SMR. All loci identified were of minor significance ($P<0.05$). For the KW analysis QTL were identified on N7/N17 (LN12), on the undesignated LN25, LN29 and LN30 groups and a number of unmapped markers as accurate identification of QTL peaks was problematic with the KW analysis. For the SMR, QTL were observed on N3/N13, N7/N17 (LN 12), N9/N15 and a single marker on N18 (Table 5.10). Accurate determination of the peak of the QTL on N3/N13 or N9/N15 was however, not feasible. This reflected the small number of lines in the sub-trial.

LN	N	Position	Locus	Signif. (KW)	Reg Fprob	Additivity (s)
LN 19	N3/N13		BN12A_303(F)		0.0192508	-7.53
LN 19	N3/N13		sS2368b		0.0192508	-7.53
LN 12	N7/N17	59.148	sN0818	$P<0.05$	0.0107424	7.93
LN 16	N9/N15		sN1988		0.0240769	7.35
LN 16	N9/N15		KBr17.27		0.0240769	7.35
N10/N19	N18		SN11670_80		0.0240769	-7.35
LN 25	N?	21.362	Ni2B03_198	$P<0.05$	0.011869	8.29
LN 25	N?	32.612	Ni2-B03_180	$P<0.05$	0.0248334	8.1
	U		Na10C08a	$P<0.05$	0.0211837	8.26
	U		sN0212b	$P<0.05$	0.0315924	7.82

Table 5.10: 2009 Intact adjusted RIT$_{50}$ Single Marker Analysis

2006/2009

A total of 16 loci were identified in the nine lines from the 2006 subset compared to the 22 markers observed to be significant in the 2009 subset (Appendix 5.26, 5.25 (pages 293 and 292, respectively)). Comparisons between the nine lines assessed from both trial years using the SMR identified 7 coincident loci and common QTL on N3/N13 and N9/N15. Although only of minor effect in 2009 ($P<0.05$), QTL on N3/N13 demonstrated a higher level of association in the 2006 subset ($P<0.01$). This may reflect the increased Intact adjusted RIT_{50} and hence levels of resistance in the population in 2006. QTL observed on N5 and N6 ($P<0.05$ and $P<0.01$, respectively) were only identified in the lines from 2006 and not in 2009, whereas significant loci on N7/N17 and N18 were not identified in the 2006 lines.

5.3.7 Broken adjusted RIT_{50}

2006

For the Broken adjusted RIT_{50} trait 30 significantly associated markers were identified with the KW approach, whereas 44 loci were elucidated utilising the SMR technique (Appendix 5.11, 5.27 (page 283 and 293, respectively). 13 coincident loci were apparent between the analyses. Adjustment for the Pod Mass covariate reduced the number of associated markers compared to Broken RIT_{50} using the KW, although a similar number of loci were identified using the SMR approach pre and post adjustment (Table 5.11).

Two putative major effect QTL were identified on N3 ($P<0.005$, $P<0.01$, respectively), another on N3/N13 ($P<0.01$) and two on N13 ($P<0.01$, $P<0.005$, respectively) with one at associated with the Ni2B03_400 locus. Major effect QTL represented by the undesignated sR11644_250/_350 ($P<0.005$) and unmapped KBrM6.12_231/_241 ($P<0.00005$), Na10C08a, Na12E01b, sORB10b ($P<0.01$) and Ol10F04a ($P<0.005$) markers were also observed. The sNRB35 was associated the most significant QTL peak on N3 ($P<0.005$), whilst AP2/4a marker (*BnaA.IND.a)* was seen to associate with the second, less significant peak ($P<0.01$). This was analogous to that observed for the markers associated to the Intact adjusted RIT_{50} indicating

the same loci are contributing to both Intact and Broken adjusted RIT$_{50}$. Minor effect QTL ($P<0.05$) on N3, both N7/N17 homeologues, N9/N15, N10/N19 and N12 were observed using the KW analysis. The TW-007a marker (*BnaX.RPL.*a), was observed to be the representative QTL on N10/N19, as was observed for Intact adjusted RIT$_{50}$ using the KW analysis.

LN	N	Position	Locus	Signif. (KW)	Reg Fprob (SMR)	Additivity (s)
LN 6	N3		AP2/4a_(281)		0.00763	-10.83
LN 6	N3	48.443	sNRB35	$P<0.05$	0.00163	-12.14
LN 19	N3/N13		Na10G10b		0.00612	-10.94
LN 16	N9/N15		sN1988		0.02216	7.32
LN 7	N13	9.884	Ni2B03_400	$P<0.01$	0.00195	-9.94
LN 38	N?	9.984	SR11644_350	$P<0.00005$	0.01266	-7.96
	U	U	CB10431_103(F)	$P<0.00005$	0.00177	-9.64
	U	U	Ol10F04a	$P<0.0001$	0.00002	-19.04
	U	U	KBrM6.12_231	$P<0.005$	0.00921	8.24
	U	U	Na10C08a	$P<0.05$	0.0062	-9.39
	U	U	Na12E01b		0.00929	-8.08
	U	U	sORB10b	$P<0.05$		

Table 5.11: 2006 Broken adjusted RIT$_{50}$ Single Marker Analysis

For the SMR, minor effect QTL ($P<0.05$) were identified on N9/N15, two on N10/N19 (LN 17, 18 respectively), N12 and for a number of unmapped and undesignated loci. The QTL on N9/N15 was observed to peak over sN1988, as had been observed for Intact adjusted RIT$_{50}$. Although a significant association ($P<0.05$) was identified with a locus on N9/N15 in the KW, this was represented by sNRB68, not sN1988. Also the minor effect QTL on N10/N10 (LN 17) peaked above sNRD49, not the adjacent TW-007a locus.

As for Intact adjusted RIT_{50} many of the lines demonstrating the greatest Broken RIT_{50} value and hence greatest relative level of shatter resistance carried Apex alleles for the most of significantly associated markers. Additivity in sNRB35 was observed at 12.14 s, 9.82 s for Ni2B03 and 19.04 s for KBrM6.12_231/241. Lines exhibiting the greatest Broken adjusted RIT_{50} values were observed to carry DK142 alleles for minor effect QTL on N9/N15 represented by sN1988 and the unmapped Na10C08a marker ($P<0.01$). The level of significance observed for the Na10C08a locus was observed to increase on adjustment for the Pod Mass covariate from $P<0.05$ to $P<0.01$. sN1998 displayed an additivity of 7 s whereas Na10C08a exhibited an additivity of 9 s.

2009

On assessment of loci associated with Broken adjusted RIT_{50} in the 2009 subset trial 13 loci were identified with the KW analysis and 25 markers with the SMR (Appendix 5.12, 5.28 (pages 283 and 294, respectively). All 13 loci identified using KW were coincident using SMR. The number of significant loci identified from the 2009 dataset was reduced compared to the full 2006 dataset. All significant associations were observed to be of minor effect ($P<0.05$) with QTL identified on N3/N13, N8, N10/N19 and N11 in both analyses (Table 5.12). Single significant markers were observed to be present on N7/N17 and N18 (sN0818 and sN11670_80, respectively). The unmapped Na10C08a locus (for which resistant lines carried B alleles) was identified to be significantly associated ($P<0.05$) with Broken adjusted RIT_{50} in both analyses on 2009 lines, whereas, the sN1988 residing on N9/N15 marker was only associated in SMR. Accurate determination of QTL peaks was problematic as described for other traits assessed in the 2009 subset.

LN	N	Position	Locus	Signif. (KW)	Reg Fprob	Additivity (s)
LN 19	N3/N13	0.000	BN12A_303(F)	*P<0.05*		
LN 19	N3/N13	25.637	sS2368b	*P<0.05*		
LN 12	N7/N17		sN0818		0.04831	8.38
LN 14	N8	27.065	Ol13B02b	*P<0.05*		
LN 17	N10/N19	0.000	BRMS-19	*P<0.05*		
LN 17	N10/N19	13.688	sNRD49	*P<0.05*		
LN 17	N10/N19	15.704	CB10079_170(F)	*P<0.05*		
LN 17	N10/N19	18.422	sORH62	*P<0.05*		
LN 17	N10/N19	21.437	BRMS-62_178	*P<0.05*		
LN1	N11	4.197	pN52f	*P<0.05*		
LN 15	N18		SN11670_80		0.04740	-8.4
U	U		Na10C08a	*P<0.05*		
U	U		AP14/15a(400)	*P<0.05*		
U	U		CB10079_205(F)	*P<0.05*		
U	U		BRMS-6_177	*P<0.05*		

Table 5.12: 2009 Broken adjusted RIT$_{50}$ Single Marker Analysis

2006/2009

Comparison of nine lines common to both 2006 and 2009 using the SMR was conducted to assess for similarities. 13 loci were significantly associated with Broken adjusted RIT$_{50}$ for the 2006 subset, whereas 25 loci were observed to be significant for the 2009 set (Appendix 5.29, 5.28 (pages 294 and 295, respectively). Five loci were coincident between years. Significant QTL were evident on N3/N13 and N7/N17 (LN 12) (*P<0.05*), as were associations with Broken adjusted half life and the unmapped Na10C08a and AP14/15a markers. Major QTL were observed on N5 and N6 (*P<0.01* and *P<0.005*, respectively) for the 2006 lines but not for those assessed in 2009. This highlights environmental effects on Broken adjusted RIT$_{50}$ between the two years.

5.3.8 Single Marker Regression in 44 POSH 1-3 lines from 2000 and 2006 trials

The SMR was utilised to assess for similarities in markers associated to Pod mass (g), Intact and Broken RIT$_{50}$ in 44 lines common to our 2006 trial and from a trial conducted in 2000 (Morgan *et al.,* Unpublished). This was performed to give a greater insight into QTL that may have been coincident across years between the two trials. It was anticipated that as more information was available from an increased number of lines that a greater degree of accuracy could be achieved than for comparisons with the 2009 subset.

Pod mass

For the Pod Mass character 32 significantly associated loci were observed for the 2000 trial and 38 for the 2006 trial ($P<0.05$) (Appendix 5.30, 5.31 (pages 295 and 296, respectively).16 coincident loci were observed between the two years. This indicated loci contributing to the Pod Mass trait were maintained across trial years. This was anticipated due to the high trait heritability calculated for the Pod Mass trait. In mapped regions of the genome, four major QTL were observed for the 2000 trial, residing on N5 ($P<0.005$), two on N10/N19 (LN 18) ($P<0.005$, $P<0.01$, respectively) and one on N18. Minor QTL were identified on N3, N4, N9/N15 and on N13 ($P<0.05$) (Table 5.13). For the 2006 trial, highly significant associations were observed on N2/N12 (LN 5) ($P<0.0005$), N3 ($P<0.005$) and a number of unmapped markers including KBrM6.12 loci and Na12E01b ($P<0.01$ and $P<0.005$, respectively), similar to that observed in the full 73 line set. Minor QTL ($P<0.05$) were observed on N2/N12 (LN 4), N5, N6, N9/N15, N10/N19 and a number of unmapped markers.

LN	N	Locus	Reg Fprob 2000 SMR	Additivity (g)	Reg Fprob 2006 SMR	Additivity (g)
LN 6	N3	AP14/15b_(400)	0.0297592	-0.4	0.0072686	-0.47
LN 6	N3	AP2/4a_(281)	0.0289109	-0.41	0.008066	-0.47
LN 6	N3	sNRB35			0.0017417	-0.57
LN 8	N4	BRMS-276_239	0.039727	0.26		
LN 8	N4	pN202a	0.0265265	0.3		
LN 10	N5	CB10487_280(F)	0.0178215	0.29		
LN 10	N5	sR9555(250)	0.0026203	0.36		
LN 10	N5	CB10487_267(F)	0.0155719	0.29		
LN 16	N9/N15	Na12E06b_231(F)			0.0106938	-0.31
LN 16	N9/N15	sORB84b	0.016297	-0.29	0.0398942	-0.24
LN 16	N9/N15	OL12F02b	0.0462506	-0.24	0.01653	-0.28
LN 16	N9/N15	OL12F02a	0.0462506	-0.24	0.01653	-0.28
LN 18	N10/N19	sN1656a	0.0018534	-0.38		
LN 18	N10/N19	sNRD93a	0.0074576	-0.33		
LN 7	N13	KBr09.8_302	0.0129986	-0.31		
LN 15	N18	CB10028(F)	0.0062139	-0.34		
	U	KBrM6.12_231			0.0095625	-0.56
	U	KBrM6.12_241			0.0095625	-0.56

Table 5.13: 2000/2006 Pod Mass SMR

Intact RIT$_{50}$

On assessment of markers associated with the Intact RIT$_{50}$ trait, 13 markers were observed in the 2000 dataset, whereas, 43 were observed for the 2006 set (Appendix 5.32, 5.33 (page 296 and 297, respectively)). In the 2000 trial only markers from unmapped regions were observed to display high levels of significance, including the CB10211_102 and KBr946 markers ($P<0.005$ and $P<0.01$, respectively). No coincident markers were identified between years, indicating that the Intact RIT$_{50}$ trait and hence PSR is environmentally sensitive, and different loci are contributing in the different trial years. Also the reduced number of lines in the analysis could have contributed to such differences.

The KBr946 marker is linked to a copy of the *BnaX.RDPG1.a* gene. Therefore this polygalacturonase may be contributing to differences in PSR in the 2000 trial. Loci of minor significance ($P<0.05$) were observed in mapped regions of the genome for the 2000 trial, with associated markers identified on N8 and N18.

For the select 44 lines from the 2006 dataset, QTL were observed to be in similar locations to those identified in the full 73 lines, but different from those that were evident in the 2000 dataset. Major QTL were identified on N3 ($P<0.001$) (AP2/4a), N7/N17 (BRAS19), N3/N13 ($P<0.01$) (sS2368b), the undesignated LN 21 ($P<0.001$) (Ol13A10) and associated with the unmapped KBrM6.12_231 and Na12E01b loci ($P<0.001$) (Table 5.14). Minor effect QTL ($P<0.05$) were observed on N13, N10/N19 and N9/N15, the latter represented by the KBr17.27 locus (*BnaX.FUL.a*).

LN	N	Locus	Reg Fprob 2000 SMR	Additivity	Reg Fprob 2006 SMR	Additivity
	U	CB10211_102(F)	0.00148	-8.44		
	U	KBr946	0.00749	-4.24		
LN 6	N3	AP2/4a_(281)			0.000865	-17.96
LN 13	N7/N17	BRAS19			0.007409	10.15
LN 19	N3/N13	sS2368b			0.004669	-11.96
LN 21	N?	Ol13A10			0.00017	-19.24
	U	KBrM6.12_231			0.000866	-26.08
	U	Na12E01b			0.000944	-15.32

Table 5.14: 2000/2006 Intact RIT$_{50}$ SMR

Broken RIT_{50}

Loci demonstrating significant association with Broken RIT_{50} were assessed in the 44 lines common to both the 2000 and 2006 datasets. 17 markers were observed to be significantly associated in the 2000 set whereas 48 were identified in the 2006 set (Appendix 5.34, 5.35 (pages 297 and 298, respectively). No coincident markers were identified between years again highlighting the environmental sensitivity of the trait and also the lack of representative lines common between mthe two trial years. For the 2000 trial major effect QTL ($P<0.01$) were only identified in unmapped regions of the genome with the greatest association with the sS2210 marker ($P<0.005$) (Table 5.15).

Minor QTL ($P<0.05$) were observed on N11, represented by the BRMS-214_261 locus and on the undesignated LN20 and LN29 marker groupings, with peaks over sNRD76 and OI13E08b, respectively. For the 2006 set, major effect QTL were identified on N2/N12 (LN4) ($P<0.01$), N3 ($P<0.005$), two putative peaks on N13 ($P<0.01$), one on N7/N17 (LN13) ($P<0.01$) and on the undesignated LN 19 grouping ($P<0.01$). Minor QTL were evident on N2/N12 (LN5), N9/N15, and N10/N19, N7/N17 (LN13) and the undesignated LN 25 and LN 38 groups. Different QTL were contributing to Broken RIT_{50} than those identified in the 2000 trial. Markers observed to be significant in the 44 lines from the 2006 were similar to those represented in the 73 lines utilised in the full SMA. Loci identified to be significantly associated with Broken RIT_{50} in the 2000 dataset were more representative of those loci observed for the Intact RIT_{50} in the 2000 trial than those associated with Broken half life from the 2006 dataset. This suggests that similar loci are contributing to Intact and Broken RIT_{50} within a year but different QTL are contributing to half-life in different years.

LN	N	Locus	Reg Fprob 2000 SMR	Additivity (g)	Reg Fprob 2006 SMR	Additivity (g)
	U	sS2210	0.0045074	-7.49		
LN 1	N11	BRMS-214_261	0.015613	-6.54		
LN 20	N?	sNRD76	0.0195401	-6.32		
LN 29	N?	Ol13E08a	0.0106626	6.98		
LN 5	N2/N12	sR94102_320R			0.0152633	-10.9
LN 6	N3	AP14/15b_(400)			0.0021879	-19.52
LN 7	N13	KBr09.8_302			0.0099857	-12.16
LN 13	N7/N17	BRAS19			0.0086906	11.89

Table 5.15: 2000/2006 Broken RIT$_{50}$ SMR

5.3.9 Multiple Marker Regression

A multiple regression analysis was utilised to assess for combinatorial relationships and also interactions between significant markers associated with Intact and Broken adjusted RIT$_{50}$ in the 2006 dataset (Appendix 5.36, 5.37 (pages 299 and 301, respectively). For Intact adjusted RIT$_{50}$the greatest amount of variance that could be explained was 58.36% using a combination of BRMS-303, IGF5298c_200, KBrM6_12_231, Ol10F04a, sN13034_140 and sN3766. For Broken adjusted RIT$_{50}$ 41.84% of the variance could be accounted for by a combination of CB10431_103(F), KBrM6.12_231 and Na12A08a loci. This highlighted the importance of multiple markers in contributing towards increases in the PSR trait.

Further analysis was performed to investigate interactions between markers significantly associated with Intact and Broken adjusted half lives to address potential interactions between loci. Multiple combinations of alleles were assessed for the greatest amount of variance that could be accounted for and identified a range of contributions to the two measures of PSR. For Intact adjusted RIT$_{50}$ approximately 65% of the variance could be accounted for by interactions between KBrM6.12_241 and BRMS_101, Ni2B03_148 and Na10C08a, and SR11644_250 and Na10C08a, respectively (Appendix 5.3). Whereas, for Broken adjusted RIT$_{50}$ approximately 67% of the variance could be accounted for through

178

interactions with Na10F06b/KBrM6_12_231, KBrM6_12_231/Ol10F04a, Ol10F04a/sORB36b, KBrM6_12_231/Na10C08a, KBrM6_12_231/Na10C08a, sORB36b/sS2368b (Appendix 5.4). This highlighted that markers of minor individual significance ($P<0.05$) contribute more significantly to increases in half life when combined with the actions of other loci. The multiple regression demonstrated that in the most pod-shatter resistant lines loci associated with Pod Mass, contributed by the Apex parent, interacted with loci associated with increases in RIT_{50} contributed by the DK142 parent. This highlights the complex, polygenic nature of the PSR trait and why this has been difficult to select for using conventional breeding strategies.

5.4 Discussion

Single Marker Analysis has been performed on POSH 1-3 trial data generated in the 2006 and 2009 trials, and also on 44 lines from a trial conducted in 2000 by Morgan *et al.* (unpublished). In the full 2006 trial we identified a range of loci which are significantly associated with Pod Mass, Seed Mass, Seed Damage and Intact/Broken RIT_{50} and Intact/Broken adjusted RIT_{50}. In the 2009 subset trial and the 2000 trial (Morgan *et al.*, unpublished) we observed loci significantly associated with Pod Mass, Intact/Broken RIT_{50} and Intact/Broken adjusted RIT_{50}. Included in these significantly associated loci were a number of markers linked directly to candidate genes of which the *Arabidopsis* orthologues demonstrate established roles in fruit development. We have observed significant associations with traits and multiple QTL and many of the traits assessed are observed to be associated with coincident QTL, reflecting common roles for gene candidates and the complex interactions between loci required to regulate to polygenic characters of this nature. We also identified differences in QTL across trial years likely to have been inferred through variation in environmental effects (E) or G x E (Genotype x Environment) effects, resulting in differences in the complement of genes regulating trait phenotypes.

Major and minor QTL associated with the Pod Mass were identified in POSH 1-3 population

For the full trial in 2006 both marker analyses identified a number of major and minor QTL associated with the Pod Mass (g) trait. Major QTL were seen to reside on N3 and N2/N12 (LN5) and associated with a number of markers which were still to be mapped. N3 is representative of the A3 chromosome whereas N2/N12 is representative of A2 or C2, showing a similar marker order to both the Parkin and TNDH *B. napus* genetic linkage maps (Parkin *et al.,* 2005, Qiu *et al.* 2006). A number of agronomically important QTL have been identified to reside on N2 and N3 for traits such as flowering time, vernalization, branch number and biomass yield (Long *et al.,* 2007, Shi *et al.,* 2009).

Significant markers identified in the 2009 sub trial were observed to be different to those identified in the full 2006 trial and nine lines common to both trials. In the 44 lines assessed between the 2000 and 2006 datasets, an increase in coincident QTL on the same linkage groups in both years was evident. The similarities between the QTL identified in the 2000/2006 trial reflects that loci contributing to Pod Mass are present in both years as was anticipated for a trait with high heritability as it should be less subject to environmental effects. Differences in QTL between the 2006 and 2009 could reflect environmental effects on Pod Mass between years but are also likely to indicate issues with utilising a reduced number of lines in which to perform QTL analysis as in the 2009 set. A reduced population size is reported to affect the accuracy in QTL identification (Young, 1999, Miles and Wayne, 2008). This is supported by the observation that accuracy in determination of the peak of QTL was reduced in the 2009 set, as was noted for the nine lines common to the 2006 subset, also resulting in ambiguity in locus significance.

Some variation in the location of QTL peaks was evident between the 2000 and 2006 subset and this is explained by differences in environment effects, genotype x environment effects or through slight variation in the physical assessment using the RIT. In lines demonstrating the greatest Pod Mass values, loci linked to major QTL major coincident across years, were identified to exhibit alleles conferred from the shatter susceptible Apex parent. This suggests that the Apex parent contributes most greatly to a larger Pod Mass in POSH lines and is supported by the observation that the Apex parent is a commercial cultivar and demonstrates a better agronomic habit compared to the synthetically derived DK142 parent resulting in longer, more fertile pods.

Homology to significantly associated markers was established for the unmapped KBrM6.12_231/241 co-segregating markers and was observed to be similar to an LRR extensin from *Arabidopsis.* Extensins are hydroxproline-rich glycoproteins found in the cell wall, are implicated in many aspects of plant development, and are also associated with increases in strength of the cell wall (Zhang *et al.,* 2008, Shirsat, Wieczorek and Kozbial,

1996). Differences in such genes may therefore have effects on variation in pod wall strength or thickness, potentially affecting Pod Mass. Identification of homology in other markers linked to QTL relating to the Pod Mass trait was confounded by the relatively low density and incomplete coverage of the POSH genome and also a lack of homology between mapped markers and *Arabidopsis* and *Brassica* sequences in the databases. Increases in the number of markers on linkage groups displaying QTL, especially those linked to candidate genes regulating Pod Mass would help elucidation of factors contributing to the trait. Further investigation into combinations of markers contributing to Pod Mass could be investigated using the multiple regression model and may shed light on the relationship between factors regulating increases in pod size and relationship with PSR.

Major and minor QTL associated with the Seed Mass in POSH 1-3 population were identified in the 2006 trial

During this assessment we have observed loci which were significantly associated with Seed Mass in the 2006 trial. These included a number of major and minor QTL, many of which were coincident with those associated with the Pod Mass trait, including the major QTL predicted on N2/N12 (LN5) and N3. We have shown previously that these traits are auto-correlated and that Seed Mass is a component of Pod Mass (Chapter Two).

It appears that genes contributing to Pod Mass are also involved in controlling Seed Mass in POSH 1-3 lines. As for Pod Mass, lines demonstrating the greatest Seed Mass were observed to carry Apex alleles for the most significantly associated loci, suggesting that the shatter susceptible parent contributes most to a greater Seed Mass. As a commercial cultivar Apex has been selected for to produce large amounts of seed. This is supported by reports from Summers *et al.* (2003) that Seed Mass in the DK142 line is reduced by 50% compared to Apex and therefore would be unlikely to contribute to larger relative Seed Mass. However, in this assessment We did not see a significant reduction in Seed Mass in the DK142 line compared to Apex. This is suggested to be a due to out-crossing in the DK142 parent after production of the POSH 1-3 population. Although Seed Mass has only been investigated in

one trial year, due to its high heritability and coincidence with QTL affecting Pod Mass, it is suggested that associated markers would likely to be identified in the other trial years if assessed. Interestingly, a minor QTL for Seed Mass was identified to coincide with an intragenic marker for the *BnaX.ALC.a* gene. This was proposed as a candidate with potential contributory roles in PSR as the orthologous *Arabidopsis ALCATRAZ* gene has been established to be involved in regulating separation layer (SL) development (Rajani and Sundarsen, 2001). *ALCATRAZ* has also been reported to be expressed in the seed and it would appear that one or two copies of the *B. napus* orthologues are contributing to differences in Seed Mass. Expression studies in the seed, such as Quantitaive Real Time PCR with primers designed for *BnaX.ALC.a,* would help to verify this finding. Further investigation in to factors contributing to Seed Mass may aid insight into components affecting seed yield and potentially have application to crop improvement. This would require repeat assessment in trials across different years and environments to establish if QTL were stable and therefore amenable targets for introgression in to breeding programmes.

Major and minor QTL associated with the Seed Damage were identified in POSH 1-3 population in the 2006 trial

Single marker analysis performed for Seed Damage has identified major and minor QTL associated with the trait. These are less numerous than QTL identified for Pod and Seed Mass, although some coincident loci of minor significance were observed between Seed Mass and Damage. Highly significant QTL were observed on both N7/N17 homeologues associated with Seed Damage. The largest QTL is observed to coincide with the TW-008b locus, which represents an intragenic marker for *BnaX.ALC.b*. This marker is thought to be a second copy of the *ALCATRAZ* gene mapping a distance of 17cM from the TW-008c marker identified as a locus contributing to differences in Seed Damage. Significance is evident for both loci, so both copies may contribute to differences in Seed Damage, but without a more developed map or repeat assessment this cannot be verified. Homology to other significantly associated loci remains elusive and increases in marker density or of loci linked

to identifiable gene candidates may improve our understanding of factors which are regulating Seed Damage.

In lines demonstrating the greatest levels of Seed Damage the majority of significantly associated loci are observed to carry a the DK142 allele, however loci from QTL on N7/N17 LN12 were observed to carry the Apex allele. Therefore differences in Seed Damage are contributed to from both the shatter resistant and susceptible parents. Negative correlations were previously identified between Seed Mass and Seed Damage with samples displaying a greater mass less subject to damage during the RIT. This may relate to greater quantities of seed in certain lines, larger seed or even differences in seed architecture allowing for a greater amount of the energy to be absorbed before damage occurs. It would be of interest to assess how *ALCATRAZ* contributes towards differences in Seed Damage by assessing seed size, number or even testa strength. This could be of direct interest, as described in Chapter Two, in relation to establishment or agronomic quality such as oil content or seed fibre content (Wittkop *et al.,* 2009).

Major and minor QTL associated with the Intact RIT$_{50}$ have been observed in POSH 1-3 population, a number of which are coincident with the Pod Mass character.

Numerous significant loci associated with the Intact RIT$_{50}$ trait were observed utilising the single marker analyses. For the 2006 trial, both KW and SMR analyses identified similar loci, although some differences were noted in minor QTL between the approaches and in the position of QTL peaks. Major and minor QTL were evident, with many coincident with Pod Mass and Seed Mass traits. This suggests that either similar genes are contributing to Pod and Seed Mass and Intact RIT$_{50}$ or that there are complex interactions between loci regulating the traits. The large number of significant loci also indicates towards the complexity of the RIT$_{50}$ character.

Loci linked to QTL on homeologous linkage groups were also observed indicating that both A and C genomes contribute to Intact RIT$_{50}$, especially with respect to markers on N3 and N13

and on N2 and N12. Major QTL were evident on N2/N12 (LN4) in the KW and N3 using the SMR, whereas a highly significant on N13 was identified using both approaches. This highlights the differences between the two marker analyses in identifying certain significantly associated QTL. This is suggested to reflect the non-parametric nature of the KW method compared to the parametric basis of the SMR. Two putative QTL may be present on N3; however without improved map density/coverage and repeated trials this cannot be fully substantiated. A lack of homology between linked markers and sequences verified in *Arabidopsis* and *Brassica* have limited the designation of gene candidates contributing to Intact RIT_{50}. One QTL peak on N3 was observed to be coincident with the AP2/4a locus, situated within the candidate *BnaA.IND.a* gene.

The *Arabidopsis IND* orthologue has been demonstrated to act as a key regulator in the dehiscent zone and endocarp layer B development (Lilijegren *et al.,* 2004). We therefore selected this as a potential candidate which may affect levels of PSR in POSH 1-3 lines. I have observed that lines demonstrating the greatest half lives carry Apex alleles for the AP2/4a locus and other highly significant markers. It appears, therefore, that alleles from the Apex parent are contributing towards PSR. It is unlikely that these markers, although highly correlated, are causal for direct increases in PSR as they are derived from the shatter susceptible parent. It is suggested such markers are conferring large pods which allow the production of the increased vasculature required to increase PSR. The addition of intragenic markers within copies of candidate genes has therefore aided map population, linkage group designation, and determination of roles for fruit development orthologues in *B. napus.*

Highly significant associations were identified with the unmapped KBrM6.12_231/241 co-segregating markers and Intact RIT_{50}. As indicated for Pod Mass these loci demonstrate homology to an LRR extensin (At3g24480) and may relate to strength of the plant cell wall (Shirsat, Wieczorek and Korbial, 1996). It is feasible that the activity of such a gene could play roles in both Pod Mass and in contributing to differences in Intact RIT_{50} and hence PSR.

Potentially variation in the strength of the cell wall may enable pods to be more or less susceptible to damage during the RIT.

Minor QTL associated with the Intact RIT_{50} were identified using both marker analyses. Included in these were QTL coincident with the sN1988 and Na10C08a markers and these are of interest as lines exhibiting the most extended Intact RIT_{50} duration carried the DK142 allele at these loci. Therefore, it is possible that these markers are linked to genes contributing directly to PSR, due to their origins in the resistant parent. Although no homology can be established for sN1988, the Na10C08a displays homology with a haloacid-dehalogenase identified to demonstrate hydrolase activity in *Arabidopsis* (At3g24480). It is proposed the *B. napus* orthologue could be a viable candidate, contributing to differences in PSR, when it is considered I have identified decreases in the breakdown of the separation layer in the most resistant POSH lines and hydrolase activity may be responsible (Chapter Three).

The observation that major QTL associated with the Intact RIT_{50} character appear to be selected from the shatter susceptible Apex parent and specific minor QTL are selected from the shatter resistant DK142 supports the suggestion of a complex, polygenic basis to the trait (Werner *et al.,* 2003a; Child *et al.,* 2003). The number of significant markers was reduced in the nine line subset from 2006 and 2009 trials. This again reflects the loss of resolution during marker analyses using a small dataset. Trait heritability was relatively high for Intact RIT_{50} and this supports the observation that similar markers linked to QTL were evident between the two years. However significant loci in the 44 lines common to the 2000 and 2006 trials were observed to be somewhat different. This could reflect the effects of environmental, G x E or differences in the assessment method. The latter is unlikely though, as similar husbandry and RIT assessment was used to investigate PSR in all trial years.

Interestingly, the KBr946 marker linked directly to the *BnaX.RDPG1.a* was observed to demonstrate highly significant associations with Intact RIT_{50} in the 2000 trial. Although not

identified in subsequent trials and even though it may potentially be subject to environmental effects, this highlights that the *RDPG1* gene targeted as an original candidate due to its established roles in *Arabidopsis,* appears to contribute to the RIT$_{50}$ character and hence PSR. Our observations reiterate the requirement for repeated field trials across multiple years and environments to establish trait stability, which is a prerequisite for selection of characters as viable targets for crop improvement (Kearsey and Pooni, 1996*;* Snape *et al.,* 2007)

Major and minor QTL associated with the Broken RIT$_{50}$ have been observed in the POSH 1-3 population, a number of which are coincident with the Intact RIT$_{50}$ and Pod Mass characters.

Major and minor effect QTL were identified to be associated with the Broken RIT$_{50}$ character. For the 2006 trial many significantly associated loci were observed to be coincident with QTL identified for Pod and Seed Mass, and Intact RIT$_{50}$ traits, including major QTL on N3 and N13. This indicates that complex interactions may exist between Pod and Seed Mass and half-life. It also highlights the anticipated relationship between Intact and Broken half life. Some variation in the position of QTL peaks and levels of significance was noted between the two types of marker analyses and is suggested to relate to the differences in each procedure as described for the Intact RIT$_{50}$ trait. Lines demonstrating the greatest Broken RIT$_{50}$ values, as with Intact RIT$_{50}$, displayed Apex alleles for loci associated with major effect QTL. The Na10C08a and sN1988 loci, although not identified in the KW, were observed to be associated with Broken RIT$_{50}$ in the SMR analysis and lines with the greatest Broken RIT$_{50}$ carried DK142 alleles for these markers. This suggests that these loci may be contributing to increases in PSR as described for Intact RIT$_{50}$.

A lack of homology between linked markers and established *Arabidopsis* and *Brassica* sequence confounded identification of gene candidates as described for other traits. Lines assessed in the 2009 subset were observed to demonstrate association with different loci than in the full and subset of lines from 2006. This reflects both differences in the number of

lines present in the analyses between the full and subset trial and also environmental or G x E effects across the two trial years. When comparing the 44 lines common to the 2000 and 2006 trial the number of significantly associated markers for the 2000 set was much reduced as observed for Intact RIT_{50}. However the loci associated with Intact and Broken in each respective trial year were observed to be quite similar. This again highlights how similar genes are contributing to the two related RIT_{50} traits and that environmental effects are causing selection for different QTL across years. This supports the suggestion of Werner *et al.* (2003a) that PSR in the POSH 1-3 population and DK142 progenitor line is environmentally sensitive.

Major and minor QTL associated with Intact adjusted RIT_{50} have been observed in the POSH 1-3 population, a number of which are coincident with Intact RIT_{50} and others which are not

Previously, Summers *et al.*, (2003) highlighted significant correlations between increases in PSR and increases in weight of pod valves and septa as well as increases in pod length. Therefore, longer, heavier pods were correlated with increases in PSR. From the perspective of identifying targets for improving pre-harvest pod shatter in commercial varieties of *B. napus,* selection of genes contributing to large pods may confound identification of the causal factors required to manifest increases in PSR. We wished to identify factors linked to increases in PSR which were independent of those ascribing larger, heavier pods. We therefore performed a covariate analysis to account for differences in Pod Mass between POSH 1-3 lines.

Significant correlation was identified between Pod Mass and mean RIT_{50} (Intact and Broken) and the covariate was observed to be highly significant for the Intact RIT_{50} trait. Post-adjustment the correlation between Pod Mass and Intact RIT_{50} was still significant but greatly reduced. This indicates that it may not be possible to completely dissociate the effects of Pod Mass on Intact RIT_{50}/adjusted RIT_{50}. We have observed that a number of QTL are coincident with Pod Mass and Intact adjusted RIT_{50}, reinforcing the suggestion that the

same QTL are regulating both traits, or that complex interactions between genes control the characters. Lines exhibiting the greatest Intact adjusted half lives were observed to carry Apex alleles for loci linked to major QTL. The AP2/4a marker situated within the 3'UTR of the *BnaA.IND.*a gene is one example of this and demonstrates how alleles from the shatter susceptible Apex parent are required to manifest the PSR phenotype in resistant POSH 1-3 lines as well as contributing to Pod Mass.

However accounting for the Pod Mass covariate does allow the identification of differences in factors contributing to Intact adjusted RIT_{50} and hence PSR; we have identified differences in both major and minor QTL observed in Intact RIT_{50} compared to Intact adjusted RIT_{50}. Interestingly, after adjustment, association with Intact adjusted RIT_{50} and the Na10C08a locus is observed to increase, indicating a greater influence on half life when Pod Mass is accounted for. A number of other loci carrying B alleles in lines demonstrating the greatest Intact adjusted RIT_{50} values were also noted to show significant associations with Intact adjusted RIT_{50} and could be potential sources of the PSR phenotype contributed from the shatter resistant DK142 parent. It is suggested that adjustment for the covariate is therefore reducing the apparent masking effect of Pod Mass on identification of loci linked to RIT_{50} and hence PSR. This is supported by the observed reduction in the correlation and level of significance between the Pod Mass and Intact adjusted RIT_{50} characters during trait analysis (Chapter Two). This indicates that our proposal to adjust Intact RIT_{50} for the covariate, to aid identification of factors contributing to PSR independently of Pod Mass, has been successful. However, repeat assessment would be required to substantiate these findings.

In lines from the 2009 sub-trial fewer QTL with lower level of significance in associated markers compared to the 2006 trial were observed. Compared to the lines common between the two trial years, some differences were noted. QTL on N5 and N6 were not apparent in 2009 as they were for the lines in 2006, but many markers were observed to be coincident, including the Na10C08a and sN212b loci. Although heritability was observed to be reduced in Intact adjusted RIT_{50} in the full trial compared to Intact RIT_{50} (55%/35%,

respectively), similarities between loci in both trials would suggest that although potentially subject to environmental and G x E effects, the Intact adjusted RIT_{50} character and hence PSR appeared to be quite robust. Therefore markers linked to QTL identified in this study may pose as viable candidates for improving pre-harvest pod shatter in *B. napus* although repeat trials would be required to validate this proposal.

As a number of QTL are still coincident with Pod Mass, Intact RIT_{50} and adjusted RIT_{50} the complex nature of this trait is clearly evident. We have observed how major QTL in lines with the greatest Intact RIT_{50} and Intact adjusted RIT_{50} values carry Apex alleles. It has also been identified how the level of significance and number of associated loci carrying DK142 alleles in resistant lines increases on adjustment for the Pod Mass covariate. It is proposed that both parents are therefore contributing to the PSR phenotype observed in a small number of POSH 1-3 lines. To assess the combinatorial effect of markers and potential interactions we performed a multiple regression on loci most significantly associated with the Intact adjusted RIT_{50} trait. We have shown how combinations of markers, of both major and minor significance, contribute to the variation accounted for by the Intact adjusted RIT_{50} trait. We have also identified how interactions between significantly associated loci can account for even greater amounts of the variation, with excesses of 65% estimated for KBrM6.12_241, BRMS_101, Ni2B03_148, Na10C08a, and SR11644_250 loci. This supports the suggestion that PSR is a highly complex character and regulated by multiple interacting genes, resulting from the contribution of combinations of alleles from the shatter susceptible Apex and shatter resistant synthetic DK142.

Major and minor QTL associated with Broken adjusted RIT_{50} have been observed in the POSH 1-3 population, a number of which are coincident with Broken RIT_{50} and others which are not

We have observed similar findings for Broken adjusted RIT_{50} as exhibited for Intact adjusted RIT_{50}. Coincident QTL were identified between Pod Mass and the linked Broken RIT_{50} characters for the 2006 trial. This was anticipated as significant correlations were observed

during the trait analysis for these characters. The KW marker analysis identified fewer major QTL compared to the SMR, although similar markers were identified at a minor level of association. This observation is suggested to be an effect of the respective non-parametric and parametric basis of the two analyses. Lines demonstrating the greatest Broken RIT_{50} values were observed to carry Apex alleles for major QTL on N3, N13 and unmapped KBrM6.12_231/241 makers as for Intact adjusted RIT_{50}.

Adjustment for the Pod Mass covariate increased the significance levels in the AP2/4a marker highlighting the contribution of *BnaA.IND.a* to increases in PSR and also the Na10C08a locus, proposed as a putative source of alleles conferring PSR from the DK142 parent. Inclusion of the covariate in the analysis negated the association of loci from N2/N12 (LN5) and identified a different QTL associated with sN1925a locus as described for Intact adjusted RIT_{50}. The observation of coincident loci between Intact and Broken adjusted RIT_{50} suggests similar QTL are affecting the both traits and could be postulated similar physiological factors are contributing to the characters. As the characters are derived from each other this finding was anticipated, although assessment of Intact and Broken pods was performed to identify if any differences between the two traits could be ascertained. The similarity in QTL may also relate to a lack of marker density, where a greater population of linked markers would increase definition of the single marker analyses and potentially identification of multiple candidate loci. For lines assessed in the 2009 we observed fewer QTL with lower level of significance in associated markers compared to the 2006 trial relating to the reduced definition due to the sample size.

Again, some differences in significant markers were noted, but many markers were observed to be coincident including the Na10C08a locus. Although heritability was observed to be reduced in Broken adjusted RIT_{50}, compared to Broken RIT_{50}, similarities between loci in both trials would suggest that although potentially subject to environmental and G x E effects between years, that loci associated with the Broken adjusted RIT_{50} character and

hence PSR appeared to be relatively stable and therefore potential candidates for improving pre-harvest pod shatter in *B. napus.*

We have observed, as with the other estimates of half life, that Broken adjusted RIT_{50} is a highly complex trait regulated by multiple genes and contributed to by both shatter resistant and susceptible progenitors. Multiple regression has identified that combinations of loci also contribute to account for a higher percentage of the trait variance than single markers alone and interactions between the KBrM6_12_231, Na10C08a, sORB36b, sS2368b accounted for approximately 67% of the variance. This indicates how highly significant markers are interacting with less significant loci to contribute towards increases in PSR in POSH 1-3 resistant lines. As with Intact half-life, lines demonstrating the greatest levels of PSR carried Apex alleles for loci linked to the majority of major QTL, whereas a number of loci linked to seemingly minor effect QTL carried the DK142 alleles. This indicates that alleles from both parents are required to produce the most shatter resistant lines. This analysis was by no means exhaustive and further investigation may identify more significant relationships as different permutations or combination may account for even higher variance percentages.

The basis of the PSR trait in POSH 1-3 lines

As originally postulated, identification of factors contributing to PSR in the POSH 1-3 population are confounded by variation in Pod Mass between different lines. When differences in Pod Mass were accounted for it became apparent that alleles from both shatter susceptible and resistant parents are required to manifest the PSR phenotype. It is suggested that alleles from Apex are conferring a beneficial agronomic background enabling plants to produce large pods, potentially grow larger or to divert more resources towards factors contributing to increases in shatter resistance, whereas the alleles from DK142 contribute to the recessive, environmentally sensitive factors linked to PSR. It is also proposed that positive heterosis could be contributing to increases in shatter resistance in POSH 1-3 DH lines resulting in the transgressive segregation.

Summers *et al.* (2003) highlighted how larger, more vigorous plants can demonstrate greater levels of PSR. In support of this, significantly associated loci are also identified to contribute to the Pod Mass (g) and Seed Mass (g) traits indicating potential roles in growth parameters as well as roles in PSR. A good agronomic background, such as that demonstrated by the Apex parent could facilitate the growth of larger healthier pods, unlike the poorer, weedier background associated with the synthetic DK142 parent. It is suggested that this could permit the diversion of resources into physiological factors, such as increases in vascular size and changes in vascular orientation as observed to contribute to PSR in the POSH progenitors by Child *et al.* 2003 and as has been established in POSH 1-3 offspring in this investigation. Also larger plants would likely have larger vasculature. It would be of interest to grow resistant lines under different growth conditions to assess how differences in drought, wind or nutrients may affect the level of shattering and vascularisation

The observation that PSR is controlled by multiple interacting factors and that the trait is variable across years emphasises why selection has been problematic even in the hands of experienced commercial plant breeders. This reinforces a requirement for suitable markers for application to MAS for crop improvement. However, further assessment with a more complete map would be required to aid accurate identification of candidate QTL for crop improvement, as would repeat trials across multiple years and environments. Due to the nature of the material, it was not possible to achieve the proposed density of 10 – 50 markers per linkage group, required for accurate QTL mapping (Kearsey, 1998). It is proposed that a higher resolution linkage map, with an increase in marker density and addition of centromeric or telomeric markers would aid accurate determination of linkage groups and therefore the chromosomal location of important QTL. A number of unmapped loci are apparent in the POSH 1-3 population and this reflects unresolved areas of the genome where it is possible also more markers linked to PSR may not have yet been identified.

After identification of suitable markers linked to QTL it would be required to validate such loci, which would require introgression into conventional material to ascertain if such factors could be used to increase shatter resistance. This is likely to be a complex and time consuming process as multiple markers are required to manifest the trait.

Using a single marker analysis it has been shown how loci associated to major and minor effect QTL contribute to Pod Mass, Seed Mass, Seed Damage and multiple measures of PSR in *B. napus.* We have identified a number of candidate genes with established roles in *Arabidopsis* fruit development with potential involvement in PSR, and observed that the genetic basis of their role in trait regulation is highly complex. Unsurprisingly, I have observed the processes such genes are involved in to be intricate and regulated by multiple factors which are difficult to elucidate due to the nature of the amphidiploid *B. napus* genome

Summary

Multiple regression analysis has identified how combinations of markers from both shatter resistant and susceptible progenitors contribute to towards manifesting the complex, polygenic PSR phenotype in POSH 1-3. The analysis has also demonstrated that alleles from both the shatter susceptible and resistant parents interact to account for more of the variance than combinations of individual loci. However, an incomplete genetic linkage map has rendered the identification of significantly associated markers on specific linkage groups problematic. This is further confounded by a paucity of genetic markers, resulting in a lack of coverage and overall map population. Determination of gene candidacy has also hampered by a lack of identifiable homology of associated markers linked to QTL to known *Arabidopsis* and *Brassica* genes*.* Therefore it is suggested continued development of the genetic map and repeated trials could be conducted to verify the loci that have already identified and also identify new QTL. However the markers we have identified have potential application for crop improvement and with continued development resources for the POSH 1-3

population appear to be an excellent source from which to obtain linked markers, with application to benefit pre-harvest pod shatter in *B. napus* and other *Brassica* oilseed crops.

Chapter 6: Investigating Variation in Pod Shatter Resistance in Natural and Mutant Accessions of *Arabidopsis thaliana* using a Novel Assay

6.1 Introduction

Fruits of flowering plants (Angiosperms) are maternally-derived organs with two primary functions: firstly they protect the developing seeds as they mature and subsequently facilitate their dissemination. *Arabidopsis* fruit development is a complex, tightly-regulated process, involving a network of transcription factors which interact with phytohormones to ensure correct tissue specification and growth (Liljegren *et al.,* 2004; Dinneny *et al.,* 2005; Girin *et al.* 2010; Arnaud *et al.*, 2010; Sorefan *et al.,* 2009). Upon maturation, fruit growth is followed by a precisely controlled degradation of the separation layer by activation of hydrolytic enzymes and desiccation of the silique resulting in mechanical tension, to enable valve detachment from the silique and allow seed dispersal (Spence *et al.* 1996; Ogawa *et al.,* 2010). Although the process of fruit development and mechanisms of pod-shattering are well documented in both cultivated *Brassica* species and *Arabidopsis thaliana,* it has yet to be investigated whether it is possible to accurately measure levels of pod shatter resistance in *Arabidopsis* or if shattering varies between ecotypes from different natural populations (Meakins and Roberts 1990 a, b; Spence *et al.,* 1996).

Arabidopsis exhibits natural variation for a wide range of characters including abiotic and biotic resistance, flowering time, drought resistance, glucosinolate content, molybdenum content and nitrogen use efficiency (Buell and Somerville, 1997; Shindo *et al.* 2005; McKay *et al.* 2008; Kleibenstein *et al.,* 2001; Baxter *et al.,* 2008; Loudet *et al.* 2007). This variation is attributed to inherent selfing, a wide distribution and adaptation to diverse environments (Lawrence, 1976, p167-190; Pigliucci, 1998).

It would be desirable to identify if differences in pod shatter exist between *Arabidopsis* accessions and to assess if natural variation in shattering is apparent in ecotypes from geographically diverse origins. This could aid in attempts to isolate genetic factors

contributing to pod shatter in *Arabidopsis* that could be potentially exploited as targets for crop improvement in cultivated *Brassica* species*.*

Differences in levels of dehiscence have been reported in mutant *Arabidopsis* lines, deficient in key transcription factors, with observation of alterations in valve margin tissues compared to wildtype (Liljegren *et al.* 2000 and 2004; Roeder *et al.,* 2003; Sundaresen *et al.,* 2001). It is also of interest to investigate if it is possible to quantify variation in shatter resistance amongst lines deficient for specific genes regulating fruit development

This chapter will describe utilisation of a novel shaking assay, termed the *Arabidopsis* Random Impact Test (ARIT), to investigate potential differences in shatter resistance in a range of different ecotypes, from a variety of geographical locations and also a number of lines deficient in specific transcription factors or biosynthetic genes associated with fruit development. Histological analyses of key lines are also illustrated in an attempt to ascertain if potential variation in PSR is associated with differences in pod structure or anatomy.

6.2 Materials and Methods

6.2.1 Plant Material

Seed was obtained from National Arabidopsis Stock Centre for Ecotypes: An-1, Bay-0, Br-0, C-24, Col-0, Cvi-0, Est-1, Kin-0, Kondara, Ler-0, Mrk-0, NFA-8, Nok-3, Oy-0, Van-0 and Ws-2. Mutant seed for lines deficient in *shp1/2, alc, ind-2,* Col-0 background/Ler-0 background were provided by Lars Østergaard. Seed was cleaned in 0.1% sodium hypochlorite solution for five mins and rinsed three times in ddH$_2$O. Seeds were stratified at 5°C in 0.1% bacto-agar for three days prior to sowing in soil (*Arabidopsis* mix: Levington's M2 compost with 4mm grit (8:1)). Plants were grown in a controlled environment room (CER) at 18°C, under long day conditions (16 hrs light/8 hrs dark) in a randomised design (Appendix 6.1, page 307). Four plants were grown per pot. Siliques were collected from four plants from each ecotype from each replicate block. Fully elongated siliques (stage 17b, smyth *et al.,* 1990) were sampled randomly across the primary and secondary branches for sectioning and staining. Siliques were cut in half and fixed in 3.7% FAA solution (described in Chapter Three). Plants were allowed to completely senesce prior to collection of siliques for shatter resistance assessment.

Siliques for shatter-testing were selected non-randomly, to avoid potential bias throughout the length of the terminal and primary branches (Figure 6.1) using forceps and fine scissors from a minimum of four individual plants and pooled to reduce environmental effects. Arrows indicate silique selection pattern, with fruits harvested from alternating sides of the along the branch to avoid positional bias. Fully elongated fruit were preferentially selected, to minimise confounding by potential variation in silique size. Pooled siliques were placed in a ventilated container and then equilibrated.

6.2.2 Plant material from mutant, reporter and over-expression lines

Fruit was obtained from mutant lines termed *delayed dehiscence 2 (dde-2), BFA (Brefeldin A) visualized endocytic trafficking defective 2 (ben-2), ga 4-3* oxidase, *spatula (spt-12)* and *indehiscent (ind-2).* Siliques from pIND>>GA2ox and *35S::BEN2* lines were also collected. Plants were grown in a CER under long day conditions and harvested at the point of

complete senescence. Sections had been prepared previously to observe potential physiological differences in certain lines (Girin *et al.,* unpublished, Arnaud *et al.,* 2010).
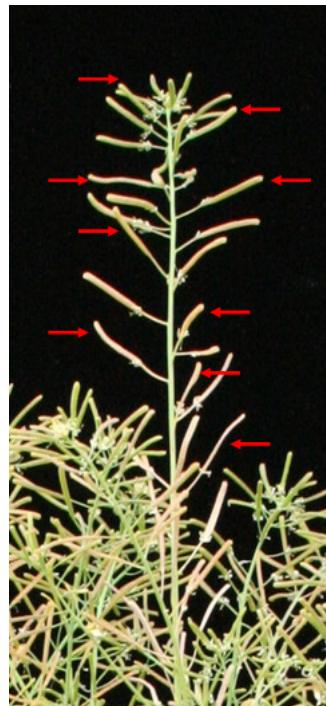
Figure 6.1: Image depicting silique selection for shatter assessment in *Arabidopsis thaliana* (Van-0) - Arrows indicate selected fruit*.*

6.2.3 Equilibration

Siliques were placed in unsealed containers in an equilibration chamber ($25°C$/50% Relative Humidity) for a minimum of seven days prior to testing. Replicate samples of 20 undamaged siliques were selected prior to shatter testing.

6.2.4 Pod Shatter assessment using the *Arabidopsis thaliana* Random Impact Test (ARIT)

The ARIT was developed to assess the relative level of resistance to shattering in *Arabidopsis thaliana* accessions. The apparatus consisted of an Eppendorf whirlimixer (Fisher Scientific, Loughborough, U.K.) modified to hold a 50 mm x 20 mm, sealed, pyrex petri dish (Figure 6.2). Parafilm was placed between the surfaces of the clamp and between the two halves of the dish to prevent slippage. Five 2 mm steel balls, with a mass of 276.25mg, were placed into the petri dish. The frequency at which the shaker oscillated was determined manually to gauge the optimal rate of silique dehiscence using Col-0 siliques as a control. The rate selected enables a progressive and quantifiable dehiscence in the siliques. The rate is kept as a standard throughout testing at approximately 900rpm (¾ full speed of shaker) for all samples. Samples of 20 siliques are placed in the petri dish, sealed and shaken for set durations of five seconds (0-60 s), ten seconds (60 – 120 s) and twenty seconds (120 s- 250 s). The number of intact/broken (fully dehisced) fruit is then recorded after each interval. Samples are assessed in triplicate.

Figure 6.2: *Arabidopsis* Random Impact Test (ARIT) shaker

6.2.5 Progress Curve Fitting

Curve fitting for silique degradation data was conducted using same model as described for the RIT utilised for assessing the POSH 1-3 population (Morgan, unpublished). A Chapman 4 parameter sigmoidal curve was fitted to each data set by the model with manual curves fitting in the event of failure. An *Arabidopsis* Random Impact Test 50 value (ARIT$_{50}$), the time point (in seconds) at which 10 siliques from a 20 silique sample remain intact, was generated for each independent curve and used as a measure of the relative level PSR in *At* ecotypes, compared to a Col-0 control. An example of a progress curve used to generate ARIT$_{50}$ data is displayed in Figure 6.3. Mean ARIT$_{50}$ values were calculated for each line assessed and were used as a comparative measure of PSR between different accessions.
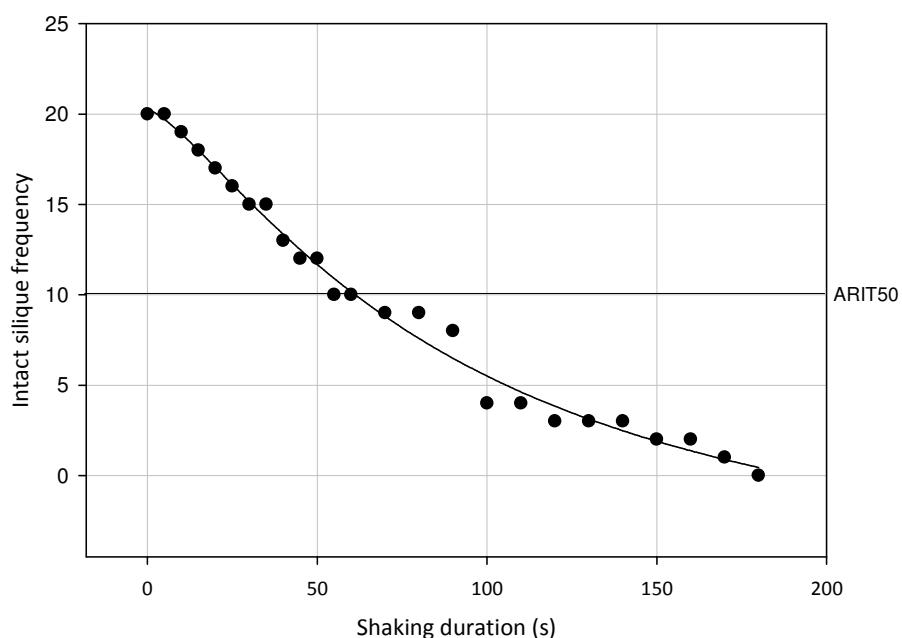
Figure 6.3: Progress curve displaying the relative decrease in intact silique frequency over increasing shaking duration in from Col-0 siliques under ARIT analysis. ARIT$_{50}$ point marked at 10 intact siliques.

6.2.6 Statistical Analyses

$ARIT_{50}$ data was analysed using Genstat V.12 software utilising two sample T-tests (paired/unpaired) to identify potential significant differences between individual lines and unbalanced GLM between lines.

6.2.7 Tissue Fixation, Sectioning and Staining of *Arabidopsis thaliana* siliques

Fully elongated siliques from select *Arabidopsis* lines were harvested (stage 17b, Smyth *et al.,* 1990), halved and immersed in 3.7% FAA. Siliques were vacuum-infiltrated for 15 mins and fixed overnight whilst on a shaker. Fixed tissue was exposed to a series of ethanol washes, cleared in a Histoclear (National Diagnostics, Hull, U.K.) series and embedded as described for *Brassica* tissue in Chapter 3. Transverse sections (8-10µm) were prepared using a microtome and mounted on slides using a water bath prior to de-waxing in Histoclear. Slides were stained in 0.1% Alcian Blue/0.05% Safranin-O for 30 mins and subsequently rinsed and mounted. Sections were visualised and imaged under Leica MZ16 dissecting microscope.

6.2.8 Lignin Specific Staining

Transverse sections (8-10µm) from fully elongated (stage 17b) Mrk-0 and Van-0 siliques were stained with 1% phloroglucinol for 2 mins and subsequently acidified with drops of 37% HCl. Lignified tissues were stained dark red. Images were visualised immediately under a Leica MZ16 microscope.

6.3 Results

6.3.1: Measuring variation in PSR in *Arabidopsis thaliana*

6.3.1.1 Differences in PSR in Columbia (Col-0), Landsberg erecta (Ler-0) and Wassilewskija (Ws-2) Ecotypes

A novel method to quantify differences in PSR in *Arabidopsis thaliana,* termed the ARIT, was developed (Figure 6.2). Initial investigations into variation in PSR using the ARIT shaking assay were performed on three common *Arabidopsis* ecotypes; Columbia (Col-0), Landsberg erecta (Ler-0) and Wassilewskija (Ws-2). Six replicate, 20 silique samples from each line were shaken over set durations and their relative decrease in number of intact fruit recorded over time. Progress curves were fitted to this intact silique data using a four-parameter, Chapman curve model (Morgan, unpublished) and Lethal Dose (ARIT$_{50}$) values estimated for each sample (the time-point (s) at which only ten fruit remain intact). A mean ARIT$_{50}$ value was then calculated for each line as a comparative measure of PSR.

Significant differences in mean ARIT$_{50}$ were observed between Col-0 and Ws-2 ($P<0.005$) (Appendix 6.2, page 307). Col-0 exhibited a mean ARIT$_{50}$ value of 58.11 seconds whereas Ws-2 displayed a mean ARIT$_{50}$ of 87.14 s (Figure 6.4). Ws-2 exhibited an increase in PSR, with an approximate 50% increase in ARIT$_{50}$ duration, compared to Col-0 during the ARIT. Ler-0 was observed to be un-testable using the ARIT, due to siliques dehiscing on the plant prior to harvest.
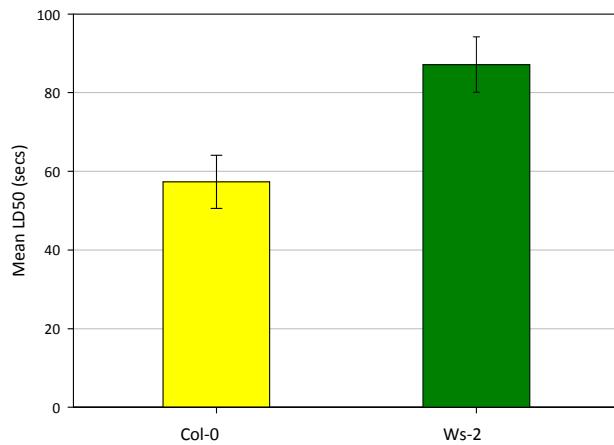
Figure 6.4: Histogram displaying mean $ARIT_{50}$ values for Col-0/Ws-2 ecotypes generated using ARIT shaking assay (including standard error bars).

6.3.1.2 Variation in Shatter Resistance in a range of *Arabidopsis thaliana* Ecotypes

A range of *Arabidopsis* ecotypes were also assessed using the ARIT to screen for differences in resistance to pod shattering. 14 ecotypes were selected for testing and mean ARIT50 values estimated from the respective silique breakdown data. Four replicate samples of 20 siliques, from two independent blocks were assessed for each line. Lines assayed included An-1, Bay-0, Br-0, C-24, Col-0, Cvi-0, Est-1, Kin-0, Kondara, Mrk-0, NFA-8, Nok-3, Oy-0, and Van-0 ecotypes. An-1 was observed to display extremely fragile siliques that could not be successfully harvested and was therefore excluded from the analysis.

The remaining 13 lines were assayed using the ARIT. Of the ecotypes tested, Cvi-0, Kin-0, Nok-3, and NFA-8 were observed to display a large range in variation between samples. The observed variation was far greater than that experienced during initial testing in Col-0 and Ws-2 ecotypes and for this reason these lines were excluded from the investigation.

Significant differences in mean $ARIT_{50}$ ($P<0.01$) were identified between the eight remaining ecotypes assayed (Figure 6.3, Appendix 6.3 (page 308)). Ecotypes displayed a range of respective mean ARIT50 values, with some varieties more susceptible to shattering than Col-0, some demonstrating a similar performance and others exhibiting increases in resistance to shattering. Br-0, Oy-0 and Van-0 ecotypes were significantly more susceptible to shattering compared to Col-0 ($P<0.001$, $P<0.05$ and $P<0.001$ respectively, Appendix 6.4 (page 308)) with respective mean $ARIT_{50}$ values of 29 s, 39 s and 30 s (compared to 58 s in Col-0). Of the ecotypes assessed, C24 was demonstrated to perform similarly to Col-0 under ARIT assessment ($P<0.281$), generating a mean $ARIT_{50}$ value of 48 s.
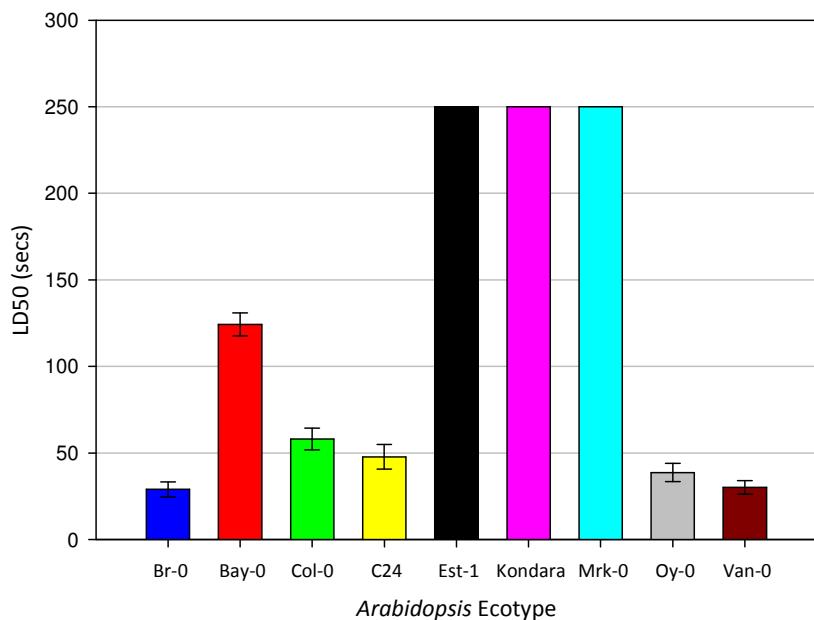
Figure 6.5: Histogram displaying mean $ARIT_{50}$ values for nine *Arabidopsis* ecotypes assessed using the ARIT shaking assay (including standard error bars).

The remaining lines tested were observed to display increases in mean $ARIT_{50}$ value and hence an increase in PSR. Bay-0 was seen to generate a significantly greater mean $ARIT_{50}$ value (124 s) in comparison to Col-0 (58 s) ($P<0.001$). Est-1, Kondara and Mrk-0 lines were

also observed to exhibit statistically significantly differences in mean $ARIT_{50}$ values compared to Col-0 ($P<0.001$) and were identified as the ecotypes most resistant to shattering when assayed with the ARIT. Although the (ARIT) assay did induce dehiscence in a small frequency of siliques from the Est-1, Kondara and Mrk-0 samples, an ARIT50 value could not be generated within the allotted testing period (250 s), for any of these ecotypes, hence no error bars were included for these lines (Figure 6.5).

A randomised planting design and pooled harvesting regime was utilised in the experimental design to attempt to reduce the effects of environmental variation between blocks. However, variation between replicate blocks ($P<0.05$) for mean $ARIT_{50}$ was identified between ecotypes (Appendix 6.5, page 313), highlighting potential environmental effects on the level of PSR in *Arabidopsis*.

6.3.1.3 Anatomical Differences in Silique Tissue Structure - Sectioning and Staining in *Arabidopsis thaliana* Ecotypes

Fully elongated fruit from select ecotypes which exhibited an increase or decrease in mean $ARIT_{50}$ value compared to Col-0 were sectioned and stained with Alcian Blue/Safranin-O dye to aid identification of potential physiological differences between them. Mrk-0 (resistant) and Van-0 (Susceptible) ecotypes were selected. Van-0 was seen to display a lignified replum, valve margin and endocarp layer B (enB) (Figure 6.6, image A). Sections of other lines cultivated in the trial were also assessed but Br-0, Col-0, Kondara, Nok-3 and Oy-0 sections were observed to be similar in appearance to Van-0 (data not shown).
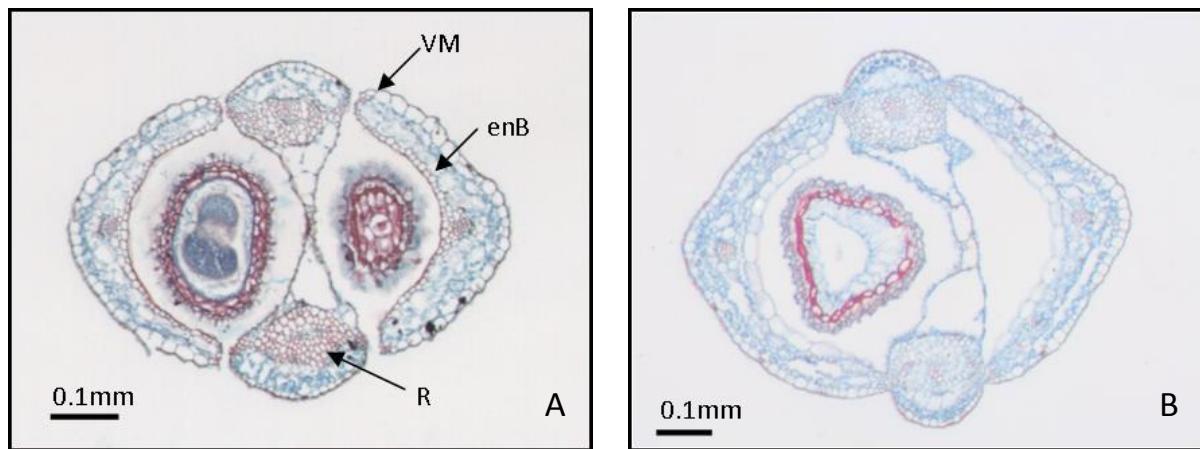
Figures 6.6 a & b: Transverse cross sections in fully elongated siliques from A. Van-0 and B. Mrk-0 ecotypes stained in Alcian Blue/Safranin-O. enB: Endocarp layer B, VM: Valve Margin and R: Replum. Note lack of lignification at enB layer, valve margin and replum in Mrk-0 line. Scale: 0.1 mm

In Mrk-0, one of the lines most resistant to shattering, a reduction in the level of lignification of the enB layer, valve margin and replum was identified, compared to other *Arabidopsis* lines (Figure 6.6 b).

To verify findings in the differences in lignification observed between Mrk-0 and Van-0, phloroglucinol was utilised to specifically stain lignin (dark-red), in transverse sections of fully elongated siliques. Clear differences in the levels lignification at the enB layer, valve margin and replum were observed between the two lines, with an apparent reduction in lignification in the shatter-resistant Mrk-0 ecotype (Figure 6.7).
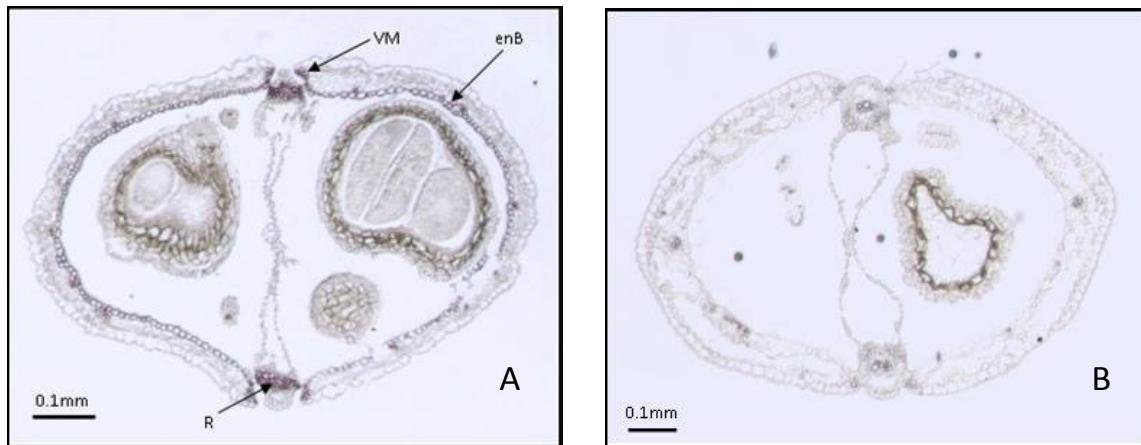
Figures 6.7 a and b: Transverse cross sections in fully elongated A. Van-0 and B. Mrk-0 siliques stained with 1% phloroglucinol. enB: Endocarp layer B, VM: Valve margin and R: Replum. Scale: 0.1 mm

6.3.2.1 Variation in PSR in Fruit Development Mutants

Potential variation for mean $ARIT_{50}$/PSR in fruit developmental mutant *Arabidopsis* lines, deficient in specific transcription factors or signalling factors regulating fruit development, were also assessed using the ARIT.

6.3.2.2 Differences in Dehiscence Identified between *alc, ind* and *shp1/2* Mutants Compared to Col-0

Fruit samples from *alcatraz* (*alc*), *indehiscent* (*ind)* and *shatterproof* (*shp1/2*) lines were observed to be completely indehiscent under the ARIT assay. Siliques could be shaken for the complete 250 s shaking duration without any dehiscence noted in any fruit (Figure 6.8). Siliques preferentially ruptured along valve walls in the three mutants (without seed dissemination) compared to conventional fracturing along valve margins in WT (Col-0). This is in agreement with previous findings that valve and replum tissues are fused in such lines due to mis-regulation during specification of valve margin tissues.
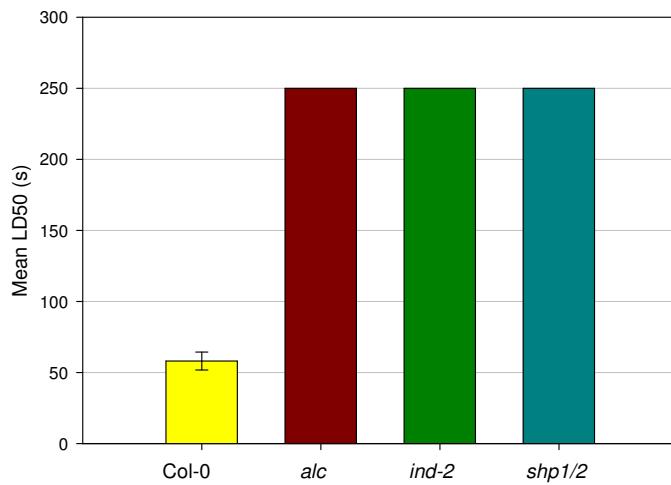
Figure 6.8: Histogram displaying mean $ARIT_{50}$ values for indehiscent *alc, ind-2* and *shp1/2* and Col-0 control (including standard error bars).

6.3.2.3 Differences in Dehiscence Identified in *spatula-12* alleles and Col-0

20 silique samples obtained from lines with weak and strong *spatula (spt)* alleles were assessed for differences in mean $ARIT_{50}$/PSR. Significant differences in mean $ARIT_{50}$ and hence PSR were observed in both weak and strong *spt* lines compared to Col-0 when assayed using the ARIT ($P<0.01$ and $P<0.001$, respectively) (Figure 6.9 Appendix 6.6, 6.7 (page 315)). Compared to the Col-0 standard (mean $ARIT_{50}$: 58 s), the weak *spt-12* allele generated a mean $ARIT_{50}$ value of 92 s and the strong line was completely indehiscent. This supports findings from cross sections of weak and strong *spt* siliques where a progressively severe phenotype between the two alleles results in incorrect patterning of tissues at the DZ has been noted (Girin, in publication).
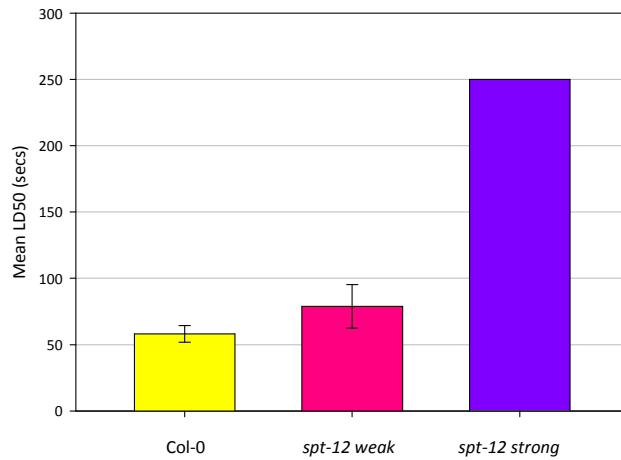
Figure 6.9: Histogram displaying mean $ARIT_{50}$ values for weak and strong *spt-12* and Col-0 control (including standard error bars).

6.3.3 Mutant Accessions Deficient in Specific Phytohormones Exhibit Differences in PSR.

The ARIT was utilised to assess PSR was in *At* lines deficient for or with modulated regulation of gibberellic acid (GA), auxin and and jasmonic acid (JA) (Arnaud *et al.* 2010, Østergaard/Girin, unpublished).

6.3.3.1 Assessment of the role of regulators of the GA pathway in fruit development and dehiscence - pIND>>ga-2 oxidase and *ga 4-1* mutant.

The role of GA on fruit patterning and dehiscence was investigated in a *ga 4-1* mutant and a pIND>>GA2ox line, using Col-0 and *ind-2* fruit as positive and negative controls, respectively. The *ga 4-1* line was deficient for a key enzyme in the biosynthetic pathway, GA 3 oxidase, resulting in a lack of GA (at the VM). In the pIND>>GA2ox line, expression of the *GA2ox* gene (encoding a GA-inactivating enzyme) is driven at the valve margin by the *IND* promoter in a two-component system resulting in GA inactivation only where IND is expressed (Moore *et al.* 1998). Mean $ARIT_{50}$ was significantly increased ($P<0.05$) in the *ga 4-* mutant compared to Col-0 (135 s/58 s), whereas fruits from the pIND>>GA2ox line exhibited complete indehiscence (Figure 6.10, Appendix 6.8 (page 6.8)).

210
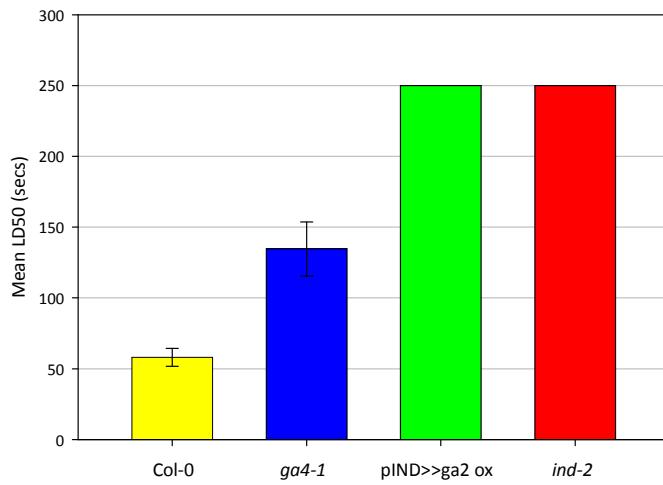
Figure 6.10: Histogram displaying mean $ARIT_{50}$ values for
Col-0, *ga4-3 oxidase*, pIND::ga-2 oxidase and *ind-2* lines
(including standard error bars).

This assessment highlights the role for correct GA regulation in the fruit development to ensure shatter susceptibility for efficient seed dispersal and has identified measurable increases in pod shatter resistance in lines deficient for GA or for transcriptions factors regulating silique GA dynamics.

6.3.3.2 Assessment of the Role of Regulators of the Auxin and JA Pathway in Fruit Development and Dehiscence

20 silique samples from *ben-2*, Col-0, *dde-2* and the constitutive expressor line *35S::BEN2* were assayed with the ARIT to identify potential differences in ARIT50 and hence PSR between lines. *ben* mutants are defective in Brefeldin A (BFA) sensitive ARF-GEF (Auxin Response Factor – GTPase Exchange Factor) regulating endosomal trafficking, affecting the distribution/localisation of the PIN1 auxin efflux carrier, whereas, *dde-2* is defective in allene oxide synthase, a key enzyme in the JA biosynthetic pathway. The mean $ARIT_{50}$ value for *ben-2,* and *35S::BEN2* were observed to have significantly reduced ($P<0.005$, $P<0.05$, respectively) compared to Col-0 and thus were more susceptible to dehiscence. Of the lines

assayed, *ben-2* displayed the shortest mean ARIT$_{50}$ s of 10.18 s and *35S::BEN2* was recorded at 20.45 s compared to 58.11s for Col-0. In contrast fruit from *dde-2* was found to display a significant increase in levels of PSR compared to the control (*p*=<0.01), with a mean ARIT50 of 96.97 s (Figure 6.11 Appendix 6.9 (page 317)).
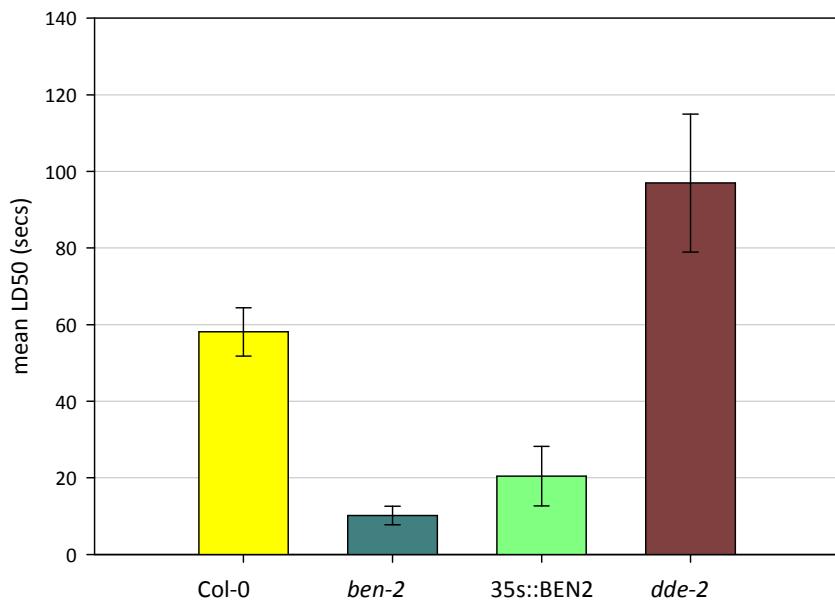
Figure 6.11: Histogram displaying mean ARIT50 values for Col-0, *ben-2*, *35s:BEN2* and *dde-2* lines (Including standard error bars)

Transverse sections of fully elongated fruit (stage 17b) from the shatter-resistant *dde-2* line were prepared in the Østergaard lab and sections stained with phloroglucinol. A large reduction in the level of lignification at the endocarp layer B (enB), valve margin and replum had been observed, compared to Col-0, similar to the lack of lignification observed in the Mrk-0 ecotype (Østergaard unpublished, data not shown).

6.4 Discussion

Summary

In this chapter it has been demonstrated that it is possible to quantify variation in shatter resistance in siliques from different *Arabidopsis thaliana* accessions using the *Arabidopsis* Random Impact Test (ARIT). We have identified significant differences in mean $ARIT_{50}$, a measure of pod shatter resistance, in both natural accessions and in mutant lines deficient in key regulators of valve margin development, compared to a Col-0. Findings support suggestions that alterations in valve margin structure in specific mutant lines affects the level of pod shatter resistance and We have also identified potential differences in PSR and lignification in resistant and susceptible lines which could contribute to variation in shattering in natural and mutant accessions (Arnaud *et al.,* 2010, Girin, Østergaard, unpublished).

We have identified variation in PSR among *Arabidopsis* ecotypes

Natural accessions displayed a range of shatter profiles with susceptible, intermediate and resistant ecotypes observed. $ARIT_{50}$ data were reproducible between replicates in nine of the thirteen ecotypes successfully tested. However, An-1 and Ler-0 ecotypes were observed to dehisce prior to testing and four ecotypes (Cvi-0, Kin-0, NFA-8 and Nok-3) exhibited large inter-sample variation so were excluded from the analysis. Variation in the PSR trait in these four ecotypes may potentially reflect a degree of genetic plasticity within an ecotype where no pressure on selection, either for or against an increased resistance to shattering has been prevalent. Genetic plasticity has previously been reported for a number of traits in *Arabidopsis* including growth rate, branching, leaf number and flowering time (Pigliucci, Schlichting and Whitton, 1995; Pigliucci,1998; Pigliucci & Schlichting, 1996, 1998).

Of the accessions assayed using the ARIT, Br-0, Oy-0 and Van-0 ecotypes exhibited significantly reduced resistance to shattering compared to a Col-0 control and Bay-0, Est-1, Kondara and Mrk-0 ecotypes demonstrated significant increases in shatter resistance. $ARIT_{50}$ values could not be generated over the standard total 250 second shaking duration for the latter three ecotypes, indicating a dramatic increase in resistance in these lines. Together,

these findings suggest a large degree of variation in pod shatter resistance between different *Arabidopsis* ecotypes (grown under the same condition). It would be of interest to identify candidate genes contributing to differences in PSR in *Arabidopsis* and the use mapping population derived from the lines tested here could be utilised to identify such loci.

Histological analysis of transverse sections from fully elongated siliques identified distinct differences in lignification pattern at the endocarp B layer, valve margin and replum between the resistant Mrk-0 ecotypes and the susceptible Van-0 lines. It is proposed that a reduction in lignification could potentially contribute to an increased level of pod shatter resistance in the Mrk-0 ecotype. It is suggested that the decrease in lignin could potentially reduce the amount of relative tension generated in/across the silique during senescence compared to more lignified varieties. A more rigorous investigation into lignification patterns, and the tensions generated in fruit in resistant and shatter susceptible ecotypes may help gain insight into physiological factors contributing to PSR in *Arabidopsis*. Assessment for variation in valve margin structure, separation layer size and relative degradation, and silique vascular architecture could also provide insight into differences in levels of PSR.

We have also identified environmental variation in PSR between replicate ecotype blocks in this investigation (p=<0.05), indicating the ability of a plant to adapt responsively to differences in the environment, at least with respect to pod shatter. It would be of great interest to test siliques from the same ecotypes in their natural habitat and those grown under conventional CER/Greenhouse conditions to ascertain the degree of differences in shattering between plants from each condition and at each location.

From a biological perspective, it could be postulated that the ability to dehisce with more or less inductive force, may provide a selective advantage under conditions where environmental pressure may be inferred. However, to begin to investigate if an environment has effects on the level of dehiscence and if natural variation in PSR in *Arabidopsis* ecotypes is evident, it would have to be established if and how shattering varies in a much broader

214

range of accessions (Borevitz, Nordberg – Personal Communication). Insight into flowering time, vernalization requirement, climate, geographical habit and population structure in respective environments for each accession would also be an important requirement for such a study. The Nordberg collection, consisting of 96 geographically diverse *Arabidopsis* ecotypes, would appear to be an excellent resource in which to investigate natural variation for pod shatter.

Interestingly, of the lines showing the greatest differences in shattering, 'susceptible' Br-0 and Van-0 ecotypes and 'resistant' Bay-0 and Mrk-0 lines are observed to be isolated from regions at the same latitude (N49) (NASC: www.arabidopsis.info). This strengthens the argument for an in depth investigation, incorporating geographical and climatic variation at collection sites for a range of different accessions to study natural variation for shattering in *Arabidopsis* as it would appear conclusions cannot be drawn simply using broad geographical distributions.

From the perspective of identifying causal genes associated with differences in shatter resistance in *Arabidopsis* genetic linkage mapping and subsequent QTL analysis and sequencing would potentially present the most amenable strategy. A range of F_2 and Recombinant Inbred Line (RILs) populations suitable for this type of analysis are already available, although differences in shatter resistance would have to be screened to identify suitable accessions (Loudet *et al.,* 2005; O'Neill *et al.,* 2008). Therefore, the Kondara x Br-0 RIL population (O'Neill *et al.,* 2008), identified to demonstrate high and low levels of shatter resistance would appear to be a good candidate in which to investigate PSR, as variation for shatter resistance has been established in the two parental lines using the ARIT during this investigation.

Variation in PSR in fruit development mutants of *Arabidopsis*

Large anatomical differences have been identified in the valve margin tissues of fruit development mutants compared to WT using SEM and sectioning thus conferring an inability to disseminate seed in the conventional manner (Liljegren *et al.* 2000 and 2004; Roeder *et*

al. 2003). Using the ARIT to attempt to quantify potential differences in PSR between them, an indehiscent phenotype was observed the *alc, ind-2, shp1/2* and (strong) *spt-12* mutants lines corroborating the importance of correct regulation in the development of the DZ by key transcription factors to enable seed dispersal.

However not all mutant alleles were observed to exhibit such a striking phenotype. The weaker *spt-12* mutant displayed an increased resistance to shattering compared to WT, with less severe 'deformation' of dehiscence zone tissues, compared to the indehiscent strong *spt-12* line (Girin, unpublished). This highlights an ability to potentially tailor dehiscence to a desirable level through identification of alleles of weaker effect. Mutations in genes such as *SPT* may therefore be amenable to manipulation as a target for *Brassica* crop improvement. This could also be true of the other genes discussed and contemporary approaches such as TILLING or RNAi in *brassica* for candidate genes identified in *Arabidopsis* may have the potential to modulate gene activities to obtain desirable agronomic phenotypes (Stephenson *et al.,* 2010, Girin *et al.* 2010).

We have also established differences in dehiscence in lines mis-regulating key biosynthetic genes from hormone signalling pathways involved in fruit development. In lines associated with the GA regulated fruit development, mean $ARIT_{50}$ and hence pod shatter resistance, was demonstrated to be significantly increased compared to Col-0 in *ga 4-1*, whereas pIND>>GA2ox was observed to be completely indehiscent. In these lines, DZ structure has been demonstrated to be altered through perturbation of the phytohormone GA, voiding its role in regulating correct development of the valve margin (Arnaud *et al.,* 2010).

Regulators in Auxin and JA signalling pathways have also been identified to be associated with differences in shattering using the ARIT. Mutant, BFA-visualized endocytic trafficking defective 2 (*ben-2*) and *35S::BEN2* lines were demonstrated to have reduced mean $ARIT_{50}$ values compared to Col-0 and thus were more susceptible to dehiscence. *ben-2* displayed the shortest mean $ARIT_{50}$ and *35S::BEN2* was only slightly increased compared to this. This

would suggest that mis-regulation of endocytic PIN1 trafficking, through knockout or over-expression of *BEN2*, effects a reduction in shattering through disrupting correct auxin distribution, potentially affecting the dehiscence mechanism in *ben-2* and *35S::BEN2* siliques.

It would appear Jasmonic Acid (JA) may also function in the regulation of patterning key elements of the fruit dehiscence machinery. Fruit from the *dde-2* mutant, which lacks a key enzyme in the JA biosynthesis pathway (Allene Oxide Synthase) (Malek *et al.,* 2002; Laudert and Weiler, 2002), displayed an increased level of PSR compared to the control, taking nearly twice as long to shatter. It was perceived, as with other lines deficient in key FD regulators, that the *dde-2* mutant may exhibit differences in physiological structures/at the tissue level.

Sectioning and subsequent staining with Phloroglucinol in the Østergaard lab revealed that there was a large reduction in the level of lignification at the endocarp layer B (enB) and at the valve margin (Østergaard, unpublished). The extended ARIT50 demonstrated in the *dde-2* line and hence an increase in shatter resistance could potentially be attributed to this reduction in lignification at the enB layer. This is in agreement with the observation in the Mrk-0 ecotype, that a decrease in lignification at the enB layer is correlated with an increase in mean ARIT50 and hence an increase in PSR.

Manipulation of regulators of hormonal signalling pathways, as has been suggested for specific transcription factors, may have the potential as targets for *Brassica* crop improvement.

Future Scope

This investigation has highlighted variation in PSR in natural accessions of *Arabidopsis* and also differences in a range of fruit development mutants, through development of a novel shaking assay. The ARIT is suggested to be an important tool for studying natural variation amongst *Arabidopsis* ecotypes and could be utilised for identification of causal genes in a

suitable mapping population, with subsequent QTL analysis. In the future it would extremely interesting to attempt to first identify and then sequence key genes (or their promoter regions) perceived to contribute to an increase in pod shatter resistance, using the ARIT as an approach to accurately phenotype PSR in *Arabidopsis.*

7.1 Pod shatter in the POSH 1-3 population and its progenitors

Pre-harvest Pod Shatter in *Brassica napus* is a serious economic and agronomic issue resulting in lost revenues and volunteer contamination of subsequent crop rotations. Pod shattering is a key domestication trait in cereals and grain crops such as wheat and rice but the character remains elusive in commercial *B. napus* varieties. This is due to the relatively narrow range of germplasm that modern cultivars have been developed from to ensure low levels of glucosinolates and erucic acid required in food oils. Resistance to shattering has been reported in a range of *Brassica* species and wild relatives, but due to the concomitant introgression of many other agronomically undesirable traits, these have not proved viable sources of useful alleles.

Efforts were therefore made to develop resources in which shatter resistance in *B. napus* could be studied and factors contributing to increases in seed retention elucidated (Morgan *et al.,* 2000; Werner *et al.* 2003 a, b). Studies into these resources have previously identified that the PSR trait is highly complex, polygenic and recessive in nature, and has also been seen to be environmentally sensitive and subject to variation by G x E effects. Lines displaying shatter resistance have been shown to have multiple physiological determinants which contribute to increases in resistance (Child *et al.*, 2003; Summers *et al.,* 2003). A doubled haploid (DH) mapping population termed POSH 1-3 was developed from a cross between the commercial cultivar Apex and a highly shatter resistant synthetic hybrid line DK142 and was shown to segregate for pod shatter resistance (PSR) (Werner *et al.,* 2003 a, b).

This population has been exploited to elucidate if similar factors controlling PSR in the resistant parent are analogous in resistant lines in the population and if QTL associated with increasing seed retention could be identified with scope for incorporation into commercial material by marker assisted selection (MAS). This approach could greatly improve the

efficacy of breeding programmes, where previous efforts to introgress alleles conferring PSR through conventional approaches have been largely unsuccessful. Also at our disposal is a wealth of knowledge and resources provided by studies into the model species and close *B. napus* relative, *Arabidopsis thaliana.* Abundant investigations into this diminutive species have yielded profound insight into the mechanisms underlying the development and regulation of the complex process of fruit growth and pod shatter which can be exploited to further our knowledge in *B. napus*.

7.2 Identification of Genetic Factors with Potential for Modulating PSR in *B. napus*

We have performed a series of investigations in the POSH 1-3 population to measure differences in a range of traits relating to PSR in *B. napus.* Studying multiple traits has allowed to the interrogation of different elements of the pod shatter character, focussing individually on factors comprising this multi-component phenotype to gather the greatest degree of information available. It has also demonstrated how many QTL are coincident between traits, suggesting that the same genes may be involved in regulating different characters or that the control of these is highly complex, with causal effects inferred by interactions between such loci. Accounting for the Pod Mass covariate during analyses has enabled the identification of factors that contribute to PSR independently, or at least partially, of differences in Pod Mass. We propose that a more thorough assessment of pod architecture, including quantification of pod length, pod wall thickness and vascular measurements in conjunction with traits already described, would provide greater clarification of the roles individual components infer on pod shattering in POSH 1-3 lines.

However, it is likely any QTL identified will have multiple roles, as has been observed for the identified candidate genes. Investigations in POSH 1-3 have identified transgressive segregation for the PSR trait with only a handful of lines demonstrating an increase in shatter resistance. This highlights the requirement for multiple, often recessive alleles, to manifest in a line to ensure increased resistance. It reiterates the polygenic, complex interactions involved in the PSR trait and emphasizes why problems have been encountered

using conventional breeding techniques. This strongly supports the use of techniques such as MAS to achieve a solution.

7.3 Validation of the Candidate Gene Approach in *B. napus*

Silique development has been shown to be highly co-ordinated in *Arabidopsis,* involving suites of transcription factors and phytohormones, interacting in distinct temporal and discrete spatial relationships to ensure correct tissue patterning (Lilijegren *et al.* 2004, Sorefan *et al.* 2009, Arnaud *et al.,* 2010, Dinneny and Yanofsky, 2005). This process may be regulated at an even greater level of complexity in *B. napus,* where up to six copies of every *Arabidopsis* gene may be present, raising issues of gene dosage, redundancy or post-transcriptional gene silencing. It is suggested that PSR may be regulated in an equally complex manner and that the level of intricacy involved may be compounded even further when it is considered differences in siliques anatomy has also been observed to contribute to increases in resistance.

This study utilised a candidate gene approach and demonstrated that genes with key regulatory roles in *Arabidopsis* are associated with pod traits in *B. napus*. This association is observed to be complex, where significant loci contributing to PSR, such as *BnaA.IND.a* are donated from the Apex shatter susceptible parent, whereas QTL with minor effects on PSR are contributed by the resistant DK142 parent. It has also been observed how copies of the *BnaX.ALC.x* gene involved in separation layer development are associated with differences in Seed Damage between POSH 1-3 lines. This reiterates the complex, multi-functional basis for genes involved in regulating fruit development in *Arabidopsis* and *Brassica.* As only a subset of the copies of candidate genes have been identified it is possible that contributions from different orthologues remain to be to be elucidated. Southern hybridisation or qPCR could be used to account for copy number in

B. napus to ensure the contributions of all candidates were accounted for when assessing a trait. However development of markers for amplifying each specific copy is problematic due to high homology in coding sequences between orthologues.

7.4 Conserved Roles for the Physical Determinants of PSR in POSH 1-3 lines

Similarities have been observed in silique development between *Arabidopsis* and *B. napus* as have roles for candidate gene orthologues. The anatomical basis of PSR in *B. napus* in resistant lines and have established key differences in the size and orientation of the main vascular bundle of the valve (MVBV) as observed in the DK142 parent line. Differences in separation layer breakdown in resistant lines were also identified, but investigations into the activity of specific hydrolytic enzymes in POSH 1-3 lines, such as RDPG1, have as yet proved inconclusive.

We did however observe a small-effect QTL associated with a marker linked to *RDPG1* for the 2000 field trial. This may reflect that differences in enzyme activity do contribute to variation in shatter resistance but that this may be environmentally sensitive. Although it has not been possible to identify clear differences in activity for hydrolytic enzymes in *Brassica*, the *Arabidopsis* orthologues of *RDPG1*, *ADPG1,* and a close relative *ADPG2*, have been demonstrated to be required for correct seed dispersal in *Arabidopsis* (Ogawa *et al.,* 2009). It is possible that immuno-labelling using antibodies specific to pectin, RDPG1, or β-1, 4-glucanase may help clarify if differences in the levels of pectiolytic activities are evident between susceptible and resistant POSH lines.

7.5 Identification of Variation in PSR in *Arabidopsis thaliana*

We have demonstrated that increased PSR in *Arabidopsis* is associated with a decrease in lignification at the enB layer in the Mrk-0 and *dde-2* ecotypes. Continued investigation into natural variation in levels of pod shatter in *Arabidopsis* ecotypes could provide information on candidates to target in *Brassica* for modulating pod shatter. It would be feasible to assess if differences in lignification in POSH 1-3 lines were evident and then ascertain if linked QTL

could be identified. Differences in vasculature and separation layer breakdown are proposed to be key components of shatter resistance in POSH lines so a screen for differences in these traits may also reveal if similar factors are contributing to variation in PSR in natural populations of *Arabidopsis.* This may also aid in the identification of suitable markers to screen for characters in *B. napus.* Studies into natural variation in *Arabidopsis* may provide important information on adaptive selection allowing us to better understand how genes conferring increases or decreases in a trait such as shattering can be advantageous in regions of environmental pressure. This could also constitute an important source of candidate genes for further dissection and manipulation of the pod shatter trait in *Brassica.*

7.6 Prospects for Developing Resources for Studying PSR in *B. napus*

These research efforts have greatly improved the POSH 1-3 genetic linkage map, doubling the number of genotyped loci compared to previous efforts, increasing coverage by a third and adding key intragenic markers for fruit development genes with identified roles in *Arabidopsis* and *Brassica.* Areas of the map are still unresolved and will require an increase in marker population and coverage, specifically with loci anchored in other mapping populations to aid linkage group designation. New mapping efforts have helped to reduce the ambiguity between associations between closely related markers or homeologues. However approximately one third of the POSH 1-3 genome remains unmapped and therefore loci linked to the PSR trait from unresolved regions may have not yet been identified. To improve resolution, the linkage map requires a greater marker density, with addition of more anchored loci, loci linked to specific gene candidates and ideally centromeric, telomeric and chromosome specific markers to aid linkage group designation. A lack of homology between significant markers and *Arabidopsis* and *Brassica* sequences in the databases has also made identification of gene candidates linked to QTL problematic. Increased marker density may also improve the likelihood of identifying loci demonstrating homology to genes of established function in related *Brassicacea*. With a more complete map, approaches such as Interval mapping or multiple QTL mapping (MQM) may be utilised

to aid identification of multiple QTL on single linkage groups, and also the amount of variation each QTL accounts for.

Efforts in POSH 1-3 mapping have been hampered by a lack of polymorphism for many of the screened markers, potential rearrangements during meiosis and apparent out-crossing in the DK142 parent. It is suggested the use of a population segregating for shatter resistance with a more diverse germplasm may aid identification of traits contributing to PSR. However it must be considered that variation for other traits, such as Pod Mass in the POSH 1-3 population, may also act to confound identification of independent characters. The Temple x MC169 population derived from an agronomically acceptable, shatter resistant POSH 1-3 line (MC169) and a high yielding, contemporary cultivar (Temple, Elsoms seeds, U.K.) is presented as a potential resource for future study of PSR as well as POSH 1-3.

Next generation sequencing, such as Solexa (Illumina), 454 (Roche) or SOLiD (ABI) is expediting the rate at which whole genome sequences will become available. Platforms such as Illumina Golden Gate ™ could be applied to greatly increase the rate of SNP genotyping, allowing densely populated linkage maps to be produced quickly and efficiently. The cost of implementing sequencing in plant breeding programmes in the U.K. may be limiting however and will require collaboration between the research community and industry to ensure both insightful and economically viable applications of the technology.

7.7 Validating Genetic Factors Suitable for Modulating PSR in *B. napus*

We have identified a number of QTL associated with increases in PSR in POSH 1-3 lines. Our studies have also revealed how combinations of these loci interact to account for considerably greater amounts of the variation observed and that alleles from both parents contribute to the PSR trait. Some ambiguity in QTL mapping was experienced when handling trial data produced in a small number of lines available in the subset trial, as there was when trying to resolve multiple QTL on the same linkage group. To improve the accuracy of QTL mapping and assess variability of the PSR trait an improved map would first be required, in

conjunction with repeated trials, performed across multiple years and environments. For successful selection characters must demonstrate high heritability. This aims to ensure the genetic component is robust and not subject to large environmental or G x E effects and therefore a trait should remain stable under different growth conditions. This is a prerequisite for agronomic traits due to the highly stringent test imposed during DUS (Distinctness, Uniformity and Stability) assessments, subsequent national list trials and also the varied agronomic conditions varieties would finally be cultivated under.

A number of loci have been shown to be linked to the PSR trait and potentially associated with genes with key roles in fruit development and shatter resistance. This study was based principally on two years of trial data and some candidates were apparent in both years. The Na10C08a locus is of interest due to its association with both Intact and Broken LD50 across years, its significance increases on adjustment for the Pod Mass covariate, as resistant lines carry DK142 alleles for this locus and it demonstrates homology with a hydrolase identified in *Arabidopsis*. A number of other loci were observed to behave similarly and repeat trials should be employed to ascertain if such markers occur in subsequent analyses across multiple years and environments. Increasing the number of lines available for trait assessment and linkage mapping could also improve the resolution of QTL identification. Presently the number of lines available in the population is limited due to the initial number of DH lines derived from the POSH 1-3 F_2 lines and a lack of selfed seed through losses due to deaths, infertility and self-incompatibility.

7.8 Future Directions

Methods to modulate PSR in *B. napus* hold the potential to reduce the economic and environmental impact associated with seed loss and volunteer contamination. A rigorous assessment of factors contributing to PSR in the POSH 1-3 DH population have been employed, improving resources through which to study pre-harvest pod shatter in *B. napus.* The number of genetic markers genotyped in the population has been increased substantially, enabling development of a new genetic linkage map, thorough

characterisation of anatomical determinants of PSR in the population and identified a number of QTL contributing to increases in shatter resistance with potential for crop improvement. With our development of a suite of robust markers positioned directly within key candidate fruit development genes it is now possible to assess these loci for contributing towards PSR and other biological processes.

Markers linked to increases in pre-harvest pod shatter need verification before application through repeat trials to establish their robustness and validity of the QTL they represent. Once validated, markers could be utilised directly to select for QTL in crosses derived for resistant POSH lines in breeding programmes and also to screen the Temple x MC169 population to investigate if the same QTL were evident as in POSH 1-3. Near isogenic lines could also be produced from the POSH material to enable fine mapping and cloning of QTL or even specific genes contributing to PSR. This could also help aid identification of small effect QTL that may have been masked by larger effect QTL.

The work presented here has also led to the generation of a novel assay to quantify shattering in *Arabidopsis thaliana* accessions. This assay allowed the identification of natural variation in shattering potential among a subset of *Arabidopsis thaliana* accessions. Although an ambitious goal, future studies involving a larger set of accessions could shed light on adaptive evolution strategies in different geographical or climatic regions where increased or decreased shatter potential may provide a selective advantage for survival. Such an analysis could also provide an important source of candidate genes for further dissection of the pod shatter trait in *Brassica.* With continued efforts, the resources developed during this investigation hold a strong potential to aid the integration of sources of pod shatter resistance into commercial *B. napus* varieties.

References

Alonso-Blanco, C., Koornneef, M. (2000). Naturally occurring variation in Arabidopsis: an underexploited resource for plant genetics. Trends in Plant Science **5,** 22-29.

Alonso-Blanco, C., and Koornneef, M. (2000). Naturally occurring variation in Arabidopsis: an underexploited resource for plant genetics. Trends Plant Sci **5,** 22-29.

Anjou, K. (1972). Cultivation of Rapeseed. (Elsevier publishing).

Appleqvist, L.A. (1972). *Rapeseed: Cultivation, Compostion, Processing and Utilization*. (Amsterdam: Elsevier).

Arnaud, N., Girin, T., Sorefan, K., Fuentes, S., Wood, T.A., Lawrenson, T., Sablowski, R., and Ostergaard, L. (2010). Gibberellins control fruit patterning in Arabidopsis thaliana. Genes Dev **24,** 2127-2132.

Ayyadevara, S., Thaden, J. J., and Shmookler Reis, R. J. (2000) Discrimination of Primer 3'-Nucleotide Mismatch by *Taq*DNA Polymerase during Polymerase Chain Reaction. Analytical Biochemistry **284,** 11–18

Bateman, A.J. (1955). Self-incompatibility systems in angiosperms. III. Cruciferae. Heredity **9,** 52-68.

Baxter, I., Muthukumar, B., Park, H.C., Buchner, P., Lahner, B., Danku, J., Zhao, K., Lee, J., Hawkesford, M.J., Guerinot, M.L., and Salt, D.E. (2008). Variation in molybdenum content across broadly distributed populations of Arabidopsis thaliana is controlled by a mitochondrial molybdenum transporter (MOT1). PLoS Genet **4,** e1000004.

Baylis, A.D. (2000). Why glyphosate is a global herbicide: strengths, weaknesses and prospects. Pest Management Science **56,** 299-308.

Belafi-Bako, K., M. Eszterle, M., Kiss, K., Nemestothy, N. and Gubicza, L. (2007). Hydrolysis of pectin by Aspergillus niger polygalacturonase in a membrane bioreactor. Journal of Food Engineering **78,** 438-442.

Bentsink, L., Yuan, K., Koornneef, M., and Vreugdenhil, D. (2003). The genetics of phytate and phosphate accumulation in seeds and leaves of Arabidopsis thaliana, using natural variation. Theor Appl Genet **106,** 1234-1243.

Berger, R.K., and Reid, P.D. (1979). Role of polygalacturonase in bean leaf abscission. Plant Physiol **63,** 1133-1137.

Berry, P. (2006). A physiological analysis of oilseed rape yields: past and future. The Journal of Agricultural Science **44,** 381-392

Bertin, I., Zhu, J.H., and Gale, M.D. (2005). SSCP-SNP in pearl millet--a new marker system for comparative genetics. Theor Appl Genet **110,** 1467-1472.

Besada, A., Tadros, N. B., Gawargious, Y. A. (1989). Copper(II)-neocuproine as colour reagent for some biologically active thiols: Spectrophotometric determination of cysteine, penicillamine, glutathione, and 6-mercaptopurine Microchimica Acta **99,** 143-146.

Bhattramakki, D., Dolan, M., Hanafey, M., Wineland, R., Vaske, D., Register, J.C., 3rd, Tingey, S.V., and Rafalski, A. (2002). Insertion-deletion polymorphisms in 3' regions of maize genes occur frequently and can be used as highly informative genetic markers. Plant Mol Biol **48,** 539-547.

Botstein, D., White, R.L., Skolnick, M., and Davis, R.W. (1980). Construction of a genetic linkage map in man using restriction fragment length polymorphisms. Am J Hum Genet **32,** 314-331.

Bowman, J.G. (1984). Commercial oilseed rape breeding. Aspects of Applied Biology **6,** 31-36.

Bradford, M.M. (1976). A rapid and sensitive method for the quantitation of microgram quantities of protein utilizing the principle of protein-dye binding. Anal Biochem **72,** 248-254.

Brookes, A.J. (1999). The essence of SNPs. Gene **234,** 177-186.

Bruce, D.M., Hobson, R. N. (1995). Rapeseed today and tomorrow. In Proceedings of the Ninth International Rapeseed Congress (Cambridge: GCIRC, Paris), 342-345.

Bruce, D.M., Farrent, J.W., Morgan, C.L., and Child, R.D. (2002). Determining the oilseed rape pod strength needed to reduce seed loss due to pod shatter. Biosystems Engineering **81,** 179-184.

Buell, C. R. and Somerville, S. C. (1997). Use of *Arabidopsis* recombinant inbred lines reveals a monogenic and novel dienic resistance mechanism to *Xanthomonas campestris* pv campestris. Plant Journal **12**, 21-29

Bundock, P.C., Cross, M.J., Shapter, F.M., and Henry, R.J. (2006). Robust allele-specific polymerase chain reaction markers developed for single nucleotide polymorphisms in expressed barley sequences. Theor Appl Genet **112,** 358-365.

Burgess, P.J., Morris, J. (2009). Agricultural technology and land use futures: THe UK case. Land Use Policy **26S,** S222-S229.

Burns, M.J., Barnes, S.R., Bowman, J.G., Clarke, M.H., Werner, C.P., and Kearsey, M.J. (2003). QTL analysis of an intervarietal set of substitution lines in Brassica napus: (i) Seed oil content and fatty acid composition. Heredity **90,** 39-48.

Chandler, J., Corbesier, L., Spielmann, P., Dettendorfer, J., Stahl, D., Apel, K., and Melzer, S. (2005). Modulating flowering time and prevention of pod shatter in oilseed rape. Molecular Breeding **15,** 87-94.

Chauvaux, N., Child, R., John, K., Ulvskov, P., Borkhardt, B., Prinsen, E., and VanOnckelen, H.A. (1997). The role of auxin in cell separation in the dehiscence zone of oilseed rape pods. Journal of Experimental Botany **48,** 1423-1429.

Cheema, J., Ellis, T.H., and Dicks, J. (2010). THREaD Mapper Studio: a novel, visual web server for the estimation of genetic linkage maps. Nucleic Acids Res **38,** W188-193.

Chen, W., Zhang, Y., Liu, X., Chen, B., Tu, J., and Tingdong, F. (2007). Detection of QTL for six yield-related traits in oilseed rape (Brassica napus) using DH and immortalized F(2) populations. Theor Appl Genet **115,** 849-858

Child, R.D., Summers, J.E., Babij, J., Farrent, J.W., and Bruce, D.M. (2003). Increased resistance to pod shatter is associated with changes in the vascular structure in pods of a resynthesized Brassica napus line. Journal of Experimental Botany **54,** 1919-1930.

Christiansen, L.C., Dal Degan, F., Ulvskov, P., and Borkhardt, B. (2002). Examination of the dehiscence zone in soybean pods and isolation of a dehiscence-related endopolygalacturonase gene. Plant Cell and Environment **25,** 479-490.

Churchill, G.A., and Doerge, R.W. (1994). Empirical threshold values for quantitative trait mapping. Genetics **138,** 963-971.

Clarke, M., Mithen, R., Brown, J. K. and Dean, C. (1995) QTL analysis of flowering time in *Arabidopsis thaliana.* Molecular and General Genetics, **248,** 3, 278-286.

Collard, B.C.Y., Jahufer, M.Z.Z., Brouwer, J.B., and Pang, E.C.K. (2005). An introduction to markers, quantitative trait loci (QTL) mapping and marker-assisted selection for crop improvement: The basic concepts. Euphytica **142,** 169-196.

Cook, S.K. (2010). Glyphosate - A necessary herbicide. Outlooks on Pest Management **21,** 280-284.

Davies, G.C., and Bruce, D.M. (1997). Fracture mechanics of oilseed rape pods. Journal of Materials Science **32,** 5895-5899.

Degan, F.D., Child, R., Svendsen, I., and Ulvskov, P. (2001). The cleavable N-terminal domain of plant endopolygalacturonases from clade B may be involved in a regulated secretion mechanism. J Biol Chem **276,** 35297-35304.

Delourme, R., Pilet-Nayel, M.L., Archipiano, M., Horvais, R., Tanguy, X., Rouxel, T., Brun, H., Renard, M., and Balesdent, M.H. (2004). A Cluster of Major Specific Resistance Genes to Leptosphaeria maculans in Brassica napus. Phytopathology **94,** 578-583.

Diepenbrock, W. (2000). Yield analysis of winter oilseed rape (*Brassica napus* L.):a review. Field Crops Research **67,** 35-49.

Ding, G., Yang, M., Hu, Y., Liao, Y., Shi, L., Xu, F., and Meng, J. (2010). Quantitative trait loci affecting seed mineral concentrations in Brassica napus grown with contrasting phosphorus supplies. Ann Bot **105,** 1221-1234.

Dinneny, J.R., and Yanofsky, M.F. (2005). Drawing lines and borders: how the dehiscent fruit of Arabidopsis is patterned. Bioessays **27,** 42-49.

Dinneny, J.R., Weigel, D., and Yanofsky, M.F. (2005). A genetic framework for fruit patterning in Arabidopsis thaliana. Development **132,** 4687-4696.

Doerge, R.W., and Churchill, G.A. (1996). Permutation tests for multiple loci affecting a quantitative character. Genetics **142,** 285-294.

Don, R.H., Cox, P.T., Wainwright, B.J., Baker, K., and Mattick, J.S. (1991). 'Touchdown' PCR to circumvent spurious priming during gene amplification. Nucleic Acids Res **19,** 4008.

Downey, R.K., Robbelen, G. (1989). *Brassica* species. In *Oils Crops of the World*, G. Robbelen, Downey, R. K. and Ashri, A., ed (New York: McGraw-Hill), 339-362.

Doyle, J.J. and Doyle, J. L. (1987). A rapid DNA isolation procedure for small quantities of fresh leaf tissue. Phytochem Bull **19,** 11-15.

Dygert, S., Li, L.H., Florida, D., and Thoma, J.A. (1965). Determination of reducing sugar with improved precision. Anal Biochem **13,** 367-374.

Ferrandiz, C., Pelaz, S., and Yanofsky, M.F. (1999). Control of carpel and fruit development in arabidopsis. Annual Review of Biochemistry **68,** 321-354.

Ferrandiz, C., Liljegren, S.J., and Yanofsky, M.F. (2000). Negative regulation of the SHATTERPROOF genes by FRUITFULL during Arabidopsis fruit development. Science **289,** 436-438.

Finlayson, A.J., Krzymanski, J., and Downey, R.K. (1973). Comparison of chemical and agronomic characteristics of two Brassica napus L. cultivars, Bronowski and Target. J Am Oil Chem Soc **50,** 407-410.

Fu, F.Y., Liu, L.Z., Chai, Y.R., Chen, L., Yang, T., Jin, M.Y., Ma, A.F., Yan, X.Y., Zhang, Z.S., and Li, J.N. (2007). Localization of QTLs for seed color using recombinant inbred lines of Brassica napus in different environments. Genome **50,** 840-854.

Gale, M.D., Youssefsen, S. (1985). Dwarfing genes in wheat. In Progress in Plant Breeding, G.E. Russel, ed (London: Butterworths), . 1-35.

Gale, M.D., and Devos, K.M. (1998 a). Plant comparative genetics after 10 years. Science **282,** 656-659.

Gale, M.D., and Devos, K.M. (1998 b). Comparative genetics in the grasses. Proc Natl Acad Sci U S A **95,** 1971-1974.

Gelderman, H. (1975). Investigation on inheritance of quantitative characters in animals by gene markers. I. Methods. Theoretical and Applied Genetics **46,** 300–319.

Giordano, M., Oefner, P.J., Underhill, P.A., Cavalli Sforza, L.L., Tosi, R., and Richiardi, P.M. (1999). Identification by denaturing high-performance liquid chromatography of numerous polymorphisms in a candidate region for multiple sclerosis susceptibility. Genomics **56,** 247-253.

Girin, T., Stephenson, P., Goldsack, C.M., Kempin, S.A., Perez, A., Pires, N., Sparrow, P.A., Wood, T.A., Yanofsky, M.F., and Ostergaard, L. (2010). Brassicaceae INDEHISCENT genes specify valve margin cell fate and repress replum formation. Plant J **63,** 329-338.

Gunstone, F.D. (2001). Production and consumption of rapeseed oil on a global scale. European Journal of Lipid Science and Technology **103,** 447-449.

Gupta, P.K., Roy, J. K., Prasad, M. (1999). DNA chips, microarrays and genomics. Current Science **77,** 875-884.

Gupta, P.K., and Varshney, R.K. (2000). The development and use of microsatellite markers for genetic analysis and plant breeding with emphasis on bread wheat. Euphytica **113,** 163-185.

Gupta, P.K., Roy, J.K., and Prasad, M. (2001). Single nucleotide polymorphisms: A new paradigm for molecular marker technology and DNA polymorphism detection with emphasis on their use in plants. Current Science **80,** 524-535.

Hackett, C.A. (2002). Statistical methods for QTL mapping in cereals. Plant Mol Biol **48,** 585-599.

Haley, C., Andersson, L. (1997). Linkage mapping of quantitative trait loci in plants and animals. In Genome mapping–A practical approach, P. Dear, ed (New York: Oxford University Press), 49–71.

Hayashi, K. (1991). PCR-SSCP: a simple and sensitive method for detection of mutations in the genomic DNA. PCR Methods Appl **1,** 34-38.

Heresbach, K. (1570). *Rei rustica libri quator*. (Cologne). Translated: Marham, G., 1631, London

Hu, J., Li, G., Struss, D., Quiros, C. F. (1999). SCAR and RAPD markers associated with 18-carbon fatty acids in rapeseed. Plant Breeding **118,** 145-150.

Hyne. V., K., M. J., Pike, D. J., Snape, J. W. (1995). QTL analysis: unreliability and bias in estimation procedure. Molecular Breeding **1,** 273-282.

Iniguez-Luy, F.L., Voort, A.V., and Osborn, T.C. (2008). Development of a set of public SSR markers derived from genomic sequence of a rapid cycling Brassica oleracea L. genotype. Theor Appl Genet **117,** 977-985.

Iniguez-Luy, F.L., Lukens, L., Farnham, M.W., Amasino, R.M., and Osborn, T.C. (2009). Development of public immortal mapping populations, molecular markers and linkage maps for rapid cycling Brassica rapa and B. oleracea. Theor Appl Genet **120,** 31-43.

Inoue, H., Nishio, T. (2004). Efficiency of PCR-RF-SSCP marker production in Brassica oleracea using Brassica EST sequences Euphytica **137,** 233-242.

Jaccoud, D., Peng, K., Feinstein, D., and Kilian, A. (2001). Diversity arrays: a solid state technology for sequence information independent genotyping. Nucleic Acids Res **29,** E25.

Jansen, R.C. (1993). Interval mapping of multiple quantitative trait loci. Genetics **135,** 205-211.

Jansen, R.C. (2003). Quantitative trait loci in inbred lines. In Handbook of Statistical Genetics, D.J. Balding, Bishop, M. and Cannings, C., ed (Chichester: John Wiley & Sons), 589-622

Jenkins, E.S., Paul, W., Craze, M., Whitelaw, C.A., Weigand, A., and Roberts, J.A. (1999). Dehiscence-related expression of an Arabidopsis thaliana gene encoding a polygalacturonase in transgenic plants of Brassica napus. Plant Cell and Environment **22,** 159-167.

Jukes, T.H. (1987). Transitions, transversions, and the molecular evolutionary clock. J Mol Evol **26,** 87-98.

Kadkol, G.P., Macmillan, R.H., Burrow, R.P., and Halloran, G.M. (1984). Evaluation of Brassica Genotypes for Resistance to Shatter .1. Development of a Laboratory Test. Euphytica **33,** 63-73.

Kaul, S., Koo, H.L., Jenkins, J., Rizzo, M., Rooney, T., Tallon, L.J., Feldblyum, T., Nierman, W., Benito, M.I., Lin, X.Y., Town, C.D., Venter, J.C., Fraser, C.M., Tabata, S., Nakamura, Y., Kaneko, T., Sato, S., Asamizu, E., Kato, T., Kotani, H., Sasamoto, S., Ecker, J.R., Theologis, A., Federspiel, N.A., Palm, C.J., Osborne, B.I., Shinn, P., Conway, A.B., Vysotskaia, V.S., Dewar, K., Conn, L., Lenz, C.A., Kim, C.J., Hansen, N.F., Liu, S.X., Buehler, E., Altafi, H., Sakano, H., Dunn, P., Lam, B., Pham, P.K., Chao, Q., Nguyen, M., Yu, G.X., Chen, H.M., Southwick, A., Lee, J.M., Miranda, M., Toriumi, M.J., Davis, R.W., Wambutt, R., Murphy, G., Dusterhoft, A., Stiekema, W., Pohl, T., Entian, K.D., Terryn, N., Volckaert, G., Salanoubat, M., Choisne, N., Rieger, M., Ansorge, W., Unseld, M., Fartmann, B., Valle, G., Artiguenave, F., Weissenbach, J., Quetier, F., Wilson, R.K., de la Bastide, M., Sekhon, M., Huang, E., Spiegel, L., Gnoj, L., Pepin, K., Murray, J., Johnson, D., Habermann, K., Dedhia, N., Parnell, L., Preston, R., Hillier, L., Chen, E., Marra, M., Martienssen, R., McCombie, W.R., Mayer, K., White, O., Bevan, M., Lemcke, K., Creasy, T.H., Bielke, C., Haas, B., Haase, D., Maiti, R., Rudd, S., Peterson, J., Schoof, H., Frishman, D., Morgenstern, B., Zaccaria, P., Ermolaeva, M., Pertea, M., Quackenbush, J., Volfovsky, N., Wu, D.Y., Lowe, T.M., Salzberg, S.L., Mewes, H.W., Rounsley, S., Bush, D., Subramaniam, S., Levin, I., Norris, S., Schmidt, R., Acarkan, A., Bancroft, I., Quetier, F., Brennicke, A., Eisen, J.A., Bureau, T., Legault, B.A., Le, Q.H., Agrawal, N., Yu, Z., Martienssen, R., Copenhaver, G.P., Luo, S., Pikaard, C.S., Preuss, D., Paulsen, I.T., Sussman, M., Britt, A.B., Selinger, D.A., Pandey, R., Mount, D.W., Chandler, V.L., Jorgensen, R.A., Pikaard, C., Juergens, G., Meyerowitz, E.M., Theologis, A., Dangl, J., Jones, J.D.G., Chen, M., Chory, J., Somerville, M.C., and In, A.G. (2000). Analysis of the genome sequence of the flowering plant Arabidopsis thaliana. Nature **408,** 796-815.

Kearsey, M.J., Hyne, V. (1994). QTL analysis: a simple 'marker regression' approach. Theoretical and Applied Genetics **89,** 698-702.

Kearsey, M.J., Pooni, H. S. (1996). The Genetical Analysis of Quantitative Traits. (London: Chapman and Hall).

Kimber, D.S., McGregor, D. I. (1995). Brassica Oilseeds. (Warwick: CAB INTERNATIONAL).

Kirk, J.T.O., Hurlstone, C. J. (1983). Varaition and inheritance of erucic acid content in *Brassica juncea*. Z. Pflanzenzüchtg **90,** 331-338.

Kliebenstein, D.J., Kroymann, J., Brown, P., Figuth, A., Pedersen, D., Gershenzon, J., and Mitchell-Olds, T. (2001). Genetic control of natural variation in Arabidopsis glucosinolate accumulation. Plant Physiol **126,** 811-825.

Koch, M.A., Haubold, B., and Mitchell-Olds, T. (2000). Comparative evolutionary analysis of chalcone synthase and alcohol dehydrogenase loci in Arabidopsis, Arabis, and related genera (Brassicaceae). Mol Biol Evol **17,** 1483-1498.

Konieczny, A., and Ausubel, F.M. (1993). A procedure for mapping Arabidopsis mutations using co-dominant ecotype-specific PCR-based markers. Plant J **4,** 403-410.

Konishi, S., Izawa, T., Lin, S.Y., Ebana, K., Fukuta, Y., Sasaki, T., and Yano, M. (2006). An SNP caused loss of seed shattering during rice domestication. Science **312,** 1392-1396.

Koornneef, M., Alonso-Blanco, C., and Vreugdenhil, D. (2004). Naturally occurring genetic variation in Arabidopsis thaliana. Annual Review of Plant Biology **55,** 141-172.

Lagercrantz, U., Putterill, J., Coupland, G., and Lydiate, D. (1996). Comparative mapping in Arabidopsis and Brassica, fine scale genome collinearity and congruence of genes controlling flowering time. Plant Journal **9,** 13-20.

Lagercrantz, U., and Lydiate, D.J. (1996). Comparative genome mapping in Brassica. Genetics **144,** 1903-1910.

Lagercrantz, U. (1998). Comparative mapping between Arabidopsis thaliana and Brassica nigra indicates that Brassica genomes have evolved through extensive genome replication accompanied by chromosome fusions and frequent rearrangements. Genetics **150,** 1217-1228.

Lander, M.J. (1976). Variations in natural populations of *Arabidopsis thaliana* (L.) Heynh. . In The Biology and Chemistry of the *Cruciferae*, J.G.a.M. Vaughan, A. J., ed (LOndon/New York/San Francisco: BMG Jones), . 167-190.

Lander, E., Abrahamson, J., Barlow, A., Daly, M., Lincoln, S., Newburg, L., and Green, P. (1987). Mapmaker a Computer Package for Constructing Genetic-Linkage Maps. Cytogenetics and Cell Genetics **46,** 642-642.

Lander, E.S., and Botstein, D. (1989). Mapping mendelian factors underlying quantitative traits using RFLP linkage maps. Genetics **121,** 185-199.

Laudert, D., and Weiler, E.W. (1998). Allene oxide synthase: a major control point in Arabidopsis thaliana octadecanoid signalling. Plant J **15,** 675-684.

Lazaro, A., Aguinagalde, I. (1998). Genetic Diversity in Brassica oleracea L. (Cruciferae) and Wild Relatives (2n=18) using RAPD Markers. Annals of Botany **82,** 829-833.

Lemieux, B. (2000). High Throughput Single Nucleotide Polymorphism Genotyping Technology Current Genomics **1,** 301-311.

Levison, G., Gutman, G. A. (1987). Slipped-strand mispairing: a major mechanism for DNA sequence evolution. Molecular Biology and Evolution **4,** 203-221.

Li, G., Quiros, C. F. (2001). Sequence- Related Amplified Polymorphism (SRAP), a new marker system based on a simple PCR reaction: Its application to mapping and gene tagging in Brassica. Theoretical and Applied Genetics **103,** 455-461.

Li, G., Gao, M., Yang, B., and Quiros, C.F. (2003). Gene for gene alignment between the Brassica and Arabidopsis genomes by direct transcriptome mapping. Theor Appl Genet **107,** 168-180.

Li, C.B., Zhou, A.L., and Sang, T. (2006). Rice domestication by reducing shattering. Science **311,** 1936-1939.

Liljegren, S.J., Ditta, G.S., Eshed, H.Y., Savidge, B., Bowman, J.L., and Yanofsky, M.F. (2000). SHATTERPROOF MADS-box genes control seed dispersal in Arabidopsis. Nature **404,** 766-770.

Liljegren, S.J., Roeder, A.H.K., Kempin, S.A., Gremski, K., Ostergaard, L., Guimil, S., Reyes, D.K., and Yanofsky, M.F. (2004). Control of fruit patterning in Arabidopsis by INDEHISCENT. Cell **116,** 843-853.

Lin, Z., Griffith, M.E., Li, X., Zhu, Z., Tan, L., Fu, Y., Zhang, W., Wang, X., Xie, D., and Sun, C. (2007). Origin of seed shattering in rice (Oryza sativa L.). Planta **226,** 11-20.

Lister, C., and Dean, C. (1993). Recombinant Inbred Lines for Mapping Rflp and Phenotypic Markers in Arabidopsis-Thaliana. Plant Journal **4,** 745-750.

Livak, K.J., Flood, S.J., Marmaro, J., Giusti, W., and Deetz, K. (1995). Oligonucleotides with fluorescent dyes at opposite ends provide a quenched probe system useful for detecting PCR product and nucleic acid hybridization. PCR Methods Appl **4,** 357-362.

Long, Y., Shi, J., Qiu, D., Li, R., Zhang, C., Wang, J., Hou, J., Zhao, J., Shi, L., Park, B.S., Choi, S.R., Lim, Y.P., and Meng, J. (2007). Flowering time quantitative trait Loci analysis of oilseed brassica in multiple environments and genomewide alignment with Arabidopsis. Genetics **177,** 2433-2444.

Lööf, B. (1972). Cultivation of Rapeseed. (Elsevier publishing).

Loudet, O., Saliba-Colombani, V., Camilleri, C., Calenge, F., Gaudon, V., Koprivova, A., North, K.A., Kopriva, S., and Daniel-Vedele, F. (2007). Natural variation for sulfate content in Arabidopsis thaliana is highly controlled by APR2. Nat Genet **39,** 896-900.

Lowe, A.J., Jones, A.E., Raybould, A.F., Trick, M., Moule, C.L., and Edwards, K.J. (2002). Transferability and genome specificity of a new set of microsatellite primers among Brassica species of the U triangle. Molecular Ecology Notes **2,** 7-11.

Lowe, A.J., Moule, C., Trick, M., and Edwards, K.J. (2004). Efficient large-scale development of microsatellites for marker and mapping applications in Brassica crop species. Theoretical and Applied Genetics **108,** 1103-1112.

Lowe A. J., M., C., Trick, M., Edwards, K.J. . (2003). Efficient large-scale development of microsatellites for marker and mapping applications in Brassica crop species. Theoretical and Applied Genetics.

Lysak, M.A., Koch, M.A., Pecinka, A., and Schubert, I. (2005). Chromosome triplication found across the tribe Brassiceae. Genome Res **15,** 516-525.

Macleod, J. (1981). Harvesting in oilseed rape. (Cambrigde: Cambrigde Agricultural publishing).

Mahmood, T., Ekuere, U., Yeh, F., Good, A.G., and Stringam, G.R. (2003). RFLP linkage analysis and mapping genes controlling the fatty acid profile of Brassica juncea using reciprocal DH populations. Theor Appl Genet **107,** 283-290.

McKay, J.K., Richards, J.H., Nemali, K.S., Sen, S., Mitchell-Olds, T., Boles, S., Stahl, E.A., Wayne, T., and Juenger, T.E. (2008). Genetics of drought adaptation in Arabidopsis thaliana II. QTL analysis of a new mapping population, KAS-1 x TSU-1. Evolution **62,** 3014-3026.

Meakin, P.J., and Roberts, J.A. (1990 a). Dehiscence of Fruit in Oilseed Rape (Brassica-Napus L) .1. Anatomy of Pod Dehiscence. Journal of Experimental Botany **41,** 995-1002.

Meakin, P.J., and Roberts, J.A. (1990 b). Dehiscence of Fruit in Oilseed Rape (Brassica-Napus L) .2. The Role of Cell-Wall Degrading Enzymes and Ethylene. Journal of Experimental Botany **41,** 1003-1011.

Mendham, N.J., Salisbury, P. A. (1995). Physiology: Crop Development, Growth and Yield. In Brassica Oilseeds: Production and Utilisation, D.S. Kimber, McGregor, D. I., ed (Warwick: CAB INTERNATIONAL), . 11-64.

Miles, C., Wayne, M. . (2008). Quantitative Trait Locus (QTL) Analysis. In Nature Education 1(1), . http://www.nature.com/scitable/topicpage/Quantitative-Trait-Locus-QTL-Analysis-53904.

Mollers, C., Iqbal, M.C.M., Robblen, G. (1994). Efficeint production of doubled haploid Brassica napus plants by colchicine treatment of microspores. Euphytica **75,** 95-104.

Moore, I., Gälweiler, L., Grosskopf, D., Schell, J., and Palme, K. (1998). A transcription activation system for regulated gene expression in transgenic plants. *Proc Natl Acad Sci* **95,** 376-381

Morgan, C.L., Bruce, D.M., Child, R., Ladbrooke, Z.L., and Arthur, A.E. (1998). Genetic variation for pod shatter resistance among lines of oilseed rape developed from synthetic B-Napus. Field Crops Research **58,** 153-165.

Morgan, C.L., Ladbrooke, Z.L., Bruce, D.M., Child, R., and Arthur, A.E. (2000). Breeding oilseed rape for pod shattering resistance. Journal of Agricultural Science **135,** 347-359.

Morgan, C., Bavage, A., Bancroft, I., Bruce, D., Child, R., Chinoy, C., Summers, J. and Arthur, E. (2003). Using novel variation in Brassica species to reduce agricultural inputs and improve agronomy of oilseed rape - a case study in pod shatter resistance. Plant Genetic Resources **1,** 59-65.

Moriguchi, K., Kimizuka, T., Ishi, I and Nomura, K. (1999). A Genetic Map Based on RAPD, RFLP, Isozyme, Morphological Markers and QTL Analysis for Clubroot Resistance in Brassica oleracea. Breeding Science **49,** 257-265.

Mullis, K.B., and Faloona, F.A. (1987). Specific synthesis of DNA in vitro via a polymerase-catalyzed chain reaction. Methods Enzymol **155,** 335-350.

Ogawa, M., Kay, P., Wilson, S., and Swain, S.M. (2009). ARABIDOPSIS DEHISCENCE ZONE POLYGALACTURONASE1 (ADPG1), ADPG2, and QUARTET2 are Polygalacturonases required for cell separation during reproductive development in Arabidopsis. Plant Cell **21,** 216-233.

Okazaki, K., Sakamoto, K., Kikuchi, R., Saito, A., Togashi, E., Kuginuki, Y., Matsumoto, S., and Hirai, M. (2007). Mapping and characterization of FLC homologs and QTL analysis of flowering time in Brassica oleracea. Theor Appl Genet **114,** 595-608.

O'Neill, C.M., and Bancroft, I. (2000). Comparative physical mapping of segments of the genome of Brassica oleracea var. alboglabra that are homoeologous to sequenced regions of chromosomes 4 and 5 of Arabidopsis thaliana. Plant J **23,** 233-243.

O'Neill, C.M., Morgan, C., Kirby, J., Tschoep, H., Deng, P.X., Brennan, M., Rosas, U., Fraser, F., Hall, C., Gill, S., and Bancroft, I. (2008). Six new recombinant inbred populations for the study of quantitative traits in Arabidopsis thaliana. Theor Appl Genet **116,** 623-634.

Ostergaard, L., and Yanofsky, M.F. (2004). Establishing gene function by mutagenesis in Arabidopsis thaliana. Plant Journal **39,** 682-696.

Ostergaard, L., Kempin, S.A., Bies, D., Klee, H.J., and Yanofsky, M.F. (2006). Pod shatter-resistant Brassica fruit produced by ectopic expression of the FRUITFULL gene. Plant Biotechnology Journal **4,** 45-51.

Ostergaard, L., Borkhardt, B. and Ulvskov, P. (2007). Dehiscence. In Plant Cell Separation and Adhesion, J.A.a.G.-C. Roberts, Z., ed (Oxford: Blackwell Publishing.

Parkin, I.A., Sharpe, A.G., Keith, D.J., and Lydiate, D.J. (1995). Identification of the A and C genomes of amphidiploid Brassica napus (oilseed rape). Genome **38,** 1122-1131.

Parkin, I.A.P., Lydiate, D.J., and Trick, M. (2002). Assessing the level of collinearity between Arabidopsis thaliana and Brassica napus for A-thaliana chromosome 5. Genome **45,** 356-366.

Parkin, I.A., Sharpe, A.G., and Lydiate, D.J. (2003). Patterns of genome duplication within the Brassica napus genome. Genome **46,** 291-303.

Parkin, I.A.P., Gulden, S.M., Sharpe, A.G., Lukens, L., Trick, M., Osborn, T.C., and Lydiate, D.J. (2005). Segmental structure of the Brassica napus genome based on comparative analysis with Arabidopsis thaliana. Genetics **171,** 765-781.

Paterson, A.H. (1996). Making genetic maps. In Genome Mapping in Plants, A.H. Paterson, ed (Sandiego, California: R. G. Landes Company; Academic Press; Austin Texas.

Payne, R.W., Murray, D.A., Harding, S.A., Baird, D.B. & Soutar, D.M. (2009). GenStat for Windows (12th Edition) (VSN International, Hemel Hempstead).

Pease, A.C., Solas, D., Sullivan, E.J., Cronin, M.T., Holmes, C.P., and Fodor, S.P. (1994). Light-generated oligonucleotide arrays for rapid DNA sequence analysis. Proc Natl Acad Sci U S A **91,** 5022-5026.

Petersen, M., Sander, L., Child, R., vanOnckelen, H., Ulvskov, P., and Borkhardt, B. (1996). Isolation and characterisation of a pod dehiscence zone-specific polygalacturonase from Brassica napus. Plant Molecular Biology **31,** 517-527.

Pflieger, S., Lefebvre, V., and Causse, M. (2001). The candidate gene approach in plant genetics: a review. Molecular Breeding **7,** 275-291.

Pigliucci, M., Whitton, J. and Schlicting, C. D. (1995). Reaction norms of Arabidopsis. I. Plasticity of charactersand correlations across water, nutrient and light gradients. Journal of Evolutionary Biology **8,** 421-438.

Pigliucci, M., Schlichting, C. D. (1996). Reaction norms of Arabidopsis IV. Relationships between plasticity and fitness. Heredity **76 (Pt 5),** 427-436.

Pigliucci, M. (1998). Ecological and evolutionary genetics of Arabidopsis. Trends in Plant Science **3,** 458-489.

Pigliucci, M., Schlichting, C. D. (1998). Reaction norms of Arabidopsis. V. Flowering time controls phenotypic architecture in response to nutrient stress. Journal of Evolutionary Biology **11,** 285-301.

Piquemal, J., Cinquin, E., Couton, F., Rondeau, C., Seignoret, E., Doucet, I., Perret, D., Villeger, M.J., Vincourt, P., and Blanchard, P. (2005). Construction of an oilseed rape (Brassica

napus L.) genetic map with SSR markers. Theoretical and Applied Genetics **111,** 1514-1523.

Powell, W., Morgante, M., Andre, C., Hanafey, M., Vogel, J., Tingey, S. and Rafalski, A. (1996). The comparison of RFLP, RAPD, AFLP and SSR (microsatellite) markers for germplasm analysis Molecular Breeding **2,** 225-238.

Pradhan, A.K., Gupta, V., Mukhopadhyay, A., Arumugam, N., Sodhi, Y.S., and Pental, D. (2003). A high-density linkage map in Brassica juncea (Indian mustard) using AFLP and RFLP markers. Theoretical and Applied Genetics **106,** 607-614.

Prakash, S., Chopra, V. L. (1988). Introgression of resistance to shattering in *Brassic napus* from *brassica napus* throughnon-homoelogous recombination. Plant Breeding **101,** 167-168.

Prakash, S., Chopra, V. L. (1990). Reconstruciton of allopolyploid Brassicas through non-homeologous recombination: introgression of resistance to pod shatter in *Brassica napus*. Genetics Research **56,** 1-2.

Pressey, R. (1986). Extraction and assay of tomato polygalacturonases. Hort Science **21,** 490-492.

Price, J.S., Hobson, R.N., Neale, M.A., and Bruce, D.M. (1996). Seed losses in commercial harvesting of oilseed rape. Journal of Agricultural Engineering Research **65,** 183-191.

Qiu, D., Morgan, C., Shi, J., Long, Y., Liu, J., Li, R., Zhuang, X., Wang, Y., Tan, X., Dietrich, E., Weihmann, T., Everett, C., Vanstraelen, S., Beckett, P., Fraser, F., Trick, M., Barnes, S., Wilmer, J., Schmidt, R., Li, J., Li, D., Meng, J., and Bancroft, I. (2006). A comparative linkage map of oilseed rape and its use for QTL analysis of seed oil and erucic acid content. Theoretical and Applied Genetics **114,** 67-80.

Quijada, P.A., Udall, J.A., Lambert, B., and Osborn, T.C. (2006). Quantitative trait analysis of seed yield and other complex traits in hybrid spring rapeseed (Brassica napus L.): 1. Identification of genomic regions from winter germplasm. Theor Appl Genet **113,** 549-561.

Radoev, M., Becker, H.C., and Ecke, W. (2008). Genetic analysis of heterosis for yield and yield components in rapeseed (Brassica napus L.) by quantitative trait locus mapping. Genetics **179,** 1547-1558.

Rajani, S., and Sundaresan, V. (2001). The Arabidopsis myc/bHLH gene ALCATRAZ enables cell separation in fruit dehiscence. Current Biology **11,** 1914-1922.

Rana, D., van den Boogaart, T., O'Neill, C.M., Hynes, L., Bent, E., Macpherson, L., Park, J.Y., Lim, Y.P., and Bancroft, I. (2004). Conservation of the microstructure of genome segments in Brassica napus and its diploid relatives. Plant J **40,** 725-733.

Riaz, A., Li, G., Quresh, Z., Swati, M. and Quiros, C. F. (2001). Genetic diversity of oilseed Brassica napus inbred lines based on sequence-related amplified polymorphism and its relation to hybrid performance. Plant Breeding **120,** 1-5.

Roeder, A.H.K., Ferrandiz, C., and Yanofsky, M.F. (2003). The role of the REPLUMLESS homeodomain protein in Patterning the Arabidopsis fruit. Current Biology **13,** 1630-1635.

Ronaghi, M. (2001). Pyrosequencing sheds light on DNA sequencing. Genome Res **11,** 3-11.

Sachidanandam, R., Weissman, D., Schmidt, S.C., Kakol, J.M., Stein, L.D., Marth, G., Sherry, S., Mullikin, J.C., Mortimore, B.J., Willey, D.L., Hunt, S.E., Cole, C.G., Coggill, P.C., Rice, C.M., Ning, Z., Rogers, J., Bentley, D.R., Kwok, P.Y., Mardis, E.R., Yeh, R.T., Schultz, B.,

Cook, L., Davenport, R., Dante, M., Fulton, L., Hillier, L., Waterston, R.H., McPherson, J.D., Gilman, B., Schaffner, S., Van Etten, W.J., Reich, D., Higgins, J., Daly, M.J., Blumenstiel, B., Baldwin, J., Stange-Thomann, N., Zody, M.C., Linton, L., Lander, E.S., and Altshuler, D. (2001). A map of human genome sequence variation containing 1.42 million single nucleotide polymorphisms. Nature **409,** 928-933.

Sander, L., Borkhardt, B., and Ulvskov, P. (1997). Characterization of beta-glucanases from pods of oilseed rape. Plant Physiology **114,** 333-333.

Sander, L., Child, R., Ulvskov, P., Albrechtsen, M., and Borkhardt, B. (2001). Analysis of a dehiscence zone endo-polygalacturonase in oilseed rape (Brassica napus) and Arabidopsis thaliana: evidence for roles in cell separation in dehiscence and abscission zones, and in stylar tissues during pollen tube growth. Plant Molecular Biology **46,** 469-479.

Sanger, F., Nicklen, S., and Coulson, A.R. (1977). DNA sequencing with chain-terminating inhibitors. Proc Natl Acad Sci U S A **74,** 5463-5467.

Sato, Y., Nishio, T. (2002). Efficient detection of DNA polymorphism in cabbage and rice cultivars by PCR-RF-SSCP (PRS) Plant Cell Reports **21,** 276-281.

Schmidt, R., Acarkan, A., and Boivin, K. (2001). Comparative structural genomics in the Brassicaceae family. Plant Physiology and Biochemistry **39,** 253-262.

Schranz, M.E., Song, B.H., Windsor, A.J., and Mitchell-Olds, T. (2007). Comparative genomics in the Brassicaceae: a family-wide perspective. Curr Opin Plant Biol **10,** 168-175.

Schuelke, M. (2000). An economic method for the fluorescent labeling of PCR fragments. Nature Biotechnology **18,** 233-234.

Sharpe, A.G., Parkin, I.A., Keith, D.J., and Lydiate, D.J. (1995). Frequent nonreciprocal translocations in the amphidiploid genome of oilseed rape (Brassica napus). Genome **38,** 1112-1121.

Shi, J., Li, R., Qiu, D., Jiang, C., Long, Y., Morgan, C., Bancroft, I., Zhao, J., and Meng, J. (2009). Unraveling the complex trait of crop yield with quantitative trait loci mapping in Brassica napus. Genetics **182,** 851-861.

Shindo, C., Aranzana, M.J., Lister, C., Baxter, C., Nicholls, C., Nordborg, M., and Dean, C. (2005). Role of FRIGIDA and FLOWERING LOCUS C in determining variation in flowering time of Arabidopsis. Plant Physiol **138,** 1163-1173.

Shirsat, A.H., Wieczorek, D., and Kozbial, P. (1996). A gene for Brassica napus extensin is differentially expressed on wounding. Plant Mol Biol **30,** 1291-1300.

Smooker, A.M., Wells, R., Morgan, C., Beaudoin, F., Cho, K., Fraser, F., and Bancroft, I. (2010). The identification and mapping of candidate genes and QTL involved in the fatty acid desaturation pathway in Brassica napus. Theoretical Applied Genetics.

Smyth, D.R., Bowman, J.L., and Meyerowitz, E.M. (1990). Early Flower Development in Arabidopsis. Plant Cell **2,** 755-767.

Snape, J.W., Foulkes M. J., Simmonds, J., Leverington, M., Fish, L. J., Wang, Y. and, and Ciavarrella, M. (2007). Dissecting gene 3 environmental effects on wheat yieldsvia QTL and physiological analysis. Euphytica **154,** 401-408.

Snowdon, R.J., Friedrich, T., Friedt, W., and Kohler, W. (2002). Identifying the chromosomes of the A- and C-genome diploid Brassica species B-rapa (syn. campestris) and B-oleracea in their amphidiploid B-napus. Theoretical and Applied Genetics **104,** 533-538.

Sobotka, R.D., L. Eurn, V. and Ovensa, J. (2004). Fluorescence-based AFLPs occur as the most suitable marker system for oilseed rape cultivar identification. Journal of Applied Genetics **45,** 161-173.

Somers, D.J., Friesen, K. R. D. and Rakow, G. (1998). Identification of molecular markers associated with linoleic acid desaturation in Brassica napus theoretical and Applied Genetics **96,** 897-903.

Sorefan, K., Girin, T., Liljegren, S.J., Ljung, K., Robles, P., Galvan-Ampudia, C.S., Offringa, R., Friml, J., Yanofsky, M.F., and Ostergaard, L. (2009). A regulated auxin minimum is required for seed dispersal in Arabidopsis. Nature **459,** 583-586.

Southern, E.D.M. (1996). DNA chips: analysing
sequence by hybridization
to oligonucleotides on a
large scale. Trends in Genetics **12,** 110-115.

Spence, J., Vercher, Y., Gates, P., and Harris, N. (1996). 'Pod shatter' in Arabidopsis thaliana, Brassica napus and B-juncea. Journal of Microscopy-Oxford **181,** 195-203.

Squires, T., Gruwel, M., Zhou, R., Sokhansanj, S., Abrams, S. and Cutler, J. (2003). Dehydration and dehiscence in siliques of Brassica napus and Brassica rapa. Canadian Journal of Botany **81,** 248-254.

Stam, P. (1993). Construction of Integrated Genetic-Linkage Maps by Means of a New Computer Package - Joinmap. Plant Journal **3,** 739-744.

Stefansson, B.R., Hougen, F. W. and Downey, R. K. (1961). Note on the isolation of rape plants with seed oil free from erucic acid. Canadian Journal of Plant Science **41,** 218-219.

Stefansson, B.R., Hougen, F. W. (1964). Selection of rape plants (*Brassica napus*) with seed oil practically free from erucic acid. Canadian Journal of Plant Science **44,** 359-364.

Stephenson, P., Baker, D., Girin, T., Perez, A., Amoah, S., King, G.J., and Ostergaard, L. (2010). A rich TILLING resource for studying gene function in Brassica rapa. BMC Plant Biol **10,** 62.

Steward, C.N., Via, L. E. (1993). A rapid CTAB DNA isolation technique useful for RAPD fingerprinting and other PCR applications. BioTechniques **14,** 748-751.

Summers, J.E., Bruce, D.M., Vancanneyt, G., Redig, P., Werner, C.P., Morgan, C., and Child, R.D. (2003). Pod shatter resistance in the resynthesized Brassica napus line DK142. Journal of Agricultural Science **140,** 43-52.

Sun, Z., Wang, Z., Tu, J., Zhang, J., Yu, F., McVetty, P.B., and Li, G. (2007). An ultradense genetic recombination map for Brassica napus, consisting of 13551 SRAP markers. Theor Appl Genet **114,** 1305-1317.

Suwabe, K., Iketani, H., Nunome, T., Kage, T., and Hirai, M. (2002). Isolation and characterization of microsatellites in Brassica rapa L. Theoretical and Applied Genetics **104,** 1092-1098.

Suwabe, K., Tsukazaki, H., Iketani, H., Hatakeyama, K., Fujimura, M., Nunome, T., Fukuoka, H., Matsumoto, S., and Hirai, M. (2003). Identification of two loci for resistance to clubroot (Plasmodiophora brassicae Woronin) in Brassica rapa L. Theor Appl Genet **107,** 997-1002.

Suwabe, K., Tsukazaki, H., Iketani, H., Hatakeyama, K., Kondo, M., Fujimura, M., Nunome, T., Fukuoka, H., Hirai, M., and Matsumoto, S. (2006). Simple sequence repeat-based

comparative genomics between Brassica rapa and Arabidopsis thaliana: The genetic origin of clubroot resistance. Genetics **173,** 309-319.

Tanksley, S.D., Young, N.D., Paterson, A.H., and Bonierbale, M. (1989). RFLP mapping in plant breeding: New tools for an old science. Biotechnology **7,** 257-264.

Tanksley, S.D., Ganal, M.W., Prince, J.P., de Vicente, M.C., Bonierbale, M.W., Broun, P., Fulton, T.M., Giovannoni, J.J., Grandillo, S., Martin, G.B., and et al. (1992). High density molecular linkage maps of the tomato and potato genomes. Genetics **132,** 1141-1160.

Tanksley, S.D. (1993). Mapping Polygenes. Annual Review of Genetics **27,** 205-233.

Tanksley, S.D., Grandillo, S., Fulton, T.M., Zamir, D., Eshed, Y., Petiard, V., Lopez, J., and BeckBunn, T. (1996). Advanced backcross QTL analysis in a cross between an elite processing line of tomato and its wild relative L-pimpinellifolium. Theoretical and Applied Genetics **92,** 213-224.

Tanksley, S.D., Nelson, J.C. (1996). Advanced backcross QTL analysis: a method for the simultaneous discovery and transfer of valuable QTLs from unadapted germplasm into elite breeding lines. Theoretical and Applied Genetics **92,** 191-203.

Teutonico, R.A., Osborn, T. C. . (1994). Mapping of RFLP and qualitative trait loci in Brassica rapa and comparison to the linkage maps of B. napus, B. oleracea, and Arabidopsis thaliana Theoretical and Applied Genetics **89,** 885-894.

Thormann, C.E., Ferreira, M. E., Camargo, L. E. A., Tivang, J. G. and Osborn, T. C. . (1994). Comparison of RFLP and RAPD markers to estimating genetic relationships within and among cruciferous species. Theoretical and Applied Genetics **88,** 973-980.

Thormann, C.E., Romero, J. , Mantet, J. and Osborn, T. C. (1996). Mapping loci controlling the concentrations of erucic and linolenic acids in seed oil of Brassica napus L. . Theoretical and Applied Genetics **93,** 282-286.

Tommasini, L., Batley, J., Arnold, G.M., Cooke, R.J., Donini, P., Lee, D., Law, J.R., Lowe, C., Moule, C., Trick, M., and Edwards, K.J. (2003). The development of multiplex simple sequence repeat (SSR) markers to complement distinctness, uniformity and stability testing of rape (Brassica napus L.) varieties. Theoretical and Applied Genetics **106,** 1091-1101.

Trick, M., Long, Y., Meng, J., and Bancroft, I. (2009). Single nucleotide polymorphism (SNP) discovery in the polyploid Brassica napus using Solexa transcriptome sequencing. Plant Biotechnol J **7,** 334-346.

Truelsen, T.A., Wyndaele, R. (1991). Cellulase in tobacco callus: regulation and purification. Journal of Plant Physiology **139,** 129-134.

U, N. (1935). Genome analysis in *Brassica* with special reference to the experimental formation of *B. napus* and peculiar mode of fertilization. *Japanese Journal of Botany* **7,** 389-452.

Udall, J.A., Quijada, P.A., and Osborn, T.C. (2005). Detection of chromosomal rearrangements derived from homologous recombination in four mapping populations of Brassica napus L. Genetics **169,** 967-979.

Udall, J.A., Quijada, P.A., Lambert, B., and Osborn, T.C. (2006). Quantitative trait analysis of seed yield and other complex traits in hybrid spring rapeseed (Brassica napus L.): 2. Identification of alleles from unadapted germplasm. Theor Appl Genet **113,** 597-609.

Van Ooijen, J.W., Voorrips, R. E. (2001). Joinmap version 3: software for the calculation of genetic linkage maps. Wageningen: Plant Research International.

Van Ooijen, J.W. (2004). MapQTL 5, Software for the mapping of quantitative trait loci in experimental populations, Kyazma B. V., Wageningen, Netherlands.

Van Os, H., Stam, P., Visser, R. G. F. and Van Eck, H. J. (2005). RECORD: a novel method for ordering loci on a genetic linkage map. Theoretical and Applied Genetics **112,** 30-40.

von Malek, B., van der Graaff, E., Schneitz, K. and Keller, B. (2002). The Arabidopsis male-sterile mutant dde2-2 is defective in the ALLENE OXIDE SYNTHASE gene encoding one of the key enzymes of the jasmonic acid biosynthesis pathway. Planta **216,** 187-192.

Vos, P., Hogers, R., Bleeker, M., Reijans, M., Vandelee, T., Hornes, M., Frijters, A., Pot, J., Peleman, J., Kuiper, M., and Zabeau, M. (1995). Aflp - a New Technique for DNA-Fingerprinting. Nucleic Acids Research **23,** 4407-4414.

Wang, R., Ripley, V. L. and Rakow, G. (2007). Pod shatter resistance evaluation in cultivars and breeding lines of Brassica napus, B. juncea and Sinapis alba. Plant Breeding **126,** 588-595.

Warwick, S.I., Black L.D. (1994). Evaluation of the subtribes Moricandiinae, Savignyinae, Vellinae and Zillinae (Brassicaceae, tribe Brassiceae) using chloroplast DNA restriction site variation. Canadian Journal of Botany **72,** 1692-1701.

Warwick, S.I.J., T. and Falka, K. C. (2008). AFLP-based molecular characterization of Brassica rapa and diversity in Canadian spring turnip rape cultivars. Plant Genetic Resources: Characterization and Utilization **6,** 11-21.

Weiss, E.A. (1983). Oilseed Crops. (London and New York: London Longman).

Wenzl, P., Carling, J., Kudrna, D., Jaccoud, D., Huttner, E., Kleinhofs, A., and Kilian, A. (2004). Diversity Arrays Technology (DArT) for whole-genome profiling of barley. Proc Natl Acad Sci U S A **101,** 9915-9920.

Werner, C., Morgan, C., Vancanneyt, G. and Arthur, A.E. (2003 (a)). The prevention of Pod Shatter in Oilseed Rape Introgression of pod shatter resistance into commercial breeding material: I F2 segregation. In HGCA document: SAPPIO LINK project 2198: The prevention of Pod Shatter in Oilseed Rape (HGCA).

Werner, C., Morgan, C., Vancanneyt, G. and Arthur, A.E. (2003 (b)). The prevention of Pod Shatter in Oilseed Rape - Introgression of pod shatter resistance into commercial breeding material: II Identification and analysis of undesireable traits. In HGCA document: SAPPIO LINK project 2198: The prevention of Pod Shatter in Oilseed Rape.

Werner, C., Morgan, C., Arthur, A.E. and Vancanneyt, G. . (2003 (c)). Introgression of pod shatter resistance into commercial breeding material: III Progress towards varieties. In HGCA document: SAPPIO LINK project 2198: The prevention of Pod Shatter in Oilseed Rape.

Whitehead, R., Wright, H. C. (1989). The incidence of weeds in winter oilseed rape in Great Britain. Aspects of Applied Biology **23,** 211-218.

Williams, J.G., Kubelik, A.R., Livak, K.J., Rafalski, J.A., and Tingey, S.V. (1990). DNA polymorphisms amplified by arbitrary primers are useful as genetic markers. Nucleic Acids Res **18,** 6531-6535.

Wittenberg, A.H., van der Lee, T., Cayla, C., Kilian, A., Visser, R.G., and Schouten, H.J. (2005). Validation of the high-throughput marker technology DArT using the model plant Arabidopsis thaliana. Mol Genet Genomics **274,** 30-39.

Wittkop, B., Snowdon, R. J. and Friedt, W. (2009). Status and perspectives of breeding for enhanced yield and quality of oilseed crops for Europe. Euphytica **170,** 131-140.

Wood, T. A., Stephenson, P. and Østergaard, L. (2011) Resources for Reverse Genetics Approaches in Brassica species, in: Genetics and Genomics in the Brassicaceae. Eds: Schmidt, R. and Bancroft, I. Springer

Yang, Y.W., Lai, K.N., Tai, P.Y., and Li, W.H. (1999). Rates of nucleotide substitution in angiosperm mitochondrial DNA sequences and dates of divergence between Brassica and other angiosperm lineages. J Mol Evol **48,** 597-604.

Yang, T.J., Kim, J.S., Lim, K.B., Kwon, S.J., Kim, J.A., Jin, M., Park, J.Y., Lim, M.H., Kim, H.I., Kim, S.H., Lim, Y.P., and Park, B.S. (2005). The Korea Brassica Genome Project: A glimpse of the Brassica genome based on comparative genome analysis with Arabidopsis. Comparative and Functional Genomics **6,** 138-146.

Ye, S., Humphries, S., and Green, F. (1992). Allele specific amplification by tetra-primer PCR. Nucleic Acids Res **20,** 1152.

Yin, X., Yi, B., Chen, W., Zhang, W., Tu, J., Dilantha Fernando, W. G. and Fu, T. (2010). Mapping of QTLs detected in a Brassica napus DH population for resistance to Sclerotinia sclerotiorum in multiple environments Euphytica **173,** 25-35.

Young, N.D. (1994). Constructing a plant genetic map with DNA markers. (Dordrecht/Boston/London: Kluwer).

Young, N.D. (1996). QTL mapping and quantitative disease resistance in plants. Annu Rev Phytopathol **34,** 479-501.

Young, N.D. (1999). A cautiously optimistic vision for marker-assisted breeding. Molecular Breeding **5,** 505-510.

Yu, B., Lydiate, D.J., Young, L.W., Schafer, U.A., and Hannoufa, A. (2008). Enhancing the carotenoid content of Brassica napus seeds by downregulating lycopene epsilon cyclase. Transgenic Res **17,** 573-585.

Zaki, M., Dickinson, H. (1991). Microspore-derived embryos in *Brassica:* the significance of division symmetry in pollen mitosis 1 to embryonic development. Sex. Plant Reproduction **4,** 48-55.

Zaki, M., Dickinson, H. (1995). Modification of cell development in vitro: The effect of colchicine on anther and isolated microspore culture in *Brassica napus*. Plant Cell, Tissue and Organ Culture**,** 255-270.

Zeng, Z.B. (1994). Precision mapping of quantitative trait loci. Genetics **136,** 1457-1468.

Zhang, X., Ren, Y., and Zhao, J. (2008). Roles of extensins in cotyledon primordium formation and shoot apical meristem activity in Nicotiana tabacum. J Exp Bot **59,** 4045-4058.

Appendix 2

2.1: POSH 1-3 2006 Intact pods raw mean dataset

Line	Samples	Pod mass	Seed mass	Seed Damage	Intact LD50	Intact Y	Intact A	Intact B	Intact C	Adj. LD50
142	5	4.65	1.854	4.2	49.1	20.02	-26.1	0.0208	1.44	31.7
142_1 (P)	4	5.672	2.628	3	101.5	19.38	-19.84	0.0147	1.27	69.4
142_2	5	3.888	1.556	4	32.4	19.88	-19.97	0.032	1.26	26.1
142_3	4	3.846	0.869	8.25	40.5	19.03	-28.49	0.0223	1.35	34.7
143	1	2.428	0.615	5	18	20.34	-18.79	0.038	0.85	32.8
144	5	2.343	0.732	3.4	18.9	19.49	-19.25	0.0699	2.25	34.9
145	5	2.764	0.94	7.6	29.4	20.17	-19.95	0.0306	1.4	39.3
147	1	1.826	0.607	3	14.2	20.1	-18.58	0.0342	0.64	37.7
148	5	5.959	2.442	4.6	162.5	20.08	-19.13	0.008	1.37	126.2
149	4	2.716	0.876	7	19.5	19.78	-20.39	0.0374	1.27	30.1
150	2	2.848	1.515	1	19.1	25.34	-36.48	0.0112	-0.58	27.8
151	2	1.551	0.141	5	17.2	20.13	-19.59	0.0534	1.3	44.7
152	4	1.844	1.023	3.25	5.5	19.96	-22.95	0.2164	1.89	28.7
153	5	4.015	1.847	3	36.3	19.2	-29.59	0.0224	1.15	28.2
155	4	2.495	0.83	4.5	27.7	20.14	-20.51	0.1048	2.19	41.6
158	5	2.168	1.22	2.501	10.1	20.01	-20.32	0.236	3.78	28.6
160	4	3.156	1.251	1	28.2	19.74	-21.53	0.0521	3.38	32.5
163	5	4.346	2.022	3	20.1	19.81	-22.95	0.0775	23.67	7.1
165	5	3.655	1.8	3.2	43.8	19.31	-20.99	0.0359	2.66	40.8
168	5	4.126	2.113	2.6	54.3	20.05	-23.04	0.0322	2.02	44.6
169	4	4.724	1.634	7.5	147.1	19.95	-19.84	0.0106	2.28	128.7
170	4	3.072	1.39	2	38.6	18.91	-26.77	0.0307	2.25	44.1
171	4	2.827	1.147	4.5	30.1	24.44	-74.61	0.0225	0.37	39.1
173	3	2.98	1.276	3.333	29.9	21.92	-26.24	0.0508	0.89	36.7
174	5	3.698	1.725	2.2	25.9	19.36	-27.58	0.0418	1.31	22.3
175	3	1.712	0.477	4.333	10.2	20.2	-24.6	0.0754	1.22	35.4
177	5	4.53	2.275	2.6	100.7	19.53	-23.57	0.0184	2.42	85.1
180	5	3.272	1.579	2.8	17.3	19.03	-24.98	0.0901	1.37	19.9
182	4	2.597	1.339	2	9.4	20.03	-19.52	0.2264	4.75	21.8
183	4	3.103	1.564	1.75	19.7	19.96	-29.54	0.0345	1.32	24.8
185	5	3.407	1.616	2.6	15	19.99	-19.91	0.0821	1.57	15.6
187	4	2.965	1.487	1.5	16.7	19.87	-19	0.1022	5.45	23.7
188	5	2.169	0.394	6.4	24	19.96	-22.52	0.0346	1.12	42.6
190	5	3.575	1.343	4	27.9	20.28	-20.9	0.0291	1.22	26.1
191	5	2.218	0.897	3.2	10.2	20.08	-20.55	0.0786	0.98	28
192	5	3.89	1.347	2.6	28.3	20.08	-19.34	0.0647	2.71	22
193	2	1.944	0.647	5	8.8	24.23	-27.29	-0.0037	-1.37	30.6
194	5	3.94	1.989	2.6	42.3	19.55	-22.42	0.0365	2.11	35.3

195	3	3.026	1.351	1	17.9	20.1	-19.79	0.0645	1.82	24.1
196	5	4.044	1.823	4.8	24	19.68	-20.57	0.0379	1.32	15.4
197	2	1.633	0.653	2	8	19.96	-22.52	0.2389	2.34	34.3
198	4	3.054	1.353	2.5	25	19.7	-27.93	0.0824	2.09	30.8
201	2	1.516	0.67	3	5.5	19.97	-27.09	0.1015	1.14	33.5
202	5	3.406	1.543	2.6	25	19.99	-28.34	0.0295	1.06	25.6
205	5	5.701	1.98	7.8	110.1	19.95	-19.68	0.011	2.53	77.5
206	2	2.179	1.152	1	6.9	20.02	-19.76	0.2051	2.22	25.3
207	5	2.265	0.692	4.2	27	20.28	-19.7	0.049	1.87	44.2
208	2	1.251	0.301	5	16.5	29.68	-28.58	0.0118	-2.39	48.3
210	5	3.486	1.688	1	14.1	19.9	-21.46	0.0711	1.44	13.6
211	5	4.996	2.621	1.4	49.5	20.08	-22.92	0.0204	1.41	27.1
213	5	4.174	1.744	3.4	56.9	19.81	-19.39	0.0331	3.42	46.4
215	5	2.597	1.116	1.4	14.6	20.07	-19.94	0.083	1.71	27
216	5	4.003	1.938	1.4	34.6	20.12	-20.44	0.0239	1.02	26.6
217	5	2.765	1.156	4	17.2	21.18	-23.84	0.0857	1.06	27.1
218	5	2.931	1.082	2.6	20.7	20.05	-20.1	0.043	1.06	28.2
222	1	2.946	0.982	5	59.9	20.72	-20.61	0.0089	0.74	67.2
223	5	3.008	1.462	3.4	15.1	19.74	-20.08	0.1004	1.68	21.5
224	4	3.611	1.721	2	21.3	19.98	-19.97	0.0956	2.39	19
226	5	4.555	2.19	1.6	65.3	22.1	-28.18	0.0131	1.43	49.3
227	5	4.121	1.908	1.8	34.4	21.12	-26.48	0.0219	0.86	24.7
228	5	4.501	2.428	1	45.8	19.92	-21.4	0.0268	1.9	30.6
233	3	2.079	0.598	2	10.2	20.03	-20.61	0.0806	1.19	30.1
234	5	3.84	1.76	3.2	36.3	19.92	-20.58	0.0249	1.27	30.7
235	5	3.531	1.19	5.8	52.3	19.94	-18.98	0.0319	1.59	51.1
238	5	3.14	1.324	2.8	28.9	19.99	-19.93	0.0438	1.58	33.4
243	4	4.085	1.617	4	60.1	19.07	-25.77	0.0091	1.08	50.9
244	5	3.971	1.976	3.2	26.8	19.15	-23.23	0.0388	1.22	19.3
245	5	3.219	1.534	3	20.2	19.95	-19.33	0.1108	2.57	23.5
246	2	3.826	1.93	3	9.1	25.78	-31.13	0.0728	-0.73	3.7
247	2	3.175	1.432	2.5	23.4	19.88	-19.62	0.0354	1.19	27.4
249	4	3.815	1.116	8.75	22.7	20.1	-20.26	0.05	1.46	17.5
253	2	3.854	1.94	1.5	34.4	20.15	-21	0.0292	1.39	28.6
259	5	3.534	1.888	2.8	18.8	20.01	-20.14	0.064	1.89	17.6
263	3	2.751	0.805	5.667	9.3	101.12	-15.77	-0.1666	-30.98	19.5
272	5	3.117	1.476	1.8	24.5	20.58	-22.53	0.1068	7.76	29.4
274	3	2.01	0.732	1	6	20.01	-25.84	0.0634	0.81	26.9
275	5	3.396	1.474	5.6	31.7	20.08	-19.63	0.048	2.49	32.5
278	1	2.003	0.314	4	22.7	144.43	-3.67	-0.0265	-22.66	43.6
280	5	2.177	0.31	8	22.4	19.74	-20.54	0.0395	1.79	40.9
281	4	2.861	1.456	3.25	12.2	20.04	-21.4	0.0433	0.83	20.7
290	1	4.35	1.174	7	56.1	20.6	-21.19	0.0178	1.51	43.1

Line	Samples	Pod mass	Seed mass	Seed Damage	Broken LD50	Broken Y	Broken A	Broken B	Broken C	Broken Adj. LD50
291	5	4.903	2.393	2.4	65	19.49	-20.32	0.0168	2	44
Apex 1(P)	4	5.195	3.137	1.75	40.2	20	-28.95	0.0294	1.73	15
Apex 2	4	4.655	2.804	1.25	30.9	20.05	-19.67	0.0557	2.11	13.5

2.2 2006 Broken pods raw mean dataset

Line	Samples	Pod mass	Seed mass	Seed Damage	Broken LD50	Broken Y	Broken A	Broken B	Broken C	Broken Adj. LD50
142	5	4.65	1.854	4.2	87.5	0.03	22.4	0.0167	3	62.2
142_1 (P)	4	5.672	2.628	3	199.8	0.48	20.51	0.0074	2	153.1
142_2	5	3.888	1.556	4	84.8	0.52	19.74	0.0187	2	75.5
142_3	4	3.846	0.869	8.25	125.8	-0.01	19.36	0.0206	8	117.4
143	1	2.428	0.615	5	27.8	-0.44	18.47	0.0287	1	49.2
144	5	2.343	0.732	3.4	26.7	0.16	18.8	0.0465	2	49.9
145	5	2.764	0.94	7.6	45.8	-0.28	19.09	0.0259	1	60.1
147	1	1.826	0.607	3	29.5	-0.62	20.04	0.015	1	63.5
148	5	5.959	2.442	4.6	208.6	0.08	18.81	0.0067	3	155.8
149	4	2.716	0.876	7	31.4	0.49	20.88	0.0396	2	46.7
150	2	2.848	1.515	1	41.9	-0.2	19.51	0.0459	3	54.5
151	2	1.551	0.141	5	34.3	0.13	19.32	0.0115	1	74
152	4	1.844	1.023	3.25	8.4	0.09	20.75	0.1326	2	42.1
153	5	4.015	1.847	3	60.7	0.06	21.32	0.0265	4	48.8
155	4	2.495	0.83	4.5	58.2	1.11	45.51	0.0119	0	78.2
158	5	2.168	1.22	2.501	9.2	0.16	21.4	0.1525	3	36.1
160	4	3.156	1.251	1	39.8	0.92	19.13	0.0738	10	45.9
163	5	4.346	2.022	3	30.6	-0.05	23.68	0.0387	2	11.8
165	5	3.655	1.8	3.2	61.1	0.46	20.14	0.039	4	56.7
168	5	4.126	2.113	2.6	84.8	-0.35	19.93	0.0211	2	70.6
169	3	4.724	1.634	7.5	164.8	0.18	18.28	0.0101	4	141.6
170	4	3.072	1.39	2	47.7	-0.51	24.11	0.0194	2	55.6
171	4	2.827	1.147	4.5	38	0.18	22.85	0.0568	3	51
173	3	2.98	1.276	3.333	50.2	-0.31	20.39	0.029	2	60
174	5	3.698	1.725	2.2	56.5	-0.29	19.54	0.0431	2	51.2
175	3	1.712	0.477	4.333	15.2	-0.16	19.51	0.0621	1	51.6
177	5	4.53	2.275	2.6	115.6	0.36	23.02	0.0145	3	92.9
180	5	3.272	1.579	2.8	17.9	0.21	19.54	0.0578	1	21.5
182	4	2.597	1.339	2	19.6	0.13	20.49	0.1484	6	37.4
183	4	3.103	1.564	1.75	20.8	-0.05	25.51	0.0361	1	28
185	5	3.407	1.616	2.6	20.4	0.13	20.59	0.0669	2	21.2
187	4	2.965	1.487	1.5	19.4	0.01	19.38	0.0811	4	29.4
188	5	2.169	0.394	6.4	48.3	-0.31	19.49	0.0254	2	75.1
190	5	3.575	1.343	4	60.6	0.42	20.25	0.0233	2	57.9

244

191	5	2.218	0.897	3.2	24.5	0.07	20.06	0.0708	2	50.2
192	5	3.89	1.347	2.6	39.3	-0.02	25.29	0.032	3	30
193	2	1.944	0.647	5	11.8	-0.03	20.2	0.0384	1	43.3
194	5	3.94	1.989	2.6	68.2	0.26	21.08	0.0229	3	57.8
195	3	3.026	1.351	1	22.5	0	20.15	0.0626	3	31.3
196	5	4.044	1.823	4.8	49.5	0.14	19.96	0.0234	2	37
197	2	1.633	0.653	2	14.2	-0.1	20.04	0.232	4	52.3
198	4	3.054	1.353	2.5	33.8	-0.44	23.87	0.0501	2	42
201	2	1.516	0.67	3	11.9	0.03	23.96	0.0816	1	52.4
202	5	3.406	1.543	2.6	76.6	0.04	21.65	0.0224	2	77.4
205	5	5.701	1.98	7.8	164.8	-1.66	24.86	0.0031	0	117.4
206	2	2.179	1.152	1	12.7	0.13	20.47	0.1359	4	39.3
207	5	2.265	0.692	4.2	43.1	-0.78	24.24	0.0344	2	67.9
208	2	1.251	0.301	5	21.6	0.13	19.29	0.0548	2	67.6
210	5	3.486	1.688	1	20.3	0.84	27.85	0.0695	2	19.4
211	5	4.996	2.621	1.4	103.5	4.08	8.33	0.0377	*	70.9
213	5	4.174	1.744	3.4	153.4	7.6	-12.43	0.0265	*	138.1
215	5	2.597	1.116	1.4	19.5	-0.02	19.71	0.0647	2	37.3
216	5	4.003	1.938	1.4	75.9	-0.23	23.02	0.0119	2	64.2
217	5	2.765	1.156	4	44.7	0.24	21.6	0.0288	2	59
218	5	2.931	1.082	2.6	38.8	0.32	21.58	0.0304	2	49.6
222	1	2.946	0.982	5	79.1	-0.68	18.58	0.0097	1	89.6
223	5	3.008	1.462	3.4	35.6	-0.15	22.08	0.0392	2	44.8
224	4	3.611	1.721	2	44.7	-0.16	20.68	0.0256	2	41.2
226	5	4.555	2.19	1.6	81.5	-0.31	27.83	0.0116	1	58.2
227	5	4.121	1.908	1.8	40.5	-0.08	21.42	0.0239	1	26.3
228	5	4.501	2.428	1	55.9	-0.48	26.97	0.019	2	33.8
233	3	2.079	0.598	2	24.1	0.13	19.1	0.0682	2	52.8
234	5	3.84	1.76	3.2	54.1	-0.11	21.42	0.0208	2	45.9
235	5	3.531	1.19	5.8	75.8	-0.34	20.74	-0.0013	0	74
238	5	3.14	1.324	2.8	42.3	0.05	21	0.0248	2	48.8
243	4	4.085	1.617	4	83.3	0.17	19.95	0.0153	2	69.9
244	5	3.971	1.976	3.2	62.6	-0.23	20.79	0.0176	2	51.6
245	5	3.219	1.534	3	50.1	1.6	28.82	0.0223	3	54.9
246	2	3.826	1.93	3	28.8	-16.53	40.64	0.0209	-1	20.9
247	2	3.175	1.432	2.5	46.2	-0.17	20.79	0.0258	1	51.9
249	4	3.815	1.116	8.75	60.5	-0.13	18.83	0.0186	2	52.8
253	2	3.854	1.94	1.5	96.6	0.17	22.76	0.0319	2	88
259	5	3.534	1.888	2.8	35.5	0.21	20.39	0.0341	2	33.7
263	3	2.751	0.805	5.667	39.8	-0.48	19.34	0.0073	1	54.3
272	5	3.117	1.476	1.8	34.7	-0.01	19.82	0.0455	2	41.6
274	3	2.01	0.732	1	18.5	1.56	34.19	0.0519	2	48.6
275	5	3.396	1.474	5.6	71	-1.59	27.12	0.0188	1	72.1

278	1	2.003	0.314	4	55.8	-0.56	20.55	0.0092	1	86
280	5	2.177	0.31	8	55	0.04	18.61	0.0346	4	81.6
281	4	2.861	1.456	3.25	30.8	0.19	21.04	0.0394	2	43
290	1	4.35	1.174	7	171	-24.46	67.3	-0.157	-162	152
291	5	4.903	2.393	2.4	82.1	0.28	20.02	0.0179	4	51.5
Apex 1(P)	4	5.195	3.137	1.75	47.1	0.01	19.75	0.0195	1	10.4
Apex 2	4	4.655	2.804	1.25	34.8	-0.36	20.07	0.0405	2	9.4

2.3 2009 Intact raw mean dataset

Line	Podwt	LD50	y	a	b	c	Adj.LD50
148	5.957	54.3	20.04	-19.8	0.0231	1.58	44.1
168	4.04	22.8	19.66	-20.4	0.0431	1.57	28.5
169	4.664	37.1	19.41	-24.2	0.0266	1.56	37.6
177	5.043	28.7	19.13	-23.4	0.0311	1.3	26
226	3.84	12.6	20.04	-20.7	0.0805	1.57	19.9
228	4.217	22.8	19.47	-34.4	0.0494	2.41	27.1
243	4.647	34.4	20	-19.5	0.0332	1.53	35
246	5.25	14	19.46	-19.7	0.0887	2.14	9.6
259	3.768	12.8	19.88	-22	0.112	4.12	20.8
Apex	4.984	17.9	19.78	-21.1	0.0564	1.45	15.7
DK142	5.765	17.8	20.09	-20.3	0.0704	1.89	9.2

2.4 2009 Broken raw mean dataset

Line	Podwt	LD50	y	a	b	c	Adj.LD50
148	5.957	85.6	0.13	19.7	0.0181	2.55	72.2
168	4.04	37	-0.18	20.7	0.0284	2.6	44.5
169	4.664	65.6	0.31	20.9	0.0172	1.95	66.3
177	5.043	52.5	0.15	25.9	0.0162	1.38	49
226	3.84	18.7	-0.36	20	0.0608	1.45	28.4
228	4.217	41.2	0.11	22.3	0.0238	1.77	46.8
243	4.647	55.7	-0.03	19.2	0.0248	2.14	56.6
246	5.25	59.6	-0.56	26.1	0.0109	1.23	53.9
259	3.768	25.1	1.41	32.2	0.0328	1.68	35.6
Apex	4.984	26.7	0.56	19.8	0.0472	2.82	23.9
DK142	5.765	46.3	0.11	19.8	0.0314	2.97	35

2.5 2006 trial Pod mass, Seed mass and Seed Damage distribution histograms
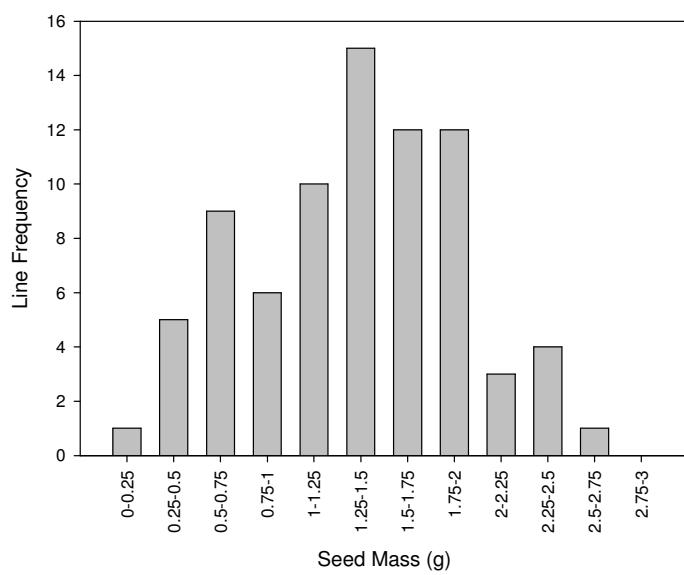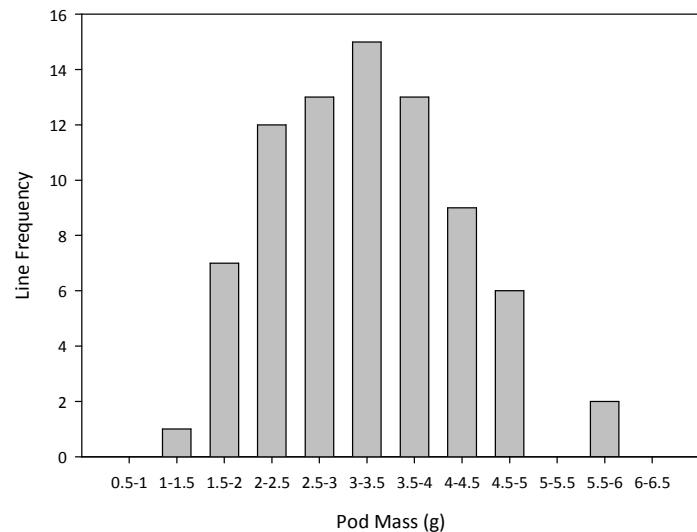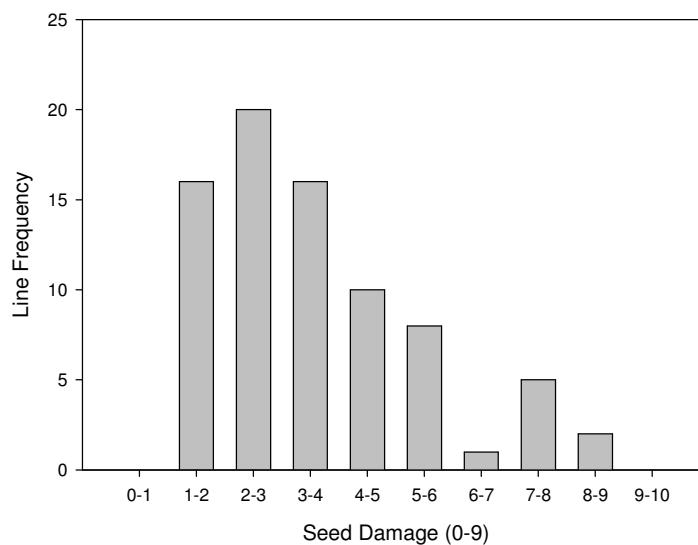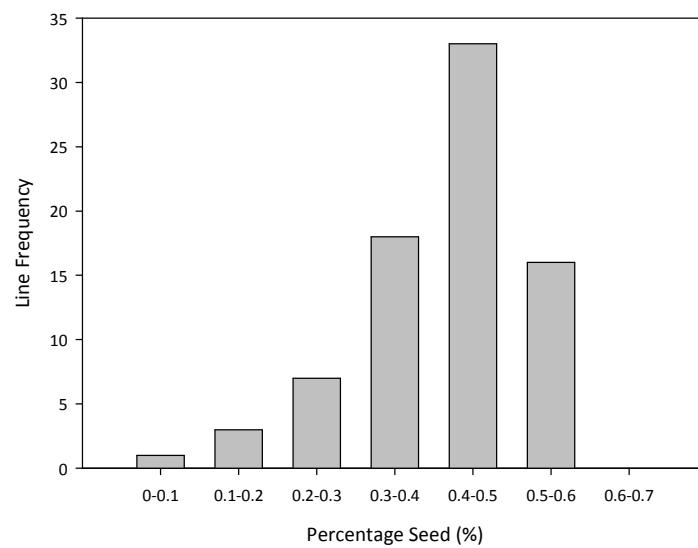
2.6 POSH 1-3 2006 trial Shapiro-Wilk test for normality for Pod mass, Seed mass and Seed damage

Data variate:	Pod_mass
Test statistic W:	0.986
Probability:	0.554

Data variate:	Seed_mass
Test statistic W:	0.9875
Probability:	0.649

Data variate:	Damage
Test statistic W:	0.9134
Probability:	<0.001

2.7 POSH 1-3 2006 trial Shapiro-Wilk test for Intact and Broken LD50 and adjusted LD50

Data variate:	Intact LD50
Test statistic W:	0.7023
Probability:	<0.001

Data variate:	Intact Adj. LD50
Test statistic W:	0.7287
Probability:	<0.001

Data variate:	Broken LD50
Test statistic W:	0.8077
Probability:	<0.001

Data variate:	Broken adj.LD50
Test statistic W:	0.8432
Probability:	<0.001

2.8 2006 Intact Line GLM outputs

Variate: podwt

Source of variation	d.f.	s.s.	m.s.	v.r.	F pr.
Line	77	276.6424	3.5928	11.04	<.001
Residual	235	76.4483	0.3253		
Total	312	353.0906			

Variate: seedwt

Source of variation	d.f.	s.s.	m.s.	v.r.	F pr.
Line	77	92.367	1.1996	10.89	<.001
Residual	234	25.7822	0.1102		
Total	311	118.0533			

Variate: damage

Source of variation	d.f.	s.s.	m.s.	v.r.	F pr.
Line	77	1067.882	13.869	8.5	<.001

Residual	234	382	1.632		
Total	311	1449.125			

Variate: y

Source of variation	d.f.	s.s.	m.s.	v.r.	F pr.
line	77	35146.4	456.4	2.65	<.001
Residual	235	40407.8	171.9		
Total	312	75554.2			

Variate: a

Source of variation	d.f.	s.s.	m.s.	v.r.	F pr.
line	77	14555.8	189	1.36	0.044
Residual	235	32778.9	139.5		
Total	312	47334.7			

Variate: b

Source of variation	d.f.	s.s.	m.s.	v.r.	F pr.
line	77	0.905897	0.011765	2.19	<.001
Residual	235	1.263187	0.005375		
Total	312	2.169084			

Variate: c

Source of variation	d.f.	s.s.	m.s.	v.r.	F pr.
line	77	6691.7	86.91	1.15	0.215
Residual	235	17762.47	75.58		
Total	312	24454.17			

Variate: lethaldose

Source of variation	d.f.	s.s.	m.s.	v.r.	F pr.
Line	77	262787.1	3412.8	5.33	<.001
Residual	235	150382.9	639.9		
Total	312	413170			

Variate: lethaldose
Covariate: podwt

Source of variation	d.f.	s.s.	m.s.	v.r.	cov.ef.	F pr.
Line	77	120871.1	1569.8	2.73	0.96	<.001

	d.f.	s.s.	m.s.	v.r.		F pr.
Covariate	1	15605.4	15605.4	27.09		<.001
Residual	234	134777.5	576		1.11	
Total	312	413170				

Variate: Percentage_seed

Source of variation	d.f.	s.s.	m.s.	v.r.	F pr.
Line	79	28774.09	364.23	11.16	<.001
Residual	239	7801.63	32.64		
Total	318	36575.72			

2.9 2006 Intact pods Block GLMs

Variate: podwt

Source of variation	d.f.	s.s.	m.s.	v.r.	F pr.
block	2	1.889	0.944	0.83	0.435
Residual	310	351.202	1.133		
Total	312	353.091			

Variate: seedwt

Source of variation	d.f.	(m.v.)	s.s.	m.s.	v.r.	F pr.
block	2		0.7175	0.3587	0.94	0.39
Residual	309	-1	117.3374	0.3797		
Total	311	-1	118.0533			

Variate: damage

Source of variation	d.f.	(m.v.)	s.s.	m.s.	v.r.	F pr.
block	2		4.279	2.139	0.46	0.633
Residual	309	-1	1444.847	4.676		
Total	311	-1	1449.125			

Variate: lethaldose

Source of variation	d.f.	s.s.	m.s.	v.r.	F pr.
block	2	3503	1751	1.33	0.267
Residual	310	409667	1322		
Total	312	413170			

Variate: lethaldose
Covariate: podwt

Source of variation	d.f.	s.s.	m.s.	v.r.	cov.ef.	F pr.
block	2	5172.7	2586.3	3.19	1	0.043
Covariate	1	159191.4	159191.4	196.39		<.001
Residual	309	250475.9	810.6		1.63	
Total	312	413170				

2.10 2006 Broken Line GLM outputs

Variate: podwt

Source of variation	d.f.	s.s.	m.s.	v.r.	F pr.
Line	77	273.4303	3.551	10.92	<.001
Residual	234	76.0946	0.3252		
Total	311	349.5249			

Variate: seedwt

Source of variation	d.f.	(m.v.)	s.s.	m.s.	v.r.	F pr.
Line	77		92.4621	1.2008	10.9	<.001
Residual	233	-1	25.6775	0.1102		
Total	310	-1	118.0439			

Variate: damage

Source of variation	d.f.	(m.v.)	s.s.	m.s.	v.r.	F pr.
Line	77		1055.012	13.701	8.36	<.001
Residual	233	-1	381.667	1.638		
Total	310	-1	1435.942			

Variate: y

Source of variation	d.f.	s.s.	m.s.	v.r.	F pr.
Line	77	1595.092	20.715	4.33	<.001
Residual	234	1118.538	4.78		
Total	311	2713.63			

Variate: a

Source of variation	d.f.	s.s.	m.s.	v.r.	F pr.
Line	77	14113.96	183.3	2.07	<.001
Residual	234	20719.48	88.54		
Total	311	34833.44			

Variate: b

Source of variation	d.f.	s.s.	m.s.	v.r.	F pr.
Line	77	0.398051	0.005169	3.1	<.001
Residual	234	0.390535	0.001669		
Total	311	0.788586			

Variate: c

Source of variation	d.f.	s.s.	m.s.	v.r.	F pr.
Line	77	3.28E+10	4.25E+08	1.73	<.001
Residual	234	5.75E+10	2.46E+08		
Total	311	9.02E+10			

Variate: lethaldose

Source of variation	d.f.	s.s.	m.s.	v.r.	F pr.
Line	77	463275	6017	5.02	<.001
Residual	234	280660	1199		
Total	311	743934			

Variate: lethaldose
Covariate: podwt

Source of variation	d.f.	s.s.	m.s.	v.r.	cov.ef.	F pr.
Line	77	209766	2724	2.53	0.96	<.001
Covariate	1	29954	29954	27.84		<.001
Residual	233	250705	1076		1.11	
Total	311	743934				

2.11 2006 Broken pod Block GLMs

Variate: podwt

Source of variation	d.f.	s.s.	m.s.	v.r.	F pr.
block	2	2.314	1.157	1.03	0.358
Residual	309	347.211	1.124		
Total	311	349.525			

Variate: seedwt

Source of variation	d.f.	(m.v.)	s.s.	m.s.	v.r.	F pr.
block	2		0.7123	0.3561	0.93	0.394
Residual	308	-1	117.3332	0.381		
Total	310	-1	118.0439			

Variate: damage

Source of variation	d.f.	(m.v.)	s.s.	m.s.	v.r.	F pr.
block	2		5.48	2.74	0.59	0.555
Residual	308	-1	1430.462	4.644		
Total	310	-1	1435.942			

Variate: lethaldose

Source of variation	d.f.	s.s.	m.s.	v.r.	F pr.
block	2	616	308	0.13	0.88
Residual	309	743318	2406		
Total	311	743934			

Variate: lethaldose
Covariate: podwt

Source of variation	d.f.	s.s.	m.s.	v.r.	cov.ef.	F pr.
block	2	2217	1109	0.75	1	0.476
Covariate	1	285065	285065	191.6		<.001
Residual	308	458254	1488		1.62	
Total	311	743934				

2.12 2009 Intact GLM outputs

Variate: podwt

Source of variation	d.f.	s.s.	m.s.	v.r.	F pr.
line	10	36.1984	3.6198	15.33	<.001
Residual	59	13.9285	0.2361		
Total	69	50.1268			

Variate: lethaldose

Source of variation	d.f.	s.s.	m.s.	v.r.	F pr.
line	10	11383.4	1138.3	6.4	<.001
Residual	59	10487.3	177.8		
Total	69	21870.7			

Variate: y

Source of variation	d.f.	s.s.	m.s.	v.r.	F pr.
line	10	6.174	0.617	0.6	0.81
Residual	59	61.022	1.034		
Total	69	67.196			

Variate: a

Source of variation	d.f.	s.s.	m.s.	v.r.	F pr.
line	10	1230.38	123.04	1.28	0.262
Residual	59	5668.12	96.07		
Total	69	6898.5			

Variate: b

Source of variation	d.f.	s.s.	m.s.	v.r.	F pr.
line	10	0.056237	0.005624	0.95	0.493
Residual	59	0.348216	0.005902		
Total	69	0.404453			

Variate: c

Source of variation	d.f.	s.s.	m.s.	v.r.	F pr.
line	10	53.47	5.35	0.47	0.904
Residual	59	673.76	11.42		
Total	69	727.24			

Variate: lethaldose
Covariate: podwt

Source of variation	d.f.	s.s.	m.s.	v.r.	cov.ef.	F pr.
line	10	7369.3	736.9	4.48	0.79	<.001
Covariate	1	956.6	956.6	5.82		0.019
Residual	58	9530.7	164.3		1.08	
Total	69	21870.7				

2.13 2009 Intact LD50 block GLM

Variate: podwt

Source of variation	d.f.	s.s.	m.s.	v.r.	F pr.
block	2	0.5198	0.2599	0.35	0.705
Residual	67	49.607	0.7404		
Total	69	50.1268			

Variate: lethaldose

Source of variation	d.f.	s.s.	m.s.	v.r.	F pr.
block	2	676.8	338.4	1.07	0.349
Residual	67	21193.8	316.3		
Total	69	21870.7			

Variate: lethaldose
Covariate: podwt

Source of variation	d.f.	s.s.	m.s.	v.r.	cov.ef.	F pr.
block	2	1012.2	506.1	2.1	0.99	0.13
Covariate	1	5306.1	5306.1	22.04		<.001
Residual	66	15887.8	240.7		1.31	
Total	69	21870.7				

2.14 2009 Broken GLM outputs

Variate: podwt

Source of variation	d.f.	s.s.	m.s.	v.r.	F pr.
line	10	36.1984	3.6198	15.33	<.001
Residual	59	13.9285	0.2361		
Total	69	50.1268			

Variate: lethaldose

Source of variation	d.f.	s.s.	m.s.	v.r.	F pr.
line	10	27545	2754.5	5.21	<.001
Residual	59	31180.4	528.5		
Total	69	58725.4			

Variate: y

Source of variation	d.f.	s.s.	m.s.	v.r.	F pr.
line	10	17.1051	1.7105	1.82	0.077
Residual	59	55.4391	0.9396		
Total	69	72.5442			

Variate: a

Source of variation	d.f.	s.s.	m.s.	v.r.	F pr.
line	10	1241.01	124.1	1.89	0.064
Residual	59	3864.34	65.5		
Total	69	5105.36			

Variate: b

Source of variation	d.f.	s.s.	m.s.	v.r.	F pr.
line	10	0.010861	0.001086	4	<.001
Residual	59	0.016014	0.000271		
Total	69	0.026876			

Variate: c

Source of variation	d.f.	s.s.	m.s.	v.r.	F pr.
line	10	20.145	2.015	0.6	0.807
Residual	59	197.959	3.355		
Total	69	218.104			

Variate: lethaldose
Covariate: podwt

Source of
variation	d.f.	s.s.	m.s.	v.r.	cov.ef.	F pr.
line	10	15276	1527.6	3	0.79	0.004
Covariate	1	1663.3	1663.3	3.27		0.076
Residual	58	29517.1	508.9		1.04	
Total	69	58725.4				

2.15 2009 Broken LD50 Block GLM

Variate: podwt

Source of
variation	d.f.	s.s.	m.s.	v.r.	F pr.
block	2	0.5198	0.2599	0.35	0.705
Residual	67	49.607	0.7404		
Total	69	50.1268			

Variate: lethaldose

Source of
variation	d.f.	s.s.	m.s.	v.r.	F pr.
block	2	1435.9	718	0.84	0.436
Residual	67	57289.4	855.1		
Total	69	58725.4			

Variate: lethaldose
Covariate: podwt

Source of
variation	d.f.	s.s.	m.s.	v.r.	cov.ef.	F pr.
block	2	2221.7	1110.9	1.72	0.99	0.187
Covariate	1	14718.1	14718.1	22.82		<.001
Residual	66	42571.4	645		1.33	
Total	69	58725.4				

2.16 GLM for 2006|2009 9 line subset:

Variate: Podwt

Accumulated analysis of variance

Change	d.f.	s.s.	m.s.	v.r.	F pr.
Line	10	9.5288	0.9529	6.18	0.004
Yr	1	0.1223	0.1223	0.79	0.394
Yr*Line	10	1.541	0.1541	1	0.5
Total	21	11.1921	0.533		

Response variate: Podwt

	Prediction
Yr	
1	4.594
2	4.743

Predictions from regression model

Response variate: Podwt

	Prediction	
Yr	1	2
Line		
148	5.959	5.957
168	4.126	4.04
169	4.552	4.664
177	4.53	5.043
226	4.555	3.84
228	4.501	4.217
243	4.085	4.647
246	3.826	5.25
259	3.534	3.768
Apex	5.195	4.984
DK142	5.672	5.765

Variate: Intact LD50

Accumulated analysis of variance

Change	d.f.	s.s.	m.s.	v.r.	F pr.

Change	d.f.	s.s.	m.s.	v.r.	F pr.
Line	10	18157.7	1815.8	2.28	0.105
Yr	1	12782.6	12782.6	16.02	0.003
Yr*Line	10	7979.3	797.9	1	0.5
Total	21	38919.6	1853.3		

Response variate: Intact LD50

		Prediction
Yr		
	1	73.22
	2	25.01

Predictions from regression model

Response variate: Int_LD50

	Prediction	
Yr	1	2
Line		
148	162.5	54.3
168	54.3	22.8
169	147.1	37.1
177	100.7	28.7
226	65.3	12.5
228	45.8	22.8
243	60.1	34.4
246	9.1	14
259	18.8	12.8
Apex	40.2	17.9
DK142	101.5	17.8

Variate:
Int_Adj_LD50

Accumulated analysis of variance

Change	d.f.	s.s.	m.s.	v.r.	F pr.
Line	10	12908.7	1290.9	2.04	0.138
Yr	1	5150	5150	8.14	0.017
Yr*Line	10	6329.1	632.9	1	0.5
Total	21	24387.7	1161.3		

Response variate: Int_Adj_LD50

	Prediction
Yr	
1	55.46
2	24.86

Predictions from regression model

Response variate: AdjLD50

	Prediction	
Yr	1	2
Line		
148	125.3	44.1
168	43.3	28.5
169	127.5	37.6
177	83.9	26
226	48.1	19.9
228	29.4	27.1
243	49.6	35
246	2.4	9.6
259	16.2	20.8
Apex	15	15.7
DK142	69.4	9.2

Variate: Broken_LD50

Accumulated analysis of variance

Change	d.f.	s.s.	m.s.	v.r.	F pr.
Line	10	30254	3025	2.06	0.135
Yr	1	15915	15915	10.84	0.008
Yr*Line	10	14676	1468	1	0.5
Total	21	60845	2897		

Response variate: Broken_LD50

	Prediction
Yr	
1	100.52
2	46.73

Predictions from regression model

Response variate: Brkn_LD50

	Prediction	
Yr	1	2
Line		
148	208.58	85.6
168	84.85	37
169	164.78	65.6
177	115.61	52.5
226	81.46	18.7
228	55.9	41.2
243	83.26	55.7
246	28.83	59.6
259	35.54	25.1
Apex	47.1	26.7
DK142	199.8	46.3

Variate: Brkn_Adj_LD50

Accumulated analysis of variance

Change	d.f.	s.s.	m.s.	v.r.	F pr.
Line	10	19820	1982	1.77	0.19
Yr	1	4680	4680	4.19	0.068
Yr*Line	10	11180	1118	1	0.5
Total	21	35679	1699		

Response variate: Brkn_Adj_LD50

	Prediction
Yr	
1	75.73
2	46.56

Predictions from regression model

Response variate: Brkn_Adj_LD50

	Prediction	
Yr	1	2

Line		
148	156.78	72.2
168	69.42	44.5
169	140.88	66.3
177	92.16	49
226	57.5	28.4
228	33.01	46.8
243	68.64	56.6
246	19.35	53.9
259	31.84	35.6
Apex	10.4	23.9
DK142	153.1	35

2.17 Apex and DK142 Pod Mass (g) T-test

2006

	Apex	DK142
	4.8836	5.491
	4.8667	5.3334
	5.251	6.2596
	5.7771	5.6025
mean	5.1946	5.6716
T-test	0.147471	

2009

	Apex	DK142
	4.13	5.75
	3.77	5.59
	3.95	5.77
	5.79	5.96
	5.43	5.84
	5.62	5.68
	5.39	
	5.48	
	5.3	
Mean	4.984	5.765
t-test	0.034549	

2.18 T-test Apex and DK142 Seed Mass (g)

Apex	DK142
3.125	2.7346
3.0201	2.6235
2.8833	2.8972
3.5186	2.2578

	Apex	DK142
Mean	3.136	2.628
T test	0.154616	

2.19 T-test Percentage Seed content in MC151/MC211 and Apex/DK142

MC151	MC211
8.206073	53.74538
9.600693	52.89858
	52.21936
	52.99478
	50.26756

	MC151	MC211
Mean	8.9	52.425
T test	1.58E-07	

Apex	DK142
63.98968	49.80149
62.05642	49.19001
54.90954	46.28411
60.90599	40.29987

	Apex	DK142
mean	60.465	46.39
T test	0.01085	

2.20 Apex/DK142 Seed Damage T-test

Apex1	DK142_1
2	3
1	3
2	3
2	3

	Apex1	DK142_1
mean	1.75	3
T-test	0.0154	

2.21 2006 Intact LD50 T-tests

	Apex	142_1
	35.71	49.34
	70	236.64
	32.15	24.35
	22.9	95.87
mean	40.19	101.55
T test	0.213966	

	142_1	MC205
	49.34	87.98
	236.64	67.1
	24.35	174.35
	95.87	95.41
		125.45
mean	101.5	110.058
T-test	0.860521	

	142_1	MC169
	49.34	123.81
	236.64	298.71
	24.35	110.19
	95.87	55.65
mean	101.5	147
T-test	0.544089	

	142_1	MC148
	49.34	75.34
	236.64	242.42
	24.35	66.69
	95.87	237.04
		191.13
mean	101.5	162.52
T-test	0.345382	

	Apex	MC205	MC148
	35.71	87.98	75.34
	70	67.1	242.42
	32.15	174.35	66.69
	22.9	95.41	237.04
		125.45	191.13
mean	40.19	110.058	162.52
T-test		0.018716	0.028556

2.22 2009 Intact LD50 T-tests

	Apex	DK142
	19.21	19.19
	12.13	24.6
	13.11	13.48
	20.88	21.33
	6.65	15.5
	23.05	12.68
	25.03	
	20.16	
	20.75	
mean	17.88	17.79
T test	0.97605	

	Apex	**MC148**
	19.21	58.13
	12.13	75.67
	13.11	84.37
	20.88	17.97
	6.65	47.09
	23.05	97.13
	25.03	29.5
	20.16	24.34
	20.75	
Mean	**17.88**	**54.275**
T test	0.002461	

	DK142	**MC148**
	19.19	58.13
	24.6	75.67
	13.48	84.37
	21.33	17.97
	15.5	47.09
	12.68	97.13
		29.5
		24.34
Mean	**17.79**	**54.275**
T test	0.011694	

2.23 2006 Broken LD50 T-tests

	Apex	DK142_1
	40.29	168.64
	76.54	297.03
	43.91	64.28
	27.71	269.13
mean	47.112	199.77
T test	0.056557	

	DK142_1	148
	168.64	104.15
	297.03	299.41
	64.28	106.13
	269.13	271.42
		261.8
mean	199.77	208.52
T test	0.899206	

	Apex	148
	40.29	104.15
	76.54	299.41
	43.91	106.13
	27.71	271.42
		261.8
mean	47.112	208.52
T test	0.013515	

2.24 2009 Broken LD50 T-tests

	Apex	DK142
	25.98	35.19
	17.27	47.45
	15.91	44.13
	39.7	33.66
	17.74	76.57
	34.64	40.81
	34.88	
	26.28	
	28.18	
Mean	26.73	46.3
T test	0.007887	

	Apex	MC148
	25.98	84.71
	17.27	90.08

	2006	2009
	15.91	186.2
	39.7	41.71
	17.74	71.1
	34.64	133.73
	34.88	37.3
	26.28	40.36
	28.18	
Mean	26.73	85.64
T test	0.004317	

2.25 2006|2009 Intact LD50 T tests

	2006	2009
	Apex	Apex
	35.71	19.21
	70	12.13
	32.15	13.11
	22.9	20.88
		6.65
		23.05
		25.03
		20.16
		20.75
Mean	40.19	17.88
T test	0.009741	

	2006	2009
	DK142_1	DK142
	49.34	19.19
	236.64	24.6
	24.35	13.48
	95.87	21.33
		15.5
		12.68
Mean	101.5	17.79
T test	0.056279	

	2006	2009
	MC148	MC148
	75.34	58.13

	242.42	75.67
	66.69	84.37
	237.04	17.97
	191.13	47.09
		97.13
		29.5
		24.34
mean	162.52	54.725
T test	0.006638	

2.26 2006|2009 Broken LD50 T tests

	2006	2009
	Apex	Apex
	25.98	40.29
	17.27	76.54
	15.91	43.91
	39.7	27.71
	17.74	
	34.64	
	34.88	
	26.28	
	28.18	
Mean	26.73	47.112
T test	0.025149	

	DK142_1	DK142
	168.64	35.19
	297.03	47.45
	64.28	44.13
	269.13	33.66
		76.57
		40.81
Mean	199.77	46.3
T test	0.006951	

	MC148	MC148
	104.15	84.71
	299.41	90.08
	106.13	186.2
	271.42	41.71
	261.8	71.1
		133.73
		37.3
		40.36
Mean	208.52	85.64
T test	0.011279	

Appendix 3

3.1: 35DAA MVBV angles GLM in Apex, DK142, MC148 and MC169 including multiple comparison test (Tukey's test)

Variate: MVBV_angle

Source of variation	d.f.	s.s.	m.s.	v.r.	F pr.
Line	3	598.331	199.444	39.51	<.001
Residual	16	80.774	5.048		
Total	19	679.106			

Line	Apex	DK142	MC148	MC169
	12	24.68	25.4	23.52

Tukey's 95% confidence intervals

	Mean	
Apex	12	a
MC169	23.52	b
DK142	24.68	b
MC148	25.4	b

3.2: 35DAA MVBV angles and T-tests in Apex, DK142, MC148 and MC169

MVBV
Angle

	APEX 1	DK142	MC148	MC169
1	11.30993	27.92898	26.18811	25.70995
2	9.039483	25.76933	25.79603	23.70265
3	9.524668	23.87528	24.19321	20.94265
4	16.76255	22.0679	27.29957	23.55226
5	13.36022	23.77235	23.53235	23.70265
Mean	**11.999**	**24.682**	**25.401**	**23.522**
stdev	3.158332	2.238132	1.527316	1.696052
sterr	1.579166	1.119066	0.763658	0.848026

T-tests

Apex/DK142	*P*=0.004278
Apex/MC148	*P*=0.000496
Apex/MC169	*P*=0.001352
DK142/MC148	*P*=0.576011
DK142/MC169	*P*=0.227245

3.3: 35DAA MVBV thickness GLM in Apex, DK142, MC148 and MC169 including multiple comparison test (Tukey's test)

Analysis of variance

Variate: MVBV_thickness

Source of variation	d.f.	s.s.	m.s.	v.r.	F pr.
Line	3	0.031253	0.0104177	21.15	<.001
Residual	16	0.0078798	0.0004925		
Total	19	0.0391328			

Line	Apex	DK142	MC148	MC169
	0.1238	0.2096	0.2148	0.2199

Tukey's 95% confidence intervals

Line

	Mean	
Apex	0.1238	a
DK142	0.2096	b
MC148	0.2148	b
MC169	0.2199	b

3.4: 35DAA MVBV thickness and T-tests in Apex, DK142, MC148 and MC169

MVBV Height

	Apex	DK142	MC148	MC169
	0.154295	0.234106	0.216049	0.249925
	0.155586	0.218811	0.198744	0.206558
	0.110535	0.197391	0.206783	0.20169
	0.09138	0.177299	0.236158	0.209258
	0.107385	0.220227	0.216065	0.232005
Mean	**0.1238**	**0.2095**	**0.2144**	**0.2198**
St dev	0.026217	0.019954	0.012502	0.018281
St error	0.014656	0.011154	0.006988	0.010219

T tests

Apex/DK142	$P=0.000428$
Apex/MC169	$P=0.001758$
Apex/MC148	$P=0.007021$
DK142/MC169	$P=0.226791$
DK142/MC148	$P=0.737109$

3.5 70DAA MVBV Widths for all four lines GLM in Apex, DK142, MC148 and MC169 including multiple comparison test (Tukey's test)

Variate: MVBV_Width

Source of variation	d.f.	s.s.	m.s.	v.r.	F pr.
Line	3	0.266674	0.088891	26.87	<.001
Residual	36	0.119102	0.003308		
Total	39	0.385775			

Variate: MVBV_Width

Grand mean 0.4211

Line	Apex	DK142	MC148	MC169
	0.3423	0.3422	0.4702	0.5298

Tukey's 95% confidence intervals

Line

	Mean	
DK142	0.3422	a
Apex	0.3423	a
MC148	0.4702	b
MC169	0.5298	b

3.6 70DAA MVBV Widths and T-tests in Apex, DK142, MC148 and MC169

MVBV Width

	Apex	DK142	MC148	MC169
1	0.35042735	0.301108	0.461538	0.600113
2	0.38034188	0.312641	0.458098	0.581945
3	0.153846154	0.351762	0.46558	0.645403
4	0.405982906	0.319693	0.416106	0.401103
5	0.35042735	0.364575	0.458949	0.585215
6	0.384615385	0.321865	0.491663	0.533228
7	0.324786325	0.34507	0.517294	0.509407
8	0.388888889	0.367796	0.530871	0.495782
9	0.384615385	0.396575	0.453574	0.512962
10	0.299145299	0.340626	0.448777	0.43277
Mean	0.3423	0.3421	0.4702	0.5297
stdev	0.073839482	0.029244	0.033978	0.075971
sterr	0.024613161	0.009748	0.011326	0.025324

T-tests	
Apex/DK142	P=0.995912
Apex/MC148	P=0.000768
Apex/MC169	P=0.00131
DK142/MC148	P=2.91E-06

DK142/MC169	P=5.22E-05

3.7 Pod Wall thickness GLM in Apex, DK142, MC148 and MC169 including multiple comparison test (Tukey's test)

Variate: Pod_Wall_Thickness

Source of variation	d.f.	s.s.	m.s.	v.r.	F pr.
Line	3	0.68519	0.228397	23.21	<.001
Residual	32	0.314879	0.00984		
Total	35	1.000069			

Line	Apex	DK142	MC148	MC169
	0.426	0.814	0.594	0.637

Tukey's 95% confidence intervals

Line

	Mean	
Apex	0.4263	a
MC148	0.5944	b
MC169	0.6369	b
DK142	0.8141	

3.8 Pod wall thickness measurements and T-tests in Apex, DK142, MC148 and MC169

	Apex	DK142	MC148	MC169
1.1	0.477009	0.72009	0.528647	0.620888
1.2	0.388349	0.667262	0.59533	0.723023
1.3	0.49752	0.782293	0.661451	0.539543
2.1	0.399635	0.931297	0.648881	0.549156
2.2	0.40546	0.626482	0.4904	0.784319
2.3	0.389929	0.810938	0.499356	0.553926
3.1	0.377407	1.08911	0.760627	0.732219
3.2	0.469426	0.772286	0.633856	0.609828
3.3	0.432091	0.92759	0.53113	0.619251
Mean	**0.4263**	**0.8141**	**0.5944**	**0.6369**
stdev	0.044492	0.146037	0.09002	0.089161
sterr	0.01573	0.051632	0.031827	0.031523

T-tests	
Apex/DK142	*P*=0.000105
Apex/MC148	*P*=0.001124
Apex/MC169	*P*=0.000632
DK142/MC148	*P*=0.000381
DK142/MC169	*P*=0.020891
MC148/MC169	*P*=0.349807

Appendix 4

Primer	Primer sequence	Target Marker
TW-001_F	5'-GAGATCGAGCTTCAAAACGA	*BnaX.SHP2*
TW-001_R	5'-TAAACCGTCCCTTGTTGATGT	*BnaX.SHP2*
TW-002_F	5'-TTGGTGAATCTCTCGGTTCC	*BnaX.SHP2*
TW-002_R	5'-TGCTGGGCGAAGAATAAAAC	*BnaX.SHP2*
TW-003 _F	5'-GAGAAGCTGAGATGATTTGAGAGG	*BnaA.ALC*
TW-003_R	5'-AGTTTCGCTACCTGGCTCCG	*BnaA.ALC*
TW-004_F	5'-CCAGAGATCGTCTTCCTGC	*BnaC.ALC*
TW-004_R1	5'-CCAAAGCGAGTGTAGTTTCACGGC	*BnaC.ALC*
TW-004_R2	5'-GAACTGTGCATCAATTTCGC	*BnaC.ALC*
TW-005_F	5'-CCAAGCTTTGAGTAGCAACG	*BnaX.RDPG1*
TW-005_F2	5'-GAATCCGATAGTTTAATCAAGC	*BnaX.RDPG1*
TW-005_F3	5'-GTTCTTTTGATGCTCGCTTGC	*BnaX.RDPG1*
TW-005_R	5'-AGTGCCTAGGATCTGGAAGC	*BnaX.RDPG1*
TW-005_R2	5'-CTCCATTTGTTGAACATGCC	*BnaX.RDPG1*
TW-005_R3	5'-GAACATGCCTTCTTCCATGC	*BnaX.RDPG1*
TW-006_F	5'-TTCGGGACATTCAGAATTCG	*BnaX.SHP1*
TW-006_R	5'-TTTCAAGCCGTCCTTCTAGG	*BnaX.SHP1*
TW-007_F	5'-TCTAAGGGCTTGGCTCTTCG	*BnaX.RPL*
TW-007_R	5'-GAGTTTGTCTGTATCAGTTGG	*BnaX.RPL*
TW-008_F	5'-CGCTATGAATGGTTTAGGCC	*BnaA.ALC*
TW-008_R1	5'-AACCAAATACTAGACTCTAC	*BnaA.ALC*
TW-008_R2	5'-GTTTTGTTCAGTCCTAAAGC	*BnaC.ALC*
TW-008_R3	5'-GCTTATTAGCATAACACTTGG	*BnaC.ALC*
TW-009_F1	5'-TTTGCCAACGTTGAGGTAGC	*BnaA.IND*
TW-009_F2	5'-TCTTGGCTAGTTATGATTCG	*BnaA.IND*
TW-009_R1	5'-AGAGATTTCACTGTATTTCG	*BnaA.IND*
TW-009_R2	5'-TATAGTTTTGGTATAGTCCC	*BnaA.IND*
TW-010_F1	5'-AGGTATATAAATGTGTGTGTG	*BnaC.IND*
TW-010_R1	5'-AACTAGCCAAAATAACTACG	*BnaC.IND*
TW-010_R2	5'-AATACTGTTAAGTGTTATCC	*BnaC.IND*
TW-010_F2	5'-GAATAAACACATGATTGCATGC	*BnaC.IND*
TW-010_R3	5'-CGCTGTGTCATTATCTGACC	*BnaC.IND*
TW-010_R4	5'-GAAGATTCAAACTACTTCGT	*BnaC.IND*
TW-010_F3	5'-TTGCCAACGTTGAGGTAGCT	*BnaC.IND*

Figure: 4.2 Candidate Gene SSCP Primer Sequences: Gene name, POSH 1-3 Marker loci and Forward and Reverse primer sequences

Appendix 5: Chapter 5 KW and SMR outputs

LN	N	Position	Locus	K*	Signif.	Allele expression ratio (A:B)
LN2	N1	0.000	BRMS-214_261	3.938	**	1.125
LN 3	N2/N12	0.000	Ol13E08c	6.225	**	0.6
LN 3	N2/N12	33.022	sN2374c	5.830	**	0.30357
LN 4	N2/N12	0.000	sN1925c	8.198	****	0.97297
LN 4	N2/N12	7.920	sR94102_320R	12.329	******	0.70732
LN 4	N2/N12	15.555	pN102c-2	10.268	****	0.64706
LN 4	N2/N12	32.647	Na10C08d	5.731	**	0.7381
LN 5	N3	29.296	sORC76c	4.946	**	0.66667
LN 5	N3	36.473	TW-010c	8.974	****	0.40816
LN 5	N3	36.964	AP14/15b_(400)	9.489	****	0.33333
LN 5	N3	37.302	AP2/4a_(281)	8.077	****	0.28
LN 5	N3	41.872	OL11G11b	12.838	******	0.22414
LN 5	N3	48.443	sNRB35	14.101	******	0.23729
LN 9	N5	0.000	Na12E01a-1	4.392	**	1.28125
LN 9	N5	10.793	BRMS-166_199	4.988	**	1.06061
LN 9	N5	13.033	sORA84_160	5.220	**	1.08824
LN 9	N5	16.224	sNRC86	4.650	**	1.05882
LN 16	N10/C9	29.305	Ol11B03a	3.892	**	0.62791
LN 6	N13	0.000	Na10F06b	6.191	**	0.87179
LN 6	N13	3.513	TW-010a	4.038	**	0.94444
LN 20	N?	0.000	Ni4-A07_250	6.038	**	0.33333
LN 20	N?	0.000	Na12E06b_231(F)	4.667	**	0.73684
LN 20	N?	6.935	Na12A08c	4.117	**	0.40385
LN 20	N?	8.968	sS1854b	4.069	**	1.29032
LN 20	N?	10.394	Ol10H02c	5.523	**	0.28571
LN 20	N?	20.145	Ol13A10	4.516	**	0.20339
LN 20	N?	21.257	Na12F12	3.889	**	0.26786
LN22	N?	36.116	KBrA14.8_221	4.176	**	0.68421
LN 22	N?	37.414	KBrA14.8_238	4.103	**	0.72973
LN 22	N?	41.380	Ol10G05	3.984	**	0.87179
	U		Na12E01b	11.696	*****	0.37736
	U		pN102c-1	10.268	****	1.54545
	U		KBrM6.12_241	9.344	****	0.375
	U		KBrM6.12_231	9.181	****	0.40625
	U		sNRC89b	8.642	****	0.7561
	U		AP14/15a_(400)	6.501	**	0.69231
	U		AP2/4b_(281)	6.171	**	0.88889
	U		sNRC89a	6.090	**	0.73171
	U		sN2187a	5.433	**	0.52083
	U		Ol9A06b	5.410	**	4.21429
	U		BRMS-314_243	4.737	**	1.2
	U		BRMS-88	4.677	**	2.3
	U		sN3766	4.400	**	2.83333
	U		Na12E01a-2	4.392	**	0.78049
	U		sS2368c	4.357	**	1.59259
	U		sS2368a	4.300	**	5.36364
	U		sS2210	4.177	**	1.48276

						Allele expression ratio (A:B)
U			Na12C08	4.038	**	1.15625
U			CB10211_267(F)	3.940	**	0.40909

Appendix 5.1: 2006 Pod Mass (g) KW single marker analysis output

**=P<0.05, ***=P<0.01, ****=P<0.005, *****=P<0.001, ******=P<0.0005, *******=P<0.0001

LN	N	Position	Locus	K*	Signif.	Allele expression ratio (A:B)
LN 12	N7/17	50.429	Na10C08b	4	**	0.3333333
LN 16	N10/N19	0	BRMS-19	4.267	**	0.5
LN 16	N10/N19	13.688	sNRD49	6	**	0.8
LN 16	N10/N19	15.704	CB10079_170(F)	6	**	0.8
LN 16	N10/N19	18.422	sORH62	6	**	0.8
LN 16	N10/N19	21.437	BRMS-62_178	6	**	0.8
U	U		Na10C01a	4.5	**	0.75
U	U		CB10045	4.2	**	0.2857143

Appendix 5.2: 2009 Pod Mass (g) KW single marker analysis output

LN	N	Position	Locus	K*	Signif.	Allele expression ratio (A:B)
LN 3	N2/N12	0.000	Ol13E08c	6.052	**	0.9730
LN 3	N2/N12	33.022	sN2374c	5.705	**	0.8718
LN 3	N2/N12	39.455	Na12H09	4.268	**	0.8889
LN 3	N2/N12	40.841	CB10026_145(F)	5.369	**	1.0606
LN 4	N2/N12	0.000	sN1925c	6.468	**	0.6000
LN 4	N2/N12	7.920	sR94102_320R	10.750	****	0.7073
LN 4	N2/N12	15.555	pN102c-2	8.230	****	0.7317
LN 4	N2/N12	32.647	Na10C08d	5.337	**	0.6977
LN 5	N3	29.296	sORC76c	5.188	**	0.8286
LN 5	N3	36.473	TW-010c	7.862	***	0.4082
LN 5	N3	36.964	AP14/15b_(400)	8.679	****	1.5455
LN 5	N3	37.302	AP2/4a_(281)	6.710	***	0.7368
LN 5	N3	41.872	OL11G11b	12.416	******	0.2241
LN 5	N3	48.443	sNRB35	12.369	******	0.2373
LN 9	N5	10.793	BRMS-166_199	4.301	**	0.6744
LN 9	N5	13.033	sORA84_160	4.269	**	0.6923
LN 9	N5	16.224	sNRC86	4.351	**	0.8947
LN 10	N6	41.380	Ol10G05	4.073	**	7.1250
LN 12	N7/N17	0.000	TW-008c	4.298	**	0.5208
LN 12	N7/N17	35.283	CB10277_619(F)	3.879	**	0.4063
LN 15	N9/N15	7.240	OL12F02b	5.186	**	0.6047
LN 15	N9/N15	8.871	OL12F02a	5.811	**	0.7381
LN 15	N9/N15	11.694	CB10305_115	6.058	**	0.8718
LN 6	N13	0.000	Na10F06b	3.940	**	1.3793
LN 21	N?	0.000	Na12E06b_231(F)	6.801	***	0.2800
LN25	N?	0.000	FITO135	4.831	**	1.8333
LN 24	N?	10.537	pN52d-1	5.526	**	1.0882
LN 38	N?	2.502	FITO66_208	4.086	**	0.8857

U			Na12E01b	10.947	*****	0.3774
U			sNRC89b	10.690	****	0.6471
U			sNRC89a	9.516	****	0.3333
U			pN102c-1	8.230	****	0.7561
U			KBrM6.12_241	6.670	***	0.3750
U			FITO66_240	6.272	**	0.3036
U			AP2/4b_(281)	6.171	**	0.4400
U			OL13C12c	6.075	**	0.5385
U			Na12C08	5.792	**	0.6667
U			KBrM6.12_231	5.660	**	1.0606
U			pN52d-2	5.526	**	1.0588
U			CB10211_116(F)	5.458	**	1.7200
U			BRMS-88	5.365	**	0.6591
U			CB10299_160	5.168	**	0.8621
U			AP14/15a_(400)	4.829	**	1.1600
U			sORA84_190	4.784	**	1.1563
U			CB10587_260(F)	4.494	**	1.9200
U			Ol9A06a	3.998	**	0.5897
U			sN2187a	3.906	**	2.3000

Appendix 5.3: 2006 Seed Mass (g) KW single marker analysis output

LN	N	Position	Locus	K*	Signif.	Allele expression ratio (A:B)
LN 3	N2/N12	82.123	sR94102_298R	7.451	***	0.6829268
LN 10	N6	25.431	Na12H04a	4.303	**	0.6511628
LN 11	N7/N17	48.386	KBr09.8_221	7.385	***	1.0967742
LN 11	N7/N17	59.148	sN0818	9.179	****	1.4642857
LN 11	N7/N17	64.825	Pw150	6.315	**	1.0606061
LN 12	N7/N17	0	TW-008c	12.282	******	1.72
LN 12	N7/N17	16.993	TW-008b	12.793	******	0.9428571
LN 12	N7/N17	18.822	TW-008d	11.558	*****	1.0909091
LN 12	N7/N17	35.283	CB10277_619(F)	4.709	**	1.0606061
LN 13	N?	0	Ol10F05a	4.403	**	1.2121212
LN 19	N?	15.439	CB10373(F)	5.47	**	1.15625
LN 37	N?	9.905	SR11644_250	5.353	**	0.5909091
LN 37	N?	9.984	SR11644_350	5.353	**	0.5909091
LN 35	N?	19.214	sN2321	5.833	**	1.1875
U			CB10258_595(F)	8.861	****	0.7368421
U			sN0212b	8.199	****	1.0909091
U			CB10443_290	8.136	****	12.8
U			CB10299_160	5.912	**	0.5897436
U			IGF5298_c(200)	6.510	**	0.9166667

Appendix 5.4: 2006 Seed Damage KW single marker analysis output

LN	N	Position	Locus	K*	Signif.	Allele expression

						ratio (A:B)
LN 2	N1	0.000	BRMS-214_261	4.036	**	1.125
LN 3	N2/N12	0.000	Ol13E08c	7.924	****	0.6
LN 3	N2/N12	18.296	Ol13E08b	3.933	**	0.46
LN 3	N2/N12	33.022	sN2374c	6.248	**	0.3035714
LN 3	N2/N12	39.455	Na12H09	6.312	**	0.44
LN 3	N2/N12	43.517	sORB10a	4.120	**	0.3877551
LN 3	N2/N12	47.328	Ol10F05b	4.306	**	0.5208333
LN 3	N2/N12	52.988	sORC76b	4.148	**	0.46
LN 4	N2/N12	15.555	pN102c-2	3.986	**	0.6470588
LN 5	N3	36.473	TW-010c	5.056	**	0.4081633
LN 5	N3	36.964	AP14/15b_(400)	5.764	**	0.3333333
LN 5	N3	37.302	AP2/4a_(281)	5.431	**	0.28
LN 5	N3	41.872	OL11G11b	6.770	***	0.2241379
LN 5	N3	48.443	sNRB35	13.685	******	0.2372881
LN 18	N3/13	37.303	Na10G10b	6.858	***	0.2545455
LN 12	N7/N17	31.586	Sn3274c	4.463	**	1.28125
LN 12	N7/N17	37.432	CB10124_297(F)	4.087	**	1.3
LN 12	N7/N17	45.038	BRAS19	4.621	**	1.4285714
LN 12	N7/N17	50.429	Na10C08b	4.252	**	0.9459459
LN 13	N8	33.581	Na12H07f	7.304	***	1.7037037
LN 13	N8	40.470	CB10026_105(F)	5.946	**	2.0909091
LN 13	N8	43.341	sS1702(298)	5.811	**	1.6153846
LN 15	N9/N15	35.933	sN1988	5.608	**	0.6363636
LN 15	N9/N15	36.783	SN1988_220	4.865	**	0.7
LN 15	N9/N15	36.783	SN1988_270	4.865	**	0.7
LN 15	N9/N15	48.928	KBr17.27	5.712	**	0.7179487
LN17	N10/N19	4.657	TW-007a	4.788	**	0.5
LN17	N10/N19	21.437	BRMS-62_178	3.938	**	1.125
LN17	N10/N19	29.305	Ol11B03a	6.606	**	0.627907
LN 6	N13	0.000	Na10F06b	9.351	****	0.8717949
LN 6	N13	3.513	TW-010a	5.171	**	0.9444444
LN 6	N13	3.939	OL11G11a	5.025	**	1.0857143
LN 6	N13	6.983	KBr09.8_302	5.547	**	1
LN 6	N13	9.884	Ni2B03_400	5.862	**	1.03125
LN 20	N?	10.394	Ol10H02c	3.938	**	0.2857143
LN 24	N?	21.362	Ni2B03_198	8.042	****	0.8611111
LN 37	N?	9.905	SR11644_250	4.422	**	0.5909091
LN 37	N?	9.984	SR11644_350	4.422	**	0.5909091
	U		KBrM6.12_231	11.178	*****	0.40625
	U		KBrM6.12_241	9.754	****	0.375
	U		Ol10F04a	9.608	****	1.25
	U		sORB10c	7.979	****	0.75
	U		Na12E01b	7.919	****	0.3773585
	U		BRMS-88	7.672	***	2.3
	U		Ol10BO4a	6.658	***	0.9459459
	U		BRMS-93_175	5.374	**	3
	U		FITO131	6.539	**	0.8648649
	U		CB10211_267(F)	6.273	**	0.4090909
	U		BRMS-23_155	5.757	**	0.4565217
	U		Na14E11	5.735	**	2.4761905
	U		sN2187a	5.708	**	0.5208333
	U		sS2368c	4.770	**	1.5925926
	U		Ol9A06c	4.526	**	1.92
	U		sORB10b	4.228	**	1.0571429
	U		sN0212b	4.049	**	1.0909091
	U		Ol9A06b	4.015	**	4.2142857
	U		Na10C08a	4.000	**	1.2903226
	U		pN102c-1	3.986	**	1.5454545

Appendix 5.5: 2006 Intact LD50 KW single marker analysis output

LN	N	Position	Locus	K*	Signif.	Allele expression ratio (A:B)
LN 10	N6	0.000	sN2837_120	4.582	**	0.75
LN 11	N7/N17	48.386	KBr09.8_221	3.872	**	0.80
LN 11	N7/N17	59.148	sN0818	4.371	**	1.25
LN 11	N7/N17	77.292	sN2567	4.083	**	1.00
LN 14	N18	17.767	SN11670_80	5.461	**	1.25
LN 15	N9/N15	35.933	sN1988	5.461	**	0.80
LN 15	N9/N15	36.783	SN1988_220	4.744	**	1.00
LN 15	N9/N15	36.783	SN1988_270	4.744	**	1.00
LN 15	N9/N15	48.928	KBr17.27	5.461	**	0.80
LN 24	N?	21.362	Ni2B03_198	5.445	**	0.50
LN 24	N?	32.612	Ni2-B03_180	5.060	**	0.60
LN 16	N10/N19	13.688	sNRD49	3.872	**	0.80
LN 16	N10/N19	15.704	CB10079_170(F)	3.872	**	0.80
LN 16	N10/N19	18.422	sORH62	3.872	**	0.80
LN 16	N10/N19	21.437	BRMS-62_178	3.872	**	0.80
LN 18	N3/N13	0.000	BN12A_303(F)	6.050	**	0.80
LN 18	N3/N13	25.637	sS2368b	6.050	**	0.80
LN 29	N?	0.000	TW-007b	4.500	**	0.75
LN 29	N?	17.013	Ol11B03b	5.445	**	2.00
LN 29	N?	30.081	BRMS-62_173	5.461	**	1.25
U	U		Na10C08a	5.333	**	1.00
U	U		Ol9A06b	4.371	**	1.25
U	U		AP14/15a(400)	6.050	**	0.80
U	U		AP2/4a(281)	3.850	**	1.33
U	U		CB10079_205(F)	4.235	**	3.50

Appendix 5.6: 2009 Intact LD50 KW single marker analysis output

LN	N	Position	Locus	K*	Signif.	Allele expression ratio (A:B)
LN 2	N1	0	BRMS-214_261	5.279	**	1.125
LN 4	N2/N12	7.92	sR94102_320R	6.12	**	0.7073171
LN 4	N2/N12	32.647	Na10C08d	5.082	**	0.7380952
LN 4	N2/N12	15.555	pN102c-2	8.039	****	0.6470588
LN 3	N2/N12	0	Ol13E08c	5.603	**	0.6
LN 3	N2/N12	39.455	Na12H09	4.118	**	0.44
LN 5	N3	41.872	OL11G11b	4.395	**	0.2241379
LN 5	N3	48.443	sNRB35	10.567	****	0.2372881
LN 9	N5	0	Na12E01a-1	4.415	**	1.28125
LN 9	N5	2.794	FITO67_233(F)	4.593	**	1.4074074
LN 9	N5	10.793	BRMS-166_199	6.053	**	1.0606061
LN 9	N5	13.033	sORA84_160	3.919	**	1.0571429
LN 10	N6	36.116	KBrA14.8_221	4.204	**	0.6842105
LN 12	N7/N17	31.586	Sn3274c	3.916	**	1.28125
LN 12	N7/N17	45.038	BRAS19	4.975	**	1.4285714
LN 12	N7/N17	50.429	Na10C08b	5.154	**	0.9459459
LN 12	N7/N17	64.018	sORE58	4.979	**	1.3461538

LN 13	N8	33.581	Na12H07f	6.377	**	1.7037037
LN 13	N8	40.47	CB10026_105(F)	5.568	**	2.0909091
LN 13	N8	43.341	sS1702(298)	5.046	**	1.6153846
LN 16	N10/N19	4.657	TW-007a	5.372	**	0.5
LN 16	N10/N19	13.688	sNRD49	4.342	**	1.2121212
LN 16	N10/N19	15.704	CB10079_170(F)	4.624	**	1.0909091
LN 16	N10/N19	18.422	sORH62	4.296	**	1.2121212
LN 16	N10/N19	21.437	BRMS-62_178	4.06	**	1.125
LN 16	N10/N19	29.305	Ol11B03a	7.601	***	0.627907
LN 6	N13	0	Na10F06b	10.933	*****	0.8717949
LN 6	N13	3.513	TW-010a	7.053	***	0.9444444
LN 6	N13	3.939	OL11G11a	6.676	***	1.0857143
LN 6	N13	6.983	KBr09.8_302	7.019	***	1
LN 6	N13	9.884	Ni2B03_400	7.665	***	1.03125
LN 13	N?	0	Ol10F05a	5.013	**	1.2121212
LN 24	N?	0	FITO135	4.968	**	0.6046512
LN 24	N?	10.537	pN52d-1	5.125	**	0.862069
LN 24	N?	21.362	Ni2B03_198	6.325	**	0.8611111
LN 27	N?	0	FITO122_113	3.843	**	1.2592593
LN 37	N?	0	Na12A08a	4.576	**	0.65
LN 37	N?	9.905	SR11644_250	8.021	****	0.5909091
LN 37	N?	9.984	SR11644_350	8.021	****	0.5909091
	U		BRMS-93_175	4.252	**	3
	U		Ol10F04a	14.585	******	1.25
	U		KBrM6.12_231	12.645	******	0.40625
	U		KBrM6.12_241	11.556	*****	0.375
	U		CB10431_103(F)	10.057	****	1.0909091
	U		pN102c-1	8.039	****	1.5454545
	U		sORB10c	7.712	***	1.0882353
	U		Na12E01b	6.941	***	0.3773585
	U		AP14/15a_(400)	4.659	**	0.6923077
	U		sORB10b	6.512	**	0.75
	U		BRMS-88	5.365	**	2.3
	U		CB10211_267(F)	5.339	**	0.4090909
	U		pN52d-2	5.125	**	1.16
	U		FITO131	4.902	**	0.8648649
	U		Na14E11	4.865	**	2.4761905
	U		pW105	4.85	**	1
	U		Ol10BO4a	4.704	**	0.9459459
	U		sN3766	4.486	**	2.8333333
	U		Na12E01a-2	4.415	**	0.7804878
	U		Na10G10a	4.396	**	1.4333333
	U		sS2368c	4.382	**	1.5925926
	U		Na12E06b_190(F)	4.314	**	2.4210526
	U		Ol9A06b	4.185	**	4.2142857
	U		BRMS-314_243	4.088	**	1.2
	U		Ni3-H07_210	3.947	**	0.8421053
	U		BRMS-6_177	3.932	**	0.8484848

Appendix 5.7: 2006 Broken LD50 KW single marker analysis output

LN	N	Position	Locus	K*	Signif.	Allele expression ratio (A:B)
LN 18	N3/N13	0.000	BN12A_303(F)	4.860	**	0.8
LN 18	N3/N13	25.637	sS2368b	4.860	**	0.8
LN 13	N8	27.065	Ol13B02b	6.000	**	0.8
LN 16	N10/N19	0.000	BRMS-19	4.267	**	0.5
LN 16	N10/N19	13.688	sNRD49	6.000	**	0.8
LN 16	N10/N19	15.704	CB10079_170(F)	6.000	**	0.8
LN 16	N10/N19	18.422	sORH62	6.000	**	0.8
LN 16	N10/N19	21.437	BRMS-62_178	6.000	**	0.8
LN 1	N11	4.197	pN52f	3.857	**	1
U	U	24	Na10C08a	4.083	**	1
U	U	62	AP14/15a(400)	4.860	**	0.8
U	U	92	CB10079_205(F)	4.200	**	3.5
U	U	115	BRMS-6_177	6.000	**	0.8

Appendix 5.8 2009 Broken LD50 KW single marker analysis output

LN	N	Position	Locus	K*	Signif.	Allele expression ratio (A:B)
LN 2	N1	18.368	CB10277_236(F)	8.182	****	1.392857143
LN 2	N1	32.954	CB10258_215(F)	4.909	**	0.914285714
LN 3	N2/N12	71.920	sN1925a	9.495	****	0.825
LN 5	N3	48.443	sNRB35	4.301	**	0.237288136
LN 18	N3/N13	0.000	BN12A_303(F)	11.059	*****	0.942857143
LN 18	N3/N13	11.315	Ni2-B03_148	16.486	*******	0.657894737
LN 18	N3/N13	18.136	BRMS-6_159	9.022	****	0.619047619
LN 18	N3/N13	25.637	sS2368b	15.378	*******	0.627906977
LN 18	N3/N13	37.303	Na10G10b	9.357	****	0.254545455
LN 18	N3/N13	39.922	CB10079_201(F)	4.736	**	0.38
LN 11	N7/N17	16.627	TW-008a	6.727	***	2.181818182
LN 11	N7/N17	22.578	Na12H07a	11.560	*****	1.769230769
LN 11	N7/N17	48.386	KBr09.8_221	7.608	***	1.096774194
LN 11	N7/N17	27.188	pN151a	5.681	**	3.133333333
LN 11	N7/N17	59.148	sN0818	4.521	**	1.464285714
LN 12	N7/N17	18.822	TW-008d	5.348	**	1.090909091
LN 12	N7/N17	31.586	Sn3274c	5.503	**	1.28125
LN 12	N7/N17	34.853	OL12B05_617(F)	5.780	**	1
LN 12	N7/N17	35.283	CB10277_619(F)	9.299	****	1.060606061
LN 12	N7/N17	37.432	CB10124_297(F)	8.546	****	1.3
LN 15	N9/N15	0.000	Na12E06b_231(F)	3.967	**	0.736842105
LN 15	N9/N15	7.240	OL12F02b	4.759	**	0.659090909
LN 15	N9/N15	8.871	OL12F02a	6.450	**	0.697674419
LN 15	N9/N15	18.704	sNRB68	5.080	**	0.666666667
LN 15	N9/N15	33.188	pW122	5.695	**	0.857142857
LN 15	N9/N15	35.933	sN1988	5.913	**	0.636363636
LN 15	N9/N15	36.783	SN1988_220	4.357	**	0.7
LN 15	N9/N15	36.783	SN1988_270	4.357	**	0.7
LN 16	N10/N19	4.657	TW-007a	5.654	**	0.5
LN 6	N13	9.884	Ni2B03_400	4.774	**	1.03125
LN 21	N?	11.694	CB10305_115	6.917	***	0.828571429
LN 24	N?	21.362	Ni2B03_198	6.646	***	0.861111111

LN	N	Position	Locus	K*	Signif.	
LN 24	N?	32.612	Ni2-B03_180	4.645	**	1.066666667
LN 23	N?	15.588	Na12H07e	5.660	**	1.181818182
LN 23	N?	20.612	Na10C01a	7.241	***	1.344827586
LN 23	N?	34.303	CB10109	6.751	***	1.296296296
LN 30	N?	0.000	CB10587_185(F)	10.734	****	1.09375
LN 33	N?	0.000	Na12H07g	6.638	***	5
LN 33	N?	5.291	sN2187c	4.383	**	3.5625
LN 37	N?	9.905	SR11644_250	3.926	**	0.590909091
LN 37	N?	9.984	SR11644_350	3.926	**	0.590909091
LN 38	N?	0.000	BN12A_266(F)	7.167	***	1.68
LN 38	N?	2.502	FITO66_208	5.546	**	1.833333333
			CB10299_160	14.356	******	0.58974359
			sN0212b	10.795	****	1.090909091
			Ol10BO4a	10.384	****	0.945945946
			Na12F03b	9.241	****	0.531914894
			OL13C12c	8.835	****	0.894736842
			KBrM6.12_231	7.451	***	0.40625
			Na10C08a	6.714	***	1.290322581
			FITO66_240	6.302	**	1.379310345
			KBrM6.12_241	6.007	**	0.375
			BRMS-93_234	5.733	**	1.208333333
			sORC20	5.423	**	1.21875
			Ni2B03_600	5.364	**	1.666666667
			BRMS-23_155	4.824	**	0.456521739
			Ol10F04a	4.372	**	1.25
			sN2187a	4.354	**	0.520833333
			sS2368a	4.234	**	5.363636364
			sORA84_190	4.084	**	0.674418605

Appendix 5.9: 2006 Intact adjusted LD50 KW single marker analysis output

LN	N	Position	Locus	K*	Signif.
LN 11	N7/N17	48.386	KBr09.8_221	6.000	**
LN 11	N7/N17	59.148	sN0818	6.000	**
LN 11	N7/N17	77.292	sN2567	5.333	**
LN 24	N?	21.362	Ni2B03_198	5.400	**
LN 24	N?	32.612	Ni2-B03_180	5.000	**
LN 28	N?	0.000	Na12H06	4.000	**
LN 28	N?	12.863	Ol10H02a	4.200	**
LN 29	N?	17.013	Ol11B03b	5.400	**
U	U	24	Na10C08a	4.083	**
U	U	34	Ol9A06b	4.860	**
U	U	49	sN0212b	5.000	**
U	U	92	CB10079_205(F)	4.200	**

Appendix 5.10: 2009 Intact adjusted LD50 KW single marker analysis output

LN	N	Position	Locus	K*	Signif.	Allele expression ratio
LN 11	N7/N17	27.188	pN151a	3.923	**	1.1333333
LN 12	N7/N17	31.586	Sn3274c	5.347	**	1.28125
LN 12	N7/N17	35.280	CB10277_619(F)	5.483	**	1.06061
LN 12	N7/N17	43.443	CB10354_297(F)	6.636	**	0.2372883
LN 11	N7/N17	22.578	Na12H07a	4.404	**	1.7692308

LN 12	N7/N17	45.038	BRAS19	5.200	**	1.4285714
LN 12	N7/N17	50.429	Na10C08b	5.154	**	0.9459459
LN 15	N9/N15	18.704	sNRB68	3.960	**	0.6666667
LN 16	N10/N19	4.657	TW-007a	5.654	**	0.5
LN 3	N2/N12	71.920	sN1925a	4.025	**	0.825
LN 6	N13	6.983	KBr09.8_302	4.713	**	1
LN 6	N13	9.884	Ni2B03_400	7.025	***	1.03125
LN 24	N?	21.362	Ni2B03_198	4.787	**	0.8611111
LN 37	N?	0.000	Na12A08a	5.095	**	0.65
LN 37	N?	9.905	SR11644_250	9.308	****	0.5909091
LN 37	N?	9.984	SR11644_350	9.308	****	0.5909091
LN 38	N?	0.000	BN12A_266(F)	3.934	**	1.68
	U		CB10431_103(F)	14.137	******	1.0909091
	U		Ol10F04a	11.713	*****	1.25
	U		KBrM6.12_231	10.435	****	0.40625
	U		KBrM6.12_241	8.867	****	0.375
	U		Ol10BO4a	6.116	**	0.9459459
	U		KBrC24.14	5.148	**	1.32
	U		pW105	5.110	**	1
	U		sORB10c	4.413	**	0.75
	U		Na10C08a	4.403	**	1.2903226
	U		Na12E06b_190(F)	4.314	**	2.4210526
	U		sORB10b	4.045	**	1.0571429
	U		CB10299_160	3.899	**	0.5897436

Appendix 5.11: 2006 Broken adjusted LD50 KW single marker analysis

LN	N	Position	Locus	K*	Signif.	Allele expression ratio (A:B)
LN 18	N3/N13	0.000	BN12A_303(F)	4.860	**	0.8
LN 18	N3/N13	25.637	sS2368b	4.860	**	0.8
LN 13	N8	27.065	Ol13B02b	6.000	**	0.8
LN 16	N10/N19	0.000	BRMS-19	4.267	**	0.5
LN 16	N10/N19	13.688	sNRD49	6.000	**	0.8
LN 16	N10/N19	15.704	CB10079_170(F)	6.000	**	0.8
LN 16	N10/N19	18.422	sORH62	6.000	**	0.8
LN 16	N10/N19	21.437	BRMS-62_178	6.000	**	0.8
LN1	N11	4.197	pN52f	3.857	**	1
U	U	24	Na10C08a	4.083	**	1
U	U	62	AP14/15a(400)	4.860	**	0.8
U	U	92	CB10079_205(F)	4.200	**	3.5
U	U	115	BRMS-6_177	6.000	**	0.8

Appendix 5.12 2009 Broken adjusted LD50 KW single marker analysis output

LN	N	Locus	Reg F prob	Additivity	Allele expression ratio (A:B)
LN 3	N2/N12	Ol13E08c	0.01043	-0.3	1.202
LN 3	N2/N12	sN2374c	0.00468	-0.37	1.25
LN 4	N2/N12	sN1925c	0.0062	-0.3	1.214
LN 4	N2/N12	sR94102_320R	0.00051	-0.4	1.279
LN 4	N2/N12	pN102c-2	0.00101	-0.43	1.318
LN 4	N2/N12	Na10C08d	0.02208	-0.26	1.178
LN 5	N3	sORC76c	0.02361	-0.27	1.18
LN 5	N3	TW-010c	0.00079	-0.42	1.284
LN 5	N3	AP14/15b_(400)	0.00049	-0.46	1.314
LN 5	N3	AP2/4a_(281)	0.00095	-0.48	1.327
LN 5	N3	OL11G11b	0.00006	-0.57	1.389
LN 5	N3	sNRB35	0.00001	-0.6	1.41
LN 9	N5	Na12E01a-1	0.02468	0.25	0.852
LN 9	N5	BRMS-166_199	0.02328	0.27	0.845
LN 9	N5	sORA84_160	0.01913	0.27	0.843
LN 9	N5	sNRC86	0.02835	0.25	0.852
LN 9	N5	Na10B08	0.02199	0.26	0.848
LN 1	N11	BRMS-214_261	0.03435	0.25	0.857
LN 6	N13	Na10F06b	0.01057	-0.29	1.199
LN 6	N13	TW-010a	0.03593	-0.24	1.162
LN 22	N?	KBrA14.8_221	0.03803	-0.26	1.175
LN 22	N?	KBrA14.8_238	0.04008	-0.26	1.172
LN 22	N?	Ol10G05	0.03835	-0.23	1.16
LN 34	N?	sS1854b	0.04906	0.23	0.866
LN 20	N?	Ni4-A07_250	0.01307	-0.33	1.22
LN 20	N?	Na12A08c	0.0404	-0.25	1.17
LN 20	N?	Ol10H02c	0.03631	-0.29	1.19
LN 20	N?	Ol13A10	0.02808	-0.33	1.22
LN 20	N?	Na12F12	0.04443	-0.28	1.187
	U	KBrM6.12_231	0.00107	-0.56	1.376
	U	KBrM6.12_241	0.00105	-0.58	1.391
	U	pN102c-1	0.00101	0.43	0.759
	U	Na12E01a-2	0.02468	-0.25	1.174
	U	Na12E01b	0.00011	-0.47	1.326
	U	Ol9A06b	0.00535	0.39	0.792
	U	sNRC89a	0.00661	-0.31	1.217
	U	sNRC89b	0.02082	-0.26	1.181
	U	sN3766	0.01906	0.31	0.827
	U	sN2187a	0.01251	-0.3	1.202
	U	sN2442a	0.01691	0.68	0.695
	U	AP14/15a(400)	0.0044	-0.34	1.232
	U	AP2/4b(281)	0.00493	-0.48	1.33
	U	Ni3-H07_210	0.03843	-0.34	1.244
	U	CB10211_267(F)	0.02222	-0.32	1.212

Appendix 5.13 2006 Pod Mass Single Marker Regression output

LN	N	Locus	Reg F prob	Additivity	Allele expression ratio (A:B)
LN 13	N8	Ol13B02b	0.0397738	-0.47	1.227
LN 16	N10/N19	BRMS-19	0.0418622	0.5	0.799

LN	N	Locus	Reg F prob	Additivity	Allele expression ratio (A:B)
LN 16	N10/N19	sNRD49	0.0052064	0.57	0.776
LN 16	N10/N19	CB10079_170(F)	0.0052064	0.57	0.776
LN 16	N10/N19	sORH62	0.0052064	0.57	0.776
LN 16	N10/N19	BRMS-62_178	0.0052064	0.57	0.776
LN 12	N7/17	Na10C08b	0.0239456	-0.63	1.293
	U	CB10045	0.0125335	-0.64	1.298
	U	sS2368a	0.035352	0.76	0.744
	U	CB10443_290	0.035352	0.76	0.744
	U	FITO122_365	0.035352	-0.76	1.344
	U	FITO122_461	0.035352	-0.76	1.344
	U	BRMS-6_177	0.0397738	-0.47	1.227
	U	Na10C01a	0.0474951	0.46	0.823

Appendix 5.14 2009 Pod Mass Single Marker Regression output

LN	N	Locus	Reg F prob	Additivity	Allele expression ratio (A:B)
LN 3	N2/N12	sORB10a	0.0497366	-0.56	1.272
LN 5	N3	SNRA56_(280)	0.0480321	-0.5	1.259
LN 5	N3	AP14/15b_(400)	0.0480321	-0.5	1.259
LN 14	N18	CB10305_265	0.0112772	-0.32	1.163
LN 14	N18	CB10179	0.0112772	-0.32	1.163
LN 22	N?	Na12H04a	0.0412923	-0.57	1.279
	U	sS2368a	0.0037995	0.87	0.707
	U	CB10443_290	0.0037995	0.87	0.707
	U	FITO122_365	0.0037995	-0.87	1.414
	U	FITO122_461	0.0037995	-0.87	1.414
	U	Na10D09b	0.0040345	0.84	0.718
	U	Na12A05a	0.0312116	-0.46	1.238
	U	BRMS-105_95	0.0347707	0.55	0.792
	U	CB10079_205(F)	0.0352336	0.55	0.793
	U	BRMS-195	0.0489534	0.68	0.742

Appendix 5.15 2006 (nine lines) Pod Mass Single Marker Regression output

LN	N	Locus	Reg F prob	Additivity	Allele expression ratio (A:B)
LN 3	N2/N12	Ol13E08c	0.0205172	-0.16	1.263
LN 3	N2/N12	sN2374c	0.0107332	-0.2	1.319
LN 3	N2/N12	CB10026_145(F)	0.0392298	-0.16	1.247
LN 4	N2/N12	sN1925c	0.0118438	-0.17	1.282
LN 4	N2/N12	sR94102_320R	0.0009194	-0.22	1.381
LN 4	N2/N12	pN102c-2	0.0045906	-0.22	1.414
LN 4	N2/N12	Na10C08d	0.0173177	-0.16	1.265
LN 5	N3	sORC76c	0.0443511	-0.14	1.229
LN 5	N3	TW-010c	0.004563	-0.21	1.331
LN 5	N3	AP14/15b_(400)	0.0030927	-0.23	1.38
LN 5	N3	AP2/4a_(281)	0.0081465	-0.23	1.373
LN 5	N3	OL11G11b	0.0005056	-0.3	1.485
LN 5	N3	sNRB35	0.0001866	-0.3	1.499
LN 9	N5	Na12E01a-1	0.0242262	0.15	0.801
LN 9	N5	BRMS-166_199	0.0172666	0.16	0.791
LN 9	N5	sORA84_160	0.0167715	0.16	0.784
LN 9	N5	sNRC86	0.0180255	0.16	0.789

LN	N	Locus	Reg F prob	Additivity	Allele expression ratio (A:B)
LN 9	N5	Na10B08	0.0463325	0.13	0.818
LN 12	N7/N17	TW-008c	0.0106836	-0.18	1.33
LN 12	N7/N17	TW-008b	0.0372321	-0.14	1.241
LN 12	N7/N17	TW-008d	0.0348412	-0.14	1.234
LN 12	N7/N17	CB10277_619(F)	0.0225814	-0.15	1.246
LN 15	N9/N15	Na12E06b_231(F)	0.0420061	-0.14	1.227
LN 15	N9/N15	OL12F02a	0.0430217	-0.14	1.223
LN 15	N9/N15	CB10305_115	0.0185892	-0.16	1.257
LN 1	N11	CB10443_281	0.049469	0.13	0.824
LN 22	N?	Na12H04a	0.0477445	-0.13	1.214
LN 22	N?	Ol10G05	0.0263502	-0.15	1.246
LN 20	N?	Ni4-A07_250	0.0381265	-0.17	1.262
LN 20	N?	Na12A08c	0.0375869	-0.15	1.244
LN 20	N?	Ol10H02c	0.0345998	-0.17	1.271
LN 24	N?	pN52d-1	0.0431131	0.16	0.77
LN 19	N?	CB10373(F)	0.0293994	-0.15	1.243
LN 34	N?	sS1854b	0.0463255	0.14	0.818
LN 38	N?	BN12A_266(F)	0.0216659	0.16	0.794
LN 38	N?	FITO66_208	0.0188473	0.16	0.791
	U	pN202b	0.0377387	-0.16	1.294
	U	KBrM6.12_231	0.0215056	-0.22	1.338
	U	KBrM6.12_241	0.0142537	-0.24	1.373
	U	pN102c-1	0.0045906	0.22	0.707
	U	pN52d-2	0.0431131	-0.16	1.298
	U	Na12E01a-2	0.0242262	-0.15	1.249
	U	Na12E01b	0.0006385	-0.25	1.412
	U	Na12C08	0.0233136	-0.15	1.261
	U	OL13C12c	0.0314905	-0.15	1.245
	U	sNRC89a	0.0024966	-0.2	1.349
	U	sNRC89b	0.0023602	-0.2	1.348
	U	sS2368a	0.0314498	-0.2	1.399
	U	sS2368c	0.048484	-0.14	1.235
	U	AP14/15a(400)	0.0367619	-0.14	1.229
	U	AP2/4b(281)	0.0075859	-0.27	1.459
	U	CB10587_260(F)	0.0476529	0.14	0.815
	U	CB10211_116(F)	0.0080955	0.26	0.718
	U	CB10299_160	0.0241935	-0.17	1.277
	U	FITO66_240	0.0323593	0.14	0.811
	U	BRMS-88	0.010726	0.19	0.765

Appendix 5.16 2006 Seed Mass Single Marker Regression output

LN	N	Locus	Reg F prob	Additivity	Allele expression ratio (A:B)
LN 3	N2/N12	sR94102_298R	0.0017726	-0.7	1.5
LN 10	N6	Na10F06a	0.0420388	-0.45	1.305
LN 11	N7/N17	KBr09.8_221	0.0027322	0.67	0.668
LN 11	N7/N17	sN0818	0.0028075	0.65	0.682
LN 11	N7/N17	Pw150	0.0120994	0.62	0.702
LN 12	N7/N17	TW-008c	0.0005468	0.8	0.635
LN 12	N7/N17	TW-008b	0.0003042	0.8	0.617
LN 12	N7/N17	TW-008d	0.0003889	0.75	0.636
LN 19	N?	CB10373(F)	0.0191599	0.53	0.73
LN 19	N?	SN11670_115	0.0207317	0.53	0.737
LN 22	N?	Na12H04a	0.0145854	0.53	0.722

LN 35	N?	sN2321	0.0156544	0.54	0.731
LN 37	N?	SR11644_250	0.026475	-0.51	1.344
LN 37	N?	SR11644_350	0.026475	-0.51	1.344
LN 38	N?	BN12A_266(F)	0.0254022	-0.53	1.397
LN 38	N?	FITO66_208	0.0294528	-0.52	1.38
	U	Ol10D10b	0.0283382	0.48	0.751
	U	sN0212b	0.0005352	0.75	0.648
	U	sNRB93	0.0329257	0.47	0.757
	U	sN2442a	0.0025321	1.61	0.506
	U	CB10258_595(F)	0.002234	0.72	0.64
	U	CB10431_59(F)	0.0230223	-0.77	1.524
	U	CB10299_160	0.0478766	0.51	0.73
	U	CB10443_290	0.0022713	1.21	0.566

Appendix 5.17 2006 Seed Damage Single Marker Regression output

LN	N	Locus	Reg F prob	Additivity	Allele expression ratio (A:B)
LN 3	N2/N12	Ol13E08c	0.01735	-8.26	1.661
LN 3	N2/N12	sN2374c	0.01109	-9.91	1.762
LN 3	N2/N12	Na12H09	0.03473	-7.65	1.588
LN 4	N2/N12	sR94102_320R	0.0454	-7.01	1.565
LN 5	N3	IGF2544_b	0.0213	-7.76	1.693
LN 5	N3	SNRA56_(280)	0.02181	-8.52	1.711
LN 5	N3	sORC76c	0.01154	-8.86	1.731
LN 5	N3	TW-010c	0.00029	-13.44	2.177
LN 5	N3	AP14/15b_(400)	0.00014	-14.85	2.261
LN 5	N3	AP2/4a_(281)	0.00009	-16.64	2.394
LN 5	N3	OL11G11b	0.00056	-14.77	2.151
LN 5	N3	sNRB35	0.00003	-16.98	2.408
LN 18	N3/N13	BN12A_303(F)	0.05064	-6.9	1.565
LN 18	N3/N13	Ni2-B03_148	0.04117	-7.86	1.621
LN 18	N3/N13	Na10G10b	0.00255	-12.85	2.003
LN 7	N4	SN13034_140	0.02784	6.93	0.615
LN 7	N4	SN13034_150	0.02784	6.93	0.615
LN 9	N5	Na10B08	0.03702	7.09	0.629
LN 10	N6	BRMS-101	0.03531	-7.52	1.637
LN 15	N9/N15	sN1988	0.04184	7.03	0.613
LN 17	N10/N19	KBr09.8_201	0.01371	-8.83	1.739
LN 16	N10/N19	Ol11B03a	0.04488	7.06	0.612
LN 6	N13	Na10F06b	0.00457	-9.35	1.843
LN 6	N13	TW-010a	0.01821	-8.07	1.701
LN 6	N13	OL11G11a	0.02458	-7.45	1.646
LN 6	N13	KBr09.8_302	0.01558	-8.54	1.746
LN 6	N13	Ni2B03_400	0.01182	-9.19	1.827
LN 17	N?	Na12H04b	0.04154	-6.9	1.568
LN 20	N?	Ni4-A07_250	0.01314	-9.98	1.738
LN 20	N?	Na12A08c	0.04452	-7.38	1.56
LN 20	N?	Ol10H02c	0.03448	-8.56	1.64
LN 20	N?	Ol13A10	0.00663	-12.13	1.917
LN 20	N?	Na12F12	0.01974	-9.7	1.739
LN 20	N?	sORB36b	0.01434	-10.05	1.75
LN 24	N?	Ni2B03_198	0.03254	7.79	0.596
LN 37	N?	Na12A08a	0.04501	-7.51	1.587
LN 37	N?	SR11644_250	0.01897	-8.16	1.686

LN 37	N?	SR11644_350	0.01897	-8.16	1.686
	U	KBrM6.12_231	0.00002	-21.83	2.844
	U	KBrM6.12_241	0.00002	-22.46	2.897
	U	BRMS-93_175	0.0342	8.94	0.597
	U	pW105	0.04796	-8.58	1.762
	U	Na12E01b	0.00004	-14.75	2.308
	U	Na12A05a	0.04413	-6.77	1.565
	U	Na10C08a	0.01609	8.27	0.587
	U	Ol10F04a	0.0275	-7.39	1.665
	U	Ol9A06b	0.00083	13.78	0.479
	U	Ol9A06c	0.00433	9.77	0.548
	U	sS1716b	0.00322	-11.22	1.951
	U	sN3766	0.00691	10.77	0.55
	U	sN0212b	0.04843	6.83	0.641
	U	sORB10b	0.02733	-7.38	1.626
	U	sN2187a	0.00075	-11.64	2.013
	U	AP14/15a(400)	0.02301	-8.31	1.691
	U	AP2/4b(281)	0.00823	-16.75	2.512
	U	Na12E06b_190(F)	0.03112	7.47	0.623
	U	CB10211_267(F)	0.02849	-9.39	1.708
	U	CB10443_290	0.03558	12.96	0.523
	U	BRMS-23_155	0.01547	-9.4	1.732

Appendix 5.18 2006 Intact LD50 Single Marker Regression output

LN	N	Locus	Reg F prob	Additivity	Allele expression ratio (A:B)
LN 18	N3/N13	BN12A_303(F)	0.00588	-10.81	2.272
LN 18	N3/N13	sS2368b	0.00588	-10.81	2.272
LN 18	N3/N13	Na10G10b	0.04299	-9.39	1.923
LN 18	N3/N13	CB10079_201(F)	0.04299	-9.39	1.923
LN 10	N6	sN2837_120	0.02694	-10.99	2.218
LN 10	N6	Ni2B03_298	0.03889	-10.36	2.072
LN 11	N7/N17	sN0818	0.02676	9.48	0.489
LN 11	N7/N17	sN2567	0.03787	10.06	0.458
LN 15	N9/N15	sNRB68	0.04299	9.39	0.52
LN 15	N9/N15	sN1988	0.01699	9.95	0.439
LN 15	N9/N15	SN1988_220	0.03223	10.09	0.435
LN 15	N9/N15	SN1988_270	0.03223	10.09	0.435
LN 15	N9/N15	KBr17.27	0.01699	9.95	0.439
LN 14	N18	SN11670_80	0.01699	-9.95	2.28
LN 24	N?	Ni2B03_198	0.02433	10.11	0.394
LN 24	N?	Ni2-B03_180	0.0441	10	0.396
LN 29	N?	TW-007b	0.02101	-11.79	2.517
LN 29	N?	Ol11B03b	0.02433	-10.11	2.539
LN 29	N?	BRMS-62_173	0.01699	-9.95	2.28
	U	Na10D09b	0.04566	14.68	0.459
	U	Na10C08a	0.00866	11.54	0.403
	U	Ol9A06b	0.02676	9.48	0.489
	U	sNRC89b	0.02544	11.4	0.486
	U	sS2368a	0.01891	15.57	0.426
	U	AP14/15a(400)	0.00588	-10.81	2.272
	U	CB10079_205(F)	0.01203	12.27	0.463
	U	CB10443_290	0.01891	15.57	0.426
	U	FITO122_365	0.01891	-15.57	2.346
	U	FITO122_461	0.01891	-15.57	2.346

Appendix 5.19 2009 Intact LD50 Single Marker Regression output

N	LN	Locus	Reg F prob	Additivity	Allele expression ratio (A:B)
LN 5	N3	AP2/4a_(281)	0.0474038	-43.31	4.161
LN 18	N3/N13	BN12A_303(F)	0.012624	-39.47	3.042
LN 18	N3/N13	Ni2-B03_148	0.0290493	-36.25	2.746
LN 18	N3/N13	sS2368b	0.012624	-39.47	3.042
LN 9	N5	KBrG23.30_185	0.018214	-38.16	2.917
LN 9	N5	CB10229_287(F)	0.0415681	-34.33	2.445
LN 9	N5	CB10487_280(F)	0.018214	-38.16	2.917
LN 10	N6	sN2837_120	0.007057	-46.57	3.135
LN 10	N6	Ni2B03_298	0.0029408	-48.47	3.435
LN 15	N9/N15	SN1988_220	0.0401249	38.58	0.323
LN 15	N9/N15	SN1988_270	0.0401249	38.58	0.323
	U	Na12A05a	0.0433108	-34.35	2.931
	U	Na10C08a	0.0240039	40.36	0.314
	U	sS1716a	0.0212319	37.57	0.299
	U	sS1716b	0.0354873	-39.87	3.91
	U	sN3766	0.0501095	34.51	0.448
	U	AP14/15a(400)	0.012624	-39.47	3.042
	U	BRMS-195	0.0232349	48.01	0.27
	U	CB10079_205(F)	0.0026271	52.11	0.327
	U	BRMS-23_155	0.0290493	-36.25	2.746

Appendix 5.20 2006 (nine line) Intact LD50 Single Marker Regression output

LN	N	Locus	Reg F prob	Additivity	Allele expression ratio (A:B)
LN 3	N2/N12	Ol13E08c	0.0100012	-11.82	1.547
LN 4	N2/N12	sR94102_320R	0.0184454	-10.94	1.514
LN 4	N2/N12	pN102c-2	0.0219332	-11.44	1.583
LN 4	N2/N12	Na10C08d	0.0233631	-10.17	1.475
LN 5	N3	TW-010c	0.0034773	-14.69	1.688
LN 5	N3	AP14/15b_(400)	0.001331	-16.83	1.766
LN 5	N3	AP2/4a_(281)	0.0003721	-20.32	1.926
LN 5	N3	OL11G11b	0.0004742	-19.79	1.883
LN 5	N3	sNRB35	6.431E-06	-23.99	2.143
LN 18	N3/N13	Na10G10b	0.0043737	-16.25	1.724
LN 9	N5	Na12E01a-1	0.0370635	9.3	0.698
LN 9	N5	Na10B08	0.0296935	9.8	0.681
LN 15	N9/N15	sN1988	0.0465238	9.16	0.687
LN 16	N10/N19	Ol11B03a	0.0186071	10.9	0.639
LN 6	N13	Na10F06b	0.0012846	-14.01	1.728
LN 6	N13	TW-010a	0.0068335	-12.24	1.617
LN 6	N13	OL11G11a	0.0099552	-11.31	1.57
LN 6	N13	KBr09.8_302	0.0068176	-12.66	1.642
LN 6	N13	Ni2B03_400	0.0051862	-13.48	1.697
LN 20	N?	Ni4-A07_250	0.0098355	-13.7	1.592
LN 20	N?	Na12A08c	0.0418071	-9.95	1.438

LN	N	Locus	Reg F prob	Additivity	Allele expression ratio (A:B)
LN 20	N?	Ol10H02c	0.0396228	-11.11	1.481
LN 20	N?	Ol13A10	0.0164665	-13.68	1.601
LN 20	N?	Na12F12	0.0153825	-13.29	1.593
LN 20	N?	sORB36b	0.0095809	-14.08	1.614
LN 24	N?	pN52d-1	0.0235681	12.06	0.606
LN 24	N?	Ni2B03_198	0.0342748	10.27	0.667
LN 37	N?	Na12A08a	0.0318987	-10.67	1.48
LN 37	N?	SR11644_250	0.0082823	-12.21	1.59
LN 37	N?	SR11644_350	0.0082823	-12.21	1.59
U	U	FITO67_233(F)	0.0469588	9.25	0.701
U	U	BRMS-166_199	0.0313096	10.18	0.673
U	U	KBr09.8_201	0.0163825	-11.47	1.543
U	U	KBrM6.12_231	8.842E-06	-30.09	2.52
U	U	KBrM6.12_241	9.693E-06	-31.09	2.571
U	U	pN102c-1	0.0219332	11.44	0.632
U	U	pN52d-2	0.0235681	-12.06	1.651
U	U	pW105	0.0284282	-11.52	1.578
U	U	Na12E01a-2	0.0370635	-9.3	1.432
U	U	Na12E01b	8.703E-05	-18.73	1.916
U	U	Na10C08a	0.0254207	10.26	0.673
U	U	Ol10F04a	0.0033617	-12.94	1.705
U	U	Ol9A06b	0.0029587	16.44	0.577
U	U	sS1716b	0.0311885	-11.07	1.495
U	U	sN3766	0.013995	13.07	0.637
U	U	sORB10b	0.0095198	-11.47	1.571
U	U	sN2187a	0.003475	-13.56	1.642
U	U	AP14/15a(400)	0.0142848	-11.71	1.559
U	U	AP2/4b(281)	0.0338558	-17.16	1.732
U	U	Ni3-H07_210	0.0363958	-13.74	1.669
U	U	CB10431_103(F)	0.0312548	-9.97	1.485
U	U	CB10443_290	0.0461983	16.42	0.596

Appendix 5.21 2006 Broken LD50 Single Marker Regression output

LN	N	Locus	Reg F prob	Additivity	Allele expression ratio (A:B)
LN 18	N3/N13	BN12A_303(F)	0.0283588	-14.26	1.786
LN 18	N3/N13	sS2368b	0.0283588	-14.26	1.786
LN 13	N8	CALSSR(F)	0.050487	-13.16	1.766
LN 13	N8	Ol13B02b	0.0093407	-15.86	1.909
LN 16	N10/N19	BRMS-19	0.0217201	15.5	0.478
LN 16	N10/N19	sNRD49	0.004441	16.65	0.478
LN 16	N10/N19	CB10079_170(F)	0.004441	16.65	0.478
LN 16	N10/N19	sORH62	0.004441	16.65	0.478
LN 16	N10/N19	BRMS-62_178	0.004441	16.65	0.478
LN 1	N11	pN52f	0.042648	-19.08	2.189
	U	Na10C08a	0.0438046	14.88	0.541
	U	sNO202	0.050487	-13.16	1.766
	U	AP14/15a(400)	0.0283588	-14.26	1.786
	U	CB10079_205(F)	0.0276755	17.1	0.548
	U	BRMS-6_177	0.0093407	-15.86	1.909

| | | U | BRMS-314_243 | 0.050487 | -13.16 | 1.766 |

Appendix 5.22 2009 Broken LD50 Single Marker Regression output

LN	N	Locus	Reg F prob	Additivity	Allele expression ratio (A:B)
LN 18	N3/13	BN12A_303(F)	0.0167656	-42.87	2.496
LN 18	N3/13	sS2368b	0.0167656	-42.87	2.496
LN 9	N5	KBrG23.30_185	0.0153444	-43.23	2.517
LN 9	N5	CB10229_287(F)	0.0360434	-39.71	2.24
LN 9	N5	CB10487_280(F)	0.0153444	-43.23	2.517
LN 10	N6	sN2837_120	0.0143109	-50.12	2.597
LN 10	N6	Ni2B03_298	0.0051531	-53	2.86
	U	Na10C08a	0.0340859	42.69	0.403
	U	sS1716a	0.033143	39.73	0.392
	U	sS2368a	0.0298752	63.65	0.39
	U	AP14/15a(400)	0.0167656	-42.87	2.496
	U	BRMS-195	0.0458076	51.99	0.359
	U	CB10443_290	0.0298752	63.65	0.39
	U	FITO122_365	0.0298752	-63.65	2.566
	U	FITO122_461	0.0298752	-63.65	2.566
	U	CB10079_205(F)	0.002085	58.67	0.371

Appendix 5.23 2006 (nine lines) Broken LD50 Single Marker Regression output

LN	N	Locus	Reg F prob	Additivity	Allele expression ratio (A:B)
LN 5	N3	BRMS-303	0.0333145	-8.32	1.545
LN 5	N3	TW-010c	0.006674	-7.4	1.516
LN 5	N3	AP14/15b_(400)	0.0048236	-8.21	1.554
LN 5	N3	AP2/4a_(281)	0.002255	-9.72	1.65
LN 5	N3	OL11G11b	0.0377203	-6.61	1.419
LN 5	N3	sNRB35	0.0051814	-8.46	1.558
LN 18	N3/N13	BN12A_303(F)	0.0027898	-7.46	1.57
LN 18	N3/N13	Ni2-B03_148	0.0003361	-9.64	1.745
LN 18	N3/N13	sS2368b	0.0008032	-8.25	1.61
LN 18	N3/N13	Na10G10b	0.003413	-9.05	1.601
LN 7	N4	pN151b	0.0441252	4.51	0.754
LN 7	N4	SN13034_140	0.0429112	4.44	0.752
LN 7	N4	SN13034_150	0.0429112	4.44	0.752
LN 10	N6	Ni2B03_298	0.0393858	-5.42	1.373
LN 10	N6	BRMS-101	0.0250542	-5.74	1.404
LN 11	N7/N17	Na12H07a	0.020453	5.83	0.716
LN 11	N7/N17	pN151a	0.0316798	6.43	0.701
LN 11	N7/N17	KBr09.8_221	0.0171255	6.28	0.689
LN 11	N7/N17	sN0818	0.0215438	5.8	0.711
LN 11	N7/N17	sN2567	0.043756	5.02	0.742
LN 15	N9/N15	pW122	0.0367569	4.65	0.739
LN 15	N9/N15	sN1988	0.0229865	5.67	0.703
LN 15	N9/N15	SN1988_220	0.0411526	5.24	0.719
LN 15	N9/N15	SN1988_270	0.0411526	5.24	0.719
LN 16	N10/N19	Ol11B03b	0.0479264	-4.92	1.358
LN 17	N10/N19	KBr09.8_201	0.0112771	-6.49	1.455
LN 17	N10/N19	Na12H04b	0.0300518	-5.33	1.369
LN 6	N13	Na10F06b	0.0313061	-5.21	1.361
LN 6	N13	OL11G11a	0.0467601	-4.8	1.335
LN 6	N13	KBr09.8_302	0.0279876	-5.57	1.392

LN	N	Locus	Reg F prob	Additivity	Allele expression ratio (A:B)
LN 6	N13	Ni2B03_400	0.0130624	-6.52	1.478
LN 20	N?	Ol13A10	0.0277287	-7.25	1.467
LN 20	N?	sORB36b	0.0307456	-6.5	1.421
LN 23	N?	Na12H07e	0.034978	5.17	0.737
LN 23	N?	Na10C01a	0.0210416	5.91	0.712
LN 24	N?	Ni2B03_198	0.0232023	5.92	0.7
LN 24	N?	Ni2-B03_180	0.0330692	5.85	0.7
LN 30	N?	CB10587_185(F)	0.0406913	-5.26	1.377
LN 37	N?	Na12A08a	0.0228951	-6.24	1.43
LN 37	N?	SR11644_250	0.0096502	-6.49	1.465
LN 37	N?	SR11644_350	0.0096502	-6.49	1.465
LN 38	N?	BN12A_266(F)	0.0213298	-6.04	1.467
LN 38	N?	FITO66_208	0.0339811	-5.57	1.427
	U	KBrM6.12_231	0.000154	-13.78	1.942
	U	KBrM6.12_241	0.0001984	-14.08	1.962
	U	Na12E01b	0.0028107	-7.95	1.544
	U	Na12A05a	0.0317026	-5.23	1.369
	U	Na12F03b	0.0290273	5.59	0.701
	U	Na10C08a	0.0064067	6.76	0.673
	U	Ol10F04a	0.0417352	-4.98	1.356
	U	Ol9A06b	0.0078817	8.06	0.654
	U	Ol9A06c	0.00753	6.66	0.684
	U	sS1716b	0.0060766	-7.7	1.546
	U	sN3766	0.0314231	6.21	0.717
	U	sN0212b	0.0066027	6.74	0.671
	U	sORB10b	0.044649	-4.91	1.341
	U	sN2187a	0.0037155	-7.34	1.511
	U	AP2/4b(281)	0.0391659	-9.79	1.689
	U	CB10258_345(F)	0.0473991	-5.17	1.355
	U	CB10299_160	0.0196754	6.58	0.659
	U	BRMS-23_155	0.0079427	-7.35	1.496
	U	IGF5298_c(200)	0.0302415	-5.41	1.39

Appendix 5.24 2006 Intact Adjusted LD50 Single Marker Regression output

LN	N	Locus	Reg F prob	Additivity	Allele expression ratio (A:B)
LN 18	N3/N13	BN12A_303(F)	0.0192508	-7.53	1.713
LN 18	N3/N13	sS2368b	0.0192508	-7.53	1.713
LN 11	N7/N17	KBr09.8_221	0.0140669	7.75	0.553
LN 11	N7/N17	sN0818	0.0107424	7.93	0.567
LN 11	N7/N17	sN2567	0.0113044	8.71	0.524
LN 15	N9/N15	sN1988	0.0240769	7.35	0.572
LN 15	N9/N15	SN1988_220	0.0475587	7.24	0.576
LN 15	N9/N15	SN1988_270	0.0475587	7.24	0.576
LN 15	N9/N15	KBr17.27	0.0240769	7.35	0.572
N10/N19	N18	SN11670_80	0.0240769	-7.35	1.749
LN 24	N?	Ni2B03_198	0.011869	8.29	0.502
LN 24	N?	Ni2-B03_180	0.0248334	8.1	0.508
LN 28	N?	Na12H06	0.033581	-7.15	1.96
LN 28	N?	Ol10H02a	0.038313	-8.29	2.112
LN 29	N?	Ol11B03b	0.011869	-8.29	1.991
LN 29	N?	BRMS-62_173	0.0240769	-7.35	1.749
	U	Na10C08a	0.0211837	8.26	0.543
	U	Ol9A06b	0.0165521	7.64	0.579
	U	sNRC89b	0.0506367	7.95	0.604
	U	sN0212b	0.0315924	7.82	0.549
	U	AP14/15a(400)	0.0192508	-7.53	1.713

					Allele expression ratio (A:B)
	U	CB10079_205(F)	0.024072	8.78	0.576

Appendix 5.25 2009 Intact Adjusted LD50 Single Marker Regression output

LN	N	Locus	Reg F prob	Additivity	Allele expression ratio (A:B)
LN 18	N3/N13	BN12A_303(F)	0.0084434	-34.35	3.464
LN 18	N3/N13	Ni2-B03_148	0.035423	-29.8	2.867
LN 18	N3/N13	sS2368b	0.0084434	-34.35	3.464
LN 9	N5	KBrG23.30_185	0.0142711	-32.93	3.26
LN 9	N5	CB10229_287(F)	0.0330836	-29.59	2.652
LN 9	N5	CB10487_280(F)	0.0142711	-32.93	3.26
LN 10	N6	sN2837_120	0.0048988	-40.72	3.644
LN 10	N6	Ni2B03_298	0.0020053	-41.55	3.852
LN 15	N9/N15	SN1988_220	0.0456683	32.01	0.3
LN 15	N9/N15	SN1988_270	0.0456683	32.01	0.3
LN 29	N?	TW-007b	0.0469771	-29.38	3.137
	U	KBrM6.12_231	0.046627	-30.92	3.471
	U	KBrM6.12_241	0.046627	-30.92	3.471
	U	Na10C08a	0.0185266	34.54	0.285
	U	sS1716a	0.019116	32.03	0.263
	U	sS1716b	0.036731	-33.12	4.211
	U	AP14/15a(400)	0.0084434	-34.35	3.464
	U	BRMS-195	0.0217055	38.36	0.266
	U	CB10079_205(F)	0.0029374	43.71	0.308
	U	BRMS-23_155	0.035423	-29.8	2.867

Appendix 5.26 2006 (nine lines) Pod Mass Single Marker Regression output

LN	N	Locus	Reg F prob	Additivity	Allele expression ratio (A:B)
LN 5	N3	AP14/15b_(400)	0.04017	-7.7	1.295
LN 5	N3	AP2/4a_(281)	0.00763	-10.83	1.415
LN 5	N3	OL11G11b	0.03669	-8.44	1.319
LN 5	N3	sNRB35	0.00163	-12.14	1.48
LN 18	N3/N13	BN12A_303(F)	0.02783	-7.16	1.299
LN 18	N3/N13	sS2368b	0.04061	-6.63	1.264
LN 18	N3/N13	Na10G10b	0.00612	-10.94	1.429
LN 15	N9/N15	pW122	0.03349	7.09	0.767
LN 15	N9/N15	sN1988	0.02216	7.32	0.76
LN 15	N9/N15	SN1988_220	0.0322	7.12	0.765
LN 15	N9/N15	SN1988_270	0.0322	7.12	0.765
LN 16	N10/N19	TW-007a	0.04602	7.21	0.751
LN 16	N10/N19	sNRD49	0.04412	6.26	0.798
LN 16	N10/N19	Ol11B03a	0.04979	6.46	0.786
LN 17	N10/N19	KBr09.8_201	0.01035	-8.28	1.341
LN 17	N10/N19	Na12H04b	0.03544	-6.6	1.266
LN 6	N13	Na10F06b	0.00682	-8.32	1.349
LN 6	N13	TW-010a	0.01786	-7.48	1.315
LN 6	N13	OL11G11a	0.01254	-7.67	1.324
LN 6	N13	KBr09.8_302	0.00675	-8.59	1.365
LN 6	N13	Ni2B03_400	0.00262	-9.82	1.431
LN 13	N?	Ol10F05a	0.04086	6.36	0.795
LN 24	N?	pN52d-1	0.03489	7.8	0.755
LN 24	N?	Ni2B03_198	0.01832	7.74	0.754
LN 24	N?	Ni2-B03_180	0.04613	7.01	0.771
LN 20	N?	Na12F12	0.04419	-7.73	1.299
LN 20	N?	sORB36b	0.01568	-9.28	1.361

LN 37	N?	Na12A08a	0.01043	-8.98	1.366
LN 37	N?	SR11644_250	0.00195	-9.94	1.423
LN 37	N?	SR11644_350	0.00195	-9.94	1.423
LN 38	N?	BN12A_266(F)	0.02656	-7.5	1.33
LN 38	N?	FITO66_208	0.03768	-7	1.305
	U	KBrM6.12_231	0.00002	-19.04	1.806
	U	KBrM6.12_241	0.00003	-19.59	1.83
	U	pN52d-2	0.03489	-7.8	1.325
	U	pW105	0.0368	-7.48	1.306
	U	Na12E01b	0.0062	-9.39	1.375
	U	Na10C08a	0.00921	8.24	0.746
	U	Ol10F04a	0.00177	-9.64	1.432
	U	Ol9A06b	0.02771	8.63	0.75
	U	sORB10b	0.00929	-8.08	1.342
	U	sN2187a	0.01945	-7.67	1.306
	U	CB10431_103(F)	0.01266	-7.96	1.343
	U	KBrC24.14	0.01814	-8.24	1.364

Appendix 5.27 2006 Broken Adjusted LD50 Single Marker Regression output

LN	N	Locus	Reg F prob	Additivity	Allele expression ratio (A:B)
LN 18	N3/N13	BN12A_303(F)	0.02574	-9.12	1.426
LN 18	N3/N13	sS2368b	0.02574	-9.12	1.426
LN 11	N7/N17	sN0818	0.04831	8.38	0.722
LN 13	N8	CALSSR(F)	0.02852	-9.01	1.441
LN 13	N8	Ol13B02b	0.00759	-10.18	1.487
LN 15	N9/N15	sN1988	0.0474	8.4	0.712
LN 15	N9/N15	KBr17.27	0.0474	8.4	0.712
LN 16	N10/N19	BRMS-19	0.0275	9.54	0.667
LN 16	N10/N19	sNRD49	0.01317	9.75	0.672
LN 16	N10/N19	CB10079_170(F)	0.01317	9.75	0.672
LN 16	N10/N19	sORH62	0.01317	9.75	0.672
LN 16	N10/N19	BRMS-62_178	0.01317	9.75	0.672
LN1	N11	pN52f	0.0301	-12.65	1.655
LN1	N11	CB10443_281	0.03611	-9.22	1.478
LN1	N11	CB10277_236(F)	0.03611	-9.22	1.478
LN 14	N18	SN11670_80	0.0474	-8.4	1.405
LN 29	N?	BRMS-62_173	0.0474	-8.4	1.405
	U	Na10C01b	0.04742	13.04	0.533
	U	Na10C08a	0.03519	9.74	0.681
	U	Ol9A06b	0.03355	8.83	0.709
	U	sNO202	0.02852	-9.01	1.441
	U	AP14/15a(400)	0.02574	-9.12	1.426
	U	CB10079_205(F)	0.01339	11.64	0.663
	U	BRMS-6_177	0.00759	-10.18	1.487
	U	BRMS-314_243	0.02852	-9.01	1.441

Appendix 5.28 2009 Broken Adjusted LD50 Single Marker Regression output

LN	N	Locus	Reg F prob	Additivity	Allele expression ratio (A:B)
LN 18	N3/N13	BN12A_303(F)	0.010422	-36.2	2.714
LN 18	N3/N13	sS2368b	0.010422	-36.2	2.714
LN 9	N5	KBrG23.30_185	0.0097911	-36.37	2.729
LN 9	N5	CB10229_287(F)	0.0241614	-33.53	2.405
LN 9	N5	CB10487_280(F)	0.0097911	-36.37	2.729
LN 10	N6	sN2837_120	0.0100089	-42.56	2.899
LN 10	N6	Ni2B03_298	0.0032891	-43.94	3.089
LN 11	N7/N17	sN0818	0.0427002	31.08	0.429
	U	Na10C08a	0.0248557	35.04	0.388
	U	sS1716a	0.0315528	32.39	0.372
	U	AP14/15a(400)	0.010422	-36.2	2.714
	U	BRMS-195	0.0488619	38.58	0.38
	U	CB10079_205(F)	0.0017775	47.85	0.357

Appendix 5.29 2006 (nine lines) Broken Adjusted LD50 Single Marker Regression output

LN	N	Locus	Reg F prob	Additivity	Allele expression ratio (A:B)
LN 5	N3	AP14/15b_(400)	0.0297592	-0.4	1.163
LN 5	N3	AP2/4a_(281)	0.0289109	-0.41	1.167
LN 7	N4	BRMS-276_239	0.039727	0.26	0.903
LN 7	N4	pN202a	0.0265265	0.3	0.889
LN 9	N5	CB10487_280(F)	0.0178215	0.29	0.894
LN 9	N5	sR9555(250)	0.0026203	0.36	0.868
LN 9	N5	CB10487_267(F)	0.0155719	0.29	0.891
LN 15	N9/N15	sORB84b	0.016297	-0.29	1.121
LN 15	N9/N15	OL12F02b	0.0462506	-0.24	1.101
LN 15	N9/N15	OL12F02a	0.0462506	-0.24	1.101
LN 6	N13	TW-010a	0.035305	-0.25	1.104
LN 6	N13	KBr09.8_302	0.0129986	-0.31	1.128
LN 14	N18	CB10028(F)	0.0062139	-0.34	1.142
LN 14	N18	sORB36a	0.0256591	-0.28	1.119
LN 17	N10/N19	sN1656a	0.0018534	-0.38	1.161
LN 17	N10/N19	KBr09.8_201	0.0376064	-0.26	1.109
LN 17	N10/N19	sNRD93a	0.0074576	-0.33	1.136
LN 17	N10/N19	Na10E08(F)	0.0051391	-0.36	1.151
LN 17	N10/N19	sS2066(250)	0.0298484	-0.28	1.115
LN 24	N?	FITO135	0.0172582	0.29	0.893
LN 29	N?	BRMS-62_173	0.0174352	-0.3	1.126
U	U	sN0539(125)	0.0279672	-0.27	1.116
	U	IGF5298_c	0.0163517	-0.29	1.121
	U	pN2	0.0323975	0.28	0.896
	U	Na10D09b	0.0498039	-0.24	1.102
	U	OL13C12c	0.0416653	-0.25	1.106
	U	sS2368c	0.0493187	-0.23	1.096
	U	sN2187a	0.0381285	-0.28	1.115
	U	AP14/15a(400)	0.0341598	-0.28	1.114
	U	Ni2-B07_175	0.0080453	0.39	0.854
	U	CB10211_89(F)	0.0253825	-0.39	1.173
	U	BRMS-54_104	0.0152693	0.35	0.876

Appendix 5.30 2000 (44 lines) Pod Mass Single Marker Regression output

LN	N	Locus	Reg F prob	Additivity	Allele expression ratio (A:B)
LN 3	N2/N12	Ol10H02c	0.0194321	-0.33	1.233
LN 3	N2/N12	Ol13A10	0.0200181	-0.4	1.28
LN 3	N2/N12	Na12F12	0.0399709	-0.33	1.235
LN 4	N2/N12	sN1925c	0.0002373	-0.41	1.32
LN 4	N2/N12	sR94102_320R	0.0001831	-0.43	1.325
LN 4	N2/N12	pN102c-2	0.0108897	-0.32	1.24
LN 5	N3	TW-010c	0.0064082	-0.4	1.282
LN 5	N3	AP14/15b_(400)	0.0072686	-0.47	1.333
LN 5	N3	AP2/4a_(281)	0.008066	-0.47	1.334
LN 5	N3	OL11G11b	0.0016926	-0.53	1.376
LN 5	N3	sNRB35	0.0017417	-0.57	1.4
LN 9	N5	sORA84_160	0.0352296	0.25	0.846
LN 10	N6	Ol11F12	0.0111577	-0.3	1.222
LN 15	N9/N15	Na12E06b_231(F)	0.0106938	-0.31	1.23
LN 15	N9/N15	sORB84b	0.0398942	-0.24	1.177
LN 15	N9/N15	OL12F02b	0.01653	-0.28	1.207
LN 15	N9/N15	OL12F02a	0.01653	-0.28	1.207
LN 16	N10/N19	CB10079_170(F)	0.0153091	0.29	0.822
LN 16	N10/N19	sORH62	0.0282608	0.26	0.839
LN 16	N10/N19	BRMS-62_178	0.0115082	0.3	0.816
LN 16	N10/N19	Ol11B03a	0.0242789	0.28	0.828
	U	KBrM6.12_231	0.0095625	-0.56	1.391
	U	KBrM6.12_241	0.0095625	-0.56	1.391
	U	CB10587_185(F)	0.011418	0.32	0.809
	U	pN102c-1	0.0108897	0.32	0.807
	U	pN52b	0.0396196	-0.26	1.2
	U	Na12E01b	0.0034188	-0.44	1.313
	U	Ol10F04b	0.0307735	-0.27	1.204
	U	OL13C12c	0.0469169	-0.24	1.175
	U	sNRC89b	0.0030015	-0.35	1.263
	U	sNO202	0.0069637	-0.31	1.233
	U	sN2187a	0.0209886	-0.31	1.218
	U	AP14/15a(400)	0.0194741	-0.3	1.215
	U	AP2/4b(281)	0.0241198	-0.44	1.308
	U	Ni4-A07_134	0.0127142	-0.34	1.242
	U	CB10258_270(F)	0.0220914	0.54	0.652
	U	FITO66_240	0.0095822	0.31	0.813
	U	BRMS-6_177	0.001398	-0.42	1.308

Appendix 5.31 2006 (44 lines) Pod Mass Single Marker Regression output

LN	N	Locus	Reg Fprob	Additivity	Allele expression ratio (A:B)
LN 13	N8	Ol10F05c	0.0483065	-3.08	1.465
LN 14	N18	SN11670_80	0.0297138	-3.44	1.531
LN 19	N?	CB10373(F)	0.0469661	-3.22	1.479
LN 19	N?	Na14B03	0.0227929	-3.67	1.593
LN 19	N?	sNRD76	0.0101583	-4.06	1.673
LN 19	N?	TW-006	0.021976	-3.59	1.544
	U	sS2210	0.0466584	-3.16	1.49
	U	sS1949(180)	0.0269593	-3.54	1.546
	U	BRMS-195	0.033984	-3.49	1.608
	U	CB10211_102(F)	0.0014778	-8.44	2.07
	U	CB10122	0.032631	3.72	0.652
	U	KBr11.30_231	0.0447411	-3.44	1.497

LN	N	Locus	Reg Fprob	Additivity	Allele expression ratio (A:B)
	U	KBr946	0.0074875	-4.24	1.678

Appendix 5.32 2000 (44 lines) Intact LD50 Single Marker Regression output

LN	N	Locus	Reg Fprob	Additivity	Allele expression ratio (A:B)
LN 5	N3	sORC76c	0.0460482	-8.14	1.777
LN 5	N3	TW-010c	0.0028158	-13.74	2.387
LN 5	N3	AP14/15b_(400)	0.0006321	-18.13	2.822
LN 5	N3	AP2/4a_(281)	0.0008653	-17.96	2.773
LN 5	N3	sNRB35	0.031404	-12.57	2.102
LN 15	N9/N15	KBr17.27	0.0460459	7.87	0.528
LN 16	N10/N19	CB10079_170(F)	0.050135	7.56	0.541
LN 16	N10/N19	sORH62	0.0487364	7.29	0.55
LN 6	N13	Na10F06b	0.0264733	-8.14	1.922
LN 6	N13	TW-010a	0.0459068	-7.53	1.829
LN 6	N13	KBr09.8_302	0.0486532	-7.95	1.861
LN 12	N7/N17	TW-008b	0.0383635	7.8	0.53
LN 12	N7/N17	TW-008d	0.0253096	8.57	0.504
LN 12	N7/N17	Sn3274c	0.0120491	9.13	0.477
LN 12	N7/N17	CB10277_619(F)	0.0320718	8.26	0.504
LN 12	N7/N17	CB10124_297(F)	0.0136828	9.39	0.466
LN 12	N7/N17	BRAS19	0.0074089	10.15	0.443
LN 12	N7/N17	Na10C08b	0.0426982	7.48	0.541
LN 12	N7/N17	sORE58	0.0417227	5.92	0.607
LN 18	N3/N13	Ni2B03_198	0.027041	-9.15	2.084
LN 18	N3/N13	BN12A_303(F)	0.0460102	-8	1.824
LN 18	N3/N13	Ni2-B03_148	0.0110817	10.42	0.459
LN 18	N3/N13	sS2368b	0.0046692	-11.96	2.194
LN 20	N?	Na12A08c	0.0086846	-10.76	2.082
LN 20	N?	Ol10H02c	0.0009002	-14.14	2.463
LN 20	N?	Ol13A10	0.0001695	-19.24	2.88
LN 20	N?	Na12F12	0.0015259	-15.74	2.543
LN 20	N?	sORB36b	0.0005322	-16.91	2.635
	U	KBrM6.12_231	0.0008661	-26.08	3.643
	U	KBrM6.12_241	0.0008661	-26.08	3.643
	U	Na12E01b	0.0009439	-15.32	2.52
	U	Na10C08a	0.0326714	8.47	0.539
	U	Ol10BO4a	0.0167949	-8.93	2.093
	U	Ol10F04a	0.0320823	-8	2.042
	U	Ol9A06b	0.0133822	14.33	0.439
	U	Ol9A06c	0.0096167	10.93	0.481
	U	Na14E11	0.0049856	11.44	0.46
	U	sS1716b	0.017164	-10.62	2.068
	U	sN2187a	0.0036009	-11.82	2.225
	U	AP14/15a(400)	0.0404251	-8.39	1.83
	U	AP2/4b(281)	0.024795	-16.56	2.437
	U	Ni4-A07_134	0.0076841	-11.2	2.126
	U	BRMS-23_155	0.0233322	-10.09	1.98

Appendix 5.33 2006 (44 lines) Intact LD50 Single Marker Regression output

LN	N	Locus	Reg Fprob	Additivity	Allele expression ratio (A:B)
LN 1	N11	BRMS-214_261	0.015613	-6.54	1.573
LN 28	N?	Ol13E08a	0.0106626	6.98	0.642
LN 28	N?	Ol10H02a	0.0306642	5.99	0.68

LN	N	Locus	Reg Fprob	Additivity	Allele expression ratio (A:B)
LN 19	N?	Na14B03	0.0270133	-6.07	1.54
LN 19	N?	sNRD76	0.0195401	-6.32	1.562
LN 19	N?	TW-006	0.0411717	-5.48	1.449
	U	pN64a	0.0305661	-5.79	1.491
	U	Ol13B02a	0.0470291	5.33	0.702
	U	OL13C12b	0.0145085	-6.5	1.551
	U	sNRC89b	0.0449033	-5.46	1.429
	U	sS2210	0.0045074	-7.49	1.728
	U	sS1949(180)	0.0371854	-5.67	1.479
	U	BRMS-195	0.01111	-7.21	1.772
	U	CB10211_102(F)	0.0484397	-9.23	1.637
	U	KBr11.30_231	0.013406	-6.94	1.575
	U	KBr946	0.0206156	-6.31	1.543

Appendix 5.34 2000 (44 lines) Broken LD50 Single Marker Regression output

LN	N	Locus	Reg Fprob	Additivity	Allele expression ratio (A:B)
LN 4	N2/N12	sN1925c	0.0377652	-9.13	1.52
LN 4	N2/N12	sR94102_320R	0.0152633	-10.9	1.609
LN 5	N3	TW-010c	0.0131473	-13.83	1.731
LN 5	N3	AP14/15b_(400)	0.0021879	-19.52	2.009
LN 5	N3	AP2/4a_(281)	0.0024196	-19.62	2.02
LN 5	N3	sNRB35	0.0230288	-15.82	1.781
LN 15	N9/N15	KBr17.27	0.036998	9.81	0.633
LN 16	N10/N19	sNRD49	0.0348205	9.27	0.653
LN 16	N10/N19	CB10079_170(F)	0.0353716	9.65	0.636
LN 16	N10/N19	sORH62	0.0279946	9.65	0.636
LN 3	N2/N12	Ol10H02c	0.0086446	-13.68	1.721
LN 3	N2/N12	Ol13A10	0.0052542	-17.69	1.9
LN 3	N2/N12	Na12F12	0.015028	-14.26	1.744
LN 3	N2/N12	sORB36b	0.0058096	-16.4	1.829
LN 6	N13	Na10F06b	0.0065442	-11.74	1.722
LN 6	N13	TW-010a	0.0123102	-11.1	1.68
LN 6	N13	OL11G11a	0.0120508	-10.93	1.676
LN 6	N13	KBr09.8_302	0.0099857	-12.16	1.753
LN 12	N7/N17	TW-008b	0.045074	9.03	0.658
LN 12	N7/N17	TW-008d	0.0345333	9.7	0.638
LN 12	N7/N17	Sn3274c	0.0150151	10.59	0.614
LN 12	N7/N17	CB10277_619(F)	0.0473936	9.14	0.649
LN 12	N7/N17	CB10124_297(F)	0.013618	11.2	0.593
LN 12	N7/N17	BRAS19	0.0086906	11.89	0.578
LN 12	N7/N17	Na10C08b	0.0314472	9.46	0.642
LN 18	N?	Ni2-B03_148	0.0076322	12.9	0.567
LN 24	N?	FITO135	0.0384002	9.53	0.637
LN 24	N?	pN52d-1	0.0248656	11.59	0.593
LN 24	N?	Ni2B03_198	0.0041983	-13.62	1.895
LN 37	N?	SR11644_250	0.0284018	-9.79	1.557
LN 37	N?	SR11644_350	0.0284018	-9.79	1.557
	U	KBrM6.12_231	0.0001333	-33.77	3.019
	U	KBrM6.12_241	0.0001333	-33.77	3.019
	U	IGF5298_c	0.0419037	-9.16	1.54
	U	pN52d-2	0.0248656	-11.59	1.686
	U	Na12E01b	0.0013983	-17.76	1.942
	U	Ol10BO4a	0.0279242	-9.84	1.588
	U	Ol10F04a	0.0008886	-14.31	2.091
	U	Ol9A06b	0.0255066	15.56	0.566
	U	Ol9A06c	0.0487073	10.1	0.659
	U	Na14E11	0.0246203	11.12	0.631

U	sORB10b	0.012874	-10.97	1.662
U	sN2187a	0.0032899	-14.25	1.782
U	sN2187b	0.0476752	-8.9	1.534
U	AP14/15a(400)	0.0047604	-13.33	1.753
U	AP2/4b(281)	0.0384484	-16.41	1.73
U	Ni4-A07_134	0.0042481	-14.1	1.756
U	BRMS-23_155	0.0502767	-10.51	1.554

Appendix 5.35 2006 (44 lines) Broken LD50 Single Marker Regression output

5.36 Intact adjusted LD50 Multiple Regression output

 Response variate: adhld50
  Number of units: 73
    Forced terms: Constant
      Forced df: 1
     Free terms: BRMS_303 + IGF5298_c_200 + KBr09_8_221 + KBrM6_12_231 +
          Na10C01a + Ni2_B03_148 + Ol10F04a + SN13034_140 +
          SR11644_250 + sN3766 + sNRB35 + sS2368b

 All possible subset selection

    Free terms: (1) BRMS_303   (7) Ol10F04a
          (2) IGF5298_c_200   (8) SN13034_140
          (3) KBr09_8_221   (9) SR11644_250
          (4) KBrM6_12_231   (10) sN3766
          (5) Na10C01a   (11) sNRB35
          (6) Ni2_B03_148   (12) sS2368b

  * MESSAGE: probabilities are based on F-statistics, i.e. on variance ratios.

 Best subsets with 1 term

 Adjusted   Cp Df (1) (2) (3) (4) (5) (6) (7) (8) (9)(10)(11)(12)
   24.77   62.39 3 - - - .00 - - - - - - - -
   16.46   76.67 3 .00 - - - - - - - - - - -
   15.83   77.76 3 - - - - - .00 - - - - - -
   13.58   81.63 3 - - - - - - - - - - - .00
   10.40   87.11 3 - - - - - - - .01 - - - -
    8.31   90.69 3 - .02 - - - - - - - - - -
    8.21   91.12 2 - - - - - - - - - - .01 -
    7.59   91.94 3 - - - - - - - - .02 - - -

 Best subsets with 2 terms

  Adjusted   Cp Df (1) (2) (3) (4) (5) (6) (7) (8) (9)(10)(11)(12)

```
32.72   49.42   5   -   -   -   .00   -   .01   -   -   -   -   -   -
31.30   51.79   5   -   -   -   .00 .02   -   -   -   -   -   -   -
31.21   51.94   5   -   -   -   .00   -   -   -   .02   -   -   -   -
30.01   53.94   5   -   .03   -   .00   -   -   -   -   -   -   -   -
29.80   54.29   5   -   -   -   .00   -   -   -   -   -   -   -   .04
28.95   55.71   5   -   -   -   .00   -   -   -   -   -   .05   -
28.94   55.72   5   -   -   -   -   -   .00   -   -   .00   -   -
27.84   57.56   5   -   -   -   .00   -   -   -   .09   -   -   -
```

Best subsets with 3 terms

```
Adjusted      Cp  Df  (1) (2) (3) (4) (5) (6) (7) (8) (9)(10)(11)(12)
 38.86   40.14   7   -   -   -   .00   -   .00   -   -   -   .02   -   -
 38.73   40.35   7   -   -   .01 .00 .00   -   -   -   -   -   -   -
 38.03   41.49   7   -   -   -   .00   -   .01   -   .02   -   -   -   -
 37.48   42.38   7   -   .03   -   .00   -   .01   -   -   -   -   -   -
 37.21   42.82   7   -   -   -   .00   -   -   -   .01   -   .02   -   -
 37.15   42.92   7   -   -   -   .00 .04 .02   -   -   -   -   -   -
 37.01   43.15   7   -   .02   -   .00 .01   -   -   -   -   -   -   -
 36.61   43.80   7   -   -   -   .01   -   .01   -   -   .05   -   -   -
```

Best subsets with 4 terms

```
Adjusted      Cp  Df  (1) (2) (3) (4) (5) (6) (7) (8) (9)(10)(11)(12)
 44.86   31.71   9   .00 .00   -   -   -   -   .00   -   -   .00   -   -
 44.84   31.74   9   -   .01   -   .00   -   .00   -   -   -   .01   -
 44.54   32.21   9   -   -   -   .00   -   .01   -   .02   -   .01   -
 43.84   33.31   9   -   -   -   .00   -   .00 .02   -   -   .00   -
 43.39   34.02   9   .00   -   -   -   -   .01 .00   -   .00   -   -
 43.28   34.19   9   .01   -   -   .01   -   -   -   .00   -   .01   -   -
 42.78   34.98   9   -   .04 .02 .00 .00   -   -   -   -   -   -   -
 42.76   35.01   9   -   .01   -   .00   -   .01 .02   -   -   -   -
```

Best subsets with 5 terms

```
Adjusted      Cp  Df  (1) (2) (3) (4) (5) (6) (7) (8) (9)(10)(11)(12)
 52.85   20.82  11   -   .00   -   .00   -   .00 .00   -   -   .00   -   -
 52.64   21.14  11   .00 .00   -   .00   -   -   .00   -   -   .00   -   -
 51.41   23.02  11   .00   -   -   .00   -   -   .00 .00   -   .00   -   -
 51.34   23.13  11   .00 .00   -   -   -   .00 .01   -   .00   -   -
 50.75   24.02  11   -   -   -   .00   -   .00 .01 .01   -   .00   -   -
 48.69   27.16  11   -   -   -   .00   -   -   .01 .01   -   .00   -   .01
 48.64   27.25  11   -   .01   -   .00   -   -   .00   -   -   .00   -   .01
 48.39   27.62  11   .00 .01   -   .01   -   -   .00 .01   -   -   -   -
```

Adjusted	Cp	Df	(1)	(2)	(3)	(4)	(5)	(6)	(7)	(8)	(9)	(10)	(11)	(12)
58.36	14.38	13	.00	.00	-	.00	-	-	.00	.01	-	.00	-	-
56.21	17.56	13	.04	.00	-	.00	-	.04	.00	-	-	.00	-	-
55.66	18.37	13	-	.02	-	.00	-	.00	.00	.06	-	.00	-	-
54.04	20.75	13	.00	.00	.15	.01	-	-	.00	-	-	.00	-	-
53.90	20.10	12	.00	.01	-	-	-	.00	.00	-	.00	.04	-	
53.88	20.99	13	.01	.01	-	-	.07	.00	.01	-	.00	-	-	
53.78	21.13	13	.00	.00	-	.00	.18	-	.00	-	-	.00	-	-
53.33	21.80	13	.07	-	-	.01	-	.11	.00	.00	-	.00	-	-

5.37 Broken adjusted LD50 Multiple Regression output

Response variate: adhld50
 Number of units: 73
  Forced terms: Constant
   Forced df: 1
   Free terms: AP2_4a_281 + BN12A_303_F + CB10431_103_F +
        KBrM6_12_231 + Na10F06b + Na12A08a + Na12H04b +
        OL11G11b + Ol10F04a + sNRB35 + sORB36b

All possible subset selection

   Free terms: (1) AP2_4a_281   (7) Na12H04b
        (2) BN12A_303_F   (8) OL11G11b
        (3) CB10431_103_F   (9) Ol10F04a
        (4) KBrM6_12_231   (10) sNRB35
        (5) Na10F06b   (11) sORB36b
        (6) Na12A08a

* MESSAGE: probabilities are based on F-statistics, i.e. on variance ratios.

Best subsets with 1 term

Adjusted	Cp	Df	(1)	(2)	(3)	(4)	(5)	(6)	(7)	(8)	(9)	(10)	(11)
27.98	23.19	3	-	-	-	.000	-	-	-	-	-	-	-
12.46	42.18	2	-	-	-	-	-	-	-	-	-	.001	-
10.96	44.50	3	-	-	-	-	-	-	-	-	.006	-	-
10.54	45.03	3	.008	-	-	-	-	-	-	-	-	-	-
8.50	47.22	2	-	-	-	-	.007	-	-	-	-	-	-
7.91	48.32	3	-	-	-	-	-	.021	-	-	-	-	-

Adjusted	Cp	Df	(1)	(2)	(3)	(4)	(5)	(6)	(7)	(8)	(9)	(10)	(11)
7.54	48.78	3	-	-	.024	-	-	-	-	-	-	-	-
6.93	49.55	3	-	-	-	-	-	-	-	.030	-	-	-

Best subsets with 2 terms

Adjusted	Cp	Df	(1)	(2)	(3)	(4)	(5)	(6)	(7)	(8)	(9)	(10)	(11)
36.09	14.75	5	-	-	.006	.000	-	-	-	-	-	-	-
34.79	16.32	5	-	-	-	.000	-	-	-	-	.013	-	-
32.31	19.35	5	-	-	-	.000	-	-	-	.045	-	-	-
32.25	19.42	5	.047	-	-	.000	-	-	-	-	-	-	-
31.80	19.96	5	-	-	-	.000	-	.058	-	-	-	-	-
28.50	23.26	4	-	-	-	.000	.223	-	-	-	-	-	-
28.12	24.44	5	-	.348	-	.000	-	-	-	-	-	-	-
27.59	25.08	5	-	-	-	.000	-	-	.447	-	-	-	-

Best subsets with 3 terms

Adjusted	Cp	Df	(1)	(2)	(3)	(4)	(5)	(6)	(7)	(8)	(9)	(10)	(11)
41.84	9.67	7	-	-	.002	.000	-	.017	-	-	-	-	-
40.76	10.94	7	-	-	.016	.000	-	-	-	-	.031	-	-
40.13	11.69	7	-	-	.006	.000	-	-	-	.043	-	-	-
38.84	13.22	7	.088	-	.013	.000	-	-	-	-	-	-	-
36.84	15.58	7	.131	-	-	.000	-	-	-	.037	-	-	-
35.90	16.68	7	-	-	-	.000	-	-	.212	-	.007	-	-
35.86	15.88	6	-	-	.005	.000	-	-	-	-	-	.389	-
35.73	16.03	6	-	-	.010	.000	.433	-	-	-	-	-	-

5.38 Intact adjusted LD50 Multiple Regression interactions output

Response variate: adhld50
 Number of units: 73
  Forced terms: Constant
   Forced df: 1
   Free terms: KBrM6_12_241 + Ni2_B03_148 + SR11644_250 +
        BRMS_101 + Na10C08a + KBrM6_12_241.Ni2_B03_148 +
        KBrM6_12_241.SR11644_250 + Ni2_B03_148.SR11644_250 +
        KBrM6_12_241.BRMS_101 + Ni2_B03_148.BRMS_101 +
        SR11644_250.BRMS_101 + KBrM6_12_241.Na10C08a +
        Ni2_B03_148.Na10C08a + SR11644_250.Na10C08a +
        BRMS_101.Na10C08a + KBrM6_12_241.Ni2_B03_148.SR11644_250 +
        KBrM6_12_241.Ni2_B03_148.BRMS_101 + Ni2_B03_148.BRMS_101.Na10C08a

All possible subset selection

Forced terms: Constant + KBrM6_12_241 + Ni2_B03_148 + SR11644_250 +
        BRMS_101 + Na10C08a

Forced df: 11
Free terms: (1) KBrM6_12_241.Ni2_B03_148
        (2) KBrM6_12_241.SR11644_250
        (3) Ni2_B03_148.SR11644_250
        (4) KBrM6_12_241.BRMS_101
        (5) Ni2_B03_148.BRMS_101
        (6) SR11644_250.BRMS_101
        (7) KBrM6_12_241.Na10C08a
        (8) Ni2_B03_148.Na10C08a
        (9) SR11644_250.Na10C08a
        (10) BRMS_101.Na10C08a
        (AFACTORIAL limit for expansion of formula = 2)

Best subsets with 1 term

Adjusted	Cp	Df	(1)	(2)	(3)	(4)	(5)	(6)	(7)	(8)	(9)	(10)
55.48	23.45	14a	-	-	-	.000	-	-	-	-	-	-
44.82	39.84	14a	-	-	-	-	.076	-	-	-	-	-
43.92	41.23	14a	-	-	-	-	-	-	-	.116	-	-
43.65	41.64	14a	-	-	-	-	-	-	-	-	.131	-
43.51	41.86	14a	.140	-	-	-	-	-	-	-	-	-
43.27	41.71	13a	-	-	-	-	-	-	-	-	-	.118
42.38	44.10	15	-	.260	-	-	-	-	-	-	-	-
41.62	44.77	14a	-	-	-	-	-	-	.318	-	-	-

Best subsets with 2 terms

Adjusted	Cp	Df	(1)	(2)	(3)	(4)	(5)	(6)	(7)	(8)	(9)	(10)
60.10	19.23	17a	-	-	-	.000	-	-	.028	-	-	-
58.65	21.34	17a	-	-	-	.000	-	-	-	.068	-	-
57.81	22.57	17a	-	-	-	.000	-	-	-	-	.113	-
57.48	23.05	17a	.136	-	-	.000	-	-	-	-	-	-
56.99	24.65	18a	-	.210	-	.000	-	-	-	-	-	-
56.49	23.63	16a	-	-	-	.000	-	-	-	-	-	.195
55.31	26.21	17a	-	-	-	.002	.434	-	-	-	-	-
54.47	27.45	17a	-	-	-	.000	-	.643	-	-	-	-

Best subsets with 3 terms

Adjusted	Cp	Df	(1)	(2)	(3)	(4)	(5)	(6)	(7)	(8)	(9)	(10)
65.22	13.95	19a	-	-	-	.000	-	-	-	.002	.004	-

```
63.92   16.83 20a .010  -   - .000  -   -   -   - .008  -
61.47   20.21 20a .185  -   - .000  -   - .042  -   -   -
61.39   21.32 21a  - .225  - .000  -   - .035  -   -   -
61.29   20.46 20a  - .056  - .000  -   -   -   - .023  -
61.23   19.56 19a  -   -   - .000  -   - .066 .172  -   -
60.63   20.40 19a  -   -   - .000  -   - .058  - .260  -
60.02   22.23 20a  -   -   - .000  - .418 .019  -   -   -
```

5.39 Broken adjusted LD50 Multiple regression interactions output

Response variate: adhld50
Number of units: 73
Forced terms: Constant
Forced df: 1
Free terms: Na10F06b + KBrM6_12_231 + Ol10F04a + sORB36b +
       Na10C08a + sS2368b + Na10F06b.KBrM6_12_231 +
       Na10F06b.Ol10F04a + KBrM6_12_231.Ol10F04a +
       Na10F06b.sORB36b + KBrM6_12_231.sORB36b +
       Ol10F04a.sORB36b + Na10F06b.Na10C08a + KBrM6_12_231.Na10C08a
+ Ol10F04a.sS2368b + sORB36b.sS2368b + Na10C08a.sS2368b + Na10F06b.KBrM6_12_231
.Ol10F04a + Na10F06b.KBrM6_12_231.sORB36b + Na10F06b.KBrM6_12_231.Na10C08a +
       Na10F06b.sORB36b.Na10C08a + Na10F06b.KBrM6_12_231.sS2368b +
       Na10F06b.Ol10F04a.sS2368b + KBrM6_12_231.Ol10F04a.sS2368b +
       Na10F06b.sORB36b.sS2368b + Na10F06b.Na10C08a.sS2368b +
       Ol10F04a.Na10C08a.sS2368b
All possible subset selection

Forced terms: Constant + Na10F06b + KBrM6_12_231 + Ol10F04a +
       sORB36b + Na10C08a + sS2368b

Forced df: 7
Free terms: (1) Na10F06b.KBrM6_12_231   (9) KBrM6_12_231.Na10C08a
       (2) Na10F06b.Ol10F04a   (10) sORB36b.Na10C08a
       (3) KBrM6_12_231.Ol10F04a   (11) Na10F06b.sS2368b
       (4) Na10F06b.sORB36b   (12) KBrM6_12_231.sS2368b
       (5) KBrM6_12_231.sORB36b   (13) Ol10F04a.sS2368b
       (6) Ol10F04a.sORB36b   (14) sORB36b.sS2368b
       (7) Na10F06b.Na10C08a   (15) Na10C08a.sS2368b
       (8) KBrM6_12_231.Na10C08a
       (AFACTORIAL limit for expansion of formula = 2)

Best subsets with 1 term

Adjusted   Cp Df (1)(2)(3)(4)(5)(6)(7)(8)(9)(10)(11)(12)(13)(14)(15)
```

```
42.48    52.51   8 - - - .0 - - - - - - - - - - -
40.42    56.44   8 .0 - - - - - - - - - - - - - -
37.60    61.79   8 - - - - - - .0 - - - - - - - -
35.88    65.07   8 - - - - - - - .0 - - - - - - -
35.72    65.37   8 - - - - - .0 - - - - - - - - -
32.99    70.57   8 - - - - .0 - - - - - - - - - -
32.82    70.91   8 - - .1 - - - - - - - - - - - -
29.94    76.39   8 - - - - - - - - - - - - - - .3
```

Best subsets with 2 terms

```
Adjusted    Cp  Df (1)(2)(3)(4)(5)(6)(7)(8)(9)(10)(11)(12)(13)(14)(15)
 45.64     46.90  9 - - .0 .0 - - - - - - - - - - -
 45.33     47.48  9 .0 - - - - .0 - - - - - - - - -
 45.30     47.55  9 - - - .0 - .0 - - - - - - - - -
 44.58     48.89  9 - - - - - .0 - .0 - - - - - - -
 44.52     49.00  9 - - - .0 - - - .1 - - - - - - -
 43.90     50.17  9 .1 - - .0 - - - - - - - - - - -
 43.89     50.17  9 .0 - - - - - .0 - - - - - - - -
 43.66     50.61  9 - - - .0 - - .1 - - - - - - - -
```

Best subsets with 3 terms

```
Adjusted    Cp  Df (1)(2)(3)(4)(5)(6)(7)(8)(9)(10)(11)(12)(13)(14)(15)
 51.11     37.21 10 .0 - - - - .0 - .0 - - - - - - -
 49.41     40.36 10 - - - .0 - .0 - .0 - - - - - - -
 48.95     41.21 10 - - - - - .0 - .0 .0 - - - - - -
 48.81     41.46 10 - - - - - .0 - .0 - - - - .0 -
 48.66     41.74 10 .0 - - - - - .0 - .0 - - - - -
 48.19     42.60 10 .0 - - - - .0 .0 - - - - - - -
 48.17     42.65 10 - - .0 .0 - - - .0 - - - - - -
 47.85     43.24 10 - - - .0 - - - .0 - - - .0 - -
```

Best subsets with 4 terms

```
Adjusted    Cp  Df (1)(2)(3)(4)(5)(6)(7)(8)(9)(10)(11)(12)(13)(14)(15)
 59.04     23.38 11 .0 - - - - .0 - .0 - - - - - .0 -
 55.88     29.12 11 .0 - - - - .0 - .0 - - - .0 - - -
 55.05     30.63 11 .0 - - - - .0 - .0 .0 - - - - - -
 54.04     32.47 11 - - - .0 - .0 - .0 - - - - - .0 -
 54.02     32.50 11 - - - .0 - .0 - .0 - - - .0 - - -
 53.28     33.85 11 - - - - - .0 - .0 .0 - - - - .0 -
 52.26     35.70 11 - - - - - .0 - .0 .0 - - .0 - - -
 52.24     35.73 11 .0 - - - - .0 - .0 - .1 - - - - -
```

Best subsets with 5 terms

```
Adjusted    Cp  Df (1)(2)(3)(4)(5)(6)(7)(8)(9)(10)(11)(12)(13)(14)(15)
  62.98    17.15 12 .0 - - - - .0 - .0 .0 - - - - .0 -
  61.03    20.62 12 .0 - - - - .0 - .0 .0 - - .0 - - -
  59.68    23.03 12 .0 - - - - .0 - .0 - - - .2 - .0 -
  59.38    23.58 12 .0 - .2 - - .0 - .0 - - - - - .0 -
  59.17    23.95 12 .0 - - - - .0 - .0 - - - - - .0 .3
  59.04    24.17 12 .0 - - - - .0 - .0 - - - - .3 .0 -
  58.81    24.59 12 .0 - - - .4 .0 - .0 - - - - - .0 -
  58.80    24.60 12 .0 - - .4 - .0 - .0 - - - - - .0 -
```

Best subsets with 6 terms

```
Adjusted    Cp  Df (1)(2)(3)(4)(5)(6)(7)(8)(9)(10)(11)(12)(13)(14)(15)
  65.34    13.91 13 .0 - .0 - - .0 - .0 .0 - - - - .0 -
  64.35    15.66 13 .0 - - - - .0 - .0 .0 - - .1 - .0 -
  63.01    18.01 13 .0 - - - - .0 - .0 .0 .3 - - - .0 -
  62.90    18.20 13 .0 - - - - .0 - .0 .0 - - - .4 .0 -
  62.74    18.49 13 .0 .4 - - - .0 - .0 .0 - - - - .0 -
  62.52    18.87 13 .0 - - - - .0 - .0 .0 - .6 - - .0 -
  62.48    18.93 13 .0 - - - - .0 - .0 .0 - - - - .0 .7
  62.40    19.07 13 .0 - - .8 - .0 - .0 .0 - - - - .0 -
```

Best subsets with 7 terms

```
Adjusted    Cp  Df (1)(2)(3)(4)(5)(6)(7)(8)(9)(10)(11)(12)(13)(14)(15)
  67.03    11.97 14 .0 - .0 - - .0 - .0 .0 - - .0 - .0 -
  65.92    13.90 14 .0 .2 .0 - - .0 - .0 .0 - - - - .0 -
  65.91    13.90 14 .0 - .0 - - .0 - .0 .0 .2 - - - .0 -
  65.33    14.92 14 .0 - .0 .3 - .0 - .0 .0 - - - - .0 -
  65.11    15.29 14 .0 - .0 - - .0 - .0 .0 - - - .4 .0 -
  64.97    15.54 14 .0 - .0 - - .0 - .0 .0 - .5 - - .0 -
  64.94    15.59 14 .0 - .0 - .6 .0 - .0 .0 - - - - .0 -
  64.80    15.83 14 .0 - .0 - - .0 - .0 .0 - - - - .0 .8
```

Appendix 6

6.1 Randomised planting design for *At* ecotypes

Block 1

An-1	Bay-0	Br-0	C24	Col-0	Cvi-0	Est-1	Ler-0
Kin-0	Kondara	Mrk-0	NFA-8	Nok-3	Oy-0	Van-0	Ws-2

Block 2

Kondara	NFA-8	Van-0	Ler-0	Kin-0	Bay-0	Est-1	Nok-3
An-1	Oy-0	Cvi-0	C24	Ws-2	Col-0	Mrk-0	Br-0

6.2 – Col-0/Ws-2 paired T-test

Genstat curve fit

	lethaldose	fprob	rsquare	Y	A	B	C
Col-0	61.44	0	99.6	20.04	-21.9542	0.0137	1.3914
Col-0	41.54	0	99.4	19.9811	-17.1068	0.0247	1.2153
Col-0	73.53	0	99.8	19.3767	-18.036	0.0134	1.3964
Col-0	54.98	3.37E-06	92.5	14.5715	-35.7076	0.0049	1.4185
Col-0	73.74	0	99.2	18.6495	-39.2248	0.0042	1.1344
Col-0	43.48	*	*	26.9082	-39.3941	-0.0061	-1.702
Ws-2	104.76	0	99.8	19.511	-17.2701	0.0159	2.8517
Ws-2	82.74	0	99.7	20.4929	-20.4997	0.0064	0.7526
Ws-2	82.67	0	96.9	15.5431	-14.6419	0.0095	1.588
Ws-2	64.65	0	99.3	20.0701	-13.4038	0.0317	2.0707
Ws-2	106.22	0	99.6	19.06	-15.2414	0.0098	1.1912
Ws-2	81.81	0	99.7	19.612	-13.726	0.0198	1.6192

Curve fitted	Col-0	Ws-2
	61.44	104.76
	41.54	82.74
	73.53	82.67
	54.98	64.65
	73.74	106.22
	43.48	81.81
mean	58.11	87.14

stdev	14.08233	15.79912
sterr	6.297811	7.06558

t test	0.006117

6.3 GLM to assess for differences between 8 ecotypes:
Analysis of variance

Variate: lethaldose

Source of variation	d.f.	s.s.	m.s.	v.r.	F pr.
Line	11	578915	52629	29.24	<.001
Residual	69	124196	1800		
Total	80	703111			

Multiple comparison

6.4 Unpaired T-tests between Col-0 and 8 ecotypes assessed:
Two-sample t-test

Variates: Bay-0, Col-0.

Test for equality of sample variances

Test statistic F = 1.78 on 8 and 5 d.f.

Probability (under null hypothesis of equal variances) = 0.54

Summary

Sample	Size	Mean	Variance	Standard deviation	Standard error of mean
C46	9	124.27	353	18.79	6.263
C52	6	58.12	198.3	14.08	5.749

Difference of means:	66.155
Standard error of difference:	9.029

95% confidence interval for difference in means: (46.65, 85.66)

Test of null hypothesis that mean of C46 is equal to mean of C52

Test statistic t = 7.33 on 13 d.f.

Probability < 0.001

Two-sample t-test

Variates: Br-/Col-0.

Test for equality of sample variances

Test statistic F = 1.05 on 5 and 10 d.f.

Probability (under null hypothesis of equal variances) = 0.88

Summary

Sample	Size	Mean	Variance	Standard deviation	Standard error of mean
C42	11	28.97	188.9	13.75	4.144
C52	6	58.12	198.3	14.08	5.749

Difference of means:	-29.149
Standard error of difference:	7.034

95% confidence interval for difference in means: (-44.14, -14.16)

Test of null hypothesis that mean of C42 is equal to mean of C52

Test statistic t = -4.14 on 15 d.f.

Probability < 0.001

Two-sample t-test

Variates: C24, Col-0.

Test for equality of sample variances

Test statistic F = 1.75 on 7 and 5 d.f.

Probability (under null hypothesis of equal variances) = 0.56

Summary

Sample	Size	Mean	Variance	Standard deviation	Standard error of mean
C50	8	47.82	346.9	18.63	6.585
C52	6	58.12	198.3	14.08	5.749

Difference of means: -10.298

Standard error of difference: 9.117

95% confidence interval for difference in means: (-30.16, 9.567)

Test of null hypothesis that mean of C50 is equal to mean of C52

Test statistic t = -1.13 on 12 d.f.

Probability = 0.281

Two-sample t-test

Variates:Est-1, Col-0.

Test for equality of sample variances

Test statistic F = * on 5 and 7 d.f.

Probability (under null hypothesis of equal variances) = 1.00

Summary

Sample	Size	Mean	Variance	Standard deviation	Standard error of mean
C56	8	250	0	0	0
C52	6	58.1	198.31	14.082	5.749

Difference of means: 191.882

Standard error of difference: 4.909

95% confidence interval for difference in means: (181.2, 202.6)

Test of null hypothesis that mean of C56 is equal to mean of C52

Test statistic t = 39.09 on 12 d.f.

Probability < 0.001

Two-sample t-test

Variates: Kondara, Col-0.

Test for equality of sample variances

Test statistic F = * on 5 and 2 d.f.

Probability (under null hypothesis of equal variances) = 1.00

Summary

Sample	Size	Mean	Variance	Standard deviation	Standard error of mean
C68	3	250	0	0	0
C52	6	58.1	198.31	14.082	5.749

Difference of means:	191.882
Standard error of difference:	8.416

95% confidence interval for difference in means: (172.0, 211.8)

Test of null hypothesis that mean of C68 is equal to mean of C52

Test statistic t = 22.80 on 7 d.f.

Probability < 0.001

Two-sample t-test

Variates:Mrk-0, Col-0.

Test for equality of sample variances

Test statistic F = * on 5 and 5 d.f.

Probability (under null hypothesis of equal variances) = 1.00

Summary

Sample	Size	Mean	Variance	Standard deviation	Standard error of mean
C60	6	250	0	0	0
C52	6	58.1	198.31	14.082	5.749

Difference of means: 191.882

Standard error of difference: 5.749

95% confidence interval for difference in means: (179.1, 204.7)

Test of null hypothesis that mean of C60 is equal to mean of C52

Test statistic t = 33.38 on 10 d.f.

Probability < 0.001

Two-sample t-test

Variates: Oy-0, Col-0.

Test for equality of sample variances

Test statistic F = 1.18 on 5 and 6 d.f.

Probability (under null hypothesis of equal variances) = 0.83

Summary

Sample	Size	Mean	Variance	Standard deviation	Standard error of mean
C64	7	38.67	168.1	12.96	4.9
C52	6	58.12	198.3	14.08	5.749

Difference of means: -19.45

Standard error of difference: 7.502

95% confidence interval for difference in means: (-35.96, -2.939)

Test of null hypothesis that mean of C64 is equal to mean of C52

Test statistic t = -2.59 on 11 d.f.

Probability = 0.025
Two-sample t-test

Variates: Van-0, Col-0.

Test for equality of sample variances

Test statistic F = 1.81 on 5 and 7 d.f.

Probability (under null hypothesis of equal variances) = 0.46

Summary

Sample	Size	Mean	Variance	Standard deviation	Standard error of mean
C72	8	30.19	109.6	10.47	3.701
C52	6	58.12	198.3	14.08	5.749

Difference of means: -27.932
Standard error of
difference: 6.538

95% confidence interval for difference in means: (-42.18, -13.69)

Test of null hypothesis that mean of C72 is equal to mean of C52

Test statistic t = -4.27 on 12 d.f.

Probability = 0.001

6.5 GLM to assess for variation between Blocks for *At* ecotypes
Screening of terms in an unbalanced design

Variate: lethaldose

Marginal and conditional test statistics and degrees of freedom

degrees of freedom for denominator (full model):   50

term	mtest	mdf	ctest	cdf
Line	433.72	7	433.72	7

P-values of marginal and conditional tests

term	mprob	cprob
Line	0	0

Analysis of an unbalanced design using GenStat regression

Variate: lethaldose

Accumulated analysis of variance

Change	d.f.	s.s.	m.s.	v.r.	F pr.
Block	2	1653.8	826.9	4.8	0.012
Line	7	523407.5	74772.5	433.72	<.001
Residual	50	8619.9	172.4		
Total	59	533681.3	9045.4		

Predictions from regression model

Response variate: lethaldose

	Prediction
Line	
Bay-0	126.6
Br-0	29.1
C24	47.5
Est-1	249.7
Kondara	251.3
Mrk-0	249.1
Oy-0	36.7
Van-0	29.9

Minimum standard error of difference	6.124
Average standard error of difference	7.498
Maximum standard error of difference	9.873

Analysis of variance

Source	d.f.	s.s.	m.s.	v.r.	F pr.
Block	2	1653.8	826.9	4.8	0.012
Line	7	523407.5	74772.5	433.72	< 0.001

Residual	50	8619.9	172.4
Total	59	533681.3	9045.4

Information summary

Design unbalanced, analysed by GenStat regression

Predictions from regression model

Response variate: lethaldose

	Prediction
Line	
Bay-0	126.6
Br-0	29.1
C24	47.5
Est-1	249.7
Kondara	251.3
Mrk-0	249.1
Oy-0	36.7
Van-0	29.9

Minimum standard error of difference	6.124
Average standard error of difference	7.498
Maximum standard error of difference	9.873

6.6: Paired t-test for Col-0 and weak *spt* allele

Col-0/spt 1-2 weak

Sample	Size	Mean	Variance	Standard deviation	Standard error of mean
C34	6	58.12	198.3	14.08	5.749
C36	3	92.3	138.4	11.77	6.793

Difference of means:	-34.178
Standard error of difference:	9.518

Test statistic t = -3.59 on 7 d.f.

Probability = 0.009

6.7 Paired t-test for Col-0 and strong *spt* allele

Col-0/spt 1-2 strong

Identifier	Values	Missing	Levels		
C37	6	0	1		

Identifier	Minimum	Mean	Maximum	Values	Missing
C38	41.54	58.12	73.74	6	0

Identifier	Values	Missing	Levels		
C39	6	3	1		

Identifier	Minimum	Mean	Maximum	Values	Missing
C40	250	250	250	6	3

Two-sample t-test

Test statistic t = -22.80 on 7 d.f.

Probability < 0.001

SPT assay (using first three Col-0 measurements)
Analysis of variance

Variate: ARIT50

Source of variation	d.f.	s.s.	m.s.	v.r.	F pr.
Line	2	62533.5	31266.7	234.88	<.001
Residual	6	798.7	133.1		
Total	8	63332.2			

Variate: ARIT50

Grand mean 133.7

Line	Col-0	*spt* 1-2 strong	*spt*1-2 weak
	58.8	250	92.3

Tukey's 95% confidence intervals

Line

	Mean
Col-0	58.8
SPT1-2 weak	92.3
spt 1-2 strong	250

316

6.8: Paired T-test to assess for variation between Col-0 and *ga 4-3 oxidase* lines

ga 4-3 oxidase	**Col-0**	*'p' value* (t-test)
154.26	61.44	
91.67	41.54	
165.95	54.98	
126.62	73.74	
mean LD50: 134.625	57.925	0.01453

6.9 Unpaired T-test to assess for variation between Col-0 and *ben-2, dde-2,* PIN1:GFP, 35s::BEN2

Two-sample t-test
Col-0/*ben-2*

Test for equality of sample variances

Test statistic F = 34.84 on 5 and 1 d.f.

Probability (under null hypothesis of equal variances) = 0.26

Summary

Sample	Size	Mean	Variance	Standard deviation	Standard error of mean
Col-0	6	58.12	198.3	14.082	5.749
ben-2	2	10.18	5.7	2.386	1.687

Difference of means: 47.94
Standard error of difference: 10.53

95% confidence interval for difference in means: (22.18, 73.69)

Test of null hypothesis that mean of Col-0 is equal to mean of *ben-2*

Test statistic t = 4.55 on 6 d.f.

Probability = 0.004

Two-sample t-test

Col-0/35s::BEN2
Test for equality of sample variances

Test statistic F = 3.31 on 5 and 1 d.f.

Probability (under null hypothesis of equal variances) = 0.79

Summary

Sample	Size	Mean	Variance	Standard deviation	Standard error of mean
Col-0	6	58.12	198.3	14.08	5.749
35s::BEN2					
	2	20.41	60.0	7.74	5.475

Difference of means:	37.71
Standard error of difference:	10.81

95% confidence interval for difference in means: (11.26, 64.16)

Test of null hypothesis that mean of Col-0 is equal to mean of 35s::BEN2

Test statistic t = 3.49 on 6 d.f.

Probability = 0.013

Two-sample t-test
Col-0/*dde-2*

Variates: C13, C15.

Test for equality of sample variances

Test statistic F = 1.64 on 2 and 5 d.f.

Probability (under null hypothesis of equal variances) = 0.57

Summary

Sample	Size	Mean	Variance	Standard deviation	Standard error of mean
Col-0	6	58.12	198.3	14.08	5.749
dde-2	3	96.97	324.7	18.02	10.404

Difference of means: -38.85
Standard error of difference: 10.83

95% confidence interval for difference in means: (-64.46, -13.25)

Test of null hypothesis that mean of Col-0 is equal to mean of *dde-2*

Test statistic t = -3.59 on 7 d.f.

Probability = 0.009